

"ROLES OF CIRCADIAN OSCILLATORS IN THE PATHOGENESIS OF DIABETES"

Thesis submitted to the Faculty of Medicine of the University of Geneva

for the degree of Privat-Docent by

Volodymyr PETRENKO

Geneva

TABLE OF CONTENTS:

ACKNOWLEDGEMENTS
SUMMARY6
INTRODUCTION
1. Circadian system as a molecular driver of rhythmic physiology7
2. Time dimension of body metabolism10
2.1. Circadian orchestration of glucose metabolism10
2.2. Lipids around-the-clock11
2.3. Circadian regulation of immunometabolism13
3. Circadian misalignment and metabolic disorders14
4. Pathogenesis of type 2 diabetes on 24 h-scale16
4.1 Insulin resistance17
4.2. Beta-cell dysfunction and apoptosis18
RESULTS AND PUBLICATIONS
1. Time zones of pancreatic islet: studying the molecular clocks in α - and β -cells in genetic mouse models, in physiology and diabetes
1.1. Pancreatic α - and β -cells bear the clocks that drive rhythmic secretion of glucagon and insulin in physiological context
PUBLICATION 1. Pancreatic α - and β -cellular clocks have distinct molecular properties and impact on islet hormone secretion and gene expression21
1.2. Roles of the islet cellular clocks in diabetes context and in β -cel

	ACATION 2. The core clock transcription factor BMAL1 drives circadian β-cell eration during compensatory regeneration of the endocrine pancreas22
2.	Translating the clocks studies in diabetes from genetic mouse models to humans
	2.1. Functional clocks operative in human pancreatic islet cells are indispensable for proper insulin secretion
	AICATION 3. A functional circadian clock is required for proper insulin secretion man pancreatic islet cells24
	2.2. Circadian clockwork is compromised in human pancreatic islet cells upon type 2 diabetes
	AICATION 4. In pancreatic islets from type 2 diabetes patients, the dampened lian oscillators lead to reduced insulin and glucagon exocytosis25
	2.3. Circadian timing of human pancreatic islet lipid metabolism in physiology and type 2 diabetes
	ICATION 5. Circadian orchestration of lipid metabolism and membrane fluidity nan pancreatic islets are disrupted upon type 2 diabetes27
CONC	CLUSIONS AND PERSPECTIVES28
1.	Circadian clocks take a part in the pathogenesis of type 2 diabetes
2.	1.3 Cell-specific entrainment signals in pancreatic islets from healthy and diabetic donors

3. Post-transplant type 2 diabetes	33
4. Defining the role of molecular clocks in human parath	yroid gland physiology and
physiopathology	34
REFERENCES	37
ANNEXES	51
Publication 1	51
Publication 2	51
Publication 3	51
Publication 4	51
Publication 5	51

ACKNOWLEDGEMENTS

I warmly thank Professor Frederic Triponez for welcoming me to the Service of Thoracic and Endocrine Surgery, his generous support with all aspects the of my clinical and scientific activities, and for inspiring me with a passion to endocrine surgery.

I also warmly thank my mentor Professor Charna Dibner, who introduced me to the circadian field and guided me through the twists and turns of this exciting scientific journey, for our fruitful scientific interaction, her unfailing support, and beyond this for her friendship over many years.

I extend my deepest thanks to:

Pr. Petra Hüppi, and for her invaluable scientific support and friendship over the last fourteen years.

Pr. Jozsef Kiss who offered me the opportunity to join his research group in Geneva within the frame "From Cortex to Classroom" Consortium. His mentorship and support have left a lasting impact on my academic journey.

My colleagues in the Service of Thoracic and Endocrine surgery for invaluable clinical mentoring, generous transmission of their expertise, and for sharing daily work next to the bed of patients.

All my ex- colleagues in the Circadian Endocrinology laboratory for our productive scientific and personal interactions over these years, and particularly Flore Sinturel for her support and professional help.

Professor Lyudmyla Stechenko, who introduced me to basic research and Dr. Vasyl Dubyna who introduced me to surgery.

I want to express special thanks to my parents and my sister, who are always there with unfailing love and support.

SUMMARY

The body circadian system governs our physiology to anticipate daily changes in geophysical time. There is accumulating evidence attributing a critical role to the cell-autonomous oscillators operative in different metabolic organs in regulation of glucose homeostasis. This work proposes a functional link between the molecular clocks of the endocrine pancreas and the pancreatic islet gene transcription and hormone secretion under physiological conditions, and in the pathogenesis of type 2 diabetes (T2D) in humans and mouse models. We provide detailed characterisation of core-clock and clock-related genes in mouse and human glucagonproducing α-cells and insulin-producing β-cells. Our experiments demonstrate that clock disruption in human islet α - and β -cells impairs the accumulation and exocytosis of insulin and glucagon granules. Furthermore, we observed that circadian oscillators operative in the islets from donors suffering from T2D bear reduced circadian amplitude and compromised synchronization capacity in vitro. Noteworthy, the clock modulator Nobiletin partly restores the amplitude of circadian oscillations concomitant with secretion of insulin by these T2D islets. Moreover, we provide evidence on circadian regulation of lipid metabolism and membrane fluidity in human pancreatic islets that are perturbed upon T2D, highlighting that circadian orchestration of sphingolipid metabolites in human pancreatic islets contributes to regulation of insulin secretion and membrane fluidity. Finally, we report that β-cell regeneration in diabetic mice exhibits daily rhythms, with the core-clock protein BMAL1 playing essential role in this conjunction.

Within the frame of circadian endocrinology, new perspectives are discussed aimed at studying of inter-organ circadian desynchrony following solid organ transplantation and its role in development of T2D, as well as at characterisation of human parathyroid cell clocks and its role in function and dysfunction of the parathyroid glands.

INTRODUCTION

1. Circadian system as a molecular driver of rhythmic physiology

The time-keeping system, dubbed "circadian" from Latin *circa diem* (about a day), has been developed by most organisms as a fundamental adaptation mechanism driving periodical oscillations of behaviour and physiology in anticipation of geophysical time changes. In mammals, this system represents a network of oscillators assembled in hierarchical manner, with a central pacemaker located in the paired suprachiasmatic nuclei (SCN) of the hypothalamus, and peripheral oscillators in the organs composed of myriads individual cellular clocks (Dibner et al. 2010; Cox and Takahashi 2021).

In humans about 100'000 clock neurons are clustered in SCN (Hofman and Swaab 2006). Within the neuronal network, they generate circadian cycles of spontaneous firing rate virtually indefinitely *in vivo* and *in vitro*, with remarkable robustness, resilience, and precision (Colwell 2011; Hastings et al. 2018). Beyond this autonomous capacity to maintain circadian rhythmicity, the SCN integrates internal and external signals allowing to adjust the whole-body oscillations to the environmental needs. The environmental cues (*Zeitgebers*) entrain the central clock daily, with light-dark cycles representing the predominant *Zeitgeber*. As a consequence, neural and hormonal rhythms emanating from SCN, along with feeding, temperature, oxygen, and metabolite levels synchronize peripheral clocks across the body (Damiola et al. 2000; Mohawk et al. 2012; Manella et al. 2021).

Like SCN neurons, the peripheral circadian oscillators maintain their cell autonomy (Balsalobre et al. 1998). However, they seem to have weaker degree of coupling strength within the peripheral organs as compared to SCN, although it differs among the tissues (Finger et al. 2020). Hence, the circadian phase-coherence relay on the integrative function of central clock. The molecular architecture of the core mechanism responsible for driving autonomous circadian oscillations in both SCN neurons and in the peripheral tissues relies on transcription-translation (TTFL) feedback loop of core-clock genes (summarized in Fig. 1). The discovery of this fundamentally conserved mechanism in a fruit fly *Drosophila melanogaster* has been awarded by the 2017 Nobel Prize in Physiology or Medicine to Jeffrey C. Hall, Michael Rosbash and Michael W. Young. The two central components of the molecular clock are the transcription factors Circadian Locomoter Output Cycles Kaput Protein (CLOCK) and Brain and Muscle Aryl hydrocarbon receptor nuclear translocator-like 1 (BMAL1), which form a heterodimeric complex triggering the rhythmic expression of their inhibitors within two

principal feedback loops within clock machinery. In the primary feedback loop, they activate the transcription of the Period (Per) and Cryptochrome (Cry) genes, encoding for the corepressor proteins PER1, PER2, CRY1 and CRY2 (Lowrey and Takahashi 2000). Once in sufficient concentrations, the PER and CRY transcriptional factors heterodimerize and inhibit the CLOCK-BMAL1 complex activity (Schmalen et al. 2014; Aryal et al. 2017). The subsequent reduction of CLOCK-BMAL1 activators leads to decreased levels of PER and CRY proteins due to their constant proteasomal degradation in the cytoplasm, until they can no longer prevent their own transcription. This evokes the beginning of a new cycle of PER and CRY protein accumulation, lasting around 24 hours. In a secondary feedback loop, the CLOCK-BMAL1 complex controls the rhythmic expression of the genes encoding for the nuclear hormone receptors REV-ERBs (REV-ERBα and REV-ERBβ), RORα, RORγ, and RORβ in neurons (Preitner et al. 2002). In turn, REV-ERBα and RORα compete for the same ROR DNA-binding elements (RORE) within the *Clock* and *Bmal1* promoter regions, resulting in the repression or activation respectively of the Clock and Bmall transcription (Fig. 1). Noteworthy, post-translational modifications of the core clock proteins, such as phosphorylation, acetylation, O-GlcNAcylation, chromatin modification, ubiquitination/degradation and more, provide an additional level of regulation of the molecular clockwork (Hirano et al. 2016). Indeed, PER and CRY stability is controlled by the casein kinase $1\varepsilon/\delta$ (CK1 ε/δ) that mediates phosphorylation of PER and CRY proteins, triggering polyubiquitination by E3 ubiquitin ligase complexes that promotes proteasomal degradation of the proteins. Importantly, activity of CLOCK-BMAL1 complex is a major driver the rhythmic expression of "clock-controlled genes" outside the clock machinery coupling autonomous circadian oscillations with cell functionality.

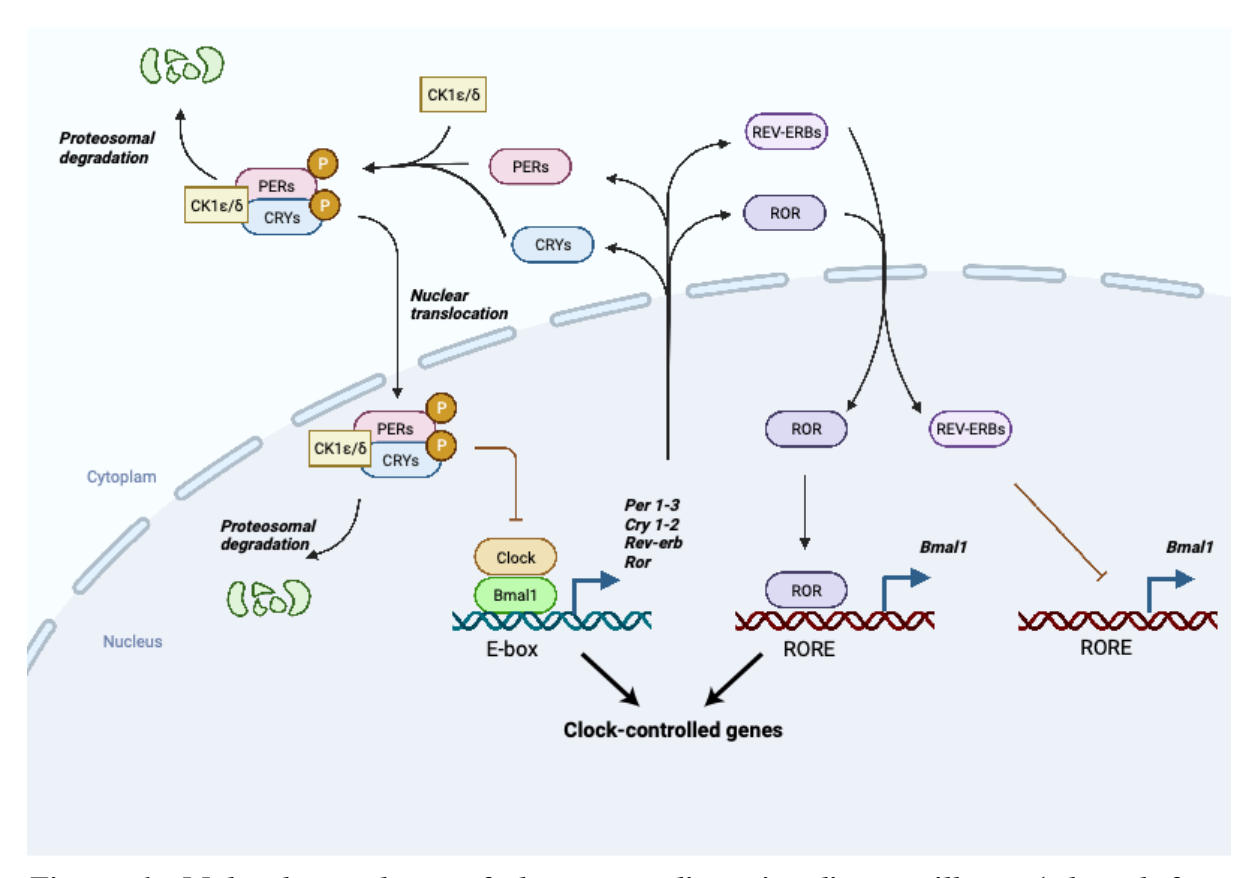


Figure 1. Molecular makeup of the mammalian circadian oscillator (adopted from (Petrenko et al. 2023)). The mammalian clock is composed of interconnected transcription-translation feedback loops. CLOCK-BMAL1 complex binds to E-box domains on gene promoters, including the genes Per1/2/3 and Cry1/2. PERs and CRYs assemble and repress their own transcription. The main loop is stabilized by the auxiliary loop consisting of REV-ERBa/β and RORa/β/γ. The ROR proteins compete with the REV-ERBs proteins for binding to RORE elements on the Bmal1 gene promoter, providing both positive (ROR) and negative (REV-ERB) regulation of Bmal1 and Clock transcription. At a post-transcriptional level, the stability of the PER and CRY proteins is regulated by kinases (casein kinase 1ε/δ (CK1ε/δ) and AMP kinase (AMPK)). The phosphorylation of the PER and CRY proteins promote polyubiquitination by E3 ubiquitin ligase complexes, which in turn tag the PER and CRY proteins for degradation by the proteasome. Additionally, core clock proteins regulate the expression of hundreds of genes outside of the circadian feedback loop (clock-controlled genes). These downstream targets are involved in a wide range of physiological processes.

2. Time dimension of body metabolism

Discovery of circadian system introduced time as an additional important dimension for the studies of mammalian physiology. The major role of the circadian clock is to enable the temporal coordination of key metabolic processes with the geophysical time, in anticipation of rest–activity and feeding–fasting behaviour. Accumulating data highlight tight interactions between molecular clock and variety of metabolic pathways, comprising those involved in glucose, lipid and immunometabolism that play an important role in the pathogenesis of T2D. Besides, the large-scale metabolomic analyses in different tissues suggest that the metabolism of nucleotides and amino acids follows daily rhythmicity (Dyar et al. 2018a; Dyar et al. 2018b). Indeed, the metabolism of purines and pyrimidines bears circadian pattern in mouse liver, and is perturbed in livers of Bmal1-deficient mice (Fustin et al. 2012). Our recent study revealed a direct link between regulatory subunit Vsp15 of class 3 phosphotidylinositol-3-kinases (PI3K) and molecular clockwork in regulation of rhythmic *de novo* purine nucleotides synthesis in liver, suggesting a complex interplay between class 3 PI3K and purine metabolism (Alkhoury et al. 2023).

This chapter summarizes the current knowledge on circadian regulation of glucose and lipid homeostasis, as well as its roles in immunometabolism.

2.1. Circadian orchestration of glucose metabolism

Maintaining blood glucose levels within a narrow range is a fundamental task of the organism, ensuring the constant cell accessibility to the principal energy source. The circadian feeding-fasting behaviour imposes high variations in glucose availability across 24-h, representing a major challenge in the regulation of body metabolism. Accumulating data suggest that both central and peripheral circadian components of timekeeping system play an important role in orchestration of glucose homeostasis. Indeed, blood glucose levels exhibit circadian rhythm in rodents and in humans, not necessarily related to feeding rhythms (Carroll and Nestel 1973; Yamamoto et al. 1987; La Fleur et al. 1999). Moreover, stimulation of SCN causes hyperglycaemia via adrenergic mechanism (Nagai et al. 1988; Fujii et al. 1989), whilst SCN lesion results in enhancement of glucose tolerance due to reduced insulin sensitivity rather than to daily oscillations of insulin concentrations (Yamamoto et al. 1987; La Fleur et al. 1999; la Fleur et al. 2001a). This phenotype relays on humoral and neuronal signals emanating from SCN via sympathetic innervation of the liver (Kalsbeek et al. 2004), and the nocturnal hormone

melatonin, depletion of which following pinealectomy attenuates circadian rhythmicity of glucose concentration (la Fleur et al. 2001b). Interestingly, recent studies in mice evoke the existence of an additional SCN-independent pathway, which may participate in light entrainment of rhythmic clock gene expression and insulin sensitivity in skeletal muscle via SIRT1 in steroidogenic factor 1 neurons of the ventromedial hypothalamic nucleus (Aras et al. 2019). The development of genetic models of clock-deficient mouse lines allowed for deciphering the roles of molecular clocks in glucose homeostasis. Indeed, most of the clockcompromised models exhibit hyperglycemia, hyperinsulinemia, impaired insulin sensitivity, and enhanced glucose tolerance (Rudic et al. 2004; Turek et al. 2005; Le Martelot et al. 2009; Marcheva et al. 2010; Zhang et al. 2010). Noteworthy, this phenotype was even more pronounced when the clock has been specifically ablated in pancreatic islets of PdxCreBmal1^{flx/flx} mice, suggesting an important role of islet-autonomous clock in regulation of glucose metabolism (Marcheva et al. 2010; Sadacca et al. 2011; Perelis et al. 2015). The discovery of autonomous functional molecular clocks operative in human islets by the Dibner group (Pulimeno et al. 2013) was the starting point for the presented here scientific publications aimed to dissect the role of molecular clock for insulin and glucagon secretion in human in physiological condition, as well as in T2D.

While the endocrine pancreas is the principal peripheral glucose-sensor and regulator of constant glucose concentration via coordinated insulin and glucagon secretion, liver, skeletal muscle, and adipose tissues represent the major sites of glucose utilization in response to insulin. Strikingly, the skeletal-muscle specific Bmall KO mice develop hyperglycemia and glucose intolerance (Harfmann et al. 2016), while the liver-specific Bmall KO mice develop fasting hypoglycemia and enhanced glucose-tolerance (Lamia et al. 2008). Furthermore, the removal of functional Bmall specifically from adipocytes (*Ad-Arntl*-/- mouse model) results in daily variations of hyperglycemia in the absence of visible changes in insulin secretion and normal plasma glucose response, which was associated with obesity. Such tissue-specific effect of core-clock component BMAL1 disruption on glucose metabolism may stem from tissue specificity of BMAL1-CLOCK binding to different regulatory sequences in these organs, as it was shown for the pancreatic islets and liver (Perelis et al. 2015).

2.2. Lipids around-the-clock

In addition to defects in glucose metabolism, majority of T2D patients develop dyslipidaemia, which is characterized by elevated triglycerides, low HDL cholesterol and increased LDL

particles in the blood (Mooradian 2009). From this perspective, the interplay between circadian system and lipid metabolism in physiological condition and under T2D pathology is of outmost interest. There is increasing evidence that molecular clocks coordinate temporal organization of different aspects of the lipid metabolism, including lipid digestion and absorption in the intestine, transportation, intracellular lipid metabolism, and accumulation. Data stemming from various whole-body clock mutant mouse models suggest that disruption of circadian rhythmicity is associated with dyslipidaemia, steatohepatitis, and obesity (Rudic et al. 2004; Turek et al. 2005; Shimba et al. 2011). At the same time, the whole-body deletion of the core clock component RORα or Cryl protected against diet-induced obesity (Lau et al. 2008; Griebel et al. 2014). Recently, a regulatory link has been established between molecular clocks, hypoxia response, fatty acid uptake, and the development of non-alcoholic fatty liver disease (NAFLD) (Pan et al. 2020). In *Clock* mutant ($Clk\Delta 19/\Delta 19$) animals this phenotype is associated with increased fatty acid uptake via enhanced levels of hypoxia-inducible factor 1α (HIF1α) protein. Moreover, recent studies in CLOCK KO mice revealed altered temporal expression of adipogenesis and proliferation markers in white adipose tissue (Ribas-Latre et al. 2021). Concordantly, loss of function of nuclear receptors REV-ERBa and REV-ERBB from auxiliary loop of clock machinery results in perturbation of lipid metabolism, including defects of lipogenesis in white adipose tissue, a marked accumulation of triacylglycerides in the liver, and development of severe hepatic steatosis (Bugge et al. 2012; Cho et al. 2012; Zhang et al. 2015). During adipogenesis, two core-clock components, BMAL1 and PER3, were shown to play a crucial role in regulating of adipocytes development from precursor cells via direct control of the pro-adipogenic gene Kruppel-Like factor 15 (Klf15) (Aggarwal et al. 2017). Finally, studies in tissue-specific models of clock disruption further dissected the differential role of peripheral clocks on lipid metabolism in these tissues. Thus, mice lacking functional Bmall specifically in adipocytes exhibit increased adipose tissue mass and develop obesity, primarily because of greater food consumption during the rest phase (daytime for mice), as compared to wild-type counterparts (Paschos et al. 2012). In contrast, intestine-specific deletion of *Bmal1* limited dietary fat absorption and protected mice from diet-induced obesity and hyperlipidemia developments (Yu et al. 2021). Surprisingly, adipocyte-specific deletion of $Rev-erb\alpha$ did not result in any detected perturbation of lipid synthesis and storage programs (Hunter et al. 2021).

Lipids do not only represent important source of energy and signalling molecules, but also essential structural components of plasma and organelle membranes. Recent lipidomic studies

revealed that nuclear and mitochondrial lipids oscillate "around-the-clock" in mouse and humans (Aviram et al. 2016; Loizides-Mangold et al. 2017). However, the functional impact of these oscillations on membrane physiology of these subcellular structures stays largely unexplored.

Taken together, these studies demonstrate that functional molecular circadian clocks are necessary for proper lipid metabolic function across tissues. The interplay between molecular clocks and different molecular processes related to the lipid metabolism is highlighted in detail in (Petrenko et al. 2023).

2.3. Circadian regulation of immunometabolism

The function of immune system is tightly coupled to the body metabolism, representing a subject of the emerging research field of immunometabolism. Molecular clocks have been characterized in different immune cell types and diurnal rhythms of multiple aspects of innate immunity have been recognized (Scheiermann et al. 2013; Cox et al. 2022). Growing body of evidence suggests that alterations of multiple components of immune system contribute to the pathogenesis of T2D (Donath and Shoelson 2011). Indeed, accumulation of islet-associated macrophages has been detected in human T2D islets, as well as in rodent models of diabetes (Ehses et al. 2007; Jourdan et al. 2013; Ying et al. 2019). However, the role of molecular oscillators in such accumulation stays obscure. Recent studies from the Scheierman's group suggest that the draining of antigen-presenting cells from tissues (Holtkamp et al. 2021) and their homing into the lymph nodes (Ince et al. 2023) exhibit daily oscillations. Furthermore, molecular systemic and paracrine immune components may affect metabolism via molecular clock. We and others have recently shown that pro-inflammatory cytokines (specifically, IL-β and interferon-gamma), may contribute to pathogenesis and progression of T2D by affecting the pancreatic islet clockwork and function via complex modulation of nitric oxide synthesis, the lysine deacetylase HDAC3, and immunoproteasome activity (Andersen et al. 2020; Javeed et al. 2020). In addition, IL-1ß stimulates postprandial insulin secretion via modulating vagal neuronal transmission upon cephalic stimulation (Wiedemann et al. 2022). Earlier clinical studies in humans showed that a elevation of IL-1β and IL6 independently increases the risk of T2D (Pradhan et al. 2001; Spranger et al. 2003). Moreover, the blockade of interleukin-1 with Anakinra improves glycemia and β-cell secretory function and reduces markers of systemic inflammation in T2D patients (Larsen et al. 2007). Collectively, these data bring circadian regulation into the interplay between immune system and metabolism, and its perturbation upon T2D pathology.

3. Circadian misalignment and metabolic disorders

Modern 24/7 society evokes the risk of circadian misalignment, or desynchrony between intrinsic body clockwork and external cues. The most common types of circadian misalignments are the discordance between intrinsic sleep-wake cycle and the time of the day; misalignment between feeding rhythms and the intrinsic sleep-wake cycle; and internal desynchrony between central and peripheral clocks. The common causes of such desynchronies in modern society are shift-work schedules that require people work during biological night; travel across between different time-zones (jet lag); and social extension of the daily activities as well as access to the electric light that may delay the timing of central circadian clocks (social jet lag). Numerous epidemiological studies report correlation between circadian disruption and human pathologies comprising cardiometabolic diseases and cancer (Fig. 2) (Innominato et al. 2014; Chellappa et al. 2019; Mukherji et al. 2019; Dibner 2020). Observational studies suggest that individuals with late chronotype exhibit increased risk of developing T2D and metabolic disorders (Merikanto et al. 2013; Yu et al. 2015), with T2D late-chronotype patients exhibiting poorer glycaemic control (Reutrakul et al. 2013; Osonoi et al. 2014; Vetter et al. 2015; Koopman et al. 2017). In line, shift workers exhibit higher risk of developing T2D, showing positive correlation with the number of night shifts per month (Gan et al. 2015; Vetter et al. 2018).

Well-controlled laboratory human studies reinforced this link between circadian misalignment and glucose metabolism. Thus, imposing of chronic sleep deprivation to healthy human individuals lowers glucose tolerance compared participants who slept 8h per night (Wilms et al. 2019), and reduces insulin sensitivity (Buxton et al. 2010; Donga et al. 2010; van Leeuwen et al. 2010; Eckel et al. 2015; Cedernaes et al. 2016). Similarly, healthy volunteers subjected to experimental circadian misalignment develop impaired glucose tolerance (Scheer et al. 2009; Leproult et al. 2014; Morris et al. 2015; Qian et al. 2018; Wefers et al. 2018).

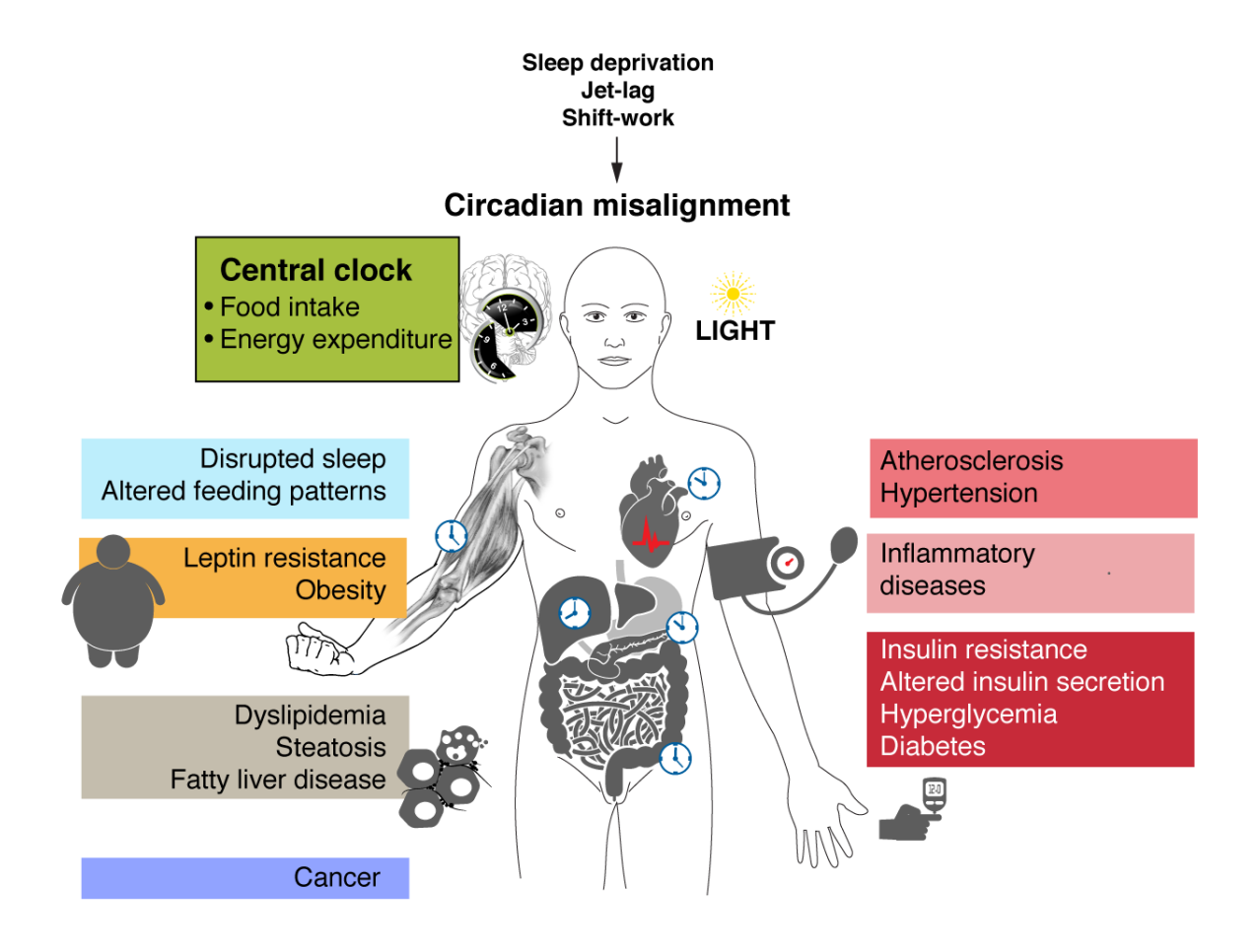


Figure 2. Human pathologies associated with circadian disruption (adopted from (Sinturel et al. 2020b))

Persistent sleep deprivation, shift work, altered eating patterns, and social jetlag are the leading causes of misalignment of the internal circadian system from the external cues. Chronic circadian misalignment is associated with the development of cardiovascular, inflammatory, and metabolic disorders such as obesity, fatty liver disease, and type 2 diabetes, along with the increased risk of cancer.

The connection between circadian misalignments and metabolic disorders may stem from the behaviour modifications. Indeed, about 95% of the circulating metabolites with a 24-h rhythmicity are driven by behavioural time rather than by the central clock (Depner et al. 2018; Skene et al. 2018). Moreover, meal timing not only modifies the plasma lipid profiles (Kessler and Pivovarova-Ramich 2019), but also impacts on the effectiveness of weight loss in obese volunteers (Garaulet et al. 2013). In line, night-shift workers consume 12-16% less calories when we sleep during daytime than when sleep occurs at night that could partially explain their weight gain (McHill et al. 2014). Interestingly, the metabolic dysregulation during the repeated

pattern of insufficient sleep cannot be compensated by *ad libitum* weekend recovery sleep (Depner et al. 2019). It was established that late eating behaviour leads to metabolic dysfunction while daytime eating protects subjects from glucose intolerance and abnormal energy expenditure (LeCheminant et al. 2013; Bandin et al. 2015; Wehrens et al. 2017). The fact that the same meal in the morning and in the evening has different postprandial consequences on the blood glucose levels and insulin secretion could be due to the direct effect of the feeding on the metabolic organ clocks (Sato et al. 2014), possibly through the nutrient-derived metabolites. On the other hand, recent studies in mice established that misalignment of feeding time with intrinsic circadian cycles of creatine-mediated adipose thermogenesis contributes to metabolic syndrome in the setting of overnutrition, suggesting a primary role of adipocyte clock in diet-induced thermogenesis (Hepler et al. 2022).

4. Pathogenesis of type 2 diabetes on 24 h-scale

According to World Health Organisation, diabetes mellitus is a chronic metabolic disorder characterized by elevated blood glucose levels which lead over the time to serious damages to the vital organs, including cardiovascular system, nervous system, eyes, kidneys. It can be classified into the following general categories (American Diabetes 2020): 1) type 1 diabetes (T1D, due to autoimmune β -cell destruction, usually leading to absolute insulin deficiency); 2) T2D, due to a progressive loss of β-cell insulin secretion frequently on the background of insulin resistance; 3) gestational diabetes mellitus (diabetes diagnosed in the second or third trimester of pregnancy that was not clearly overt diabetes prior to gestation); and 4) specific types of diabetes (monogenic diabetes syndromes, diseases of exocrine pancreas, drug-induced diabetes and others). T2D exhibits an alarming epidemiological trend not only in adults but also in children and young adults, currently accounting for nearly 90% of the approximately 537 million cases of diabetes worldwide (Ahmad et al. 2022). Although the exact etiology of T2D is not defined, a combination of multiple pathophysiological factors, comprising inflammation, islet cell dysfunction, increased insulin resistance in metabolic tissues, as well as kidney, and gastrointestinal tract dysfunctions, has been attributed to the progression of the disease (Skyler et al. 2017; Ahmad et al. 2022). In addition, the extensive research in humans (described in chapter 3) suggests that chronic circadian misalignment contributes to the development of metabolic diseases, including T2D (Maury et al. 2014; Kumar Jha et al. 2015; Saini et al. 2015; Bass 2017; Javeed and Matveyenko 2018; Wefers et al. 2018; Gao et al. 2020; Hemmer et al. 2021), although the molecular mechanism underlying this conjunction stays largely unexplored.

Importantly, T2D may be not unique nosology, but comprise different entities with regards to etiology and pathogenesis. Indeed, recent clinical study in T2D patients distinguished 5 subtypes of T2D in Scandinavian population by applying data-drive cluster analysis, attributing different disease progression and risk of diabetes complications to distinct subtypes (Ahlqvist et al. 2018).

Combination of β -cell disfunction and insulin resistance in metabolic tissues are currently recognized as two major pathogenic factors contributing to the development of T2D. Both these processes show hyperbolic relationship over the T2D time course: when insulin sensitivity is high, large changes in insulin sensitivity produce relatively small changes in insulin levels and responses, whereas when insulin sensitivity is low, small changes in insulin sensitivity produce relatively large changes in insulin levels and responses (Kahn et al. 1993; Weir et al. 2020).

4.1. Insulin resistance

Insulin resistance is defined as a defect in insulin-mediated regulation of glucose metabolism in metabolic tissues, mainly in muscle, fat, and liver. It leads to the significant reduction in postprandial glucose clearance primarily by skeletal muscles and adipose tissue, as well as altered insulin suppression of hepatic glucose output resulting in enhanced gluconeogenesis. The mechanism of insulin resistance is not fully understood (James et al. 2021). It comprises a combination of factors, including intracellular insulin signalling, defective intracellular GLUT 4 trafficking, reduced glycogen accumulation, decreased oxidation of glucose, and altered activity of mitochondria (Muoio and Newgard 2008; James et al. 2021). In addition, recent studies evoke a role of impaired glucose-regulated microcirculation of skeletal muscle as a pathogenic mechanism involved in the development of the myocyte or whole-body insulin resistance in vivo (Carmichael et al. 2022).

The core insulin signalling pathway may be divided on proximal components comprising the insulin receptor, insulin receptor substrate, phosphoinositide 3/kinase, AKT; and on its downstream components: Rab GTPase-regulating protein TBC1D4, glycogen synthase-3 (GSK3) and phosphodiesterase 3 (PDE3B). Impaired AKT activation is the key element in metabolic perturbations involving insulin resistance and is modulated by deacetylase SIRT1 (Liang et al. 2009; Zhou et al. 2018). Importantly, SIRT1 also regulates circadian clock gene expression via deacetylation of Per2 (Asher et al. 2008), providing a molecular link between insulin signalling and molecular clockwork. Indeed, recent studies directly show that insulin resets clock gene expression vin metabolic tissues via intracellular insulin signalling (Crosby et al. 2019; Tuvia et al. 2021). Hence, impaired insulin signalling in T2D may participate in

disruption of intracellular circadian oscillators. In turn, alteration of molecular clockwork in human myotubes by siRNA against *CLOCK* induces insulin resistance, negatively regulating genes involved in insulin signalling pathway and in GLUT4 trafficking (Perrin et al. 2018). Furthermore, defects in skeletal muscle glycogen accumulation also play a role in development of insulin resistance upon T2D (Shulman et al. 1990). Interestingly, the experiments on Neurospora Crassa suggest that glycogen synthase is under control of core-clock machinery (Baek et al. 2019). Concordantly, rodent studies shows that CLOCK regulates glycogen synthase 2 (Gys2), a rate-limiting enzyme in liver glycogen synthesis (Doi et al. 2010). Finally, mitochondrial dysfunction in T2D skeletal muscles, characterized by morphological and metabolic abnormalities, is recognized as a pivotal mechanism in progression of insulin resistance (Kelley et al. 2002; Finck et al. 2005; Koves et al. 2005; Koves et al. 2008). Recent

Together, these data highlight an intimate interplay between different elements involved in the development of insulin resistance and molecular clock suggesting molecular clock as an important element in the progression of T2D.

studies revealed bidirectional communication between mitochondrial dysfunction and

molecular clock perturbation in myotubes derived from T2D patients (Gabriel et al. 2021).

However, the exact mechanism underlying this link stays unexplored.

4.2. Beta-cell dysfunction

Beta cell failure manifests as an impaired glucose-stimulated insulin secretion leading to the β -cell secretory dysfunction and loss of β -cell mass due to increased apoptosis and dedifferentiation (Butler et al. 2003; Talchai et al. 2012; Kahn et al. 2014). The mechanism of these changes is largely unexplored. It has been attributed to activation of oxidative and endoplasmic reticulum (ER) stress due to permanent exposure of β cells to toxic factors such as hyperglycemia, hyperlipidemia, and islet amyloid peptide oligomers (Haataja et al. 2008; Poitout and Robertson 2008; Scheuner and Kaufman 2008). Accumulating evidence suggest the role of molecular clocks in intracellular perturbations leading to β -cell loss. Indeed, it was recently proposed that loss of core clock component Bmal1 enhances the NADPH oxidase-mediated generation of reactive oxygen species in β -cells (de Jesus et al. 2022). In line, the imposed disruption of circadian rhythms in rodent model accelerates development of diabetes through pancreatic β -cell dysfunction and apoptosis (Gale et al. 2011). The changes might be reciprocal, since it was shown that ER stress may modify the expression of core-clock genes in NIH3T3 cells via an ATF4-dependent mechanism (Gao et al. 2019).

Beyond β -cell dysfunction, the deregulation within diabetic islet involves an impaired glucagon secretion, although the mechanism of α -cell dysfunction is not well understood. It has been attributed to an increase in α -cell numbers and alterations of their function in diabetes (Meier et al. 2006; Schrader et al. 2009), supporting a bihormonal-abnormality hypothesis as a part of T2D pathogenesis (Unger and Orci 1975).

RESULTS AND PUBLICATIONS

1. Time zones of pancreatic islet: studying the molecular clocks in α - and β -cells in genetic mouse models, in physiology and diabetes

Pancreatic islets harbour endocrine cells with different physiological functions, among which α - and β -cells represent two predominant populations, secreting the counterregulatory hormones glucagon and insulin, respectively. While previous studies in the field were referring to pancreatic islet as a whole, we aimed to zoom into the α - and β - islet cell-specific molecular clocks, in order to dissect their interplay and functional roles in physiological context and in diabetic conditions. To study circadian properties of α - and β -cells in parallel, we generated a triple-reporter mouse line encompassing proglucagon (Gcg)-Venus reporter (Reimann et al. 2008) allowing for specific labelling of α cells, rat insulin2 promoter (RIP)-Cherry reporter labelling of β cells (Zhu et al. 2015), and the Period2::Luciferase (Per2::Luc) knock-in reporter (Yoo et al. 2004) allowing for continuous monitoring of molecular clockwork at population and single-cell levels.

The following two publications focus on the molecular characterization of the α - and β -cellular clocks, their interactions, and impact on daily orchestration of gene transcription and islet hormone secretion under physiological conditions, and following massive β -cell loss, which represent a common element in the development of T1D and T2D.

1.1. Pancreatic α - and β -cells bear the clocks that drive rhythmic secretion of glucagon and insulin in physiological context (PUBLICATION 1)

This work reports the first analysis of the molecular properties of circadian clocks operative in α - and β -cells conducted in parallel in mouse primary islet cells. It provides novel insights into the complex regulation of the islet cell temporal physiology at the transcriptional and functional levels. Employing advanced reporter mouse model, we assessed the α -cell and β -cell-specific clock entrainment properties, along with daily landscape of the islet cell transcriptome and hormone secretion *in vivo* and *in vitro*, at the islet cell population and single-cell levels. Diurnal transcriptome analyses in separated α - and β -cells revealed thousands of functional genes playing the key roles in the islet physiology including regulators of glucose sensing and hormone secretion, follow diurnal rhythmicity in the islet cells. Interestingly, the phase of key core clock components was shifted between α -cell and β -cell clocks in vivo. Indeed, the expression pattern of Bmall, Rev-erb α and Cry1, exhibited distinct rhythmic properties in α -

and β -cells, with the β -cell core-clock genes being phase- advanced compared to their α -cell counterparts. Population and single-cell analyses of isolated α - and β -cells synchronized in vitro by forskolin confirmed that islet cellular clocks bear circadian oscillators with distinct molecular properties. The observed phase shift between α - and β -cellular clocks may account for the temporal separation of insulin and glucagon secretion profiles, exhibiting oscillatory profiles in vivo in the blood and in vitro as recorded by cell perifusion.

Altogether, our data indicate that differential entrainment characteristics of circadian α -cell and β -cell clocks are an important feature in the temporal coordination of endocrine function and gene expression. We propose that, along with feeding–fasting cycles, the described distinct properties of α -cellular and β -cellular clocks might contribute to orchestrating temporal secretion patterns of glucagon and insulin.

PUBLICATION 1. Pancreatic α - and β -cellular clocks have distinct molecular properties and impact on islet hormone secretion and gene expression.

1.2. Roles of the islet cellular clocks in diabetes context and in β -cell regeneration (PUBLICATION 2)

Rodent studies suggest that β -cells have a limited potential for regeneration. Core-clock components may play a role in regulating β -cell division. Unraveling mechanisms of circadian regulation of β -cell regeneration is of a fundamental clinical importance in the search of new therapeutic approaches for management of *diabetes mellitus*.

In this study, we induced massive β -cell ablation to identify mechanisms participating in the regulation of islet cell regeneration and to characterize the transcriptional landscape in separated α - and residual β -cells. To this end, we utilized a well-established mouse model of doxycycline-induced expression of diphtheria toxin A (DTA) in Insulin-rtTA/TET-DTA mice (Nir et al. 2007). Since we crossed reporter genes expressing α - and β -cell- specific fluorescent proteins into these mice, we could follow the fate of α - and β cells separately. As expected, DTA induction resulted in an acute hyperglycemia, which was accompanied by dramatic changes in gene expression in residual β cells as assessed by RNA-sequencing. In contrast, only temporal alterations of gene expression were observed in α -cells. Our results provide evidence that proliferation of residual β -cells triggered by massive ablation follows a circadian pattern. Virtually no compensatory β -cell regeneration occurred in arrhythmic mice lacking Bmal1 (Bmal1^{st/st}) that may suggest a role of the functional oscillators in coordinating β -cell division. Importantly, massive β -cell ablation led to a fatal non-compensated diabetes in the absence of the core clock transcription factor BMAL1.

In summary, our data strongly suggest that regeneration of β cells is tightly coupled to diurnal rhythm. Moreover, loss of functional clocks aggravates the development of diabetic phenotype in mice.

PUBLICATION 2. The core clock transcription factor BMAL1 drives circadian β -cell proliferation during compensatory regeneration of the endocrine pancreas.

2. Translating the clocks studies in diabetes from genetic mouse models to humans

The existence of cell-autonomous, self-sustained circadian oscillators, operative in human pancreatic islets, has been first described in our laboratory (Pulimeno et al. 2013). Despite accumulating evidence on the role of the molecular clock in the regulation of insulin secretion and glucose homeostasis in rodents (as highlighted in introduction), the molecular link between the human islet clockwork and insulin secretion in physiological condition and upon T2D stays largly unexplored. In the serie of presented here publications we explored the role of circadian oscillator for regulation of insulin secretion by disrupting functionnal clock in non-diabetic islets from one hand and characterized specific changes in molecular clockwork of pancreatic islet cells derived from T2D donors – from another. Taken together, these works provide novel evidence on the role of islet-autonomous clocks in pathogenesis of T2D in humans.

2.1. Functional clocks operative in human pancreatic islet cells are indispensable for proper insulin secretion (PUBLUCATION 3)

In this study we aimed to explore the physiological relevance of islet-authonomous molecular clock for regulating insulin secretion and its impact on islet cell transcriptome. We used small interfering RNA-mediated knockdown of CLOCK to efficiently disrupt circadian clockwork in non-diabetic human pancreatic islet cells. Human islet secretory function was assessed in the presence or absence of a functional circadian clock by stimulated insulin secretion assays, and by continuous around-the-clock monitoring of basal insulin secretion. We demonstrated time that basal insulin secretion by human islet cells synchronized in vitro exhibits a circadian rhythmic pattern, which was perturbed upon clock disruption. Moreover, circadian clock disruption results in significant attenuation of glucose-stimulated insulin secretion. Large-scale transcriptome analysis by RNA sequencing revealed alterations in 352 transcript levels upon circadian clock disruption. Among them, key regulators of the insulin secretion pathway (GNAQ, ATP1A1, ATP5G2, KCNJ11) and transcripts required for granule maturation and release (VAMP3, STX6, SLC30A8) were affected.

These data show for the first time that a functional β -cell clock is required for proper basal and stimulated insulin secretion. Moreover, clock disruption has a profound impact on the human

islet transcriptome, in particular, on the genes involved in insulin secretion at the levels of granular maturation, membrane fusion and intracellular signal transduction in human islet cells.

PUBLICATION 3. A functional circadian clock is required for proper insulin secretion by human pancreatic islet cells.

2.2. Circadian clockwork is compromised in human pancreatic islet cells upon type 2 diabetes (PUBLICATION 4)

In this study, we examine whether compromised clocks play a role in the pathogenesis of T2D in humans. We assessed human islet clockwork by introducing two antiphasic circadian reporters, Bmall-Luciferase or Per2-Luciferase, allowing for continuous bioluminescence monitoring in human primary cells following in vitro synchronization (Pulimeno et al. 2013). We quantified parameters of molecular clocks operative in human T2D islets at population, single islet, and single islet cell levels. Strikingly, our experiments reveal that islets from T2D patients contain clocks with diminished circadian amplitudes and reduced in vitro synchronization capacity compared to their nondiabetic counterparts.

Complementary to our previous study (Saini et al. 2016), here we uncover the temporal coordination of insulin, proinsulin, and glucagon secretion profiles by the circadian oscillators, operative in human pancreatic islet cells. We establish that such temporal coordination is exerted via an exocytosis process, since our experiments reveal that functional islet clocks are indispensable for proper secretory granule docking and exocytosis of insulin and glucagon. Moreover, temporal coordination of the islet hormone secretion was perturbed in human T2D islets, concomitant with the islet molecular clock alterations, implying a role for the islet cell-autonomous clocks in T2D progression. Treating the T2D islets with the clock modulator Nobiletin, an agonist of the core-clock proteins $ROR\alpha/\gamma$, boosted circadian amplitude and insulin secretion by these islets.

This study uncovers a link between human molecular clockwork and T2D, thus considering clock modulators as putative pharmacological intervention to combat this disorder.

PUBLICATION 4. In pancreatic islets from type 2 diabetes patients, the dampened circadian oscillators lead to reduced insulin and glucagon exocytosis.

2.3. Circadian timing of human pancreatic islet lipid metabolism in physiology and type 2 diabetes (PUBLICATION 5)

Dysregulation of lipid metabolism plays a key role in pathophysiology of metabolic diseases (as highlighted in the introduction section). Although the roles of lipid metabolites in β -cell function and dysfunction upon T2D development have been raised in several studies (Boslem et al. 2011; MacDonald et al. 2015; Sanchez-Archidona et al. 2021), no data on human islet lipidomics and its regulation by the circadian system have been provided so far.

In this study we assessed circadian regulation of lipid homeostasis in human pancreatic islets under physiological conditions and in T2D by employing large-scale mass spectrometry-based shotgun lipidomics allows quantification of that for over 1'000 phospholipids, sphingolipids, and triacylglycerides with high accuracy (Loizides-Mangold et al. 2021). Among 329 detected lipid species across 8 major lipid classes, 5% exhibited circadian rhythmicity in non-diabetic human islets synchronized in vitro. Two-time point-based lipidomic analyses in T2D human islets revealed global and temporal alterations in phospho- and sphingolipids. Concomitant with the oscillating patterns of lipid species, we describe rhythmic expression of the genes encoding for the key enzymes regulating turnover of sphingolipids in non-diabetic islets. This rhythmicity was perturbed in the islets bearing si-Clock mediated clock disruption, and in those derived from T2D donors. Strikingly, T2D human islet cells exhibit reduced cellular membrane fluidity, as measured by a Nile Red derivative NR12S. This phenotype was reproduced in ND donors' islets with disrupted circadian clockwork or those treated with sphingolipid pathway modulators. Moreover, inhibiting the glycosphingolipid biosynthesis led to strong reduction of insulin secretion triggered by glucose or KCl, whereas inhibiting earlier steps of de novo ceramide synthesis resulted in milder inhibitory effect on insulin secretion by ND islets. Finally, our data suggest a reciprocal connection between the islet circadian clocks and ceramide metabolism, since the treatment of in vitro synchronized non-diabetic human islets with ceramide turnover inhibitors myriocin and PDMP alter circadian oscillations of Per2-lucioferase reporter.

Altogether, in this work we provide a novel link between disruption of circadian clock, temporal coordination of lipid metabolism in human pancreatic islet, and islet dysfunction upon T2D in humans, highlighting both molecular oscillator and sphingolipid metabolites as important regulators of insulin secretion and membrane fluidity.

PUBLICATION 5. Circadian orchestration of lipid metabolism and membrane fluidity in human pancreatic islets are disrupted upon type 2 diabetes.

CONCLUSIONS AND PERSPECTIVES

1. Circadian clocks take a part in the pathogenesis of type 2 diabetes

In humans, studies on peripheral clocks in organs and isolated cells still represent the only way to dissect the role of molecular clocks in physiological and pathophysiological conditions. This is particularly the case for studying the pancreatic islets because of the difficult access to these structures in human. We report that the islets derived from T2D patients contain compromised molecular clocks with diminished circadian amplitudes and reduced in vitro synchronization capacity compared to their nondiabetic counterparts. These observations in combination with our experimental data suggest the role of islet-autonomous circadian oscillator in β -cell dysfunction upon T2D via deregulation of islet hormone exocytosis, perturbation of islet lipid metabolism and membrane fluidity, circadian uncoupling between endocrine cells within pancreatic islets, defective synchronization response of islet cells to the physiologically relevant signals, and disruption of compensatory β -cells regeneration.

1.1. Disruption of circadian clocks in the pancreatic islets of type 2 diabetic patients

In order to study whether modifications of the clock participate in the pathogenesis of T2D in humans, we assessed key parameters of molecular clockwork in the pancreatic islets derived from donors with T2D at different scales - from islet population, to isolated islets, and isolated cells (Petrenko et al. 2020). Surprisingly, our experiments show that islets from T2D patients have clocks whose circadian amplitude is reduced and whose in vitro synchronization capacity is weakened compared to clocks present in islets from healthy donors. Time lapse microscopy analysis of pancreatic islets suggests that the reduction in amplitude is associated with a reduced synchronization capacity between T2D islets, but also between different endocrine cells within the same islet. In line with previous transcriptomic screening data (Stamenkovic et al. 2012), we observed an alteration in the expression of clock genes in non-synchronized pancreatic islets from diabetic individuals. Furthermore, our data suggest that circadian profiles of insulin and glucagon secretion are disrupted in diabetic donors, highlighting the role of cellular clocks in the progression of T2D. These results, obtained in vitro, are consistent with data obtained in vivo, demonstrating that the rhythmic profile of insulin secretion in the blood,

measured in healthy volunteers (Boden et al. 1996), disappears in individuals first degree relatives of patients with T2D (Boden et al. 1999).

1.2. Functional clocks in human islets are required for proper absolute and temporal secretion of insulin and glucagon.

Using RNA interference to target the key clock gene Clock (siCLOCK), allowed us to alter the circadian oscillator in human islet cells in vitro (Saini et al. 2016). Decreasing CLOCK expression to 80% causes increased transcription of other clock genes such as BMAL1 and CRY1 and decreased expression of REV-ERBa, PER3 and DBP, measured by quantitative PCR (qPCR). Moreover, such disruption of core clock gene expression flattened the circadian amplitude of the Bmal1-luciferase reporter gene oscillations in forskolin-synchronized islet cells. These results are in agreement with recent observations observed in human skeletal myotubes transfected with siCLOCK (Perrin et al. 2015), and with data from transgenic mice lacking Clock (Marcheva et al. 2010). Above all, this technique allowed us to establish the important role of functional clocks in insulin secretion, since islet cells transfected with siCLOCK secrete less insulin compared to control cells, not only in basal conditions, but also after stimulation with glucose, KCL, carbachol and theophylline. Our continuous perifusion experiments for 48 hours demonstrated that isolated islet cells secrete insulin in a circadian manner in vitro, a phenomenon which is also disrupted in cells whose expression of CLOCK was attenuated. These results are in agreement with data previously obtained from transgenic rodent models in which circadian clocks are essential for insulin secretion (Marcheva et al. 2010; Gale et al. 2011), suggesting that disruption of this mechanism may be involved in the development of T2D (Marcheva et al. 2010; Qian et al. 2013; Qian et al. 2015). This discovery was then supported by whole transcriptome analysis assessed by RNA sequencing, which identified alterations in several groups of genes whose function is associated with insulin secretion. Indeed, according to Gene Ontology analysis, treatment with siCLOCK disrupts the expression of transcripts involved in protein synthesis and in the formation and exocytosis of granules. For example, the expression of the zinc transporter SLC30A8, necessary for the formation and secretion of insulin granules (Davidson et al. 2014), is attenuated by siCLOCK. In mice, deletion of this gene modifies insulin secretion in vivo (Nicolson et al. 2009), thus supporting our results. Appropriate secretion of insulin by exocytosis requires the functionality of the SNAP25/VAMP/STX complex (Regazzi et al. 1995; Kuliawat et al. 2004). We reported that the expression of components of this complex in human β cells, the VAMP3 and STX6

genes, is attenuated following siCLOCK treatment. Noteworthy, the expression of the same genes is also modified in arrhythmic mice following the mutation of the Clock gene (Marcheva et al. 2010). Interestingly, the expression of genes participating in insulin secretion following stimulation by glucose is similarly affected, in particular those for the ATP5G2, ATP1A1 and KCNJ11 genes. While the expression of ATP5G2, ATP1A1 is decreased, the level of KCNJ11 mRNA is increased. Mutation of the KCNJ11 gene (component of the voltage-gated potassium ion channel) reduces insulin secretion in humans (Gloyn et al. 2006). Likewise, activation of the specific expression of Kcnill in β cells triggers, in diabetic mice, hyperpolarization, disrupting not only basal insulin secretion, but also the stimulated one (Girard et al. 2009). Our data, associated with other recent work obtained in transgenic mice, support the hypothesis that the circadian clock controls exocytosis (Dibner and Schibler 2015). Using total internal reflection fluorescence (TIRF) microscopy, we were able to provide for the first time direct evidence of a disruption in the exocytosis of insulin and glucagon granules in siCLOCK-treated β- and α-cells (Petrenko et al. 2020). Interestingly, a similar disruption of the exocytosis of these insulin granules was recently described in β-cells from T2DM patients (Gandasi et al. 2018), suggesting a potential role for molecular clocks in the pathogenesis of this disease. Moreover, due to altered circadian lipid metabolism in the pancreatic islets upon T2D, the islet cell membranes are more rigid than the those of their ND counterparts (Petrenko et al. 2022). This phenotype is reproduced by clock disruption. Changes in membrane fluidity impacts on cell communication with the environment by affecting the receptor function, signal transduction, endo-, and exocytosis. This might additionally contribute to the reduced capacity for insulin and glucagon secretion of islet cells of patients with T2D.

1.3. Cell-specific entrainment signals in pancreatic islets from healthy and diabetic donors

At the organismal level, the circadian synchronization of the islet cellular clocks represents a complex integration of different extrinsic triggers such as feeding-fasting cycles, and is controlled by neuronal, endocrine and paracrine stimuli (Perelis et al. 2016; Gachon et al. 2017; Petrenko and Dibner 2018; Sinturel et al. 2020a). Numerous systemic signals couple the function of the endocrine pancreas to metabolic needs, in part via modulation of circadian rhythmicity of α - and β -cells. In mice, physiologically relevant stimuli including adrenaline, insulin, glucagon, somatostatin and GLP-1 analogues (liraglutide and exenatide) synchronize efficiently circadian rhythmicity of α - and β -cells in vitro, in a cell-specific manner (Petrenko

et al. 2017; Petrenko and Dibner 2018). Forskolin, dexamethasone, and temperature cycles are also effective synchronizers of human islet cells in vitro (Pulimeno et al. 2013; Perelis et al. 2015). In the islets isolated from normoglycemic human donors, adrenaline, octreotide and liraglutide demonstrated prominent synchronizing effects. Strikingly, a pulse of adrenaline and octreotide failed to synchronize the T2D islets, while liraglutide remained efficient synchronizer, indicating that its therapeutic effect may rely, at least in part, on adjustment of the molecular clocks. Furthermore, the chronic application of high concentration of glucose, primary regulator of the islet hormone secretion, for several days lengthens the circadian period of non-diabetic islets, but not of the islets derived from T2D donors. The synchronizing effect of glucose pulse on the cellular clocks of non-diabetic pancreatic islets might be mediated by the attenuation of the expression of the immediate early clock genes Per1 and Per2, as has been shown for cultured rat fibroblasts (Hirota et al. 2002). This mechanism could be altered in diabetic islets. Physiological hormonal or blood sugar changes, such as increased adrenaline levels under stress or postprandial increase in glucose levels, could contribute to the regulation of islet cell oscillators, suggesting that disruption of this mechanism contributes to the development of T2D.

1.4. Interplay between β cell regeneration and circadian clocks

The mechanism of β -cell regeneration remains poorly understood, despite decades of extensive research in this direction. The multiplication of differentiated β cells, rather than the differentiation of stem cells, represents a major source of newly generated β cells after birth, under physiological conditions, but also during regeneration following injury (Dor et al. 2004; Brennand et al. 2007; Nir et al. 2007; Teta et al. 2007; Klochendler et al. 2016). Furthermore, in the absence of residual β cells during near-total ablation, the conversion of α or δ cells into insulin-producing cells has also been described (Thorel et al. 2010; Chera et al. 2014). We were able to demonstrate that the regeneration of β cells following a significant ablation (~80%) is organized rhythmically and that it depends on the clock gene Bmal1. Indeed, the proliferation rate is greater during the activity phase in the middle of the night, concomitantly with the peak expression of genes involved in the cell cycle. Moreover, mice lacking the essential component of molecular clocks BMAL1 are incapable of regenerating lost β cells. Furthermore, it has been shown that the absence of a single allele of the Bmal1 gene in the β cells of mice fed a high-fat diet is sufficient to prevent the expansion of these cells (Rakshit et al. 2016). However, cell

regeneration and expansion are two different mechanisms. Unlike the expansion of β cells in obese mice, we show that regeneration requires a functional clock and that it is maintained in control rhythmic mice heterozygous for the Bmall allele. In the regenerating liver, the entry into mitosis of hepatocytes also follows a rhythm of 24 hours (Matsuo et al. 2003). Unlike β cells which regenerate slowly, the entry of hepatocytes into the S phase of the cell cycle is not under the control of cellular clocks. Additionally, in arrhythmic Cry1/Cry2 mice liver regeneration is delayed, but still exist. In contrast, β-cell regeneration is virtually abolished in the absence of functional BMAL1 causing severe and fatal diabetes in mice. By searching for the molecular mechanism linking circadian clock and the regeneration of β cells, we analysed by RNAseq the circadian rhythmic genes in β cells undergoing regeneration and identified the transcription factor FOXM1, which expression is altered in the absence of BMAL1. Indeed, at birth, this gene is essential for the proliferation of β cells in physiological conditions (Zhang et al. 2006; Ackermann Misfeldt et al. 2008). Furthermore, its expression is increased in different experimental models that allow the study of β -cell expansion (Ackermann Misfeldt et al. 2008; Davis et al. 2010; Yamamoto et al. 2017). Together, these data propose the FOXM1 as a candidate molecule coupling the cell cycle and the molecular clock. Additional studies are required to test this hypothesis.

2. Modulation of molecular clocks holds promise as a therapeutic or preventive approach for the management of metabolic diseases

Modern lifestyle, including social jet lag and shift work, is associated with the development of metabolic syndrome and T2D (Marcheva et al. 2013; Bass 2017; Sinturel et al. 2020a). As T2D reaches epidemic scope in our society, the novel link between functional molecular clocks in human pancreatic islets and endocrine pancreas function, but also the pathogenesis of T2D, could represent an important target for future clinical investigations. Our experimental data on transgenic mice suggest that disruption of molecular clocks worsens diabetes and increases mortality. We found that Nobiletin, an agonist of the ROR α/γ clock proteins, stimulates the amplitude of islet clocks derived from donors with T2D as well as the secretion of insulin by these islets. At the same time, the nuclear receptor agonist REVERB α/β , SR9001, attenuates insulin secretion by diabetic islets, suggesting that ROR element controls secretion of this hormone. In rodents, Nobiletin showed beneficial protective effects against atherosclerosis, obesity, metabolic syndrome and insulin resistance (Mulvihill et al. 2011; Lee et al. 2013; He et al. 2016). Notably, no significant toxicity has yet been detected for this molecule in our in

vitro study, but also when it is applied in vivo in rodents (He et al. 2016). These data allow us to imagine that clock modulators could be considered as potential therapeutic substances against diabetes. Loss of β cells represents the main cause of T1D and is part of the pathogenesis of advanced T2D. In humans, the potential of β cells to regenerate is limited, without the reasons being known (Zhou and Melton 2018; Zhong and Jiang 2019). By studying diabetic mice, we established that their β -cell regeneration mechanisms are under the influence of cellular clocks and in particular the BMAL1. Deciphering this phenomenon and, above all, finding how to stimulate β -cell regeneration could be a game-changer in the therapeutic approach for diabetes. Understanding these mechanisms will perhaps make it possible to trigger the regeneration of β cells in humans, a current hope cure of diabetes.

In summary, this series of studies proposes a functional link between the molecular clocks of the endocrine pancreas, its function in physiological conditions and the pathogenesis of T2D in humans. Moreover, it paves the way for development of new therapeutic approaches for T2D by modulating the perturbed clocks via life-style adaptations (timely scheduled light, meals, physical exercise) and small molecules dubbed clock modulators.

3. Post-transplant type 2 diabetes

There is accumulating evidence attributing a critical role to the local oscillators operative in different metabolic organs in regulation of glucose homeostasis (Sinturel et al. 2020a). Thus, liver-specific Bmal1KO mice exhibit hypoglycemia during fasting period due to increased glucose clearance, while a liver-specific depletion of Cry1 and Cry2 stimulates gluconeogenesis (Lamia et al. 2008; Zhang et al. 2010). Removal of core-clock component Bmal1 exclusively from skeletal muscles leads to impaired insulin-stimulated glucose uptake and perturbations in fatty acid, triglyceride, and phospholipid metabolism (Dyar et al. 2014; Dyar et al. 2018a). Withdrawal of Bmal1 from nephrons decreased oxidative phosphorylation-to-glycolysis ratio in kidney and induced systemic perturbation of protein and lipid metabolism (Nikolaeva et al. 2016). Islet-specific Bmal1KO mice developed more pronounced hypoinsulinemia and features of T2D at younger age as compared to the whole-body Bmal1KO mice or *Clock* mutants (Marcheva et al. 2010; Sadacca et al. 2011; Perelis et al. 2015). Concordantly, siRNA-mediated clock disruption in non-diabetic human islet cells attenuated insulin secretion by these cells (Saini et al. 2016). In turn, human pancreatic islets from T2D donors displayed compromised

molecular oscillators *in vitro* (Petrenko et al. 2020). Collectively, these studies strongly suggest that circadian desynchrony between the orangs may have greater impact on glucose metabolism than whole body arrhythmicity.

Mouse models of organ-specific clock ablation were instrumental in exploring the function of individual peripheral clocks. Yet, they have not allowed to assess the degree of autonomy of the organ clocks from each other, and from the SCN pacemaker. It has been recently shown that liver bearing restored clocks in otherwise arrhythmic mice maintains certain level of circadian functionality (Sinturel et al. 2021), specifically for NAD⁺ salvage pathway and glycogen turnover (Koronowski et al. 2019). How such circadian autonomy from rest of the body clocks affects glucose homeostasis, and whether it is specific to liver, has not yet been addressed.

Transplantation of metabolic organs carrying functional clocks to the hosts with dysfunctional oscillators (associated with aging and/or metabolic disease) may represent a clinically relevant example of inter-organ circadian misalignment due to circadian autonomy of the graft. Indeed, engraftment of solid metabolic organs, such as liver and kidney, is associated with development of post-transplant diabetes mellitus (PTDM) in up to 74% of transplantations (Hecking et al. 2013; Han et al. 2016; Alnasrallah et al. 2019; Chowdhury 2019). In addition to established risk factors of T2D, the immunosuppressive therapy and graft-related inflammation are thought to play a role in the pathogenesis of PTDM (Shivaswamy et al. 2016), although the mechanism is still obscure.

As the perspective of this research line, I would like to investigate the link between inter-organ circadian desynchrony following solid organ transplantation and development of T2D.

4. Defining the role of molecular clocks in human parathyroid gland physiology and physiopathology.

Among other tissues, the molecular circadian clock was also described in rodent parathyroid gland (PG) (Egstrand et al. 2020). Moreover, downregulation of Bmal1 in mice lead to perturbed proliferation of parathyroid cells in response to uremia (Egstrand et al. 2022). In humans, the variation of parathyroid hormone (PTH) levels in blood exhibit circadian rhythm, with the highest level in the early morning (Jubiz et al. 1972). However, the characterization of molecular oscillators in human PGs is still lacking. Hyperparathyroidism is a common surgical pathology of PG associated with unadapted PTH secretion to calcium levels (Walker

and Silverberg 2018). While circadian rhythm of serum PTH level seems to be disrupted in patients with primary hypoparathyroidism (HPT1) as compared to healthy volunteers (Logue et al. 1990), the removal of the parathyroid gland adenoma restores the serum PTH rhythmicity in patients (Lobaugh et al. 1989). Our previous study revealed that the differential expression analysis of selected mRNA targets in post-operative biopsies of parathyroid tissues assessed by Nanostring and qPCR revealed clock genes NFIL3 and PER1 among transcripts significantly altered in HPT1 adenoma compared with normal PG (Sadowski et al. 2018), evoking a hypothesis on the role of core-clock machinery in the development of the PG adenoma. However, the role of molecular clocks in human parathyroid function and tumorigenesis has not been unraveled. It is therefore of scientific and clinical importance to provide insight into the potential application of the circadian clock alterations upon the parathyroid cell transformation, its potential impact on altered hormone secretion, and on how this knowledge may be translated into diagnostics or therapeutic applications.

This research line aims at characterizing molecular makeup of circadian clocks in human primary parathyroid cell culture, its role in PG function and at establishing differential transcriptional patterns of normal and pathological PGs. To evaluate dynamic alterations in molecular patterns as a function of the type of parathyroid gland pathology, a comparative transcript and miRNA analysis shell be conducted in subgroups of healthy samples, sporadic HPT1 adenoma and hyperplasia. This analysis will also allow us to identify molecular signature of parathyroid neoplasms. Furthermore, we will assess the role of molecular clock in PG cell physiology. The efficient circadian clock disruption will achieved primary parathyroid cell cultures by small interfering RNA-mediated knockdown of *CLOCK*. The functionality of circadian clock machinery will be assessed by continuous recording of circadian bioluminescence introduced via lentivectors and paralleled with around-the-clock measurement of PTH secretion using perifusion system.

Importantly, parathyroid tissue exhibit a near-infrared autofluorescence (NIRAF) pattern which allowed to develop new reliable imaging methods for intraoperative localization of these glands (Paras et al. 2011; McWade et al. 2013; McWade et al. 2014; McWade et al. 2019). However, the biochemical mechanisms and the fluorophores responsible for the autofluorescence of the parathyroid involved in NIRAF remain poorly understood. Noteworthy, the PG adenoma exhibits heterogeneous near-infrared autofluorescence pattern, with adenoma tissue documented being significantly less autofluorescent than the rim of normal parathyroid tissue (Demarchi et al. 2021). Understanding the molecular difference between healthy and adenoma tissues with different autofluorescence intensity may help in

identifying the fluorophore responsible for NIRAF fluorescence in parathyroid tissue, in addition to the above-mentioned goals.

REFERENCES

- Ackermann Misfeldt A, Costa RH, Gannon M. 2008. Beta-cell proliferation, but not neogenesis, following 60% partial pancreatectomy is impaired in the absence of FoxM1. *Diabetes* 57: 3069-3077.
- Aggarwal A, Costa MJ, Rivero-Gutierrez B, Ji L, Morgan SL, Feldman BJ. 2017. The Circadian Clock Regulates Adipogenesis by a Per3 Crosstalk Pathway to Klf15. *Cell Rep* 21: 2367-2375.
- Ahlqvist E, Storm P, Karajamaki A, Martinell M, Dorkhan M, Carlsson A, Vikman P, Prasad RB, Aly DM, Almgren P et al. 2018. Novel subgroups of adult-onset diabetes and their association with outcomes: a data-driven cluster analysis of six variables. *Lancet Diabetes Endocrinol* 6: 361-369.
- Ahmad E, Lim S, Lamptey R, Webb DR, Davies MJ. 2022. Type 2 diabetes. *Lancet* **400**: 1803-1820.
- Alkhoury C, Henneman NF, Petrenko V, Shibayama Y, Segaloni A, Gadault A, Nemazanyy I, Le Guillou E, Wolide AD, Antoniadou K et al. 2023. Class 3 PI3K coactivates the circadian clock to promote rhythmic de novo purine synthesis. *Nat Cell Biol* **25**: 975-988.
- Alnasrallah B, Goh TL, Chan LW, Manley P, Pilmore H. 2019. Transplantation and diabetes (Transdiab): a pilot randomised controlled trial of metformin in impaired glucose tolerance after kidney transplantation. *BMC Nephrol* **20**: 147.
- American Diabetes A. 2020. 2. Classification and Diagnosis of Diabetes: Standards of Medical Care in Diabetes-2020. *Diabetes Care* 43: S14-S31.
- Andersen PAK, Petrenko V, Rose PH, Koomen M, Fischer N, Ghiasi SM, Dahlby T, Dibner C, Mandrup-Poulsen T. 2020. Proinflammatory Cytokines Perturb Mouse and Human Pancreatic Islet Circadian Rhythmicity and Induce Uncoordinated beta-Cell Clock Gene Expression via Nitric Oxide, Lysine Deacetylases, and Immunoproteasomal Activity. *Int J Mol Sci* 22.
- Aras E, Ramadori G, Kinouchi K, Liu Y, Ioris RM, Brenachot X, Ljubicic S, Veyrat-Durebex C, Mannucci S, Galie M et al. 2019. Light Entrains Diurnal Changes in Insulin Sensitivity of Skeletal Muscle via Ventromedial Hypothalamic Neurons. *Cell Rep* 27: 2385-2398 e2383.
- Aryal RP, Kwak PB, Tamayo AG, Gebert M, Chiu PL, Walz T, Weitz CJ. 2017. Macromolecular Assemblies of the Mammalian Circadian Clock. *Mol Cell* 67: 770-782 e776.
- Asher G, Gatfield D, Stratmann M, Reinke H, Dibner C, Kreppel F, Mostoslavsky R, Alt FW, Schibler U. 2008. SIRT1 regulates circadian clock gene expression through PER2 deacetylation. *Cell* **134**: 317-328.
- Aviram R, Manella G, Kopelman N, Neufeld-Cohen A, Zwighaft Z, Elimelech M, Adamovich Y, Golik M, Wang C, Han X et al. 2016. Lipidomics Analyses Reveal Temporal and Spatial Lipid Organization and Uncover Daily Oscillations in Intracellular Organelles. *Mol Cell* 62: 636-648.
- Baek M, Virgilio S, Lamb TM, Ibarra O, Andrade JM, Goncalves RD, Dovzhenok A, Lim S, Bell-Pedersen D, Bertolini MC et al. 2019. Circadian clock regulation of the glycogen synthase (gsn) gene by WCC is critical for rhythmic glycogen metabolism in Neurospora crassa. *Proc Natl Acad Sci U S A* **116**: 10435-10440.
- Balsalobre A, Damiola F, Schibler U. 1998. A serum shock induces circadian gene expression in mammalian tissue culture cells. *Cell* **93**: 929-937.
- Bandin C, Scheer FA, Luque AJ, Avila-Gandia V, Zamora S, Madrid JA, Gomez-Abellan P, Garaulet M. 2015. Meal timing affects glucose tolerance, substrate oxidation and

- circadian-related variables: A randomized, crossover trial. *Int J Obes (Lond)* **39**: 828-833.
- Bass JT. 2017. The circadian clock system's influence in health and disease. *Genome Med* **9**: 94.
- Boden G, Chen X, Polansky M. 1999. Disruption of circadian insulin secretion is associated with reduced glucose uptake in first-degree relatives of patients with type 2 diabetes. *Diabetes* **48**: 2182-2188.
- Boden G, Ruiz J, Urbain JL, Chen X. 1996. Evidence for a circadian rhythm of insulin secretion. *Am J Physiol* **271**: E246-252.
- Boslem E, MacIntosh G, Preston AM, Bartley C, Busch AK, Fuller M, Laybutt DR, Meikle PJ, Biden TJ. 2011. A lipidomic screen of palmitate-treated MIN6 beta-cells links sphingolipid metabolites with endoplasmic reticulum (ER) stress and impaired protein trafficking. *Biochem J* **435**: 267-276.
- Brennand K, Huangfu D, Melton D. 2007. All beta cells contribute equally to islet growth and maintenance. *PLoS Biol* **5**: e163.
- Bugge A, Feng D, Everett LJ, Briggs ER, Mullican SE, Wang F, Jager J, Lazar MA. 2012. Rev-erbalpha and Rev-erbbeta coordinately protect the circadian clock and normal metabolic function. *Genes Dev* 26: 657-667.
- Butler AE, Janson J, Bonner-Weir S, Ritzel R, Rizza RA, Butler PC. 2003. Beta-cell deficit and increased beta-cell apoptosis in humans with type 2 diabetes. *Diabetes* **52**: 102-110.
- Buxton OM, Pavlova M, Reid EW, Wang W, Simonson DC, Adler GK. 2010. Sleep restriction for 1 week reduces insulin sensitivity in healthy men. *Diabetes* **59**: 2126-2133.
- Carmichael L, Keske MA, Betik AC, Parker L, Brayner B, Roberts-Thomson KM, Wadley GD, Hamilton DL, Kaur G. 2022. Is vascular insulin resistance an early step in dietinduced whole-body insulin resistance? *Nutr Diabetes* 12: 31.
- Carroll KF, Nestel PJ. 1973. Diurnal variation in glucose tolerance and in insulin secretion in man. *Diabetes* **22**: 333-348.
- Cedernaes J, Lampola L, Axelsson EK, Liethof L, Hassanzadeh S, Yeganeh A, Broman JE, Schioth HB, Benedict C. 2016. A single night of partial sleep loss impairs fasting insulin sensitivity but does not affect cephalic phase insulin release in young men. *J Sleep Res* 25: 5-10.
- Chellappa SL, Vujovic N, Williams JS, Scheer F. 2019. Impact of Circadian Disruption on Cardiovascular Function and Disease. *Trends Endocrinol Metab* **30**: 767-779.
- Chera S, Baronnier D, Ghila L, Cigliola V, Jensen JN, Gu G, Furuyama K, Thorel F, Gribble FM, Reimann F et al. 2014. Diabetes recovery by age-dependent conversion of pancreatic delta-cells into insulin producers. *Nature* **514**: 503-507.
- Cho H, Zhao X, Hatori M, Yu RT, Barish GD, Lam MT, Chong LW, DiTacchio L, Atkins AR, Glass CK et al. 2012. Regulation of circadian behaviour and metabolism by REV-ERB-alpha and REV-ERB-beta. *Nature* **485**: 123-127.
- Chowdhury TA. 2019. Post-transplant diabetes mellitus. Clin Med (Lond) 19: 392-395.
- Colwell CS. 2011. Linking neural activity and molecular oscillations in the SCN. *Nat Rev Neurosci* **12**: 553-569.
- Cox KH, Takahashi JS. 2021. Introduction to the Clock System. *Adv Exp Med Biol* **1344**: 3-20.
- Cox SL, O'Siorain JR, Fagan LE, Curtis AM, Carroll RG. 2022. Intertwining roles of circadian and metabolic regulation of the innate immune response. *Semin Immunopathol* 44: 225-237.

- Crosby P, Hamnett R, Putker M, Hoyle NP, Reed M, Karam CJ, Maywood ES, Stangherlin A, Chesham JE, Hayter EA et al. 2019. Insulin/IGF-1 Drives PERIOD Synthesis to Entrain Circadian Rhythms with Feeding Time. *Cell* **177**: 896-909 e820.
- Damiola F, Le Minh N, Preitner N, Kornmann B, Fleury-Olela F, Schibler U. 2000. Restricted feeding uncouples circadian oscillators in peripheral tissues from the central pacemaker in the suprachiasmatic nucleus. *Genes Dev* 14: 2950-2961.
- Davidson HW, Wenzlau JM, O'Brien RM. 2014. Zinc transporter 8 (ZnT8) and beta cell function. *Trends Endocrinol Metab* **25**: 415-424.
- Davis DB, Lavine JA, Suhonen JI, Krautkramer KA, Rabaglia ME, Sperger JM, Fernandez LA, Yandell BS, Keller MP, Wang IM et al. 2010. FoxM1 is up-regulated by obesity and stimulates beta-cell proliferation. *Mol Endocrinol* **24**: 1822-1834.
- de Jesus DS, Bargi-Souza P, Cruzat V, Yechoor V, Carpinelli AR, Peliciari-Garcia RA. 2022. BMAL1 modulates ROS generation and insulin secretion in pancreatic beta-cells: An effect possibly mediated via NOX2. *Mol Cell Endocrinol* 555: 111725.
- Demarchi MS, Karenovics W, Bedat B, De Vito C, Triponez F. 2021. Autofluorescence pattern of parathyroid adenomas. *BJS Open* **5**.
- Depner CM, Melanson EL, Eckel RH, Snell-Bergeon JK, Perreault L, Bergman BC, Higgins JA, Guerin MK, Stothard ER, Morton SJ et al. 2019. Ad libitum Weekend Recovery Sleep Fails to Prevent Metabolic Dysregulation during a Repeating Pattern of Insufficient Sleep and Weekend Recovery Sleep. *Curr Biol* **29**: 957-967 e954.
- Depner CM, Melanson EL, McHill AW, Wright KP, Jr. 2018. Mistimed food intake and sleep alters 24-hour time-of-day patterns of the human plasma proteome. *Proc Natl Acad Sci U S A* **115**: E5390-E5399.
- Dibner C. 2020. The importance of being rhythmic: Living in harmony with your body clocks. *Acta Physiol (Oxf)* **228**: e13281.
- Dibner C, Schibler U. 2015. METABOLISM. A pancreatic clock times insulin release. *Science* **350**: 628-629.
- Dibner C, Schibler U, Albrecht U. 2010. The mammalian circadian timing system: organization and coordination of central and peripheral clocks. *Annu Rev Physiol* **72**: 517-549.
- Doi R, Oishi K, Ishida N. 2010. CLOCK regulates circadian rhythms of hepatic glycogen synthesis through transcriptional activation of Gys2. *J Biol Chem* **285**: 22114-22121.
- Donath MY, Shoelson SE. 2011. Type 2 diabetes as an inflammatory disease. *Nat Rev Immunol* **11**: 98-107.
- Donga E, van Dijk M, van Dijk JG, Biermasz NR, Lammers GJ, van Kralingen KW, Corssmit EP, Romijn JA. 2010. A single night of partial sleep deprivation induces insulin resistance in multiple metabolic pathways in healthy subjects. *J Clin Endocrinol Metab* **95**: 2963-2968.
- Dor Y, Brown J, Martinez OI, Melton DA. 2004. Adult pancreatic beta-cells are formed by self-duplication rather than stem-cell differentiation. *Nature* **429**: 41-46.
- Dyar KA, Ciciliot S, Wright LE, Bienso RS, Tagliazucchi GM, Patel VR, Forcato M, Paz MI, Gudiksen A, Solagna F et al. 2014. Muscle insulin sensitivity and glucose metabolism are controlled by the intrinsic muscle clock. *Mol Metab* 3: 29-41.
- Dyar KA, Hubert MJ, Mir AA, Ciciliot S, Lutter D, Greulich F, Quagliarini F, Kleinert M, Fischer K, Eichmann TO et al. 2018a. Transcriptional programming of lipid and amino acid metabolism by the skeletal muscle circadian clock. *PLoS Biol* **16**: e2005886.
- Dyar KA, Lutter D, Artati A, Ceglia NJ, Liu Y, Armenta D, Jastroch M, Schneider S, de Mateo S, Cervantes M et al. 2018b. Atlas of Circadian Metabolism Reveals System-wide Coordination and Communication between Clocks. *Cell* **174**: 1571-1585 e1511.

- Eckel RH, Depner CM, Perreault L, Markwald RR, Smith MR, McHill AW, Higgins J, Melanson EL, Wright KP, Jr. 2015. Morning Circadian Misalignment during Short Sleep Duration Impacts Insulin Sensitivity. *Curr Biol* **25**: 3004-3010.
- Egstrand S, Mace ML, Morevati M, Nordholm A, Engelholm LH, Thomsen JS, Bruel A, Naveh-Many T, Guo Y, Olgaard K et al. 2022. Hypomorphic expression of parathyroid Bmall disrupts the internal parathyroid circadian clock and increases parathyroid cell proliferation in response to uremia. *Kidney Int* **101**: 1232-1250.
- Egstrand S, Nordholm A, Morevati M, Mace ML, Hassan A, Naveh-Many T, Rukov JL, Gravesen E, Olgaard K, Lewin E. 2020. A molecular circadian clock operates in the parathyroid gland and is disturbed in chronic kidney disease associated bone and mineral disorder. *Kidney Int* **98**: 1461-1475.
- Ehses JA, Perren A, Eppler E, Ribaux P, Pospisilik JA, Maor-Cahn R, Gueripel X, Ellingsgaard H, Schneider MK, Biollaz G et al. 2007. Increased number of islet-associated macrophages in type 2 diabetes. *Diabetes* **56**: 2356-2370.
- Finck BN, Bernal-Mizrachi C, Han DH, Coleman T, Sambandam N, LaRiviere LL, Holloszy JO, Semenkovich CF, Kelly DP. 2005. A potential link between muscle peroxisome proliferator- activated receptor-alpha signaling and obesity-related diabetes. *Cell Metab* 1: 133-144.
- Finger AM, Dibner C, Kramer A. 2020. Coupled network of the circadian clocks: a driving force of rhythmic physiology. *FEBS Lett* **594**: 2734-2769.
- Fujii T, Inoue S, Nagai K, Nakagawa H. 1989. Involvement of adrenergic mechanism in hyperglycemia due to SCN stimulation. *Horm Metab Res* **21**: 643-645.
- Fustin JM, Doi M, Yamada H, Komatsu R, Shimba S, Okamura H. 2012. Rhythmic nucleotide synthesis in the liver: temporal segregation of metabolites. *Cell Rep* 1: 341-349.
- Gabriel BM, Altintas A, Smith JAB, Sardon-Puig L, Zhang X, Basse AL, Laker RC, Gao H, Liu Z, Dollet L et al. 2021. Disrupted circadian oscillations in type 2 diabetes are linked to altered rhythmic mitochondrial metabolism in skeletal muscle. *Sci Adv* 7: eabi9654.
- Gachon F, Loizides-Mangold U, Petrenko V, Dibner C. 2017. Glucose Homeostasis: Regulation by Peripheral Circadian Clocks in Rodents and Humans. *Endocrinology* **158**: 1074-1084.
- Gale JE, Cox HI, Qian J, Block GD, Colwell CS, Matveyenko AV. 2011. Disruption of circadian rhythms accelerates development of diabetes through pancreatic beta-cell loss and dysfunction. *J Biol Rhythms* **26**: 423-433.
- Gan Y, Yang C, Tong X, Sun H, Cong Y, Yin X, Li L, Cao S, Dong X, Gong Y et al. 2015. Shift work and diabetes mellitus: a meta-analysis of observational studies. *Occup Environ Med* 72: 72-78.
- Gandasi NR, Yin P, Omar-Hmeadi M, Ottosson Laakso E, Vikman P, Barg S. 2018. Glucose-Dependent Granule Docking Limits Insulin Secretion and Is Decreased in Human Type 2 Diabetes. *Cell Metab* **27**: 470-478 e474.
- Gao L, Chen H, Li C, Xiao Y, Yang D, Zhang M, Zhou D, Liu W, Wang A, Jin Y. 2019. ER stress activation impairs the expression of circadian clock and clock-controlled genes in NIH3T3 cells via an ATF4-dependent mechanism. *Cell Signal* 57: 89-101.
- Gao Y, Gan T, Jiang L, Yu L, Tang D, Wang Y, Li X, Ding G. 2020. Association between shift work and risk of type 2 diabetes mellitus: a systematic review and dose-response meta-analysis of observational studies. *Chronobiol Int* **37**: 29-46.
- Garaulet M, Gomez-Abellan P, Alburquerque-Bejar JJ, Lee YC, Ordovas JM, Scheer FA. 2013. Timing of food intake predicts weight loss effectiveness. *Int J Obes (Lond)* **37**: 604-611.
- Girard CA, Wunderlich FT, Shimomura K, Collins S, Kaizik S, Proks P, Abdulkader F, Clark A, Ball V, Zubcevic L et al. 2009. Expression of an activating mutation in the gene

- encoding the KATP channel subunit Kir6.2 in mouse pancreatic beta cells recapitulates neonatal diabetes. *J Clin Invest* **119**: 80-90.
- Gloyn AL, Diatloff-Zito C, Edghill EL, Bellanne-Chantelot C, Nivot S, Coutant R, Ellard S, Hattersley AT, Robert JJ. 2006. KCNJ11 activating mutations are associated with developmental delay, epilepsy and neonatal diabetes syndrome and other neurological features. *Eur J Hum Genet* **14**: 824-830.
- Griebel G, Ravinet-Trillou C, Beeske S, Avenet P, Pichat P. 2014. Mice deficient in cryptochrome 1 (cry1 (-/-)) exhibit resistance to obesity induced by a high-fat diet. *Front Endocrinol (Lausanne)* **5**: 49.
- Haataja L, Gurlo T, Huang CJ, Butler PC. 2008. Islet amyloid in type 2 diabetes, and the toxic oligomer hypothesis. *Endocr Rev* **29**: 303-316.
- Han E, Kim MS, Kim YS, Kang ES. 2016. Risk assessment and management of post-transplant diabetes mellitus. *Metabolism* **65**: 1559-1569.
- Harfmann BD, Schroder EA, Kachman MT, Hodge BA, Zhang X, Esser KA. 2016. Muscle-specific loss of Bmall leads to disrupted tissue glucose metabolism and systemic glucose homeostasis. *Skelet Muscle* **6**: 12.
- Hastings MH, Maywood ES, Brancaccio M. 2018. Generation of circadian rhythms in the suprachiasmatic nucleus. *Nat Rev Neurosci* **19**: 453-469.
- He B, Nohara K, Park N, Park YS, Guillory B, Zhao Z, Garcia JM, Koike N, Lee CC, Takahashi JS et al. 2016. The Small Molecule Nobiletin Targets the Molecular Oscillator to Enhance Circadian Rhythms and Protect against Metabolic Syndrome. *Cell Metab* 23: 610-621.
- Hecking M, Kainz A, Werzowa J, Haidinger M, Doller D, Tura A, Karaboyas A, Horl WH, Wolzt M, Sharif A et al. 2013. Glucose metabolism after renal transplantation. *Diabetes Care* **36**: 2763-2771.
- Hemmer A, Mareschal J, Dibner C, Pralong JA, Dorribo V, Perrig S, Genton L, Pichard C, Collet TH. 2021. The Effects of Shift Work on Cardio-Metabolic Diseases and Eating Patterns. *Nutrients* **13**.
- Hepler C, Weidemann BJ, Waldeck NJ, Marcheva B, Cedernaes J, Thorne AK, Kobayashi Y, Nozawa R, Newman MV, Gao P et al. 2022. Time-restricted feeding mitigates obesity through adipocyte thermogenesis. *Science* **378**: 276-284.
- Hirano A, Fu YH, Ptacek LJ. 2016. The intricate dance of post-translational modifications in the rhythm of life. *Nat Struct Mol Biol* **23**: 1053-1060.
- Hirota T, Okano T, Kokame K, Shirotani-Ikejima H, Miyata T, Fukada Y. 2002. Glucose down-regulates Per1 and Per2 mRNA levels and induces circadian gene expression in cultured Rat-1 fibroblasts. *J Biol Chem* **277**: 44244-44251.
- Hofman MA, Swaab DF. 2006. Living by the clock: the circadian pacemaker in older people. *Ageing Res Rev* **5**: 33-51.
- Holtkamp SJ, Ince LM, Barnoud C, Schmitt MT, Sinturel F, Pilorz V, Pick R, Jemelin S, Muhlstadt M, Boehncke WH et al. 2021. Circadian clocks guide dendritic cells into skin lymphatics. *Nat Immunol* 22: 1375-1381.
- Hunter AL, Pelekanou CE, Barron NJ, Northeast RC, Grudzien M, Adamson AD, Downton P, Cornfield T, Cunningham PS, Billaud JN et al. 2021. Adipocyte NR1D1 dictates adipose tissue expansion during obesity. *Elife* **10**.
- Ince LM, Barnoud C, Lutes LK, Pick R, Wang C, Sinturel F, Chen CS, de Juan A, Weber J, Holtkamp SJ et al. 2023. Influence of circadian clocks on adaptive immunity and vaccination responses. *Nat Commun* 14: 476.
- Innominato PF, Roche VP, Palesh OG, Ulusakarya A, Spiegel D, Levi FA. 2014. The circadian timing system in clinical oncology. *Ann Med* **46**: 191-207.

- James DE, Stockli J, Birnbaum MJ. 2021. The aetiology and molecular landscape of insulin resistance. *Nat Rev Mol Cell Biol* **22**: 751-771.
- Javeed N, Brown MR, Rakshit K, Her T, Sen SK, Matveyenko AV. 2020. Pro-inflammatory Cytokine Interleukin 1beta Disrupts beta cell Circadian Clock Function and Regulation of Insulin Secretion. *Endocrinology*.
- Javeed N, Matveyenko AV. 2018. Circadian Etiology of Type 2 Diabetes Mellitus. *Physiology* (*Bethesda*) **33**: 138-150.
- Jourdan T, Godlewski G, Cinar R, Bertola A, Szanda G, Liu J, Tam J, Han T, Mukhopadhyay B, Skarulis MC et al. 2013. Activation of the Nlrp3 inflammasome in infiltrating macrophages by endocannabinoids mediates beta cell loss in type 2 diabetes. *Nat Med* 19: 1132-1140.
- Jubiz W, Canterbury JM, Reiss E, Tyler FH. 1972. Circadian rhythm in serum parathyroid hormone concentration in human subjects: correlation with serum calcium, phosphate, albumin, and growth hormone levels. *J Clin Invest* **51**: 2040-2046.
- Kahn SE, Cooper ME, Del Prato S. 2014. Pathophysiology and treatment of type 2 diabetes: perspectives on the past, present, and future. *Lancet* **383**: 1068-1083.
- Kahn SE, Prigeon RL, McCulloch DK, Boyko EJ, Bergman RN, Schwartz MW, Neifing JL, Ward WK, Beard JC, Palmer JP et al. 1993. Quantification of the relationship between insulin sensitivity and beta-cell function in human subjects. Evidence for a hyperbolic function. *Diabetes* **42**: 1663-1672.
- Kalsbeek A, La Fleur S, Van Heijningen C, Buijs RM. 2004. Suprachiasmatic GABAergic inputs to the paraventricular nucleus control plasma glucose concentrations in the rat via sympathetic innervation of the liver. *J Neurosci* **24**: 7604-7613.
- Kelley DE, He J, Menshikova EV, Ritov VB. 2002. Dysfunction of mitochondria in human skeletal muscle in type 2 diabetes. *Diabetes* **51**: 2944-2950.
- Kessler K, Pivovarova-Ramich O. 2019. Meal Timing, Aging, and Metabolic Health. *Int J Mol Sci* **20**.
- Klochendler A, Caspi I, Corem N, Moran M, Friedlich O, Elgavish S, Nevo Y, Helman A, Glaser B, Eden A et al. 2016. The Genetic Program of Pancreatic β-Cell Replication In Vivo. *Diabetes* **65**: 2081.
- Koopman ADM, Rauh SP, van 't Riet E, Groeneveld L, van der Heijden AA, Elders PJ, Dekker JM, Nijpels G, Beulens JW, Rutters F. 2017. The Association between Social Jetlag, the Metabolic Syndrome, and Type 2 Diabetes Mellitus in the General Population: The New Hoorn Study. *J Biol Rhythms* **32**: 359-368.
- Koronowski KB, Kinouchi K, Welz PS, Smith JG, Zinna VM, Shi J, Samad M, Chen S, Magnan CN, Kinchen JM et al. 2019. Defining the Independence of the Liver Circadian Clock. *Cell* 177: 1448-1462 e1414.
- Koves TR, Li P, An J, Akimoto T, Slentz D, Ilkayeva O, Dohm GL, Yan Z, Newgard CB, Muoio DM. 2005. Peroxisome proliferator-activated receptor-gamma co-activator lalpha-mediated metabolic remodeling of skeletal myocytes mimics exercise training and reverses lipid-induced mitochondrial inefficiency. *J Biol Chem* 280: 33588-33598.
- Koves TR, Ussher JR, Noland RC, Slentz D, Mosedale M, Ilkayeva O, Bain J, Stevens R, Dyck JR, Newgard CB et al. 2008. Mitochondrial overload and incomplete fatty acid oxidation contribute to skeletal muscle insulin resistance. *Cell Metab* 7: 45-56.
- Kuliawat R, Kalinina E, Bock J, Fricker L, McGraw TE, Kim SR, Zhong J, Scheller R, Arvan P. 2004. Syntaxin-6 SNARE involvement in secretory and endocytic pathways of cultured pancreatic beta-cells. *Mol Biol Cell* **15**: 1690-1701.
- Kumar Jha P, Challet E, Kalsbeek A. 2015. Circadian rhythms in glucose and lipid metabolism in nocturnal and diurnal mammals. *Mol Cell Endocrinol* **418 Pt 1**: 74-88.

- La Fleur SE, Kalsbeek A, Wortel J, Buijs RM. 1999. A suprachiasmatic nucleus generated rhythm in basal glucose concentrations. *J Neuroendocrinol* 11: 643-652.
- la Fleur SE, Kalsbeek A, Wortel J, Fekkes ML, Buijs RM. 2001a. A daily rhythm in glucose tolerance: a role for the suprachiasmatic nucleus. *Diabetes* **50**: 1237-1243.
- la Fleur SE, Kalsbeek A, Wortel J, van der Vliet J, Buijs RM. 2001b. Role for the pineal and melatonin in glucose homeostasis: pinealectomy increases night-time glucose concentrations. *J Neuroendocrinol* 13: 1025-1032.
- Lamia KA, Storch KF, Weitz CJ. 2008. Physiological significance of a peripheral tissue circadian clock. *Proc Natl Acad Sci U S A* **105**: 15172-15177.
- Larsen CM, Faulenbach M, Vaag A, Volund A, Ehses JA, Seifert B, Mandrup-Poulsen T, Donath MY. 2007. Interleukin-1-receptor antagonist in type 2 diabetes mellitus. *N Engl J Med* **356**: 1517-1526.
- Lau P, Fitzsimmons RL, Raichur S, Wang SC, Lechtken A, Muscat GE. 2008. The orphan nuclear receptor, RORalpha, regulates gene expression that controls lipid metabolism: staggerer (SG/SG) mice are resistant to diet-induced obesity. *J Biol Chem* **283**: 18411-18421.
- Le Martelot G, Claudel T, Gatfield D, Schaad O, Kornmann B, Lo Sasso G, Moschetta A, Schibler U. 2009. REV-ERBalpha participates in circadian SREBP signaling and bile acid homeostasis. *PLoS Biol* 7: e1000181.
- LeCheminant JD, Christenson E, Bailey BW, Tucker LA. 2013. Restricting night-time eating reduces daily energy intake in healthy young men: a short-term cross-over study. *Br J Nutr* **110**: 2108-2113.
- Lee YS, Cha BY, Choi SS, Choi BK, Yonezawa T, Teruya T, Nagai K, Woo JT. 2013. Nobiletin improves obesity and insulin resistance in high-fat diet-induced obese mice. *J Nutr Biochem* **24**: 156-162.
- Leproult R, Holmback U, Van Cauter E. 2014. Circadian misalignment augments markers of insulin resistance and inflammation, independently of sleep loss. *Diabetes* **63**: 1860-1869.
- Liang F, Kume S, Koya D. 2009. SIRT1 and insulin resistance. *Nat Rev Endocrinol* **5**: 367-373.
- Lobaugh B, Neelon FA, Oyama H, Buckley N, Smith S, Christy M, Leight GS, Jr. 1989. Circadian rhythms for calcium, inorganic phosphorus, and parathyroid hormone in primary hyperparathyroidism: functional and practical considerations. *Surgery* **106**: 1009-1016; discussion 1016-1007.
- Logue FC, Fraser WD, Gallacher SJ, Cameron DA, O'Reilly DS, Beastall GH, Patel U, Boyle IT. 1990. The loss of circadian rhythm for intact parathyroid hormone and nephrogenous cyclic AMP in patients with primary hyperparathyroidism. *Clin Endocrinol (Oxf)* 32: 475-483.
- Loizides-Mangold U, Perrin L, Vandereycken B, Betts JA, Walhin JP, Templeman I, Chanon S, Weger BD, Durand C, Robert M et al. 2017. Lipidomics reveals diurnal lipid oscillations in human skeletal muscle persisting in cellular myotubes cultured in vitro. *Proc Natl Acad Sci U S A* **114**: E8565-E8574.
- Loizides-Mangold U, Petrenko V, Dibner C. 2021. Circadian Lipidomics: Analysis of Lipid Metabolites Around the Clock. *Methods Mol Biol* **2130**: 169-183.
- Lowrey PL, Takahashi JS. 2000. Genetics of the mammalian circadian system: Photic entrainment, circadian pacemaker mechanisms, and posttranslational regulation. *Annu Rev Genet* **34**: 533-562.
- MacDonald MJ, Ade L, Ntambi JM, Ansari IU, Stoker SW. 2015. Characterization of phospholipids in insulin secretory granules and mitochondria in pancreatic beta cells and their changes with glucose stimulation. *J Biol Chem* **290**: 11075-11092.

- Manella G, Sabath E, Aviram R, Dandavate V, Ezagouri S, Golik M, Adamovich Y, Asher G. 2021. The liver-clock coordinates rhythmicity of peripheral tissues in response to feeding. *Nat Metab* **3**: 829-842.
- Marcheva B, Ramsey KM, Buhr ED, Kobayashi Y, Su H, Ko CH, Ivanova G, Omura C, Mo S, Vitaterna MH et al. 2010. Disruption of the clock components CLOCK and BMAL1 leads to hypoinsulinaemia and diabetes. *Nature* **466**: 627-631.
- Marcheva B, Ramsey KM, Peek CB, Affinati A, Maury E, Bass J. 2013. Circadian clocks and metabolism. *Handb Exp Pharmacol*: 127-155.
- Matsuo T, Yamaguchi S, Mitsui S, Emi A, Shimoda F, Okamura H. 2003. Control mechanism of the circadian clock for timing of cell division in vivo. *Science* **302**: 255-259.
- Maury E, Hong HK, Bass J. 2014. Circadian disruption in the pathogenesis of metabolic syndrome. *Diabetes Metab* **40**: 338-346.
- McHill AW, Melanson EL, Higgins J, Connick E, Moehlman TM, Stothard ER, Wright KP, Jr. 2014. Impact of circadian misalignment on energy metabolism during simulated nightshift work. *Proc Natl Acad Sci U S A* 111: 17302-17307.
- McWade MA, Paras C, White LM, Phay JE, Mahadevan-Jansen A, Broome JT. 2013. A novel optical approach to intraoperative detection of parathyroid glands. *Surgery* **154**: 1371-1377; discussion 1377.
- McWade MA, Paras C, White LM, Phay JE, Solorzano CC, Broome JT, Mahadevan-Jansen A. 2014. Label-free intraoperative parathyroid localization with near-infrared autofluorescence imaging. *J Clin Endocrinol Metab* **99**: 4574-4580.
- McWade MA, Thomas G, Nguyen JQ, Sanders ME, Solorzano CC, Mahadevan-Jansen A. 2019. Enhancing Parathyroid Gland Visualization Using a Near Infrared Fluorescence-Based Overlay Imaging System. *J Am Coll Surg* **228**: 730-743.
- Meier JJ, Kjems LL, Veldhuis JD, Lefebvre P, Butler PC. 2006. Postprandial suppression of glucagon secretion depends on intact pulsatile insulin secretion: further evidence for the intraislet insulin hypothesis. *Diabetes* **55**: 1051-1056.
- Merikanto I, Lahti T, Puolijoki H, Vanhala M, Peltonen M, Laatikainen T, Vartiainen E, Salomaa V, Kronholm E, Partonen T. 2013. Associations of chronotype and sleep with cardiovascular diseases and type 2 diabetes. *Chronobiol Int* **30**: 470-477.
- Mohawk JA, Green CB, Takahashi JS. 2012. Central and peripheral circadian clocks in mammals. *Annu Rev Neurosci* **35**: 445-462.
- Mooradian AD. 2009. Dyslipidemia in type 2 diabetes mellitus. *Nat Clin Pract Endocrinol Metab* **5**: 150-159.
- Morris CJ, Yang JN, Garcia JI, Myers S, Bozzi I, Wang W, Buxton OM, Shea SA, Scheer FA. 2015. Endogenous circadian system and circadian misalignment impact glucose tolerance via separate mechanisms in humans. *Proc Natl Acad Sci U S A* 112: E2225-2234.
- Mukherji A, Bailey SM, Staels B, Baumert TF. 2019. The circadian clock and liver function in health and disease. *J Hepatol* **71**: 200-211.
- Mulvihill EE, Assini JM, Lee JK, Allister EM, Sutherland BG, Koppes JB, Sawyez CG, Edwards JY, Telford DE, Charbonneau A et al. 2011. Nobiletin attenuates VLDL overproduction, dyslipidemia, and atherosclerosis in mice with diet-induced insulin resistance. *Diabetes* **60**: 1446-1457.
- Muoio DM, Newgard CB. 2008. Mechanisms of disease:Molecular and metabolic mechanisms of insulin resistance and beta-cell failure in type 2 diabetes. *Nat Rev Mol Cell Biol* **9**: 193-205.
- Nagai K, Fujii T, Inoue S, Takamura Y, Nakagawa H. 1988. Electrical stimulation of the suprachiasmatic nucleus of the hypothalamus causes hyperglycemia. *Horm Metab Res* **20**: 37-39.

- Nicolson TJ, Bellomo EA, Wijesekara N, Loder MK, Baldwin JM, Gyulkhandanyan AV, Koshkin V, Tarasov AI, Carzaniga R, Kronenberger K et al. 2009. Insulin storage and glucose homeostasis in mice null for the granule zinc transporter ZnT8 and studies of the type 2 diabetes-associated variants. *Diabetes* **58**: 2070-2083.
- Nikolaeva S, Ansermet C, Centeno G, Pradervand S, Bize V, Mordasini D, Henry H, Koesters R, Maillard M, Bonny O et al. 2016. Nephron-Specific Deletion of Circadian Clock Gene Bmall Alters the Plasma and Renal Metabolome and Impairs Drug Disposition. *J Am Soc Nephrol* 27: 2997-3004.
- Nir T, Melton DA, Dor Y. 2007. Recovery from diabetes in mice by beta cell regeneration. *J Clin Invest* **117**: 2553-2561.
- Osonoi Y, Mita T, Osonoi T, Saito M, Tamasawa A, Nakayama S, Someya Y, Ishida H, Kanazawa A, Gosho M et al. 2014. Morningness-eveningness questionnaire score and metabolic parameters in patients with type 2 diabetes mellitus. *Chronobiol Int* **31**: 1017-1023.
- Pan X, Queiroz J, Hussain MM. 2020. Nonalcoholic fatty liver disease in CLOCK mutant mice. *J Clin Invest* **130**: 4282-4300.
- Paras C, Keller M, White L, Phay J, Mahadevan-Jansen A. 2011. Near-infrared autofluorescence for the detection of parathyroid glands. *J Biomed Opt* **16**: 067012.
- Paschos GK, Ibrahim S, Song WL, Kunieda T, Grant G, Reyes TM, Bradfield CA, Vaughan CH, Eiden M, Masoodi M et al. 2012. Obesity in mice with adipocyte-specific deletion of clock component Arntl. *Nat Med* **18**: 1768-1777.
- Perelis M, Marcheva B, Ramsey KM, Schipma MJ, Hutchison AL, Taguchi A, Peek CB, Hong H, Huang W, Omura C et al. 2015. Pancreatic beta cell enhancers regulate rhythmic transcription of genes controlling insulin secretion. *Science* **350**: aac4250.
- Perelis M, Ramsey KM, Marcheva B, Bass J. 2016. Circadian Transcription from Beta Cell Function to Diabetes Pathophysiology. *J Biol Rhythms* **31**: 323-336.
- Perrin L, Loizides-Mangold U, Chanon S, Gobet C, Hulo N, Isenegger L, Weger BD, Migliavacca E, Charpagne A, Betts JA et al. 2018. Transcriptomic analyses reveal rhythmic and CLOCK-driven pathways in human skeletal muscle. *Elife* 7.
- Perrin L, Loizides-Mangold U, Skarupelova S, Pulimeno P, Chanon S, Robert M, Bouzakri K, Modoux C, Roux-Lombard P, Vidal H et al. 2015. Human skeletal myotubes display a cell-autonomous circadian clock implicated in basal myokine secretion. *Mol Metab* 4: 834-845.
- Petrenko V, Dibner C. 2018. Cell-specific resetting of mouse islet cellular clocks by glucagon, glucagon-like peptide 1 and somatostatin. *Acta Physiol (Oxf)* **222**: e13021.
- Petrenko V, Gandasi NR, Sage D, Tengholm A, Barg S, Dibner C. 2020. In pancreatic islets from type 2 diabetes patients, the dampened circadian oscillators lead to reduced insulin and glucagon exocytosis. *Proc Natl Acad Sci U S A* 117: 2484-2495.
- Petrenko V, Saini C, Giovannoni L, Gobet C, Sage D, Unser M, Heddad Masson M, Gu G, Bosco D, Gachon F et al. 2017. Pancreatic alpha- and beta-cellular clocks have distinct molecular properties and impact on islet hormone secretion and gene expression. *Genes Dev* 31: 383-398.
- Petrenko V, Sinturel F, Loizides-Mangold U, Montoya JP, Chera S, Riezman H, Dibner C. 2022. Type 2 diabetes disrupts circadian orchestration of lipid metabolism and membrane fluidity in human pancreatic islets. *PLoS Biol* **20**: e3001725.
- Petrenko V, Sinturel F, Riezman H, Dibner C. 2023. Lipid metabolism around the body clocks. *Prog Lipid Res* **91**: 101235.
- Poitout V, Robertson RP. 2008. Glucolipotoxicity: fuel excess and beta-cell dysfunction. *Endocr Rev* **29**: 351-366.

- Pradhan AD, Manson JE, Rifai N, Buring JE, Ridker PM. 2001. C-reactive protein, interleukin 6, and risk of developing type 2 diabetes mellitus. *JAMA* **286**: 327-334.
- Preitner N, Damiola F, Lopez-Molina L, Zakany J, Duboule D, Albrecht U, Schibler U. 2002. The orphan nuclear receptor REV-ERBalpha controls circadian transcription within the positive limb of the mammalian circadian oscillator. *Cell* 110: 251-260.
- Pulimeno P, Mannic T, Sage D, Giovannoni L, Salmon P, Lemeille S, Giry-Laterriere M, Unser M, Bosco D, Bauer C et al. 2013. Autonomous and self-sustained circadian oscillators displayed in human islet cells. *Diabetologia* **56**: 497-507.
- Qian J, Block GD, Colwell CS, Matveyenko AV. 2013. Consequences of exposure to light at night on the pancreatic islet circadian clock and function in rats. *Diabetes* **62**: 3469-3478.
- Qian J, Dalla Man C, Morris CJ, Cobelli C, Scheer F. 2018. Differential effects of the circadian system and circadian misalignment on insulin sensitivity and insulin secretion in humans. *Diabetes Obes Metab* **20**: 2481-2485.
- Qian J, Yeh B, Rakshit K, Colwell CS, Matveyenko AV. 2015. Circadian Disruption and Diet-Induced Obesity Synergize to Promote Development of beta-Cell Failure and Diabetes in Male Rats. *Endocrinology* **156**: 4426-4436.
- Rakshit K, Hsu TW, Matveyenko AV. 2016. Bmall is required for beta cell compensatory expansion, survival and metabolic adaptation to diet-induced obesity in mice. *Diabetologia* **59**: 734-743.
- Regazzi R, Wollheim CB, Lang J, Theler JM, Rossetto O, Montecucco C, Sadoul K, Weller U, Palmer M, Thorens B. 1995. VAMP-2 and cellubrevin are expressed in pancreatic beta-cells and are essential for Ca(2+)-but not for GTP gamma S-induced insulin secretion. *EMBO J* 14: 2723-2730.
- Reimann F, Habib AM, Tolhurst G, Parker HE, Rogers GJ, Gribble FM. 2008. Glucose sensing in L cells: a primary cell study. *Cell Metab* 8: 532-539.
- Reutrakul S, Hood MM, Crowley SJ, Morgan MK, Teodori M, Knutson KL, Van Cauter E. 2013. Chronotype is independently associated with glycemic control in type 2 diabetes. *Diabetes Care* **36**: 2523-2529.
- Ribas-Latre A, Santos RB, Fekry B, Tamim YM, Shivshankar S, Mohamed AMT, Baumgartner C, Kwok C, Gebhardt C, Rivera A et al. 2021. Cellular and physiological circadian mechanisms drive diurnal cell proliferation and expansion of white adipose tissue. *Nat Commun* 12: 3482.
- Rudic RD, McNamara P, Curtis AM, Boston RC, Panda S, Hogenesch JB, Fitzgerald GA. 2004. BMAL1 and CLOCK, two essential components of the circadian clock, are involved in glucose homeostasis. *PLoS Biol* 2: e377.
- Sadacca LA, Lamia KA, deLemos AS, Blum B, Weitz CJ. 2011. An intrinsic circadian clock of the pancreas is required for normal insulin release and glucose homeostasis in mice. *Diabetologia* **54**: 120-124.
- Sadowski SM, Pusztaszeri M, Brulhart-Meynet MC, Petrenko V, De Vito C, Sobel J, Delucinge-Vivier C, Kebebew E, Regazzi R, Philippe J et al. 2018. Identification of Differential Transcriptional Patterns in Primary and Secondary Hyperparathyroidism. *J Clin Endocrinol Metab* **103**: 2189-2198.
- Saini C, Brown SA, Dibner C. 2015. Human peripheral clocks: applications for studying circadian phenotypes in physiology and pathophysiology. *Front Neurol* **6**: 95.
- Saini C, Petrenko V, Pulimeno P, Giovannoni L, Berney T, Hebrok M, Howald C, Dermitzakis ET, Dibner C. 2016. A functional circadian clock is required for proper insulin secretion by human pancreatic islet cells. *Diabetes Obes Metab* 18: 355-365.

- Sanchez-Archidona AR, Cruciani-Guglielmacci C, Roujeau C, Wigger L, Lallement J, Denom J, Barovic M, Kassis N, Mehl F, Weitz J et al. 2021. Plasma triacylglycerols are biomarkers of beta-cell function in mice and humans. *Mol Metab* **54**: 101355.
- Sato M, Murakami M, Node K, Matsumura R, Akashi M. 2014. The role of the endocrine system in feeding-induced tissue-specific circadian entrainment. *Cell Rep* **8**: 393-401.
- Scheer FA, Hilton MF, Mantzoros CS, Shea SA. 2009. Adverse metabolic and cardiovascular consequences of circadian misalignment. *Proc Natl Acad Sci U S A* **106**: 4453-4458.
- Scheiermann C, Kunisaki Y, Frenette PS. 2013. Circadian control of the immune system. *Nat Rev Immunol* **13**: 190-198.
- Scheuner D, Kaufman RJ. 2008. The unfolded protein response: a pathway that links insulin demand with beta-cell failure and diabetes. *Endocr Rev* **29**: 317-333.
- Schmalen I, Reischl S, Wallach T, Klemz R, Grudziecki A, Prabu JR, Benda C, Kramer A, Wolf E. 2014. Interaction of circadian clock proteins CRY1 and PER2 is modulated by zinc binding and disulfide bond formation. *Cell* **157**: 1203-1215.
- Schrader H, Menge BA, Breuer TG, Ritter PR, Uhl W, Schmidt WE, Holst JJ, Meier JJ. 2009. Impaired glucose-induced glucagon suppression after partial pancreatectomy. *J Clin Endocrinol Metab* **94**: 2857-2863.
- Shimba S, Ogawa T, Hitosugi S, Ichihashi Y, Nakadaira Y, Kobayashi M, Tezuka M, Kosuge Y, Ishige K, Ito Y et al. 2011. Deficient of a clock gene, brain and muscle Arnt-like protein-1 (BMAL1), induces dyslipidemia and ectopic fat formation. *PLoS One* **6**: e25231.
- Shivaswamy V, Boerner B, Larsen J. 2016. Post-Transplant Diabetes Mellitus: Causes, Treatment, and Impact on Outcomes. *Endocr Rev* **37**: 37-61.
- Shulman GI, Rothman DL, Jue T, Stein P, DeFronzo RA, Shulman RG. 1990. Quantitation of muscle glycogen synthesis in normal subjects and subjects with non-insulin-dependent diabetes by 13C nuclear magnetic resonance spectroscopy. *N Engl J Med* **322**: 223-228.
- Sinturel F, Gos P, Petrenko V, Hagedorn C, Kreppel F, Storch KF, Knutti D, Liani A, Weitz C, Emmenegger Y et al. 2021. Circadian hepatocyte clocks keep synchrony in the absence of a master pacemaker in the suprachiasmatic nucleus or other extrahepatic clocks. *Genes Dev* **35**: 329-334.
- Sinturel F, Petrenko V, Dibner C. 2020a. Circadian Clocks Make Metabolism Run. *J Mol Biol.* -. 2020b. Circadian Clocks Make Metabolism Run. *J Mol Biol* 432: 3680-3699.
- Skene DJ, Skornyakov E, Chowdhury NR, Gajula RP, Middleton B, Satterfield BC, Porter KI, Van Dongen HPA, Gaddameedhi S. 2018. Separation of circadian- and behavior-driven metabolite rhythms in humans provides a window on peripheral oscillators and metabolism. *Proc Natl Acad Sci U S A* 115: 7825-7830.
- Skyler JS, Bakris GL, Bonifacio E, Darsow T, Eckel RH, Groop L, Groop PH, Handelsman Y, Insel RA, Mathieu C et al. 2017. Differentiation of Diabetes by Pathophysiology, Natural History, and Prognosis. *Diabetes* 66: 241-255.
- Spranger J, Kroke A, Mohlig M, Hoffmann K, Bergmann MM, Ristow M, Boeing H, Pfeiffer AF. 2003. Inflammatory cytokines and the risk to develop type 2 diabetes: results of the prospective population-based European Prospective Investigation into Cancer and Nutrition (EPIC)-Potsdam Study. *Diabetes* **52**: 812-817.
- Stamenkovic JA, Olsson AH, Nagorny CL, Malmgren S, Dekker-Nitert M, Ling C, Mulder H. 2012. Regulation of core clock genes in human islets. *Metabolism* **61**: 978-985.
- Talchai C, Xuan S, Lin HV, Sussel L, Accili D. 2012. Pancreatic beta cell dedifferentiation as a mechanism of diabetic beta cell failure. *Cell* **150**: 1223-1234.
- Teta M, Rankin MM, Long SY, Stein GM, Kushner JA. 2007. Growth and regeneration of adult beta cells does not involve specialized progenitors. *Dev Cell* 12: 817-826.

- Thorel F, Nepote V, Avril I, Kohno K, Desgraz R, Chera S, Herrera PL. 2010. Conversion of adult pancreatic alpha-cells to beta-cells after extreme beta-cell loss. *Nature* **464**: 1149-1154.
- Turek FW, Joshu C, Kohsaka A, Lin E, Ivanova G, McDearmon E, Laposky A, Losee-Olson S, Easton A, Jensen DR et al. 2005. Obesity and metabolic syndrome in circadian Clock mutant mice. *Science* **308**: 1043-1045.
- Tuvia N, Pivovarova-Ramich O, Murahovschi V, Luck S, Grudziecki A, Ost AC, Kruse M, Nikiforova VJ, Osterhoff M, Gottmann P et al. 2021. Insulin Directly Regulates the Circadian Clock in Adipose Tissue. *Diabetes* **70**: 1985-1999.
- Unger RH, Orci L. 1975. The essential role of glucagon in the pathogenesis of diabetes mellitus. *Lancet* 1: 14-16.
- van Leeuwen WM, Hublin C, Sallinen M, Harma M, Hirvonen A, Porkka-Heiskanen T. 2010. Prolonged sleep restriction affects glucose metabolism in healthy young men. *Int J Endocrinol* **2010**: 108641.
- Vetter C, Dashti HS, Lane JM, Anderson SG, Schernhammer ES, Rutter MK, Saxena R, Scheer F. 2018. Night Shift Work, Genetic Risk, and Type 2 Diabetes in the UK Biobank. *Diabetes Care* 41: 762-769.
- Vetter C, Devore EE, Ramin CA, Speizer FE, Willett WC, Schernhammer ES. 2015. Mismatch of Sleep and Work Timing and Risk of Type 2 Diabetes. *Diabetes Care* 38: 1707-1713.
- Walker MD, Silverberg SJ. 2018. Primary hyperparathyroidism. *Nat Rev Endocrinol* **14**: 115-125.
- Wefers J, van Moorsel D, Hansen J, Connell NJ, Havekes B, Hoeks J, van Marken Lichtenbelt WD, Duez H, Phielix E, Kalsbeek A et al. 2018. Circadian misalignment induces fatty acid metabolism gene profiles and compromises insulin sensitivity in human skeletal muscle. *Proc Natl Acad Sci U S A* 115: 7789-7794.
- Wehrens SMT, Christou S, Isherwood C, Middleton B, Gibbs MA, Archer SN, Skene DJ, Johnston JD. 2017. Meal Timing Regulates the Human Circadian System. *Curr Biol* **27**: 1768-1775 e1763.
- Weir GC, Gaglia J, Bonner-Weir S. 2020. Inadequate beta-cell mass is essential for the pathogenesis of type 2 diabetes. *Lancet Diabetes Endocrinol* 8: 249-256.
- Wiedemann SJ, Trimigliozzi K, Dror E, Meier DT, Molina-Tijeras JA, Rachid L, Le Foll C, Magnan C, Schulze F, Stawiski M et al. 2022. The cephalic phase of insulin release is modulated by IL-1beta. *Cell Metab* **34**: 991-1003 e1006.
- Wilms B, Leineweber EM, Molle M, Chamorro R, Pommerenke C, Salinas-Riester G, Sina C, Lehnert H, Oster H, Schmid SM. 2019. Sleep Loss Disrupts Morning-to-Evening Differences in Human White Adipose Tissue Transcriptome. *J Clin Endocrinol Metab* **104**: 1687-1696.
- Yamamoto H, Nagai K, Nakagawa H. 1987. Role of SCN in daily rhythms of plasma glucose, FFA, insulin and glucagon. *Chronobiol Int* **4**: 483-491.
- Yamamoto J, Imai J, Izumi T, Takahashi H, Kawana Y, Takahashi K, Kodama S, Kaneko K, Gao J, Uno K et al. 2017. Neuronal signals regulate obesity induced β-cell proliferation by FoxM1 dependent mechanism. *Nature Communications* 8: 1930.
- Ying W, Lee YS, Dong Y, Seidman JS, Yang M, Isaac R, Seo JB, Yang BH, Wollam J, Riopel M et al. 2019. Expansion of Islet-Resident Macrophages Leads to Inflammation Affecting beta Cell Proliferation and Function in Obesity. *Cell Metab* **29**: 457-474 e455.
- Yoo SH, Yamazaki S, Lowrey PL, Shimomura K, Ko CH, Buhr ED, Siepka SM, Hong HK, Oh WJ, Yoo OJ et al. 2004. PERIOD2::LUCIFERASE real-time reporting of circadian dynamics reveals persistent circadian oscillations in mouse peripheral tissues. *Proc Natl Acad Sci U S A* **101**: 5339-5346.

- Yu F, Wang Z, Zhang T, Chen X, Xu H, Wang F, Guo L, Chen M, Liu K, Wu B. 2021. Deficiency of intestinal Bmall prevents obesity induced by high-fat feeding. *Nat Commun* 12: 5323.
- Yu JH, Yun CH, Ahn JH, Suh S, Cho HJ, Lee SK, Yoo HJ, Seo JA, Kim SG, Choi KM et al. 2015. Evening chronotype is associated with metabolic disorders and body composition in middle-aged adults. *J Clin Endocrinol Metab* **100**: 1494-1502.
- Zhang EE, Liu Y, Dentin R, Pongsawakul PY, Liu AC, Hirota T, Nusinow DA, Sun X, Landais S, Kodama Y et al. 2010. Cryptochrome mediates circadian regulation of cAMP signaling and hepatic gluconeogenesis. *Nat Med* **16**: 1152-1156.
- Zhang H, Ackermann AM, Gusarova GA, Lowe D, Feng X, Kopsombut UG, Costa RH, Gannon M. 2006. The FoxM1 transcription factor is required to maintain pancreatic beta-cell mass. *Mol Endocrinol* **20**: 1853-1866.
- Zhang Y, Fang B, Emmett MJ, Damle M, Sun Z, Feng D, Armour SM, Remsberg JR, Jager J, Soccio RE et al. 2015. GENE REGULATION. Discrete functions of nuclear receptor Rev-erbalpha couple metabolism to the clock. *Science* **348**: 1488-1492.
- Zhong F, Jiang Y. 2019. Endogenous Pancreatic beta Cell Regeneration: A Potential Strategy for the Recovery of beta Cell Deficiency in Diabetes. *Front Endocrinol (Lausanne)* **10**: 101.
- Zhou Q, Melton DA. 2018. Pancreas regeneration. Nature 557: 351-358.
- Zhou S, Tang X, Chen HZ. 2018. Sirtuins and Insulin Resistance. *Front Endocrinol (Lausanne)* 9: 748.
- Zhu X, Hu R, Brissova M, Stein RW, Powers AC, Gu G, Kaverina I. 2015. Microtubules Negatively Regulate Insulin Secretion in Pancreatic beta Cells. *Dev Cell* **34**: 656-668.

ANNEXES

PUBLICATION 1.

Petrenko V, Saini C, Giovannoni L, Gobet C, Sage D, Unser M, Heddad Masson M, Gu G, Bosco D, Gachon F, Philippe J, Dibner C. Pancreatic α- and β-cellular clocks have distinct molecular properties and impact on islet hormone secretion and gene expression. Genes Dev. 2017 Feb 15;31(4):383-398. doi: 10.1101/gad.290379.116. Epub 2017 Mar 8. PMID: 28275001; PMCID: PMC5358758.

PUBLICATION 2.

Petrenko V, Stolovich-Rain M, Vandereycken B, Giovannoni L, Storch KF, Dor Y, Chera S, Dibner C. The core clock transcription factor BMAL1 drives circadian β-cell proliferation during compensatory regeneration of the endocrine pancreas. Genes Dev. 2020 Dec 1;34(23-24):1650-1665. doi: 10.1101/gad.343137.120. Epub 2020 Nov 12. PMID: 33184223; PMCID: PMC7706703.

PUBLICATION 3.

Saini C, Petrenko V, Pulimeno P, Giovannoni L, Berney T, Hebrok M, Howald C, Dermitzakis ET, Dibner C. A functional circadian clock is required for proper insulin secretion by human pancreatic islet cells. Diabetes Obes Metab. 2016 Apr;18(4):355-65. doi: 10.1111/dom.12616. Epub 2016 Jan 22. PMID: 26662378.

PUBLICATION 4.

Petrenko V, Gandasi NR, Sage D, Tengholm A, Barg S, Dibner C. In pancreatic islets from type 2 diabetes patients, the dampened circadian oscillators lead to reduced insulin and glucagon exocytosis. Proc Natl Acad Sci U S A. 2020 Feb 4;117(5):2484-2495. doi: 10.1073/pnas.1916539117. Epub 2020 Jan 21. PMID: 31964806; PMCID: PMC7007532.

PUBLICATION 5.

Petrenko V, Sinturel F, Loizides-Mangold U, Montoya JP, Chera S, Riezman H, Dibner C. Type 2 diabetes disrupts circadian orchestration of lipid metabolism and membrane fluidity in human pancreatic islets. PLoS Biol. 2022 Aug 3;20(8):e3001725. doi: 10.1371/journal.pbio.3001725. PMID: 35921354; PMCID: PMC9348689.

Pancreatic α - and β -cellular clocks have distinct molecular properties and impact on islet hormone secretion and gene expression

Volodymyr Petrenko,^{1,2,3} Camille Saini,^{1,2,3,9} Laurianne Giovannoni,^{1,2,3,9} Cedric Gobet,^{4,5,9} Daniel Sage,⁶ Michael Unser,⁶ Mounia Heddad Masson,¹ Guoqiang Gu,⁷ Domenico Bosco,⁸ Frédéric Gachon,^{4,5,10} Jacques Philippe,^{1,10} and Charna Dibner^{1,2,3}

¹Endocrinology, Diabetes, Hypertension, and Nutrition, University Hospital of Geneva, CH-1211 Geneva, Switzerland; ²Department of Cellular Physiology and Metabolism, Diabetes Center, Faculty of Medicine, University of Geneva, CH-1211 Geneva, Switzerland; ³Institute of Genetics and Genomics in Geneva (iGE3), University of Geneva, CH-1211 Geneva, Switzerland; ⁴Department of Diabetes and Circadian Rhythms, Nestlé Institute of Health Sciences, CH-1015 Lausanne, Switzerland; ⁵School of Life Sciences, Ecole Polytechnique Fédérale de Lausanne (EPFL), CH-1015 Lausanne, Switzerland; ⁶Biomedical Imaging Group, EPFL, CH-1015 Lausanne, Switzerland; ⁷Department of Cell and Developmental Biology, Vanderbilt University Medical Center, Nashville, Tennessee 37240, USA; ⁸Department of Surgery, Cell Isolation and Transplantation Centre, University Hospital of Geneva, CH-1211 Geneva, Switzerland

A critical role of circadian oscillators in orchestrating insulin secretion and islet gene transcription has been demonstrated recently. However, these studies focused on whole islets and did not explore the interplay between α -cell and β -cell clocks. We performed a parallel analysis of the molecular properties of α -cell and β -cell oscillators using a mouse model expressing three reporter genes: one labeling α cells, one specific for β cells, and a third monitoring circadian gene expression. Thus, phase entrainment properties, gene expression, and functional outputs of the α -cell and β -cell clockworks could be assessed in vivo and in vitro at the population and single-cell level. These experiments showed that α -cellular and β -cellular clocks are oscillating with distinct phases in vivo and in vitro. Diurnal transcriptome analysis in separated α and β cells revealed that a high number of genes with key roles in islet physiology, including regulators of glucose sensing and hormone secretion, are differentially expressed in these cell types. Moreover, temporal insulin and glucagon secretion exhibited distinct oscillatory profiles both in vivo and in vitro. Altogether, our data indicate that differential entrainment characteristics of circadian α -cell and β -cell clocks are an important feature in the temporal coordination of endocrine function and gene expression.

[Keywords: mouse α cells and β cells, circadian clock; insulin/glucagon secretion; RNA sequencing; single-cell bioluminescence–fluorescence time-lapse microscopy]

Supplemental material is available for this article.

Received September 9, 2016; revised version accepted February 2, 2017.

The circadian timing system is a mechanism developed in virtually all organisms from bacteria to humans that allows one to anticipate the changes of geophysical time (Partch et al. 2014). The mammalian circadian clock is organized in a hierarchical structure, with a master pacemaker residing in the suprachiasmatic nuclei (SCNs) of the hypothalamus that establishes phase coherence in the body by synchronizing every day the slave oscillators residing in the periphery, encompassing billions of individual cellular clocks (Partch et al. 2014). While light in-

put represents the dominant timing cue (Zeitgeber) for the oscillators of SCN neurons, feeding cycles driven by rest-activity rhythms have a major impact on the entrainment of peripheral clocks (Dibner and Schibler 2015a). Metabolism and circadian rhythms are therefore tightly linked through complex behavioral and molecular pathways (Perelis et al. 2015b). Moreover, cell-autonomous self-sustained peripheral clocks operative in nearly every cell in the body are connected to the metabolic state of

⁹These authors contributed equally to this work.

¹⁰These authors contributed equally to this work.

Corresponding author: charna.dibner@hcuge.ch

Article published online ahead of print. Article and publication date are online at http://www.genesdev.org/cgi/doi/10.1101/gad.290379.116.

© 2017 Petrenko et al. This article is distributed exclusively by Cold Spring Harbor Laboratory Press for the first six months after the full-issue publication date (see http://genesdev.cshlp.org/site/misc/terms.xhtml). After six months, it is available under a Creative Commons License (Attribution-NonCommercial 4.0 International), as described at http://creativecommons.org/licenses/by-nc/4.0/.

the cell (Asher and Schibler 2011; Asher and Sassone-Corsi 2015; Perrin et al. 2015).

Circadian oscillators in the endocrine pancreas have been demonstrated recently to play an essential role in driving transcription and function of the pancreatic islet in mice and humans (Marcheva et al. 2010; Sadacca et al. 2011; Pulimeno et al. 2013; Qian et al. 2013; Perelis et al. 2015a; Saini et al. 2016). Moreover, ablation of the islet clock in mouse models, including islet clock perturbation induced at an adult age, directly triggers the onset of type 2 diabetes (T2D) (Marcheva et al. 2010; Sadacca et al. 2011; Perelis et al. 2015a). These findings provide a direct functional link between the molecular clock operative in pancreatic islets, its function under physiological conditions, and the etiology of T2D.

Pancreatic islets represent an intricate model comprising α and β cells as main endocrine cell types, secreting the counterregulatory hormones glucagon and insulin, respectively. Beyond the primordial role of β -cell dysfunction in T2D development, alterations in α -cell function and resulting hyperglucagonemia are important components of the metabolic aberrations associated with T2D (Unger and Orci 1975). Therefore, studies of α -cell physiology and regulation of glucagon secretion have caught more attention, particularly with respect to potential T2D treatment (Gromada et al. 2007; Thorel et al. 2010; Zaret and White 2010).

In the pancreas, circadian regulation of its endocrine function has been studied at the level of whole islets, therefore mostly unravelling clock regulations occurring in β cells, representing >80% of the mouse islet cell content. Consequently, the circadian physiology of a cells, representing ~10%-15% of islet cells in mice, stayed largely unexplored. We therefore focused on the physiological importance of the α-cell clock and its impact on transcription and glucagon secretion. Furthermore, we assessed αcell and β-cell circadian properties in parallel by developing experimental settings that allowed us to simultaneously monitor the molecular makeup of the clock and the circadian physiology of separated α and β cells. Diurnal transcriptome analysis in separated populations of α and β cells, assessed through next-generation RNA sequencing (RNA-seq), revealed that a high number of key functional genes in both islet cell types exhibited rhythmic expression patterns with either common or distinct properties. Interestingly, the phase of key core clock components was shifted between α -cell and β -cell clocks in vivo. Furthermore, a similar effect was observed by in vitro population analysis of separated α and β cells synchronized with physiologically relevant cues and by high-resolution single-cell bioluminescence-fluorescence time-lapse microscopy (Pulimeno et al. 2013). The distinct coordination between α -cellular and β -cellular clocks may account for the regulation of insulin and glucagon secretion profiles, exhibiting oscillatory profiles in vivo in the blood and in vitro as recorded by cell perifusion (Saini et al. 2016). This work is the first integrative analysis on the molecular properties of circadian clocks operative in α and β cells that brings new insights into the complex regulation of islet cell physiology at the transcriptional and functional level.

Results

RNA-seq analysis reveals distinct expression patterns in α and β cells

To analyze the α-cell and β-cell transcriptome and function in parallel, we combined the proglucagon (Gcg)-Venus reporter mouse (Reimann et al. 2008) with the βcell-specific rat insulin2 promoter (RIP)-Cherry reporter mouse for specific labeling of α cells (Zhu et al. 2015) and with the Period2::Luciferase (Per2::Luc) knock-in mouse (Yoo et al. 2004) for assessment of circadian clock properties (Supplemental Fig. S1). To identify the transcripts expressed in a rhythmic manner in α and β cells, separated populations of these two cell types were isolated from triple reporter islets at six time points over 24 h and subjected to genome-wide transcriptome analysis by RNA-seq (data available at Gene Expression Omnibus [http://www.ncbi.nlm.nih.gov/geo] through accession number GSE95156) (Materials and Methods; Supplemental Figs. S1, S2). A total of 12,452 transcripts expressed with log₂ reads per kilobase per million mapped reads (RPKM) > 0 in at least one cell type were identified (Supplemental Data Set 1). Two types of analyses were applied to each identified transcript: (1) differential expression level analysis between α and β cells and (2) assessment of 24-h period rhythmicity of the transcript (Fig. 1A). Based on the average expression of six time points, we considered genes exhibiting an expression difference of >16 (absolute log₂ fold change >4, false discovery rate [FDR]adjusted P-value < 0.05) between the two cell types as differentially expressed. Such differential expression analysis, illustrated in Figure 1B, identified 284 transcripts that were highly enriched in α or β cells and detected in either both cell types (40 genes; group A) (Supplemental Data Set 1) or one cell type only (244 genes; group B). An additional group of 997 genes demonstrated a lower cellspecific differential expression (absolute log2 fold change <4; group D). These transcripts were expressed in one cell type only at a globally lower level (maximum log₂) RPKM < 4) (Supplemental Fig. S3A). Finally, the remaining ~90% of all identified transcripts were expressed in both cell types with nondifferential (<16-fold difference) absolute levels (11,171 genes; group C).

The temporal patterns of all analyzed transcripts were divided into 18 models according to their rhythmic properties in one or both cell types and with respect to their differential expression (Fig. 1A and legend). Importantly, along with the high number of key functional transcripts exhibiting a similar rhythmic pattern in both cell types (models 4 and 13) (Fig. 1A), numerous transcripts harboured distinct temporal profiles in α and β cells.

Temporal patterns of functional genes differentially expressed in α and β cells

Most of the classical α -cell- and β -cell-specific transcripts were differentially expressed (group A and B) (Supplemental Data Set 1), confirming the accuracy of our cell separation approach. As expected, hormone transcripts *Ins1* and

Circadian physiology of a and B cells

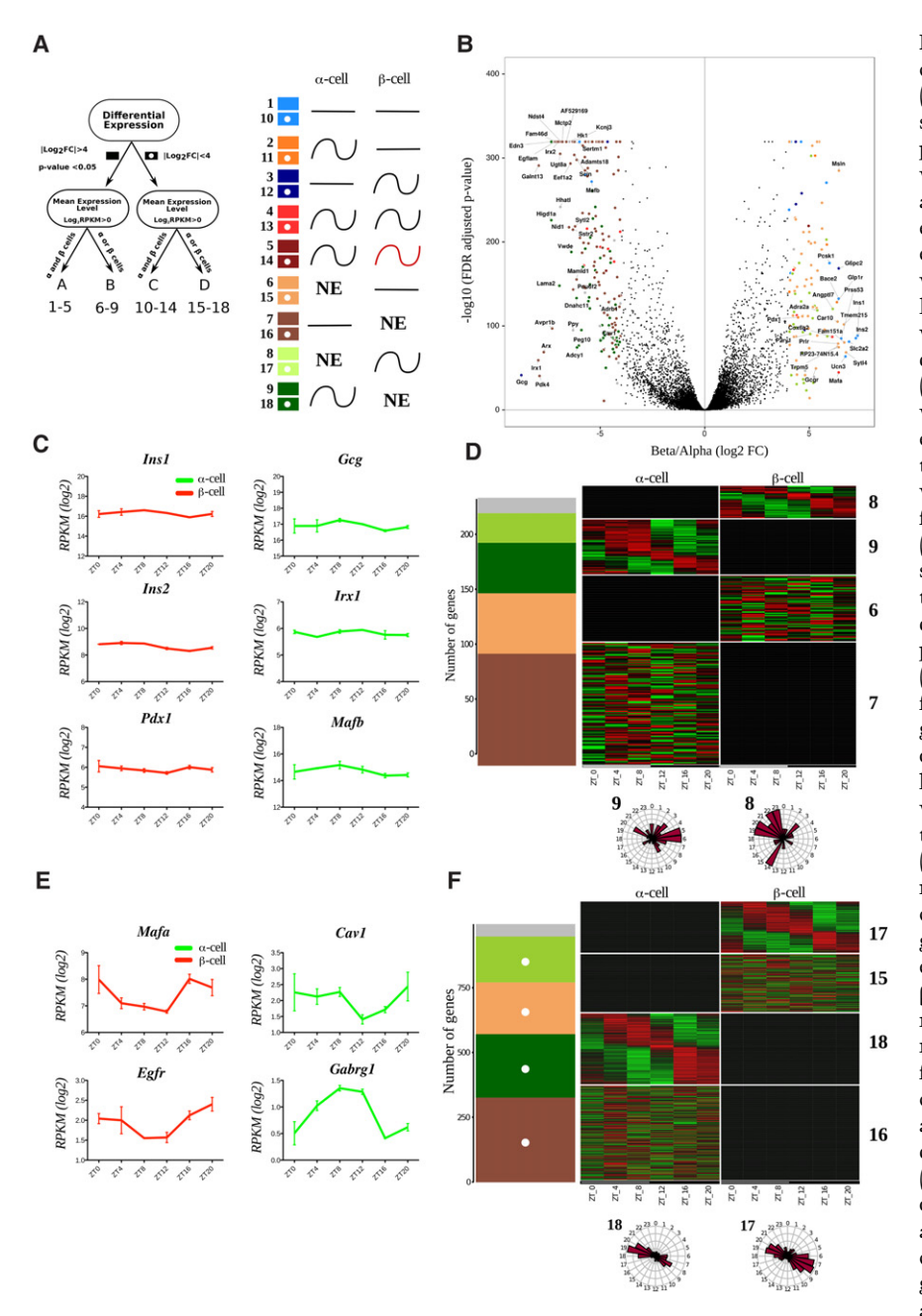


Figure 1. Temporal pattern of transcripts differentially expressed in α and β cells. (A) Groups and models assigned to transcripts with respect to their differential expression and rhythmic pattern. Transcripts with expression levels of log_2 RPKM > 0 in at least one of the cell types were considered as expressed in this cell type and nonexpressed (NE) in the other cell type. Genes with expression differences >16-fold (absolute log₂ fold change >4; FDR-adjusted Pvalue < 0.05) between two cell types were considered as differentially expressed (groups A and B; solid-colored squares), while those with expression level differences <16-fold were considered as nondifferentially expressed (groups C and D; squares with white dots). We therefore obtained four independent groups of genes: group A (differentially expressed α-cell- and β-cellspecific transcripts detectable in both cell types), group B (differentially expressed αcell- and β-cell-specific transcripts expressed in one single cell type), group C (genes expressed in α and β cells with lower fold change), and group D (genes in one single cell type with lower fold change). Based on harmonic regression with a period of 24 h, model selection to assess rhythmicity was applied to these four groups. An arbitrary threshold of 0.4 was set on BIC weight (BICW). Genes were assigned to one of the nine pairs of models: groups A and C: genes defined as nonrhythmic (models 1 and 10), genes defined as rhythmic in a cells (models 2 and 11), genes defined as rhythmic in β cells (models 3 and 12), genes defined as rhythmic in both cell types with similar parameters (models 4 and 13), and genes defined as rhythmic in both cell types with different parameters (models 5 and 14); and groups B and D: genes expressed in β cells only and defined as nonrhythmic (models 6 and 15), genes expressed in α cells only and defined as nonrhythmic (models 7 and 16), genes expressed in β cells only and defined as rhythmic (models 8 and 17), and genes expressed in a cells only and defined as rhythmic (models 9 and 18). (NE) Gene

is not expressed. Genes with lower BICWs were considered as undefined (model 0) and are represented as a gray bar in D and F. (B) Volcano plot presenting the transcripts differentially expressed in α cells (\log_2 fold change less than -4) or β cells (\log_2 fold change >4). Differentially expressed genes are identified by colored dots corresponding to their respective model. (C, E) Temporal expression profiles for selected non-rhythmic (E) transcripts differentially expressed in β cells (left) and α cells (right). Only the profile on the higher-expression cell type is shown. Data represent the mean of two biological replicates per time point (each replicate is a mix of cells from six mice). Error bars express the SD of two independent experiments. (D, F) Rhythmic expression heat maps for transcripts of groups B and D. The number of genes distributed by models (described in A) is depicted in the left panel. (Right panels) Corresponding heat maps showing relative expression indicated in green (low) and red (high). Phase distribution of rhythmic genes is presented in the adjacent polar histograms.

Ins2 and β-cell-specific transcription factors (*Mafa, Ucn3, Nkx6-1, Mnx1,* and *Pdx1*) were expressed in β cells with highest significance, while Gcg and α-cell-specific transcription factors (*Mafb, Irx1, Irx2,* and *Arx*) were significantly differentially expressed in α cells, validating the specificity of the cell populations in our experimental

conditions. Most of the above-mentioned cell-specific transcription factors as well as genes encoding for insulin and glucagon were nonrhythmic (Fig. 1C), except for *Mafa*, which was oscillating (Fig. 1E). The low-level expression of classical α -cell- and β -cell-specific transcripts in the opposite cell type might be attributed to the actual

expression in this cell type or minor cross-contamination between two cell populations during the fluorescence-activated cell sorting (FACS) procedure.

With respect to the assessment of rhythmic expression patterns (groups A and B), 34 transcripts (seven in group A and 27 in group B; models 3 and 8, respectively) were qualified as rhythmic in β cells, and 51 (five in group A and 46 in group B; models 2 and 9, respectively) were qualified as rhythmic in α cells (Fig. 1D,E; Supplemental Fig. S3B; Supplemental Data Set 1). According to gene ontology (GO) term analysis, the rhythmic β-cell-specific genes were enriched in biological processes such as cell adhesion, protein and hormone transport and secretion, and neuroactive ligand-receptor interaction. Rhythmic genes in α cells were enriched in processes such as cell signalling, development, and synaptic transmission and for pathways of the complement and coagulation cascade (Supplemental Data Sets 2, 3; Supplemental Table 1). Of note, the peak phase for the expression of α -cell-specific transcripts was mainly during the day, whereas the peak phase for β-cell genes occurred mainly during the end of the night (Fig. 1D; Supplemental Fig. S3B; Supplemental Data Set 1).

Among the genes defined as group D (Fig. 1A), 245 transcripts exhibited rhythmic expression in β cells (model 17), whereas 177 transcripts exhibited rhythmic expression in α cells (model 18) (Fig. 1F; Supplemental Data Set 1). The oscillatory profile of these transcripts showed two principal peaks at Zeitgeber time 8 (ZT8) and ZT20 in both cell types (Fig. 1F). β -Cell-specific transcripts from this group of genes were involved mainly in ion transport, while α -cell-specific transcripts were associated with intracellular component movement and morphology, cell signalling, and developmental processes (Supplemental Data Set 5).

Temporal patterns of genes nondifferentially expressed in α and β cells

Most transcripts with nondifferential levels of expression in the two cell types, classified as group C, were distributed between five models (models 10-14) according to their temporal expression pattern (Figs. 1A, 2A). Genes comprising this group were involved in a high number of different basal metabolic processes (Supplemental Data Set 4). Interestingly, most of the genes involved in hormone secretion were rhythmic, with similar circadian parameters in both cell types (Supplemental Data Set 4, model 13). While no significant GO term enrichment could be identified for this group due to the large number of genes with a wide range of different functions (Supplemental Data Set 1, 4), many key genes involved in intracellular signalling, granule trafficking and exocytosis, mitochondrial ATP production, and ion channels were present in this group (Fig. 2, model 13; Supplemental Data Set 1; Supplemental Table 1). Of note, a group of 751 genes exhibited a rhythmic pattern in α cells only (model 11), comprising Pcsk2, Vegfa, and Ccnd3 (Fig. 2B). On the other hand, 1126 genes were rhythmic in β cells only (model 12), comprising those involved in endoplasmic reticulum-associated functions and glucose metabolism (Fig. 2A,B; Supplemental Data Set 1, 4; Supplemental Table 1). Finally, 352 genes were rhythmic in both cell types, with distinct oscillatory parameters in α and β cells (Fig. 2A,B, model 14; Supplemental Data Set 1, 4).

RNA-seq reveals distinct rhythmic phases for the expression profiles of core clock transcripts in α and β cells

Surprisingly, the most enriched biological function in the above-mentioned group of genes with distinct oscillatory parameters (group C model 14) was the GO term "circadian rhythm" (Fig. 3A,B; Supplemental Fig. S4; Supplemental Data Set 4). Indeed, several core clock transcripts, including Bmall (Arntl), Reverba (Nr1d1), and Cry1, exhibited distinct rhythmic patterns of expression in α and β cells, with the β-cell core clock genes being phase-advanced ~4 h compared with their α-cell counterparts (Fig. 3C; Supplemental Fig. S4). The phase coherence between the rhythmic profiles of these transcripts expressed in α and β cells was further confirmed by quantitative RT-PCR (qRT-PCR\(Fig. 3C\). Collectively, these data suggest that α-cellular and β-cellular clocks exhibit comparable rhythmic amplitudes but distinct phases in vivo, with β-cell clocks being phase-advanced compared with α-cell clocks.

 α -Cellular and β -cellular clocks synchronized in vitro by forskolin exhibit distinct circadian profiles at the population and single-cell levels

Since different rhythmic phases observed for core clock transcripts in vivo might be attributed to distinct entrainment properties of α and β cells, analysis of circadian properties of α-cell and β-cell populations was further undertaken in vitro. PER2::Luc profiles were recorded in intact islets and for dispersed islet cells synchronized with forskolin, which has been shown previously to be an efficient synchronizer for intact mouse and human islets (Perelis et al. 2015a; Saini et al. 2016). No difference was observed between the circadian profiles of whole islets and a mixed islet cell population (Supplemental Fig. S5A). Next, we conducted population analysis of separated pure α and β cells synchronized with forskolin (Fig. 4A). Forskolin induced high-amplitude oscillations in both cell types compared with the respective controls stimulated with medium change only (Supplemental Fig. S5B). Of note, separated α cells exhibited significantly earlier circadian phase in comparison with β cells, with no significant change in the circadian period length (Fig. 4A; Supplemental Table 2).

To explore individual cellular rhythms, we performed single-cell analysis of mouse α and β cells using a high-resolution combined bioluminescence–fluorescence time-lapse microscopy approach (Pulimeno et al. 2013). Dispersed triple transgenic islet cells synchronized with forskolin were subjected to time-lapse microscopy (Fig. 4B, C; Supplemental Movies S1, S2). The PER2::Luc bioluminescence profiles of α cells (Venus-positive) and β cells (Cherry-positive) were analyzed (Fig. 4D). Based on the analysis of 49 α cells and 55 β cells in eight time-lapse

Circadian physiology of α and β cells

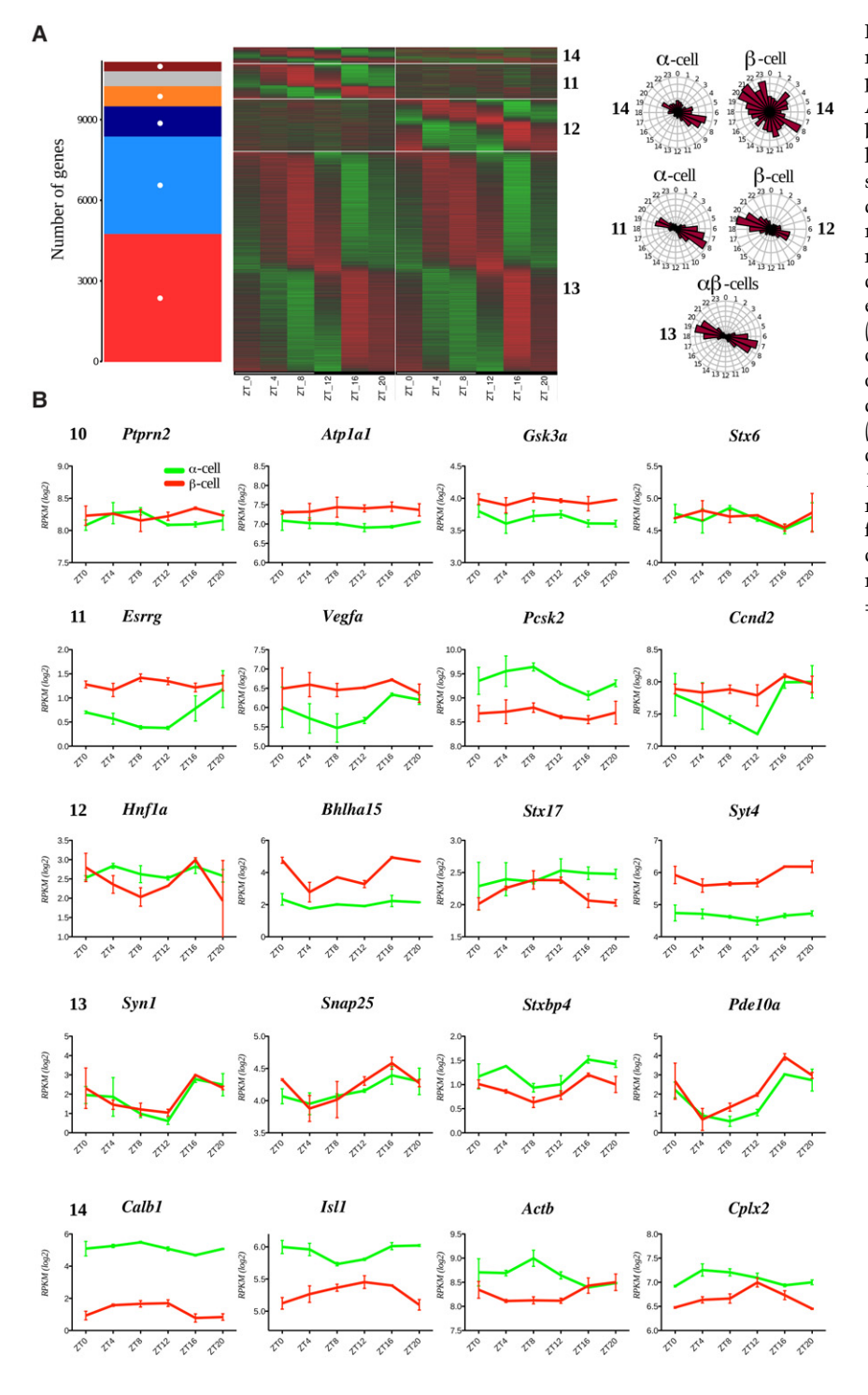


Figure 2. Comparative analysis of temporal expression patterns of the transcripts expressed in α and β cells (group C in Fig. 1A). A total of 11,171 transcripts expressed in both α and β cells (log₂ RPKM > 0) and exhibiting the expression level differences absolute log₂ fold change <4 between the two cell types were assigned to one of the five models (models 10-14 in Fig. 1A). (A) The number of genes assigned in models and corresponding heat maps showing relative expression indicated in green (low) and red (high). The gray bar represents genes not classified in any models. Phase distribution of rhythmic genes is presented on the adjacent polar histograms for rhythmic genes in (1) one cell type (models 11 and 12), (2) both cell types with the same parameters (model 13), or (3) both cell types with different parameters (model 14). (B) Temporal profiles for selected transcripts expressed in both cell types delineated to one of the rhythmicity models. Data are expressed as mean ± SD of two independent experiments.

microscopy experiments, the circadian phase of PER2::Luc bioluminescence profile was significantly advanced in α cells when compared with β cells (Fig. 4E), in agreement with the population analysis (cf. Fig. 4A). Of note, we observed an opposite tendency for the phase shift between α -cellular and β -cellular clocks in vivo (Fig. 3B,C) compared with in vitro following forskolin synchronization (Fig. 4A,E).

Adrenaline, but not insulin, exerts differential synchronizing effects on α -cellular and β -cellular clocks in vitro

To decipher potential differences in the α -cellular and β -cellular clock entrainment properties in vitro, the physiologically relevant synchronizers insulin and adrenaline were applied to the islet cells. In vitro synchronization

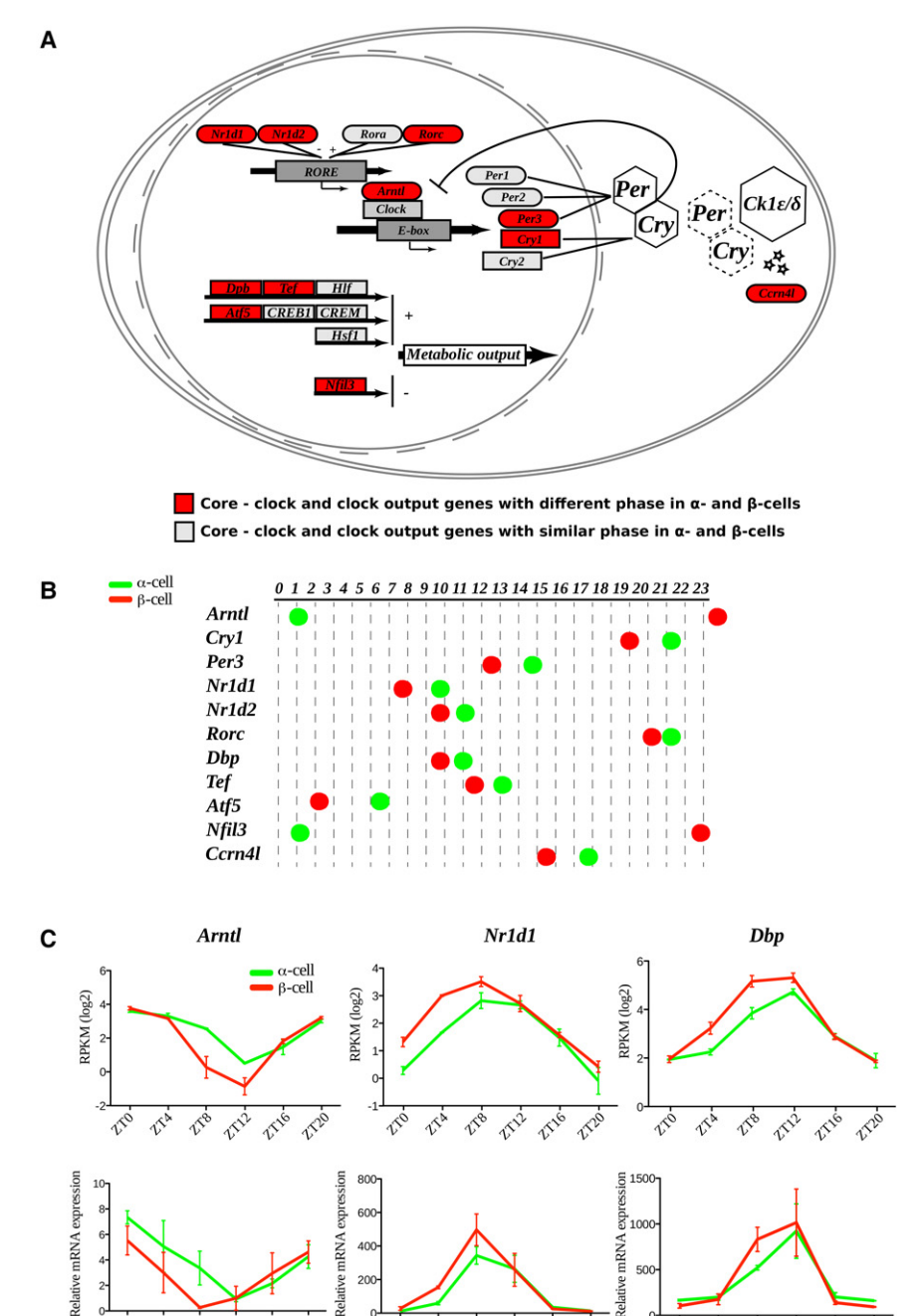


Figure 3. Core clock transcripts expressed in α and β cells exhibit distinct rhythmic phases in vivo. (A) Mapping of identified α-cell and β-cell molecular clock and clock-controlled transcripts into modified "circadian rhythm" KEGG (Kyoto Encyclopedia of Genes and Genomes) pathways. Transcripts exhibiting distinct rhythmic phases in α and β cells are marked in red, and those with similar phases are marked in gray. (B) Rhythmic phases of core clock and clock-controlled transcripts in α and β cells. (C) Temporal profiles of selected core clock transcripts with distinct rhythmic phases in α and β cells assessed by RNA-seq data (top panels) and qRT-PCR analysis (bottom panels). Data represent the mean of two biological replicates per time point (each replicate is a mix of cells from six mice). Error bars express the SD of two independent experiments.

with insulin and adrenaline pulses proved to be efficient for intact pancreatic islets (Supplemental Fig. S5C). When applied to isolated α and β cells, insulin induced similar profiles of circadian bioluminescence in both cell types (Fig. 5A; Supplemental Table 2). In contrast, separated α cells synchronized by adrenaline exhibited distinct oscillation properties when compared with β cells, with α cells being phase-delayed behind their β -cell counterparts (Fig. 5B; Supplemental Table 2). Thus, the phase shift between α and β cells induced by adrenaline (Fig. 5B) was in the opposite direction when compared with the one observed for forskolin synchronization in vitro

(Fig. 4A,E) and coherent with the phases of core clock transcripts expressed in α and β cells in vivo (Fig. 3C).

To gain mechanistic insights into the observed differences, we compared expression profiles of the adrenaline hormone receptors in α and β cells. Importantly, while *Inst* exhibited similar levels and temporal expression profiles in both cell types (Fig. 5A), adrenergic receptors were differentially expressed in α and β cells (Adrb1 in α cells and Adra2a in β cells) (Fig. 5B). Therefore, the observed differences in the circadian properties of α -cellular and β -cellular clocks might be attributed to the distinct repertoire of these hormone receptors expressed on α and β cells and

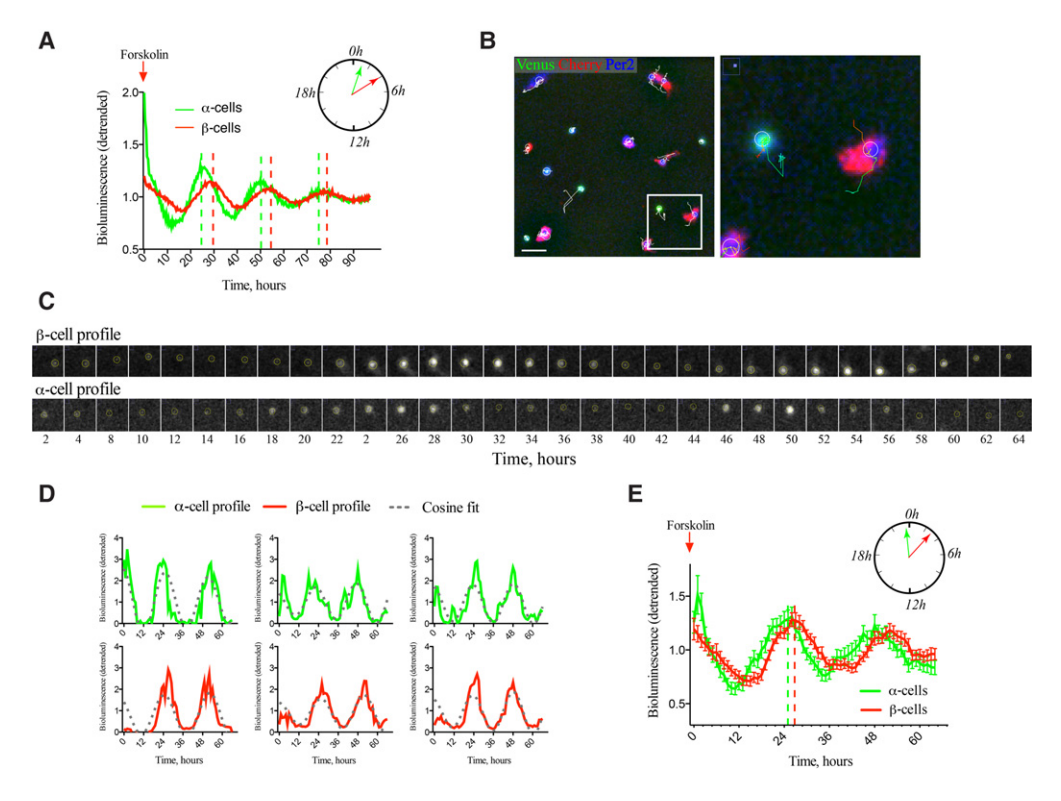


Figure 4. α-Cell and β-cell clocks synchronized in vitro by forskolin exhibit distinct circadian phases at the population (A) and single-cell (B–E) levels. (A) Average PER::Luc oscillation profiles of forskolin-synchronized FACS separated α-cell and β-cell populations (50,000 cells per well) in n = 4 and n = 5 experiments (with an average of five animals used per experiment), respectively. Data are presented as detrended values (Pulimeno et al. 2013). Significant phase shift between the two cell types (see Supplemental Table 2) is presented schematically in the polar diagram. (B) Representative full bioluminescence–fluorescence image (512×512 pixels) of proGcg-Venus/RIP-Cherry/PER2:: Luc-dissociated mouse islet cells subjected to time-lapse bioluminescence–fluorescence microscopy (Supplemental Movies S1–2). α Cells are Venus-positive (green labeling), and β cells are Cherry-positive (red labeling). Bioluminescence signal (blue in the image) was quantified for each cell over the nucleus within the circled area. Representative trajectories are overplayed in white over the image. (Right panel) The cropped image presents two traced cells. Bar, 40 μm. (C) Time-lapse microscopy of circadian PER2::Luc bioluminescence of a representative β cell (top row) and β cells (top row). Images were taken every 2 h during 64 h. (top) Analyzed bioluminescence tracks (detrended) for three representative β cells (top row). Images were taken every 2 h during 64 h. (top) Analyzed bioluminescence tracks (detrended) for three representative β cells (top row) and top cells (top row). Images were taken every 2 h during 64 h. (top) Analyzed bioluminescence tracks (detrended) for three representative top cells (top row). (top row) and top cells (top row) and top cells and

possibly due to their distinct temporal profiles, as demonstrated by RNA-seq analysis (Fig. 5B; Supplemental Data Set 1). To further explore this hypothesis, $\alpha 2$ adrenergic receptor (ADRA2) antagonist yohimbine was applied to β cells prior to adrenaline synchronization, resulting in a perturbed cellular circadian rhythm compared with adrenaline synchronization alone (Fig. 5C, left panel; Supplemental Table 3). Moreover, application of the selective $\beta 1$ adrenergic receptor antagonist attenolol to α cells prior to adrenaline synchronization led to a significant attenuation of the circadian profile (Fig. 5C right panel; Supplemental Table 3).

Blood levels of the islet hormones are oscillating over 24 h

To unravel the impact of the islet cellular clocks on physiology, the temporal pattern of islet hormones was assessed around the clock. Blood levels of glucose, insulin,

and glucagon were measured in night-fed animals every 4 h during 24 h (Fig. 6A) following the same design developed for islet cell transcript analysis (Supplemental Fig. S1). In agreement with previous publications, insulin levels exhibited a rhythmic profile with a peak in the middle of night (ZT16; Fig. 6A). On the other hand, glucagon levels were not considered circadian according to CosinorJ analysis, whereas a clear peak at ZT20–ZT0 following the peak of insulin was observed (Fig. 6A). Glucose levels did not show a clear rhythmic pattern in the same serum samples.

To distinguish between the clock-driven and food-driven origins of the observed rhythms, islet hormone blood levels were assessed in fasted animals (Fig. 6B). The rhythmic profiles of glucagon and insulin persisted in the absence of feeding, although the secretion peak for both hormones was advanced ~8 h in fasted animals as compared with night-fed mice. Thus, the phase coherence between the peaks of insulin and glucagon levels was

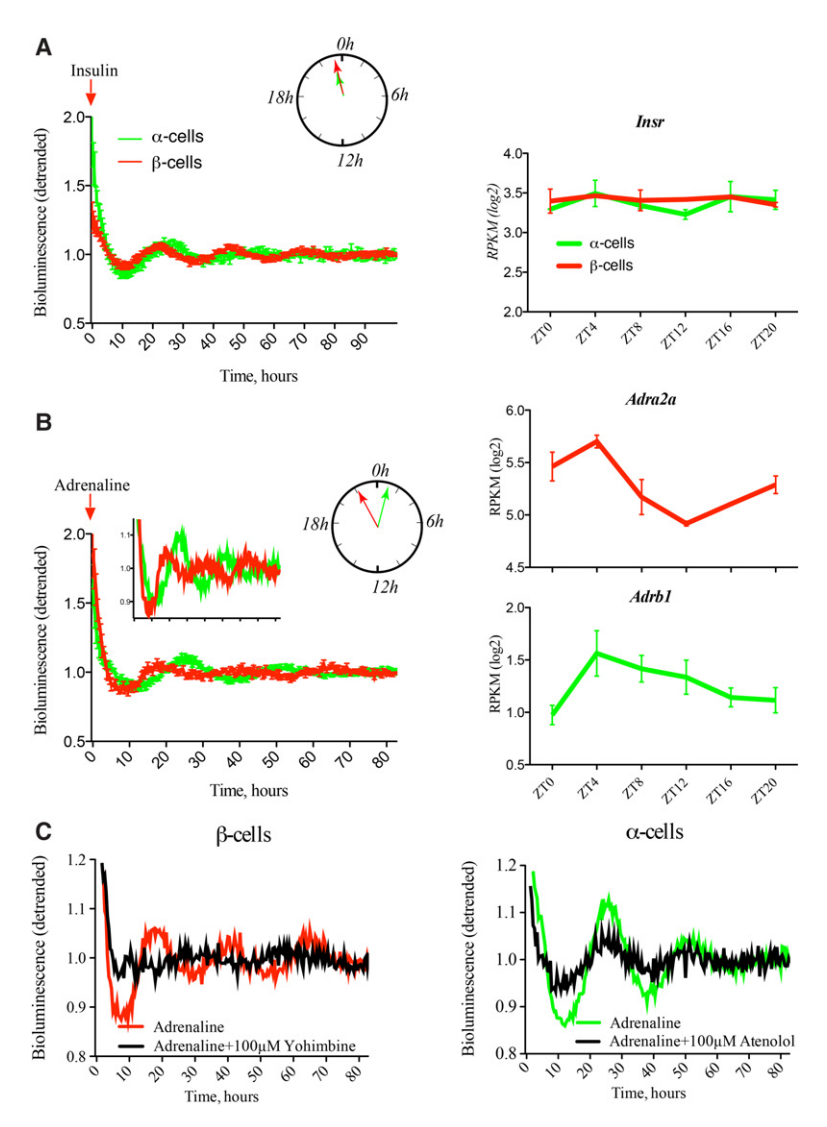


Figure 5. α -Cell and β -cell clocks synchronized in vitro by adrenaline, but not by insulin, exhibit distinct circadian phases. (Left panels) Average detrended PER2::Luc bioluminescence profiles for separated αcell and β-cell populations synchronized in vitro with a 1-h pulse of 100 nM insulin (A) or 5 μM adrenaline (B). Circadian phases of the PER2::Luc bioluminescence profiles recorded from α -cell and β -cell populations, presented in the polar diagrams, were similar (A) or delayed for α -cell population (B). Mean circadian parameters for these experiments are in Supplemental Table 2. (Right panels) In vivo temporal expression transcript profiles over 24 h obtained by RNA-seq (Supplemental Data Set 1) for insulin receptor (Insr) and adrenergic receptors (Adra2a and Adrb1) in α and β cells. Data are expressed as mean \pm SEM for the *left* panels. (A) n = 5 experiments for α cells; n = 6experiments for β cells. (B) n = 6 experiments for α cells; n=3 experiments for β cells. An average of five mice was used per experiment. Mean ± SD for the *right* panels. n = 2 independent experiments. (C) Average detrended PER2::Luc bioluminescence profiles for separated α -cell and β -cell populations synchronized with adrenaline alone or in the presence of adrenergic receptor antagonists. n = 6 experiments for α cells with adrenaline alone; n = 3 experiments for β cells with adrenaline alone; n = 3 independent experiments with antagonists for each cell type. An average of five mice was used per experiment. Coincubation of α and β cells with antagonists of $\beta 1$ adrenergic receptor (100 μM atenolol) and α2 adrenergic receptor (100 µM yohimbine), respectively, attenuated the synchronizing effect of adrenaline. Mean circadian parameters for these experiments are in Supplemental Table 3.

maintained in the night-fed and fasted mice (Fig. 6A,B). As expected, the blood glucose levels were strongly diminished in fasted animals without any clear diurnal rhythmicity pattern (Fig. 6A,B, cf. right panels).

To assess the impact of a functional clock on insulin and glucagon blood levels, the islet hormone measurements were performed in clock-deficient Bmal1 knockout mouse serum samples. During the light phase, both insulin and glucagon secretion levels were significantly diminished in Bmal1 knockout mice compared with the Bmal1 wild-type littermates (Fig. 6C). During the dark phase, only insulin exhibited a tendency for dampened secretion levels in Bmal1 knockout mice, which did not reach statistical significance (P = 0.06, paired t-test), while glucagon levels remained unchanged (Fig. 6C).

Rhythmic basal secretion of glucagon and insulin by isolated α and β cells synchronized in vitro

To understand whether the oscillatory profiles of islet hormones observed in the blood might be regulated to some

extent by cell-autonomous clocks, we used an in-house-developed perifusion system connected to a LumiCycle chamber (Saini et al. 2016). Basal insulin and glucagon secretion was monitored around the clock under a constant flow of culture medium in a dispersed mixed islet cell population (Fig. 6E) and FACS-sorted α and β cells (Fig. 6G) synchronized in vitro by a forskolin pulse. In parallel, PER::Luc bioluminescence was recorded from the same cells (Fig. 6D,F). These perifusion experiments suggested that both basal insulin secretion by synchronized β cells and basal glucagon secretion by synchronized α cells are circadian. Of note, the peak of glucagon secretion was delayed compared with that of insulin secretion by \sim 2 h in the mixed cell population and \sim 4 h in FACS-sorted α and β cells (Fig. 6E,G, cf. right panels).

Discussion

This study represents the first parallel molecular analysis of α -cell and β -cell oscillators and their impact on the gene

Circadian physiology of a and β cells

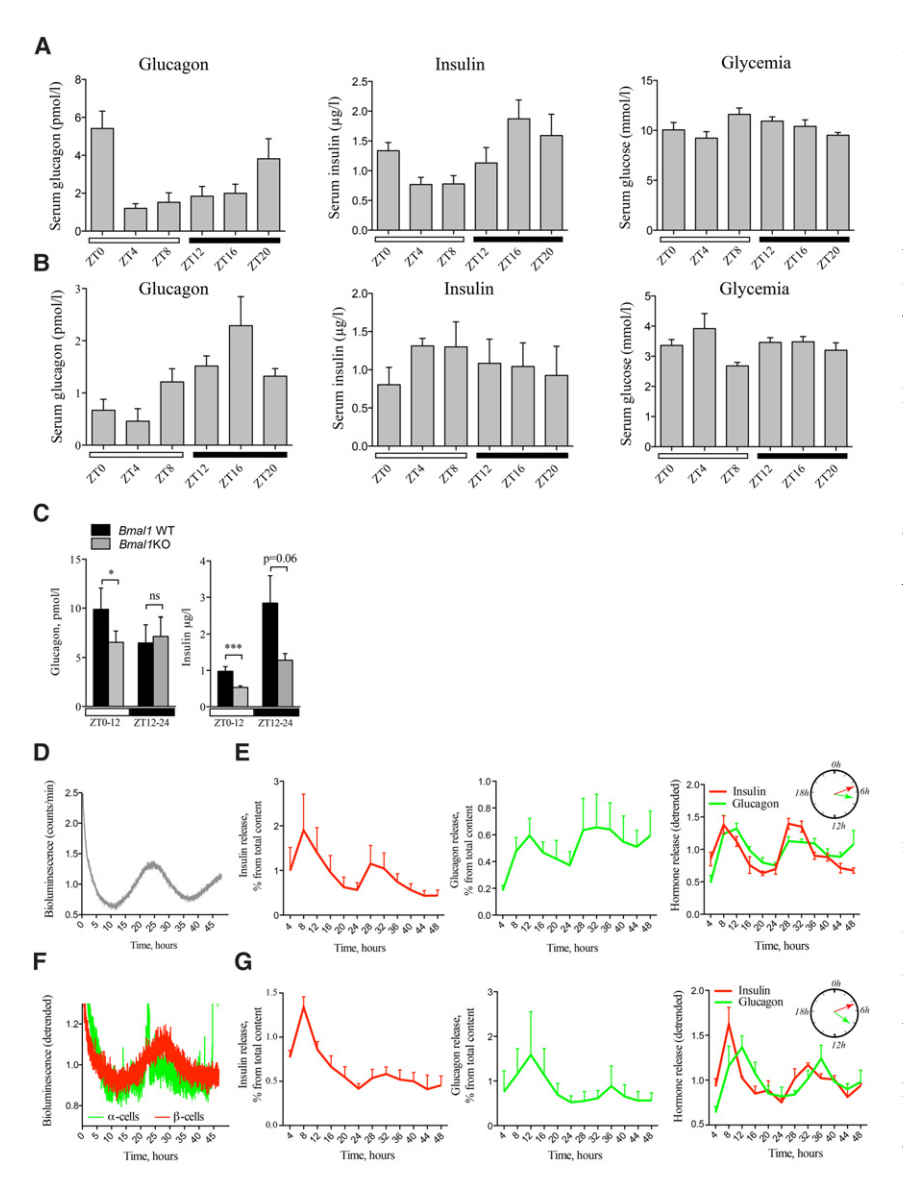


Figure 6. Secretion of insulin and glucagon in vivo and in vitro exhibits rhythmic profiles altered in circadian mutant mice. In vivo insulin, glucagon, and glucose levels were assessed in the sera collected from night-fed animals (A) or animals fasted for 12 h prior to the experiment and during the entire period of serum collection (B). Obtained profiles were analyzed by CosinorJ and qualified as 24-h rhythmic for χ^2 < 0.5 within the period length range of 18– 30 h and nonrhythmic if $\chi^2 \ge 0.5$ or outside this period length range. (A) Mouse sera were collected around the clock every 4 h (see Supplemental Fig. S1 for the design). n = 6-15 animals for each time point. Average serum insulin levels were $\chi^2 = 0.0069$ for period $22.05~h\pm2.2~h$ and phase $18.83~h\pm6.45~h$ (rhythmic), $\chi^2 = 3.39$ (nonrhythmic) for glucagon, and $\chi^2 = 0.73$ (nonrhythmic) for glucose. (B) Mouse sera were collected as described in A from n = 3-5 mice per time point. CosinorJ analysis results for average serum insulin levels were $\chi^2 = 0.055$ for period 20.1 h ± 6.04 h (rhythmic), $\chi^2 = 0.21$ for glucagon for period 24.0 h ± 1.59 h (rhythmic), and χ^2 = 0.16 for glucose for period $10.5 \text{ h} \pm 2.17 \text{ h}$ (nonrhythmic). (C) In vivo insulin and glucagon levels were assessed in mouse serum samples collected during the light phase (ZT0-ZT12; white square) and dark phase (ZT12-ZT24; black square) in night-fed Bmal1 knockout animals and their Bmal1 wild-type littermates. Light-phase insulin was assessed in n = 27 paired samples from Bmal1 knockout and Bmal1 wild-type mice (total of 54 animals). Dark phase insulin was assessed in 12 paired animal samples. Light-phase glucagon was measured in the blood samples from n = 16 pairs of animals (n = 12 pairs for the dark phase). Data are expressed as mean \pm SEM. (***) P = 0.0006 for light-phase insulin; (*) P = 0.034 for light-phase glucagon, two-tailed paired t-test. (D,E) Circadian bioluminescence recording (D) with parallel assessment of hormone secretion (E) in

perifused mixed islet cell populations after forskolin synchronization. n=4 independent experiments with an average of four mice used per experiment. The perifusion medium contained 5.5 mM glucose and was collected every 4 h during 48 h. Hormone concentrations in the outflow medium were normalized to the total hormone content in the cell lysate at the end of each experiment and are expressed as the percentage of total content (mean ± SEM) (*left* and *middle* panels) or as superimposed detrended values (mean ± SEM) (*right* panel). CosinorJ analysis results for insulin levels were $\chi^2 = 0.22$ for period 19.49 h ± 1.17 h and phase 5.13 h ± 0.37 h (rhythmic) and $\chi^2 = 0.064$ for glucagon level for period 25.79 h ± 2.19 h and phase 7.05 h ± 0.75 h (rhythmic). (*F,G*) Circadian bioluminescence recording (*F*) with parallel assessment of insulin secretion in a separated β-cell population (*G, left* panel) and glucagon secretion in a separated α-cell population (*G, middle* panel). n = 3 independent experiments for α and for β cells, with and average of five mice used per experiment. α-Cell and β-cell populations were separated by FACS, plated, synchronized with forskolin pulse, and continuously perifused with culture medium containing 5.5 mM glucose for 48 h following synchronization. The outflow medium was collected every 4 h. Hormone concentrations in the outflow medium samples were normalized to the total hormone content in the cell lysate at the end of each experiment and are expressed as the percentage of total content (mean ± SEM) (*left* and *middle* panels) or as superimposed detrended values (mean ± SEM) (*right* panel). CosinorJ analysis results were $\chi^2 = 0.19$ for insulin level for period 23.17 h ± 0.56 h and phase 4.94 h ± 0.88 h (rhythmic) and $\chi^2 = 0.04$ for glucagon level for period 23.03 ± 1.14 h and phase 8.4 h ± 0.93 h (rhythmic).

expression and functional regulation of islet cells. We demonstrate that α -cell and β -cell clocks harbor different circadian properties in vivo and in vitro in response to physiologically relevant stimuli such as adrenaline (Fig. 7). Parallel large-scale in vivo transcriptome analysis in

separated α and β cells showed oscillatory profiles for a high number of key islet genes in either one or both cell types (Figs. 1–3; Supplemental Data Set 1). Rhythmically expressed transcripts with similar or distinct characteristics in α and β cells comprised those encoding for glucose

transporters, glucose metabolism enzymes, and regulators of granule trafficking and exocytosis (Fig. 7; Supplemental Data Set 1; Supplemental Table 1). We propose that, along with feeding–fasting cycles, the described distinct properties of α -cellular and β -cellular clocks (Figs. 3–5) might contribute to orchestrating temporal secretion patterns of glucagon and insulin (Fig. 6), possibly due to differential circadian expression of functional genes in α and β cells (Figs. 1, 2, 7).

Pancreatic α -cellular and β -cellular clocks exhibit distinct molecular properties in vivo and in vitro

Parallel RNA-seq analysis of the temporal pattern of transcripts expressed in separated α and β cells suggested important phase differences between the two cell types (Fig. 3). Opposite phase relationships were found in isolated α and β cells synchronized by forskolin in vitro (Fig. 4A; Supplemental Table 2). These data were supported by single-cell analysis of α and β cells in mixed populations (Fig. 4B-E), raising the question of which endocrine and paracrine regulators might be relevant for islet cell clock synchronization in vivo. Synchronization of islet cellular clocks is a highly complex and dynamic process comprising feeding-fasting cycles, neural regulation, and endocrine and paracrine stimuli (Dibner and Schibler 2015b; Perelis et al. 2015a,b). Since insulin and catecholamines are key regulators of islet physiology during feeding and fasting, respectively, their synchronization properties on islet cell clocks were assessed. Indeed, these hormones had pronounced synchronizing capacity on α-cell and βcell clocks (Fig. 5; Supplemental Fig. S5C). Insulin, which has been suggested to have a weak synchronizing effect on cultured rat fibroblasts through the transcriptional induction of core clock genes Per1 and Per2 (Balsalobre et al. 2000), is acting via its specific receptors. Insulin receptor exhibited similar expression levels and temporal patterns in both cell types according to our data (Fig. 5; Supplemental Data Set 1) and previously published data sets (Benner et al. 2014; Adriaenssens et al. 2016; DiGruccio et al. 2016). In response to a high dose of insulin, α-cellular and β-cellular clocks exhibit a similar circadian phase (Fig. 5; Supplemental Table 2).

In contrast, the adrenaline pulse generates a significant phase shift between α and β cells, similar to the phase shift observed in vivo (cf. Figs. 5B and 3C). Responses of the αcell and β-cell clocks to adrenaline synchronization are likely to be mediated through adrenergic receptors, which are expressed differentially in α and β cells according to our RNA-seq data set (Fig. 5B, right panels). Importantly, inhibition of the β-cell-specific ADRA2A receptor with the α2 adrenergic antagonist vohimbine or of the α-cell-enriched ADRB1 receptor with the selective β1 adrenergic antagonist atenolol altered the synchronizing effect of adrenaline in these cells, respectively (Fig. 5C), further supporting a receptor-specific effect of adrenaline on islet cells. The intracellular effect of ADRB1 is mediated via activation of adenylyl cyclase (Vieira et al. 2004), while ADRA2A inhibits this enzyme (Rosengren et al. 2010). According to our RNA-seq analysis, different isoforms of

adenylyl cyclase (Adcy3, Adcy1, and Adcy9) are rhythmic only in a cells and are either nonrhythmic or nonexpressed in β cells (Supplemental Data Set 1). Additionally, distinct isoforms of protein kinase C (Prkcb and Prkce) and phospholipase C (Plcb1, Plcb4, and Plcg1), second messengers of the GNAQ-activated pathway downstream from ADRA2A, exhibited differential expression levels and temporal patterns in α and β cells (Supplemental Data Set 1). Collectively, the data presented in Figure 5C together with the RNA-seq analysis imply that the distinct circadian response of α-cell and β-cell clocks to adrenaline might be mediated by the cell-specific expression of adrenergic receptors and their second messengers in these cells. This islet cell-specific synchronizing effect of adrenaline observed in vitro may also account for the phase difference of α-cellular and β-cellular clocks demonstrated in vivo (Fig. 3) due to the essential role of the sympathetic innervation for islet function (Thorens 2014).

Additionally, oscillatory patterns of blood insulin (Fig. 6A) and adrenaline (De Boer and Van der Gugten 1987) may feed back on islet clocks by influencing their circadian phase. Transient changes of these hormones levels—for instance, increase of adrenaline concentration upon stress or increase of insulin after food ingestion—may contribute to the regulation of islet cell oscillators. In summary, our experiments suggest that adrenaline and insulin may coordinate the cell-specific resetting of α -cellular and β -cellular clocks, resulting in their phase difference in vivo (Figs. 3, 5, 7).

Of note, Per2 expression exhibited a similar rhythmic expression profile in α and β cells in vivo but not in vitro, as reflected by the circadian PER2::Luc reporter (see Figs. 3B, 4, 5B). It has been demonstrated that, unlike other core clock genes, Per2 expression might be uncoupled from the core clock and driven by systemic cues independently of the local oscillator (Kornmann et al. 2007). Therefore, the observed discrepancy might be explained by the dominant effect of food entrainment on Per2, overriding the input of local oscillators in vivo and its absence in vitro under constant medium conditions.

Differential rhythmic expression pattern of the α -cell and β -cell transcriptome

Computational analysis of large-scale temporal gene expression profiles with high resolution in separated α-cell and β-cell populations resulted in establishing a unique database (Supplemental Data Set 1) comprising α-celland β-cell-specific genes and those expressed in both cell types and the assessment of their rhythmicity. In total, ~60% of all detected transcripts exhibited rhythmicity in one or both cell types (Figs. 1D,F, 2A; Supplemental Fig. S3), which is higher in comparison with the recently reported fraction in whole islets (Perelis et al. 2015a). This difference might be explained by transcripts exhibiting distinct phases in two cell types (models 5 and 14), which may not be detectable as rhythmic in the whole islets. Previous studies suggested that the ratio of cycling and noncycling genes is tissue-specific, with metabolically active tissues exhibiting a greater number of rhythmic

Circadian physiology of a and B cells

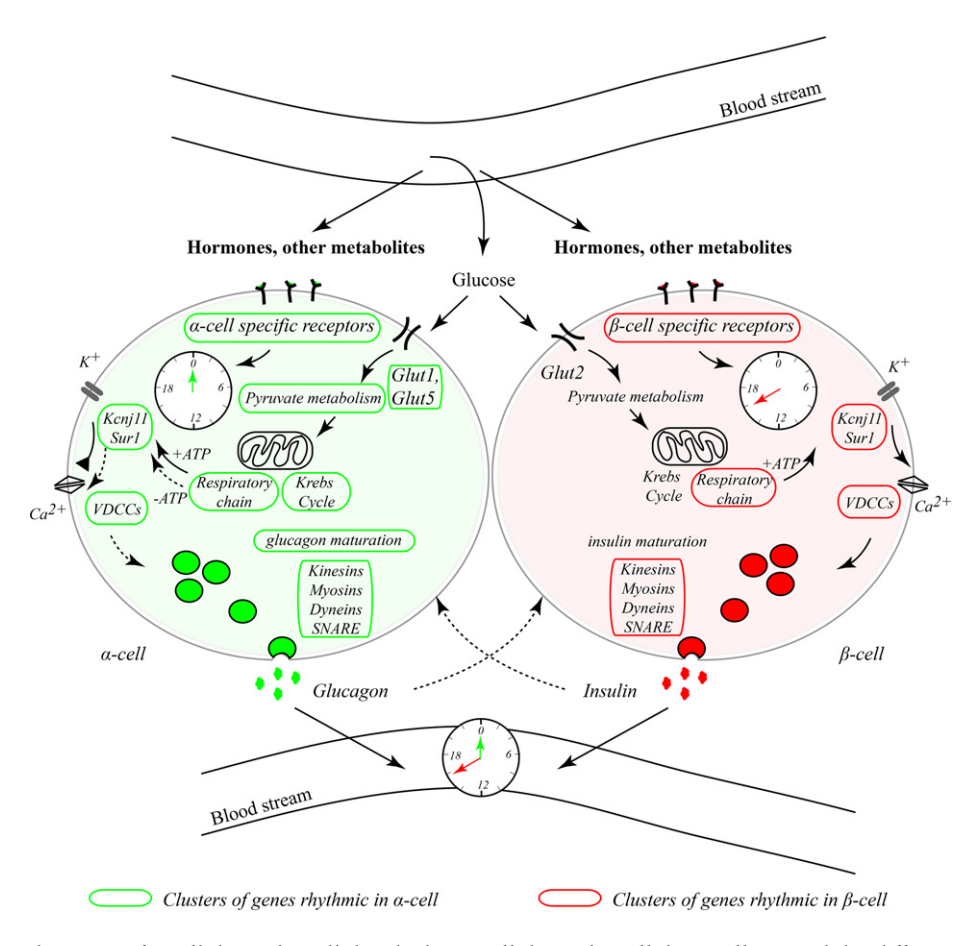


Figure 7. Inputs and outputs of α-cellular and β-cellular clocks. α-Cellular and β-cellular oscillators exhibit different circadian phases in vivo and in vitro in response to physiologically relevant stimuli, such as adrenaline, possibly due to a distinct repertoire of surface receptors and signal transduction molecules specific for each cell type. Key functional genes exhibit similar or distinct temporal patterns in α and β cells, comprising those encoding for glucose transporters, enzymes catalyzing glucose metabolism reactions (glycolysis, pyruvate metabolism, and Krebs cycle), K_{ATP} channels, voltage-dependent calcium channels (VDCCs), genes involved in glucagon maturation (but not insulin maturation), and genes responsible for granule trafficking and exocytosis. Clusters of rhythmic genes in β cells are highlighted in red, and those rhythmic in α cells are highlighted in green. We hypothesize that the distinct properties of α-cellular and β-cellular clocks, along with feeding–fasting cycles, might contribute to orchestrating different oscillating secretory patterns of glucagon and insulin stemming from the differential temporal orchestration of the functional gene transcription in α and β cells.

transcripts (Zhang et al. 2014). Playing a key role in glucose metabolism, α and β cells represent populations with high metabolic activities closely associated with feeding behavior. Most of the observed rhythmic transcripts exhibited peak expression levels in the middle of the light or dark phase (Figs. 1, 2), which might be attributed to the strong synchronizing effect exerted by rhythmic feeding on α -cell and β -cell clocks, as was demonstrated for other metabolically active tissues (Damiola et al. 2000; Atger et al. 2015). Among the rhythmically expressed transcripts, we found genes required for granule biogenesis, trafficking, and exocytosis (Fig. 7; Supplemental Data Set 1; Supplemental Table 1).

Rhythmic transcriptional regulation of islet hormone biogenesis

Biogenesis of insulin and glucagon shares similarities at principal steps, including hormone production, maturation, and secretory granule formation, trafficking, and exocytosis. The expression levels of insulin and glucagon were constant throughout the day (Fig. 1C), in line with previous reports on mouse and human insulin gene expression (Marcheva et al. 2010; Pulimeno et al. 2013). While the profile of the β -cell-specific proprotein convertase Pcsk1 (determining the first step of insulin maturation) (Orci et al. 1987) was nonrhythmic, expression of Pcsk2 (which regulates proinsulin processing in β cells) and the first steps of Gcg maturation in α cells (Furuta et al. 2001) were rhythmic only in α cells. Its expression was in opposite phase to the maximum of glucagon secretion, possibly to allow refilling of glucagon stores (Fig. 2B). Genes encoding for COPII proteins as well as members of common vesicle trafficking pathways and SNARE proteins—regulating immediate and delayed granule exocytosis (Regazzi et al. 1995) and their accessory factors were rhythmically expressed, peaking in the middle of the night (Fig. 7; Supplemental Table 1; Supplemental

Data Set 1). In line with our data, previous studies suggested circadian profiles for granule assembly and exocytosis regulators in in vitro synchronized islets, which were affected by clock disruption in transgenic mice (Perelis et al. 2015a) and human islet cells (Saini et al. 2016).

Rhythmic regulation of stimulus–secretion-coupling pathways in α and β cells

Furthermore, differential rhythmic control was exerted over transcripts encoding for proteins involved in basal and stimulated insulin and glucagon secretion (Fig. 7). Indeed, high glucose uptake in β cells is mediated by the nonrhythmic expression of the Glut2 transporter (Slc2a2 transcript) (Orci et al. 1989), while, in α cells, the principal glucose transporters Glut1 and Glut5 (Slc2a1 and Slc2a5 transcripts) were rhythmic. Glucokinase (Gck transcript) exhibited a rhythmic expression pattern in both cell types, simultaneously peaking at night. Genes responsible for the initial steps in glucose metabolism (pyruvate metabolism [Pdha1 and Pcx] and Krebs cycle [Aco2]) were rhythmic in α cells but not β cells. In contrast, the expression of respiratory chain components (complex V transcripts) was similarly rhythmic in both cell types, peaking at daytime (Supplemental Data Set 1; Supplemental Table 1). These data suggest a rhythmic transcriptional regulation of energy metabolism processes in mouse islet cells (in line with previous findings in clock-disrupted mice) (Lee et al. 2011) and human islet cells (Saini et al. 2016). In the liver, most of these rate-limiting mitochondrial enzymes are oscillating at the protein level (Neufeld-Cohen et al. 2016). Mitochondrial glucose metabolism differentially raises the ATP/ADP ratio in α and β cells, regulating the function of ion channels responsible for triggering insulin secretion and inhibiting glucagon release (Gromada et al. 2007). Elevated levels of ATP lead to the closure of ATP-sensitive K⁺ (K_{ATP}) channels (complex of KCNJ11 and sulfonylurea receptor SUR-1 encoded by Abcc8, resulting in cell depolarization and opposite regulation of glucose-induced insulin and glucagon secretion (Gromada et al. 2004). Here, we report that the rhythmic expression peaks for *Kcnj11* and *Abcc8* in α and β cells are temporally separated: ZT6 for *Kcnj11* and ZT20 for *Abcc8*. Interestingly, in human islet cells, the KCNI11 transcript was up-regulated upon siRNA-mediated CLOCK disruption (Saini et al. 2016), suggesting an inhibitory effect of the BMAL1/ CLOCK complex on KCNJ11 expression. Activation of K_{ATP} upon high glucose concentration opens voltage-dependent calcium channels (VDCCs) in β cells, resulting in calcium influx, SNARE-mediated insulin granule release, and closure of these channels in α cells, inhibiting glucagon secretion (Gromada et al. 2004; Gustavsson et al. 2009). Low glucose concentrations result in low ATP levels in α cells and moderately activate K_{ATP} channels, allowing the opening of VDCCs (Fig. 7, dotted arrow), leading to Ca^{2+} influx in α cells and SNAREmediated release of glucagon granules. Interestingly, multiple genes encoding for VDCC members (Supplemental Table 1) exhibited rhythmic expression, in line with the previously reported circadian regulation of VDCC expression in the SCNs (Nahm et al. 2005). Hence, the fact that the activity of VDCCs in islet cells is regulated by glucose makes them good candidates for coupling feeding regimen to intracellular molecular clocks.

Rhythmic profiles of insulin and glucagon are not aligned in vivo and in vitro

Turning to the functional output of α and β cells, plasma insulin levels exhibited significant circadian oscillation, peaking in the middle of the dark phase in night-fed mice (Fig. 6A), in agreement with previous studies reporting higher plasma insulin levels during the activity (night) phase (Marcheva et al. 2010; Perelis et al. 2015a). Parallel assessment of plasma glucagon content in the same samples suggested the oscillatory fluctuation over 24 h with the peak of secretion in the morning hours (ZTO), lagging ~8 h after the insulin peak (Figs. 6A, 7). These data are consistent with previous work detecting weak daily rhythms in plasma glucagon levels, peaking at the end of the night in ad libitum fed rats (Ruiter et al. 2003). It is noteworthy that rhythmic profiles of both insulin and glucagon secretion were preserved in fasted animals, with peaks strongly and similarly advanced for both hormones as compared with night-fed animals (Fig. 6A,B), suggesting that the circadian clock impacts on islet hormone secretion also in the absence of rhythmic feeding. In line with a previous report (Ruiter et al. 2003), introducing a fasting period prior to the blood collection influenced the daily glucagon secretion pattern by significantly enhancing its amplitude and advancing the phase (Fig. 6A, B, cf. left panels). Interestingly, the opposite tendency has been observed for the circadian amplitude of insulin secretion, which was lower in fasted animals compared with their night-fed counterparts (Fig. 6A,B, cf. middle panels). This finding is in line with human data indicating that the circadian amplitude of blood insulin is positively correlated with blood glucose levels (Boden et al. 1996). Of note, previous experiments with SCN lesioned animals (Yamamoto et al. 1987) demonstrated a role of the central clock in generating daily rhythms of glucagon secretion. Moreover, the studies by Bass and colleagues (Marcheva et al. 2010; Perelis et al. 2015a) provided compelling evidence that insulin secretion is strongly compromised in clock-deficient mice and that this effect is cell-autonomous. Similarly, in human islets, clock disruption reduced the amount of insulin at both basal and highglucose conditions (Saini et al. 2016). In strong agreement with these studies, our data imply that the presence of a functional clock is essential for proper islet hormone secretion, as clock-disrupted Bmal1 knockout mice had significantly altered blood levels of both insulin and glucagon (Fig. 6C), further strengthening the importance of a functional clock in regulating glucose homeostasis.

In line with in vivo data, our perifusion experiments demonstrate that mixed islet cells and pure α cells synchronized in vitro by forskolin secrete basal glucagon in a circadian manner (Fig. 6E,G, middle panels). The suggested role of the α -cell clock in regulating glucagon secretion is supported by a previous study demonstrating an

Circadian physiology of α and β cells

inhibitory effect of the core clock component *Reverba* on glucagon secretion in αTC1–9 cells (Vieira et al. 2013).

A rhythmic pattern of basal insulin secretion was obtained from mixed cells and pure β cells exhibiting similar circadian phases in this case (Fig. 6E,G), consistent with earlier in vitro studies in rodent and human islet cells, suggesting a circadian profile of insulin secretion by isolated islets or islet cells in rodents and humans (Peschke and Peschke 1998; Perelis et al. 2015a; Saini et al. 2016). Remarkably, this temporal separation of glucagon and insulin secretion observed in vivo persists also in vitro, with the glucagon profile being phase-delayed compared with insulin (Fig. 6E,G, right panels). This phase shift was particularly pronounced in separated α -cell and β -cell populations, suggesting differential autonomous circadian regulation of hormone secretion in α and β cells (Fig. 7).

While the dietary glucose intake has an acute effect on regulating insulin and glucagon secretion, cell-autonomous islet cellular clocks are likely to modulate this process in a temporal manner through the diurnal regulation of genes involved in secretion (Dibner and Schibler 2015b). Similar to rodents, endocrine body rhythms in humans, including those of insulin, are tightly regulated by the circadian system (Philippe and Dibner 2014). Such oscillatory profiles of metabolically active hormones may represent an important anticipatory mechanism, allowing for the optimal metabolic orchestration at the organism level.

The incidence of metabolic diseases, including T2D, is growing exponentially in modern societies (Krug 2016). This tendency might be attributed to sleep perturbations related to the increasing rate of acute and social jet lag and the rise of shifted work schedules (Maury et al. 2014; Saini et al. 2015). Accumulating data suggest a key role of α -cell dysfunction in the development of T2D (D'Alessio 2011; Lee et al. 2016). Our data will help to dissect the contribution of the circadian clock in α -cell and β -cell physiology and pave the way for future studies aiming at deciphering α -cell and β -cell dysfunction in the etiology of metabolic diseases.

Materials and methods

Animal care and reporter mouse strain

Animal studies were performed according to the regulations of the veterinary office of the State of Geneva. The triple reporter mouse strain was established by crossing Gcg-Venus reporter (Reimann et al. 2008), RIP-Cherry (Zhu et al. 2015), and Per2:: Luc (Yoo et al. 2004) mice (Supplemental Fig. S1). ProGcg-Venus and RIP-Cherry reporters exhibited very high specificity and expression levels in α and β cells, respectively (Supplemental Fig. S1; Zhu et al. 2015; Dusaulcy et al. 2016). Bmal1 knockout mice have been described previously by Jouffe et al. (2013). All experiments were done in mice between 7 and 16 wk of age under standard animal housing conditions with free access to food and water and in 12-h light/12-h dark cycles (LD). For the in vivo sample collection, animals were subjected to night-restricted feeding (Supplemental Fig. S1) 2 wk prior to the experiments and during the entire period of sample collection, allowing us to reduce the effect of individual feeding rhythms (Atger et al. 2015). For sample

collection covering the 24-h period, half of the animals were entrained by inverted LD and feeding cycles during the 3 wk preceding the experiments. Fasted blood collection around the clock was performed in the absence of feeding and following 12 h of fasting prior to the first time point. For *Bmal1* knockout mice and their control littermates, serum samples were collected during the light phase (ZT0–ZT12) and dark phase (ZT12–ZT24).

Pancreatic islet isolation and separation of α and β cells

Islets of Langerhans were isolated by standard procedure based on collagenase (type XI; Sigma) digestion of the pancreas followed by Ficoll purification (Wojtusciszyn et al. 2009). Islet cells were gently dissociated by trypsin (GIBCO) resuspended in KRB solution (pH 7.4) supplemented with 0.3 % free fatty acid bovine serum albumin (BSA) (Sigma), 1.4 mM glucose, and 0.5 mM EDTA). $\alpha\text{-Cell}$ and $\beta\text{-cell}$ populations were separated by flow cytometry FACS (Astrios sorter, Beckman Coulter) based on fluorescence wavelength and intensity and cell singlet nature, size, and viability (Supplemental Fig. S2).

In vitro islets/islet cell culture, synchronization, and bioluminescence monitoring

For in vitro culture, the intact islets or dissociated or sorted cells were recovered in RPMI 1640 complete medium (11.2 mM glucose, 110 µg/mL sodium pyruvate) supplemented with 10% fetal calf serum, 110 U/mL penicillin, 110 µg/mL streptomycin, and 50 μg/mL gentamycin and attached to 35-mm dishes or multiwell plates precoated with a laminin-5-rich extracellular matrix (Parnaud et al. 2008). Adherent islets/cells were synchronized by a 1-h pulse of 10 µM forskolin (Sigma), 100 nM insulin (NovoRapid), or 5 µM adrenaline (Geneva Hospital Pharmacy) prior to continuous bioluminescence recording in RPMI supplemented with 100 µM luciferin (NanoLight Technology) (Saini et al. 2016). For detrended time series, raw luminescence signals were processed by a moving average with a window of 24 h (Saini et al. 2016). β1 adrenergic receptor antagonist atenolol (100 μM), and 100 μM α2 adrenergic receptor antagonist yohimbine were applied to α and β cells, respectively, 15 min prior to adding adrenaline for the synchronization, and cells were kept in the medium during a 1-h synchronization period.

Combined bioluminescence-fluorescence time-lapse microscopy and data analysis

Dispersed islet cells attached to glass-bottomed dishes (WillCo Wells BV) were synchronized by forskolin and subjected to combined bioluminescence–fluorescence imaging (Pulimeno et al. 2013). An Olympus LV200 workstation equipped with a 63× UPLSAPO objective and EM CCD camera (Image EM C9100-13, Hamamatsu) was used. The recorded time-lapsed images were analyzed on ImageJ 1.50 (Schneider et al. 2012), with individual cells tracked in the bioluminescence and fluorescence channels using a modified version of ImageJ plug-in CGE (Sage et al. 2010). Measuring of expression levels was performed on the labeled and tracked cells in the bioluminescence images over time. To assess the circadian characteristics of single-cell profiles, a Cosine fitting method (CosinorJ) was applied (Mannic et al. 2013).

RNA-seq

Total RNA was prepared from FACS-sorted α and β cells collected every 4 h around the clock in duplicates (total of 24 samples

representing an RNA pool of six to 12 mice each) using RNeasy Plus Micro Kit (Qiagen). RNA-seq was performed on the Institute of Genetics and Genomics in Geneva genomics platform (University of Geneva, Switzerland). The TruSeq stranded total RNA with Ribo-Zero Gold kit (Illumina) was used for library preparation with 100 ng of total RNA as input. Library molarity and quality were assessed with Qubit (Life Technologies) and Tapestation using a DNA high-sensitivity chip (Agilent Technologies). Paired-end reads of 50 bases were generated using TruSeq SBS HS version 3 chemistry on an Illumina HiSeq 2500 sequencer. RNA-seq mapping and quantification and model selection and rhythmicity assessment are described in the Supplemental Material.

Measurements of insulin, glucagon, and glucose levels in the blood serum

Mice were sacrificed by decapitation at ZTO, ZT4, ZT8, ZT12, ZT16, and ZT20 with subsequent blood collection and serum preparation by immediate centrifugation at 3000 rpm for 15 min at 4°C (Supplemental Fig. S1) and storage at -80°C. Protease inhibitors PMSF (Axon), aprotinin (Sigma), and DPP4 (Millipore) were added to the samples to preserve the hormones from degradation. Insulin and glucagon concentrations were assessed by ultrasensitive mouse insulin and glucagon ELISA kits (Mercodia), and serum glucose was assessed by Accu-Chek glucometer (Roche).

Islet cell continuous perifusion

Dispersed islet cells or FACS-separated α and β cells were attached and forskolin-synchronized as described above, placed into an in-house-developed two-well horizontal perifusion chamber connected to a LumiCycle, and continuously perifused with RPMI (without sodium pyruvate) containing 5.5 mM glucose and 100 μ M luciferin as described (Saini et al. 2016). Bioluminescence recordings were performed in parallel to the 4-h interval automated collection of the outflow medium. Basal insulin and glucagon levels were quantified in the outflow medium by mouse insulin and glucagon ELISA kits (Mercodia) and normalized to the total cellular content with subsequent moving average transformation. Circadian parameters of the secreted profiles were evaluated by the CosinorJ algorithm (Mannic et al. 2013).

Acknowledgments

We thank Ueli Schibler, Claes Wollheim, Eric Feraille, Hans Reinke, and Ursula Loizides-Mangold for constructive discussions; Pedro Luis Herrera and his colleagues-Simona Chera, Luiza Ghila, Fabirizio Thorel, and Olivier Fazio-for generous help with the reporter mice; Yvan Gosmain and Christian Vesin for helping with islet isolation; Andre Liani and George Severi for helping with perifusion experiments; Mylene Docquier and Brice Petit for performing RNA-seq experiments; Jean-Pierre Aubry-Lachainaye for his exceptional help with FACS experiments; and Christoph Bauer and Jerome Bosset for helping with bioimaging experiments. This work was funded by Swiss National Science Foundation grant 31003A_166700/1, the Novartis Consumer Health Foundation, the Fondation Romande pour la Recherche sur le Diabète, the European Foundation for the Study of Diabetes/Boehringer Ingelheim Basic Research Programme, the Fondation Privée des Hôpitaux Universitaires de Genève, the Bo Hjelt Foundation, and the Olga Mayenfisch Foundation (C.D.).

References

- Adriaenssens AE, Svendsen B, Lam BY, Yeo GS, Holst JJ, Reimann F, Gribble FM. 2016. Transcriptomic profiling of pancreatic α , β and δ cell populations identifies δ cells as a principal target for ghrelin in mouse islets. *Diabetologia* **59:** 2156–2165.
- Asher G, Sassone-Corsi P. 2015. Time for food: the intimate interplay between nutrition, metabolism, and the circadian clock. *Cell* **161:** 84–92.
- Asher G, Schibler U. 2011. Crosstalk between components of circadian and metabolic cycles in mammals. *Cell Metab* 13: 125–137
- Atger F, Gobet C, Marquis J, Martin E, Wang J, Weger B, Lefebvre G, Descombes P, Naef F, Gachon F. 2015. Circadian and feeding rhythms differentially affect rhythmic mRNA transcription and translation in mouse liver. *Proc Natl Acad Sci* 112: E6579–E6588.
- Balsalobre A, Marcacci L, Schibler U. 2000. Multiple signaling pathways elicit circadian gene expression in cultured Rat-1 fibroblasts. Curr Biol 10: 1291–1294.
- Benner C, van der Meulen T, Caceres E, Tigyi K, Donaldson CJ, Huising MO. 2014. The transcriptional landscape of mouse β cells compared to human β cells reveals notable species differences in long non-coding RNA and protein-coding gene expression. *BMC Genomics* **15**: 620.
- Boden G, Ruiz J, Urbain JL, Chen X. 1996. Evidence for a circadian rhythm of insulin secretion. *Am J Physiol* **271:** E246–E252.
- D'Alessio D. 2011. The role of dysregulated glucagon secretion in type 2 diabetes. *Diabetes Obesity Metab* **13:** 126–132.
- Damiola F, Le Minh N, Preitner N, Kornmann B, Fleury-Olela F, Schibler U. 2000. Restricted feeding uncouples circadian oscillators in peripheral tissues from the central pacemaker in the suprachiasmatic nucleus. *Genes Dev* 14: 2950–2961.
- De Boer SF, Van der Gugten J. 1987. Daily variations in plasma noradrenaline, adrenaline and corticosterone concentrations in rats. *Physiol Behav* **40**: 323–328.
- Dibner C, Schibler U. 2015a. Circadian timing of metabolism in animal models and humans. *J Intern Med* **277:** 513–527.
- Dibner C, Schibler U. 2015b. Metabolism. A pancreatic clock times insulin release. *Science* **350**: 628–629.
- DiGruccio MR, Mawla AM, Donaldson CJ, Noguchi GM, Vaughan J, Cowing-Zitron C, van der Meulen T, Huising MO. 2016. Comprehensive α , β and δ cell transcriptomes reveal that ghrelin selectively activates δ cells and promotes somatostatin release from pancreatic islets. *Mol Metab* 5: 449–458.
- Dusaulcy R, Handgraaf S, Heddad-Masson M, Visentin F, Vesin C, Reimann F, Gribble F, Philippe J, Gosmain Y. 2016. α-Cell dysfunctions and molecular alterations in male insulinopenic diabetic mice are not completely corrected by insulin. *Endocrinology* **157:** 536–547.
- Furuta M, Zhou A, Webb G, Carroll R, Ravazzola M, Orci L, Steiner DF. 2001. Severe defect in proglucagon processing in islet A-cells of prohormone convertase 2 null mice. *J Biol Chem* **276**: 27197–27202.
- Gromada J, Ma X, Hoy M, Bokvist K, Salehi A, Berggren PO, Rorsman P. 2004. ATP-sensitive K^+ channel-dependent regulation of glucagon release and electrical activity by glucose in wild-type and $SUR1^{-/-}$ mouse α -cells. *Diabetes* **53**: S181–S189.
- Gromada J, Franklin I, Wollheim CB. 2007. α-Cells of the endocrine pancreas: 35 years of research but the enigma remains. *Endocr Rev* **28:** 84–116.
- Gustavsson N, Wei SH, Hoang DN, Lao Y, Zhang Q, Radda GK, Rorsman P, Sudhof TC, Han W. 2009. Synaptotagmin-7 is a

- principal Ca^{2+} sensor for Ca^{2+} -induced glucagon exocytosis in pancreas. *J Physiol* **587**: 1169–1178.
- Jouffe C, Cretenet G, Symul L, Martin E, Atger F, Naef F, Gachon F. 2013. The circadian clock coordinates ribosome biogenesis. PLoS Biol 11: e1001455.
- Kornmann B, Schaad O, Bujard H, Takahashi JS, Schibler U. 2007. System-driven and oscillator-dependent circadian transcription in mice with a conditionally active liver clock. *PLoS Biol* **5:** e34.
- Krug EG. 2016. Trends in diabetes: sounding the alarm. *Lancet* **387:** 1485–1486.
- Lee J, Kim MS, Li R, Liu VY, Fu L, Moore DD, Ma K, Yechoor VK. 2011. Loss of Bmal1 leads to uncoupling and impaired glucosestimulated insulin secretion in β-cells. *Islets* 3: 381–388.
- Lee YH, Wang MY, Yu XX, Unger RH. 2016. Glucagon is the key factor in the development of diabetes. *Diabetologia* **59:** 1372–1375.
- Mannic T, Meyer P, Triponez F, Pusztaszeri M, Le Martelot G, Mariani O, Schmitter D, Sage D, Philippe J, Dibner C. 2013. Circadian clock characteristics are altered in human thyroid malignant nodules. J Clin Endocrinol Metab 98: 4446–4456.
- Marcheva B, Ramsey KM, Buhr ED, Kobayashi Y, Su H, Ko CH, Ivanova G, Omura C, Mo S, Vitaterna MH, et al. 2010. Disruption of the clock components CLOCK and BMAL1 leads to hypoinsulinaemia and diabetes. *Nature* **466**: 627–631.
- Maury E, Hong HK, Bass J. 2014. Circadian disruption in the pathogenesis of metabolic syndrome. *Diabetes Metab* **40**: 338–346.
- Nahm SS, Farnell YZ, Griffith W, Earnest DJ. 2005. Circadian regulation and function of voltage-dependent calcium channels in the suprachiasmatic nucleus. *J Neurosci* **25:** 9304–9308.
- Neufeld-Cohen A, Robles MS, Aviram R, Manella G, Adamovich Y, Ladeuix B, Nir D, Rousso-Noori L, Kuperman Y, Golik M, et al. 2016. Circadian control of oscillations in mitochondrial rate-limiting enzymes and nutrient utilization by PERIOD proteins. *Proc Natl Acad Sci* 113: E1673–E1682.
- Orci L, Ravazzola M, Storch MJ, Anderson RG, Vassalli JD, Perrelet A. 1987. Proteolytic maturation of insulin is a post-Golgi event which occurs in acidifying clathrin-coated secretory vesicles. *Cell* **49:** 865–868.
- Orci L, Thorens B, Ravazzola M, Lodish HF. 1989. Localization of the pancreatic β cell glucose transporter to specific plasma membrane domains. *Science* **245**: 295–297.
- Parnaud G, Bosco D, Berney T, Pattou F, Kerr-Conte J, Donath MY, Bruun C, Mandrup-Poulsen T, Billestrup N, Halban PA. 2008. Proliferation of sorted human and rat β cells. *Diabetologia* 51: 91–100.
- Partch CL, Green CB, Takahashi JS. 2014. Molecular architecture of the mammalian circadian clock. *Trends Cell Biol* **24**: 90–99.
- Perelis M, Marcheva B, Ramsey KM, Schipma MJ, Hutchison AL, Taguchi A, Peek CB, Hong H, Huang W, Omura C, et al. 2015a. Pancreatic β cell enhancers regulate rhythmic transcription of genes controlling insulin secretion. *Science* **350**: aac4250
- Perelis M, Ramsey KM, Bass J. 2015b. The molecular clock as a metabolic rheostat. *Diabetes Obesity Metab* **17:** 99–105.
- Perrin L, Loizides-Mangold U, Skarupelova S, Pulimeno P, Chanon S, Robert M, Bouzakri K, Modoux C, Roux-Lombard P, Vidal H, et al. 2015. Human skeletal myotubes display a cell-autonomous circadian clock implicated in basal myokine secretion. *Mol Metab* **4:** 834–845.
- Peschke E, Peschke D. 1998. Evidence for a circadian rhythm of insulin release from perifused rat pancreatic islets. *Diabetologia* **41:** 1085–1092.

- Philippe J, Dibner C. 2014. Thyroid circadian timing: roles in physiology and thyroid malignancies. *J Biol Rhythms* 2: 76–83.
- Pulimeno P, Mannic T, Sage D, Giovannoni L, Salmon P, Lemeille S, Giry-Laterriere M, Unser M, Bosco D, Bauer C, et al. 2013. Autonomous and self-sustained circadian oscillators displayed in human islet cells. *Diabetologia* **56**: 497–507.
- Qian J, Block GD, Colwell CS, Matveyenko AV. 2013. Consequences of exposure to light at night on the pancreatic islet circadian clock and function in rats. *Diabetes* 62: 3469–3478.
- Regazzi R, Wollheim CB, Lang J, Theler JM, Rossetto O, Montecucco C, Sadoul K, Weller U, Palmer M, Thorens B. 1995. VAMP-2 and cellubrevin are expressed in pancreatic β -cells and are essential for Ca²⁺-but not for GTP γ S-induced insulin secretion. *EMBO J* **14**: 2723–2730.
- Reimann F, Habib AM, Tolhurst G, Parker HE, Rogers GJ, Gribble FM. 2008. Glucose sensing in L cells: a primary cell study. *Cell Metab* 8: 532–539
- Rosengren AH, Jokubka R, Tojjar D, Granhall C, Hansson O, Li DQ, Nagaraj V, Reinbothe TM, Tuncel J, Eliasson L, et al. 2010. Overexpression of α2A-adrenergic receptors contributes to type 2 diabetes. *Science* **327**: 217–220.
- Ruiter M, La Fleur SE, van Heijningen C, van der Vliet J, Kalsbeek A, Buijs RM. 2003. The daily rhythm in plasma glucagon concentrations in the rat is modulated by the biological clock and by feeding behavior. *Diabetes* **52:** 1709–1715.
- Sadacca LA, Lamia KA, deLemos AS, Blum B, Weitz CJ. 2011. An intrinsic circadian clock of the pancreas is required for normal insulin release and glucose homeostasis in mice. *Diabetologia* 54: 120–124.
- Sage D, Unser M, Salmon P, Dibner C. 2010. A software solution for recording circadian oscillator features in time-lapse live cell microscopy. *Cell Div* 5: 17.
- Saini C, Brown SA, Dibner C. 2015. Human peripheral clocks: applications for studying circadian phenotypes in physiology and pathophysiology. Front Neurol 6: 95.
- Saini C, Petrenko V, Pulimeno P, Giovannoni L, Berney T, Hebrok M, Howald C, Dermitzakis ET, Dibner C. 2016. A functional circadian clock is required for proper insulin secretion by human pancreatic islet cells. *Diabetes Obesity Metab* 18: 355–365
- Schneider CA, Rasband WS, Eliceiri KW. 2012. NIH Image to ImageJ: 25 years of image analysis. *Nat Methods* 9: 671–675.
- Thorel F, Nepote V, Avril I, Kohno K, Desgraz R, Chera S, Herrera PL. 2010. Conversion of adult pancreatic α -cells to β -cells after extreme β -cell loss. *Nature* **464**: 1149–1154.
- Thorens B. 2014. Neural regulation of pancreatic islet cell mass and function. *Diabetes Obesity Metab* **16**(Suppl 1): 87–95.
- Unger RH, Orci L. 1975. The essential role of glucagon in the pathogenesis of diabetes mellitus. *Lancet* 1: 14–16.
- Vieira E, Liu YJ, Gylfe E. 2004. Involvement of α1 and β-adrenoceptors in adrenaline stimulation of the glucagon-secreting mouse α-cell. *Naunyn Schmiedebergs Arch Pharmacol* **369:** 179–183
- Vieira E, Marroqui L, Figueroa AL, Merino B, Fernandez-Ruiz R, Nadal A, Burris TP, Gomis R, Quesada I. 2013. Involvement of the clock gene Rev–erbα in the regulation of glucagon secretion in pancreatic α-cells. *PLoS One* **8:** e69939.
- Wojtusciszyn A, Andres A, Morel P, Charvier S, Armanet M, Toso C, Choi Y, Bosco D, Berney T. 2009. Immunomodulation by blockade of the TRANCE co-stimulatory pathway in murine allogeneic islet transplantation. *Transpl Int* 22: 931–939.
- Yamamoto H, Nagai K, Nakagawa H. 1987. Role of SCN in daily rhythms of plasma glucose, FFA, insulin and glucagon. *Chro-nobiol Int* 4: 483–491.

- Yoo SH, Yamazaki S, Lowrey PL, Shimomura K, Ko CH, Buhr ED, Siepka SM, Hong HK, Oh WJ, Yoo OJ, et al. 2004. PERIOD2:: LUCIFERASE real-time reporting of circadian dynamics reveals persistent circadian oscillations in mouse peripheral tissues. *Proc Natl Acad Sci* 101: 5339–5346.
- Zaret KS, White MF. 2010. Diabetes forum: extreme makeover of pancreatic α-cells. *Nature* **464**: 1132–1133.
- Zhang R, Lahens NF, Ballance HI, Hughes ME, Hogenesch JB. 2014. A circadian gene expression atlas in mammals: implications for biology and medicine. *Proc Natl Acad Sci* 111: 16219–16224.
- Zhu X, Hu R, Brissova M, Stein RW, Powers AC, Gu G, Kaverina I. 2015. Microtubules negatively regulate insulin secretion in pancreatic β cells. *Dev Cell* **34:** 656–668.



Pancreatic $\alpha\text{-}$ and $\beta\text{-}cellular$ clocks have distinct molecular properties and impact on islet hormone secretion and gene expression

Volodymyr Petrenko, Camille Saini, Laurianne Giovannoni, et al.

Genes Dev. 2017, **31:** originally published online March 8, 2017 Access the most recent version at doi:10.1101/gad.290379.116

Supplemental Material	http://genesdev.cshlp.org/content/suppl/2017/03/08/gad.290379.116.DC1
References	This article cites 59 articles, 14 of which can be accessed free at: http://genesdev.cshlp.org/content/31/4/383.full.html#ref-list-1
Creative Commons License	This article is distributed exclusively by Cold Spring Harbor Laboratory Press for the first six months after the full-issue publication date (see http://genesdev.cshlp.org/site/misc/terms.xhtml). After six months, it is available under a Creative Commons License (Attribution-NonCommercial 4.0 International), as described at http://creativecommons.org/licenses/by-nc/4.0/ .
Email Alerting Service	Receive free email alerts when new articles cite this article - sign up in the box at the top right corner of the article or click here .



The core clock transcription factor BMAL1 drives circadian β-cell proliferation during compensatory regeneration of the endocrine pancreas

Volodymyr Petrenko, ^{1,2,3,4} Miri Stolovich-Rain, ⁵ Bart Vandereycken, ⁶ Laurianne Giovannoni, ^{1,2,3,4} Kai-Florian Storch, ^{7,8} Yuval Dor, ⁵ Simona Chera, ⁹ and Charna Dibner ^{1,2,3,4}

¹Division of Endocrinology, Diabetes, Nutrition, and Patient Education, Department of Medicine, University of Geneva, 1211 Geneva, Switzerland; ²Department of Cell Physiology and Metabolism, Faculty of Medicine, University of Geneva, 1211 Geneva, Switzerland; ³Diabetes Center, Faculty of Medicine, University of Geneva, 1211 Geneva, Switzerland; ⁴Institute of Genetics and Genomics in Geneva (iGE3), 1211 Geneva, Switzerland; ⁵Department of Developmental Biology and Cancer Research, The Institute for Medical Research Israel-Canada, The Hebrew University-Hadassah Medical School, Jerusalem 91120, Israel; ⁶Section of Mathematics, University of Geneva, 1211 Geneva, Switzerland; ⁷Department of Psychiatry, McGill University, Montreal, Quebec H4H 1R3, Canada; ⁸Douglas Mental Health University Institute, Montreal, Quebec H4H 1R3, Canada; ⁹Department of Clinical Science, University of Bergen, 5021 Bergen, Norway

Circadian clocks in pancreatic islets participate in the regulation of glucose homeostasis. Here we examined the role of these timekeepers in β -cell regeneration after the massive ablation of β cells by doxycycline-induced expression of diphtheria toxin A (DTA) in Insulin-rtTA/TET-DTA mice. Since we crossed reporter genes expressing α - and β -cell-specific fluorescent proteins into these mice, we could follow the fate of α - and β cells separately. As expected, DTA induction resulted in an acute hyperglycemia, which was accompanied by dramatic changes in gene expression in residual β cells. In contrast, only temporal alterations of gene expression were observed in α cells. Interestingly, β cells entered S phase preferentially during the nocturnal activity phase, indicating that the diurnal rhythm also plays a role in the orchestration of β -cell regeneration. Indeed, in arrhythmic *Bmal1*-deficient mice, which lack circadian clocks, no compensatory β -cell proliferation was observed, and the β -cell ablation led to aggravated hyperglycemia, hyperglucagonemia, and fatal diabetes.

[Keywords: circadian clockwork; pancreatic α and β cells; Insulin-rtTA/TET-DTA mouse model; diabetes; glucose metabolism; β -cell proliferation; β -cell regeneration]

Supplemental material is available for this article.

Received August 25, 2020; revised version accepted October 8, 2020.

The circadian system allows organisms to synchronize physiology and behavior to the changes of geophysical time repeatable every 24 h. In mammals, the clock network is organized in a hierarchical manner. It comprises a master pacemaker, located in the paired suprachiasmatic nuclei (SCN) of the hypothalamus, that orchestrates the timing of peripheral oscillators situated in all organs on a daily basis (Dibner 2020). The molecular clocks rely on two coupled auto-regulatory transcriptional–translational negative feedback loops (TTFLs). In the primary TTFL, the transcriptional activators BMAL1 and CLOCK form a heterodimer that activates transcription of the genes encoding the negative limb members *PER1*–3 and *CRY1*–2 (Cox and Takahashi 2019; Sinturel et al. 2020). CRY and PER proteins form complexes that translocate to the nu-

Corresponding author: charna.dibner@hcuge.ch

Article published online ahead of print. Article and publication date are online at http://www.genesdev.org/cgi/doi/10.1101/gad.343137.120.

cleus and inhibit the action of BMAL1 and CLOCK on their own transcription (Aryal et al. 2017). In the secondary TTFL, members of the nuclear orphan receptor families ROR and REV-ERB drive the circadian transcription of the positive limb members *BMAL1* and *CLOCK* (Dibner et al. 2010).

A coupling between the circadian oscillator and the cell division cycle has been observed in cultured fibroblasts (Nagoshi et al. 2004) and in tissues with high proliferative activity, such as oral mucosa, skin (Bjarnason et al. 2001), and intestinal epithelium (Karpowicz et al. 2013; Stokes et al. 2017). Indeed, core clock components were demonstrated to directly drive the expression of key cell cycle

© 2020 Petrenko et al. This article is distributed exclusively by Cold Spring Harbor Laboratory Press for the first six months after the full-issue publication date (see http://genesdev.cshlp.org/site/misc/terms.xhtml). After six months, it is available under a Creative Commons License (Attribution-NonCommercial 4.0 International), as described at http://creativecommons.org/licenses/by-nc/4.0/.

genes comprising *Wee1*, *Cyclins*, and *Myc1* (Matsuo et al. 2003), and to gate cytokinesis to a specific time within the circadian cycle (Nagoshi et al. 2004; Bieler et al. 2014). Both the cell division cycle and the circadian clock undergo significant changes upon malignant transformation, although no clear causal links between the two processes are known (Mannic et al. 2013; Gaucher et al. 2018).

The importance of temporal coordination of cell proliferation has emerged in the context of reparative regeneration in tissues that bear intrinsic regenerative capacity, such as liver, intestine, and skeletal muscle (Matsuo et al. 2003; Karpowicz et al. 2013; Chatterjee et al. 2015; Bellet et al. 2016; Stokes et al. 2017). Rodent studies suggest that β cells have a limited potential for regeneration via replication of existing β cells (Dor et al. 2004; Nir et al. 2007; Stolovich-Rain et al. 2012; Klochendler et al. 2016) or trans-differentiation from adjacent ductal epithelial cells (Xu et al. 2008), a cells (Thorel et al. 2010; Chakravarthy et al. 2017), and δ cells (Chera et al. 2014). Unlike fast regenerating tissues including liver, the regeneration of β cells is a long-lasting process that takes a few weeks and even months in mice (Nir et al. 2007; Cheng et al. 2017). Core clock components may play a role in regulating β -cell division. Indeed, mice lacking at least one allele of Bmall in β cells fail to increase β -cell mass in response to diet-induced obesity (Rakshit et al. 2016), and siRNA-mediated down-regulation of RORy attenuated glucose-driven induction of cell cycle-related genes and the proliferation rate in INS-1E cell line (Schmidt et al. 2016). Unraveling mechanisms of regulation of βcell regeneration is of a fundamental clinical importance in the search of new therapeutic approaches for management of diabetes mellitus.

Molecular clocks operative in pancreatic islets (Pulimeno et al. 2013) play a critical role in islet cell physiology and in regulating glucose homeostasis (Marcheva et al. 2010; Petrenko et al. 2017b; Sinturel et al. 2020). Indeed, mice harboring whole-body or tissue-specific null alleles for essential core clock components develop hyperglycemia, hypoinsulinemia and glucose intolerance (Marcheva et al. 2010; Dyar et al. 2014; Perelis et al. 2015; Rakshit et al. 2016). Although perturbation of the islet clocks emerges as a part of type 2 diabetes (T2D) pathogenesis in humans (Petrenko et al. 2020), it remains unclear whether alterations of the molecular clockwork precede development of T2D or stem from the disease progression. Thus, understanding the functional link between changes of the molecular clockwork, islet dysfunction and β-cell regeneration potential is an important challenge. In this work we studied the diurnal regulation of β-cell proliferation and profiled the circadian transcriptomes of α and β cells following massive β-cell ablation in the Insulin-rtTA/TET-DTA mouse model in the presence or absence of functional clocks.

Results

 β -Cell regeneration follows a diurnal pattern

In order to study the impact of the circadian system on β -cell dysfunction and regeneration, we used Insulin-

rtTA/TET-DTA transgenic mice, in which the ablation of ~80% of β cells can be induced in a controlled manner (Nir et al. 2007). This mouse strain was crossed with triple-reporter mice (Petrenko et al. 2017b) that expressed fluorescent protein reporters specific for a cells (ProGlucagon [Gcg]-Venus) and β cells (rat Insulin2 promoter [RIP]-Cherry), along with the ubiquitously expressed circadian bioluminescence reporter Period2::Luciferase (Per2::Luc) (Supplemental Fig. S1A). The resulting mouse model encompassing five transgenes permitted to conduct parallel analyses of the transcriptional landscape separately in residual β cells and neighboring α cells following massive β cell ablation. Administration of doxycycline (DOX) to the drinking water during 7–10 d induced a massive β -cell loss in Insulin-rtTA/TET-DTA mice (Supplemental Fig. S1B), resulting in acute hyperglycaemia sustained for at least 14 d (Supplemental Fig. S1C), consistent with previous publications (Nir et al. 2007).

We first assessed whether entry into the S phase of the cell cycle of remnant β cells exhibited a diurnal profile. This was done by injecting 5-bromo-2'-deoxyuridine (BrdU), a marker of DNA replication during S phase, 2 h prior to sacrificing the animals at 6 time points with 4-h intervals across 24 h. In accordance to previously published data (Nir et al. 2007), we observed overall increased BrdU incorporation in the nuclei of insulin-labeled cells following massive β-cell loss when averaging the results across all time points (Supplemental Fig. S1D). Most importantly, the incorporation of BrdU by residual β cells was not only augmented overall, but it also exhibited a circadian rhythmicity (adjusted P-value = 0.032; BH.Q = 0.065) when examined using the JTK_Cycle paradigm (Fig. 1A,B; Supplemental Fig. S2; Hughes et al. 2010). These data suggest that the proliferative response in residual β cells after ablation gains a circadian pattern, with a peak observed in the middle of activity phase.

The acute loss of β -cell mass affects gene expression in residual β cells, but not in adjacent α cells

In an attempt to explore the mechanism of β -cell proliferation following massive ablation, we profiled the temporal transcriptome of FACS sorted α - and β -cell populations. Temporal analyses were conducted 7-10 d following DOX administration in Insulin-rtTA/TET-DTA-triple-reporter transgenic mice. Remnant islets were isolated every 4 h at six time points across 24 h (Supplemental Fig. S1A,B; Petrenko et al. 2017a; Petrenko and Dibner 2018). α-Cell and \beta-cell fractions from DOX group and untreated control counterparts were subjected to genome-wide transcriptome analysis by RNA sequencing (RNA-seq). We identified 12,912 transcripts after filtering for genes with at least 1 count per million (CPM) in at least half of all measurements (cell type, condition, and time points). A multidimensional scaling with a distance measure for microarrays (plotMDS from limma [Ritchie et al. 2015]) run on all samples showed clear separation between a and β cells (Fig. 2A, dimension 1) and major differences between β cells in intact islets and residual β cells following ablation (Fig. 2A, dimension 2). In contrast, almost no

Circadian clocks drive **\beta-cell** regeneration

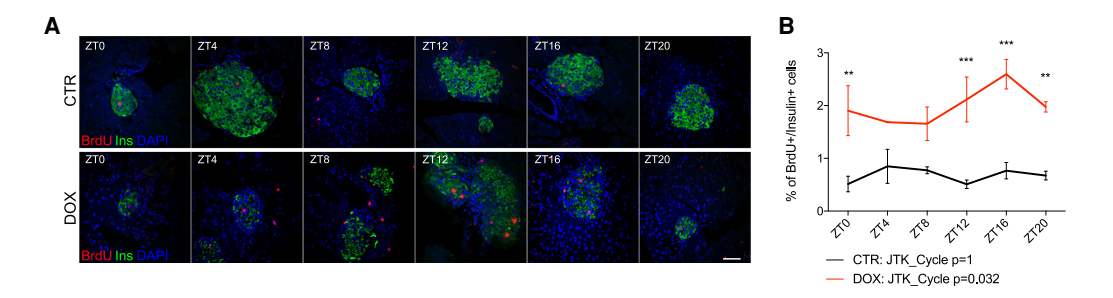


Figure 1. Circadian regulation of β-cell regeneration following massive ablation. (A,B) Around-the-clock assessment of β-cell proliferation conducted 12 d after beginning of DOX administration. BrdU was injected intraperitoneally 2 h prior to sacrificing the animals every 4 h across 24 h. (A) Representative confocal images of pancreatic islets show localization of proliferation marker BrdU (red staining) in the nucleus of insulin-producing β cells (green) at the indicated time points (see also Supplemental Fig. S2). Scale bar, 50 μm. (B) Daily profile of β-cell proliferation. Data are expressed as mean ± SEM for n = 3 mice per time point. Two-way ANOVA test with Bonferroni post-test was used to assess the difference between control and DOX groups. (**) P < 0.001. [TK_Cycle was used to assess circadian rhythmicity of the averaged profiles.

differences among α -cell samples were detected between control and DOX groups (Fig. 2A, dimension 2).

Differential transcript expression analysis that compared average values across all six time points per cell type and per condition identified 924 differentially expressed genes between residual β cells from the DOX group and the untreated control counterparts (733 up-regulated and 268 down-regulated) (Fig. 2B; Supplemental Data Set S1). In contrast, only one gene (B2m) was differentially expressed in neighboring α cells after ablation as compared with controls (Supplemental Data Set S1). We next validated the changes of selected transcripts differentially expressed in β cells from the DOX group in an independent set of experimental animals by qRT-PCR analyses. Concordant with the RNA-seq results, miKi67, AurkB, and Pappa2 were up-regulated, whereas Mafa was down-regulated (Fig. 2C). Ingenuity pathway analysis (IPA) identified in the top canonical pathways characterizing the transcriptional landscape of the residual β cells the signaling pathways involved in cell cycle regulation. Based on the observed regulation of their molecular components, these were predicted as activated (Fig. 2D). Moreover, Foxm1 was predicted as a top upstream transcriptional regulator for the observed regulatory landscape (Fig. 2E).

When the analysis was conducted separately per time point, the number of differentially expressed transcripts (Supplemental Fig. S3A) was similarly distributed in β cells compared with a cells in the control condition (Supplemental Fig. S3B). Small differences across the time points were observed between α and residual β cells in the DOX group (Supplemental Fig. S3C-E). In contrast, the number of differentially regulated transcripts in β cells between DOX-treated and control mice varied greatly among the time points (Fig. 2F). There was a higher number of differentially expressed transcripts observed during the inactivity phase (between ZT0 and ZT8), and a minimal number of differentially expressed transcripts at the time point of light to dark transition (ZT12) (Fig. 2F). All in all, our findings suggest that transcripts whose expression levels change after β-cell ablation exhibit daily variability.

The temporal expression of transcripts is differentially affected in residual β - and neighboring α cells following massive β -cell loss

To study temporal regulation of α - and β -cell transcriptional landscapes we analyzed RNA-seq data sets collected at six time points every 4 h across 24 h from DOX Insulin-rtTA/TET-DTA-triple-reporter mice following β-cell ablation and the untreated CTR counterparts (Supplemental Fig. S1A; Supplemental Data Sets S2–S5). The rhythmicity of each gene was determined based on the best circadian profile with a 20- to 28-h period and a classification by logistic regression (Materials and Methods). Temporal gene expression profiles were grouped into a number of models, which are summarized in Figure 3, E and F. Heat maps for five selected models for the alteration of temporal gene expression between α and β cells in control and DOX groups are presented in Figure 3, A and B, respectively. The five groups of profile changes encompassed the genes expressed in both cell types that exhibited a flat (nonrhythmic) profile across 24 h in one cell type, but a circadian profile in the other cell type (NC and CN, where N stands for "nonrhythmic" and C stands for "circadian"). The CC group comprised genes that were rhythmically expressed in both cell types, with similar or distinct circadian properties. The last two categories referred to the genes that were not expressed (Ne) in one cell type but expressed in a circadian fashion in the other (CNe and NeC). A gene was considered to be expressed if it had an average RPKM across all time points of >1. Consistent with our previous study (Petrenko et al. 2017b), close to half of the detected transcripts (45.15%) exhibited a rhythmic expression in at least one cell type (Fig. 3A; Supplemental Data Set S2). Following massive β-cell loss, the overall proportion of genes defined as rhythmic in at least one cell type slightly increased to 48.5%. The number of rhythmic genes common to both cell types increased from 1505 to 1645, and the number of transcripts exclusively rhythmic in residual β cells increased from 1668 to 2128 in the DOX group (Fig. 3B; Supplemental Data Set S3). We next conducted a similar comparison of

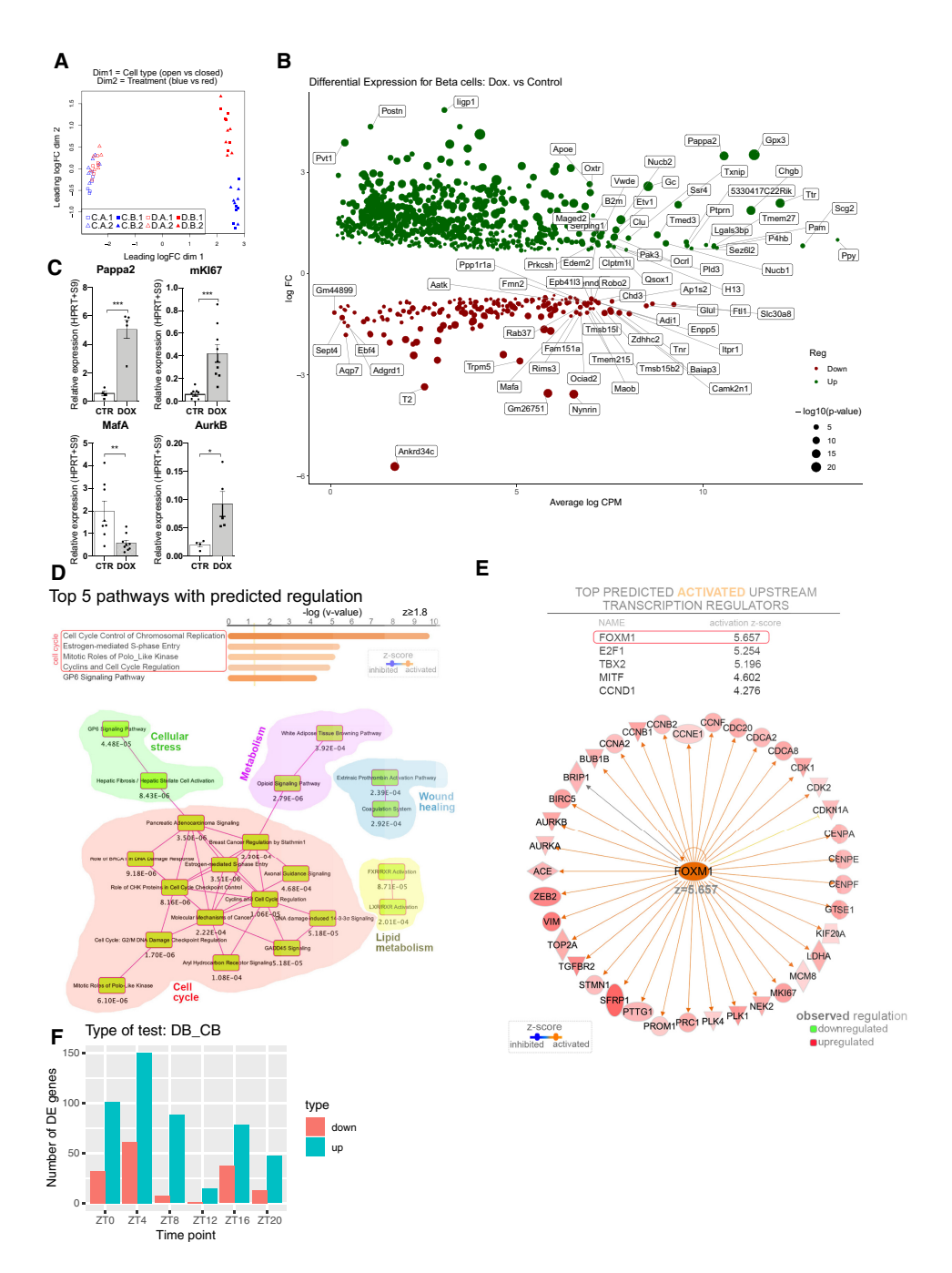


Figure 2. Differential analysis of gene expression in α and β cells following massive β-cell ablation. A total of 12,912 transcripts were identified by RNA-seq analyses, following the experimental settings presented in Supplemental Figure S1A. (A) Multidimensional scaling across all the samples (α and β cells from mice treated or not with DOX in six time points, two experimental repetition each, total of 24 samples). (Dimension 1) Cell type, (dimension 2) treatment (DOX vs CTR). "C.A" and "C.B" (experimental repetition 1 and 2) correspond to α and β cells, respectively, from the CTR group; D.A and D. B (repetition 1 and 2) correspond to the DOX group counterparts. Note the clear separation between the transcripts specific for α and β cells, and between CTR and DOX β cells. (B) Volcano plot presents transcripts that were differentially expressed between CTR β cells and residual β cells in DOX group. For differential analysis, the average across six time points per each of four conditions (a and β cells, treated or not with DOX) was considered. Up-regulated genes (924 genes) are labeled in green; down-regulated (190 genes) are labeled in red ($\log_2 FC > 0.5$ and $\log_2 FC < -0.5$, respectively). Sizes of dots correspond to the $\log_{10} P$ value. Volcano plots that compare α and β cells in control and DOX groups are presented in Supplemental Figure S3, A and C, respectively. (C) Examples of differentially expressed genes in β cells following ablation identified by RNA-seq (shown in B) and assessed by qRT-PCR analysis in an independent set of mice. Data are expressed as mean \pm SEM for n = 4-9 mice. (*) P < 0.05, (**) P < 0.01, (***) P < 0.001. (D_rE) $Results of the Ingenuity \ Pathway \ Analysis \ (IPA) \ of \ differentially \ expressed \ transcripts \ (shown in \ B), indicating the top \ canonical \ pathways \ differentially \ expressed \ transcripts \ (shown in \ B), indicating the top \ canonical \ pathways \ differentially \ expressed \ transcripts \ (shown in \ B), indicating the top \ canonical \ pathways \ differentially \ expressed \ transcripts \ (shown in \ B), indicating \ the top \ canonical \ pathways \ differentially \ expressed \ transcripts \ (shown in \ B), indicating \ the top \ canonical \ pathways \ differentially \ expressed \ transcripts \ (shown in \ B), indicating \ the top \ canonical \ pathways \ differentially \ expressed \ transcripts \ (shown in \ B), indicating \ the top \ canonical \ pathways \ differentially \ expressed \ transcripts \ (shown in \ B), indicating \ the top \ canonical \ pathways \ differentially \ expressed \ transcripts \ (shown in \ B), indicating \ the top \ canonical \ pathways \ differentially \ expressed \ transcripts \ (shown in \ B), indicating \ the top \ canonical \ pathways \ differentially \ expressed \ transcripts \ (shown in \ B), indicating \ the top \ canonical \ pathways \ differentially \ expressed \ transcripts \ (shown in \ B), indicating \ the top \ canonical \ pathways \ differentially \ expressed \ transcripts \ (shown in \ B), indicating \ the top \ canonical \ pathways \ differentially \ expressed \ transcripts \ expressed \ expre$ predicted regulated ($z \ge 1.8$) as well as the overlapping canonical pathways map with at least five common molecules (D) and the top activated predicted upstream transcription regulators $(z \ge 2)$ (E). (F) Histograms presenting differential expression (number of up- and downregulated genes) in residual β cells (DB) compared with control condition (CB) at each of six time points. See Supplemental Figure S1 for the experimental design and related Supplemental Figure S3.

4 GENES & DEVELOPMENT

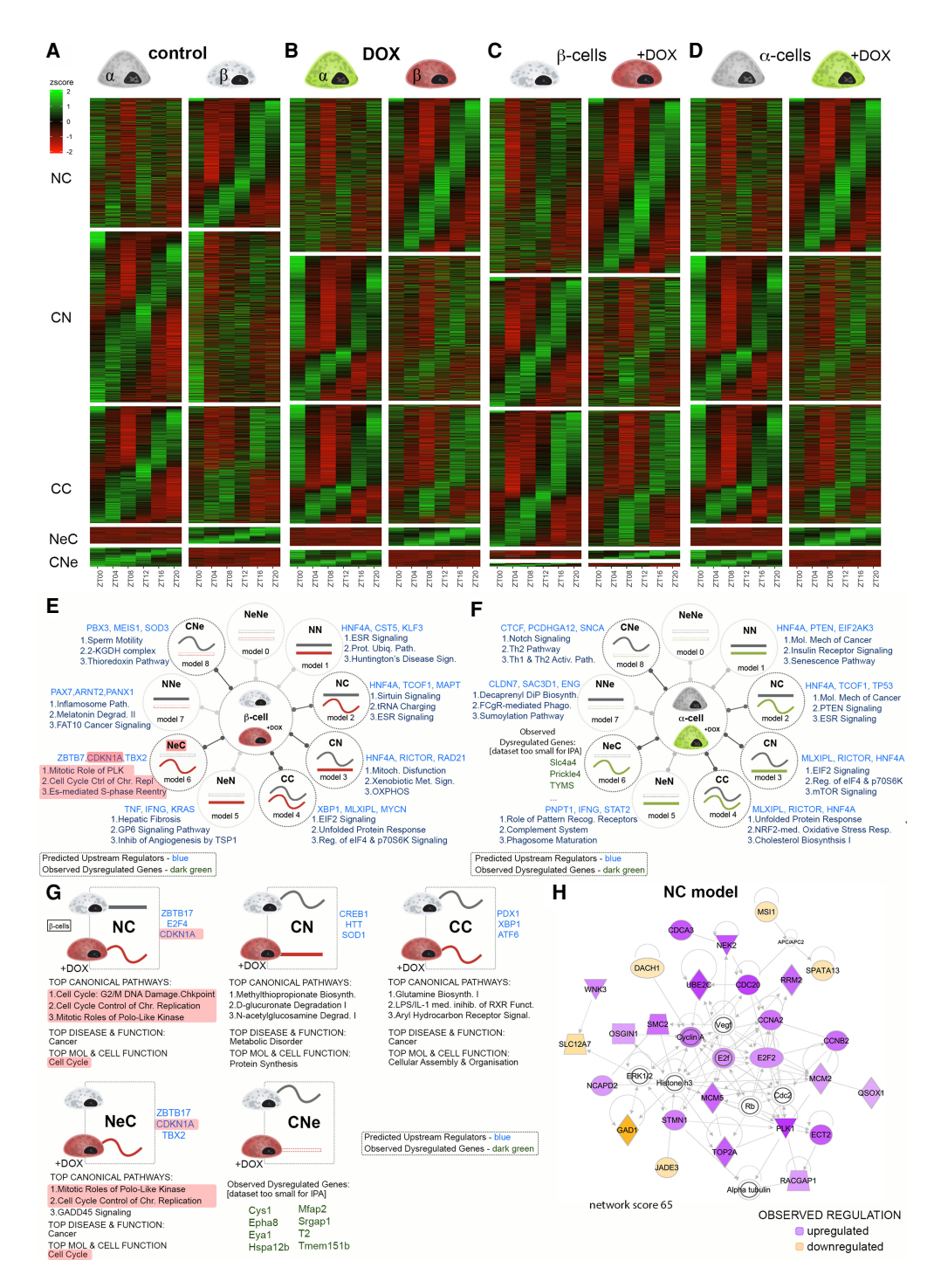


Figure 3. Temporal analysis of gene expression in α and residual β cells following partial β-cell ablation. (A–D) Heat maps comparing temporal profiles of transcripts between α and β cells in control condition (A) or following β-cell ablation (DOX condition; B), between α cells in control and DOX groups (C), and between β cells (D) in control and DOX groups for the temporal transcript profile changes from nonrhythmic to circadian (NC), circadian to nonrhythmic (CN), circadian rhythmic in both conditions (CC), nonexpressed in one condition and circadian rhythmic in the other (NeC and CNe), nonexpressed in one condition and nonrhythmic in the other (NeN and NNe), and nonexpressed in both conditions (NeNe). (E,F) IPA of different models of rhythmic transcripts expressed in β cells (E) and in α cells (F), in control versus DOX-treated conditions. Three predicted upstream regulators (blue) and three most enriched functional pathways are listed next to the model drawings. For data sets too small to allow pathway analysis, a selection of genes belonging to the respective model is indicated (green). (G) IPA of sub-groups of rhythmic transcripts (Fig. 3C, models CC, NC, CN, NeC, and CNe) that were differentially expressed in β cells between control and DOX-treated conditions. Predicted upstream regulators (blue) are listed next to the schematic drawing of the temporal profile change. For data sets too small to allow pathway analysis, a selection of DEGs (green) is indicated. Top canonical pathways, disease, and molecular/cellular function are listed *below* the drawing. (H) Leading IPA-generated organic network of up-regulated and down-regulated transcripts that acquired rhythmicity following DOX treatment in the model NC in presented in G displaying the regulation of cell cycle related genes.

Petrenko et al.

temporal gene expression in each cell type between control and DOX conditions (Fig. 3C,D). In the β-cell fraction, 1635 genes that were circadianly expressed in the control lost their rhythmic expression in the DOX group (Fig. 3C; Supplemental Data Set S4, model CN). Remarkably, 2208 transcripts that were nonrhythmic in the control group acquired rhythmicity after ablation (Fig. 3C; Supplemental Data Set S4, model NC). Noteworthy, despite the lack of differential changes in the average values of the transcript expression across all the time points in $\boldsymbol{\alpha}$ cells following DOX treatment, the ablation of neighboring β cells strongly affected the temporal landscape of the α cell transcriptome. Indeed, 2266 transcripts that were rhythmic in the control group became flat in the DOX group (Fig. 3D, model CN), and as many as 2225 nonrhythmic transcripts in the control α cells acquired a rhythmicity in DOX-treated mice (Fig. 3D, model NC; Supplemental Data Set S5).

We next performed pathway analysis by applying IPA to each of the five groups of transcripts that presented temporal profile changes in β and α cells between the control and DOX groups (Fig. 3E,F, respectively, referring to the temporal heat maps in Fig. 3C,D). Interestingly, nonrhythmic transcripts that acquired rhythmicity in residual β cells were involved into Sirtuin signaling, tRNA charging, and estrogen receptor (ESR) signaling (Fig. 3E). Those in neighboring α cells were related to ESR and PTEN signaling, and to molecular mechanisms related to cancer (Fig. 3F). In turn, rhythmic transcripts that lost rhythmicity in residual β cells were related to mitochondrial dysfunctions, oxidative phosphorylation, and xenobiotic metabolism. Those in neighboring α - cells were related to mTOR signaling, to EIF2 signaling, and to the regulation of eIF4 and the ribosomal protein p70S6k, which are involved in the tuning of protein synthesis.

Two additional groups of genes were identified in each cell type: (1) genes that were defined as nonexpressed in control condition, and that were up-regulated and acquired rhythmic profiles following DOX treatment (model NeC in Fig. 3E,F); and (2) rhythmically expressed genes in the control condition that became silent following DOX treatment (model CNe in Fig. 3E,F). Interestingly, newly expressed rhythmic genes in residual β cells were related to mitosis, with the mitotic role of Polo-like kinase, cell cycle control of chromosome replication, and estrogen-mediated S-phase reentry signaling being identified as the top three canonical pathways (Fig. 3E).

Finally, we applied IPA to the genes that were both differentially expressed according to the analyses of mean values (Fig. 2B) and exhibited distinct temporal rhythmic profiles in β cells following the β -cell ablation compared with the control group (Fig. 3C). Strikingly, a high number of genes coding for the key regulators of the cell cycle were comprised in this group. The transcripts of cell cycle regulators exhibited higher expression in residual β cells (Fig. 2B) and became rhythmic after ablation (models NC and NeC in Fig. 3G,H). This further supports the possibility that compensatory β -cell proliferation is controlled in a circadian fashion. Accordingly, the top-rated network of differentially expressed genes within the NC model con-

sisted of genes involved in cell cycle regulation (Fig. 3H), further substantiating the role of circadian regulation in the proliferation of β cells during regeneration.

The temporal expression of core clock and cell cycle-controlling genes in residual β cells and adjacent α cells following β -cell ablation

Remarkably, a comparison of the circadian phases between the transcripts that exhibited rhythmic expression profiles in control and DOX groups in β cells (Fig. 3C) revealed that most of the transcripts rhythmic in the DOX group had a phase delay of ~2.5 h when compared with the corresponding transcripts of the control group (Fig. 4A, red bars; Supplemental Data Set S6). In contrast, no significant phase shifts were found for the transcripts that were rhythmically expressed in α cells between control and DOX conditions (Fig. 4A, green bars; Supplemental Data Set S6).

To address the question of whether the core clock machinery operative in the islet cells had been altered by massive β -cell ablation, we compared profiles of the core clock components in DOX and control groups in α and β cells. Rorc, Bmal1 (Arntl), and Cry1 oscillatory profiles were phase-advanced in β cells compared with α cells in untreated control mice, concordant with our previous findings (Petrenko et al. 2017b). Noteworthy, these transcript profiles were phase-delayed in β cells following DOX treatment when compared with β cells of untreated mice. However, these phase differences could not be observed in the neighboring a cells (Fig. 4B). This finding was further supported by a KEGG pathway enrichment analysis of RNA-seq database (Supplemental Data Set S6), with circadian clock pathway appearing among the most altered ones (Supplemental Fig. S4A). We next assessed the molecular clockwork in isolated remnant islets after massive β -cell ablation and in separated α and β cells synchronized by a forskolin pulse in vitro (Supplemental Fig. S4B,C). These experiments suggest that cell-autonomous molecular clocks are fully operative in isolated a and β cells of remnant pancreatic islets following massive β-cell ablation.

An additional prominent group of transcripts whose accumulation appeared altered following DOX treatment by IPA analysis was related to the regulation of the cell cycle. Noteworthy, most of the up-regulated cell cycle-related transcripts exhibited a circadian expression profile (see Fig. 3G). These transcripts include mRNAs encoding the proliferation regulators mKi67, Foxm1, Pbk, E2f2, cyclins (Ccna2 and Ccnb2), aurora kinases (Aurkb and Aurka), Cdk1, Cdc20, and other regulators of cellular cycle progression (Fig. 4C; Supplemental Data Set S3).

The essential core clock transcription factor BMAL1 is required for β -cell proliferation following massive β -cell ablation

To scrutinize the role of the molecular clocks in the development of diabetic phenotypes and in the regulation of compensatory β -cell regeneration, β -cell ablation was

Circadian clocks drive **\beta-cell** regeneration

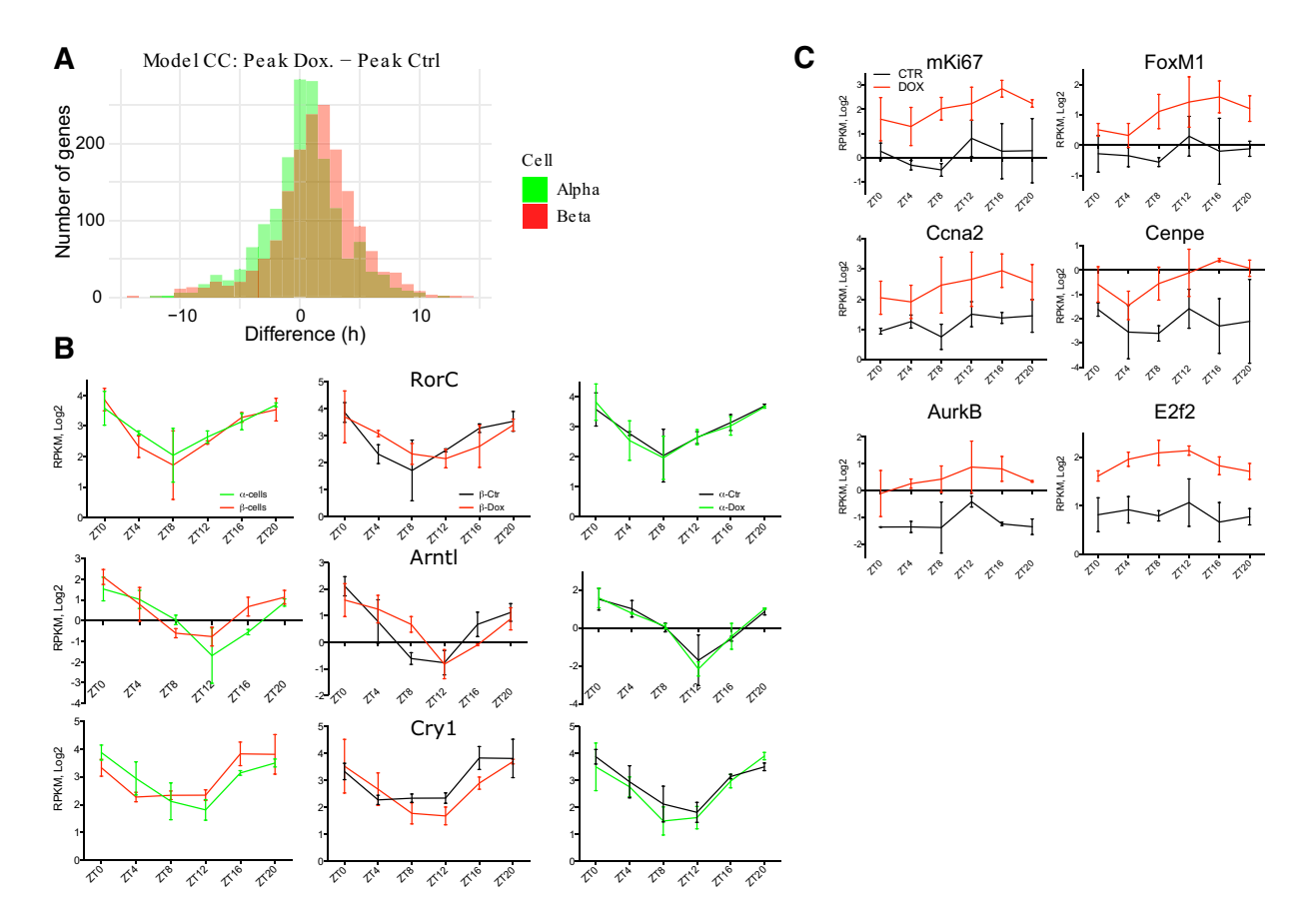


Figure 4. Temporal profiles of core clock and proliferation regulating genes in residual β cells and adjacent α cells following massive ablation. (A) Phase shift between rhythmically expressed transcripts in CTR and DOX conditions (model CC) identified in α cells (in green) and β cells (in red) according to the temporal analysis of RNA-seq presented in Figure 3. Phase differences were calculated for each rhythmic transcript and plotted on the graph. 0 corresponds to identical phase between the transcript expression in CTR and DOX conditions. (B) Temporal profiles of selected core clock transcripts (RorC, Arntl [Bmal1], and Cry1) in control α and β cells (in green and in red, respectively; left panels), in control β cells versus residual counterparts (middle panels), and in control and DOX-treated α cells (right panels) assessed by RNA-seq. (C) Temporal profiles of selected transcripts encoding for the proliferation regulating proteins (see also Fig. 3G) in sorted β cells. Data are expressed as mean ± SD for two experimental repetitions per each time point with at least three mice in each plicate.

triggered in arrhythmic Bmal1 deficient mice. To this end, we crossed mice in which BMAL1 expression was blocked by a transcriptional-translational stop cassette knock-in into the *Bmal1* locus (*Bmal1* st/st mice) (Supplemental Fig. S5A) with Insulin-rtTA/TET-DTA-triple-reporter mice. As expected, the absence of functional clocks in isolated islets from these transgenic animals resulted in a flat Per2-luc bioluminescence profile following forskolin synchronization (Supplemental Fig. S5B). Clockcompromised Bmal1st/stDTA mice and their heterozygous Bmal1+/stDTA counterparts were treated with DOX according to the design depicted in Supplemental Figure S1A. Of note, nontreated Bmal1+/st mice and their Bmal1+/+ counterparts exhibited comparable levels of glucose, insulin, and glucagon (Supplemental Fig. S6A-C). Induction of β -cell loss in *Bmal1*^{st/st} mice led to a significantly more severe hyperglycemia as compared with DOX-treated heterozygous mice (Fig. 5A, cf. Bmal1+/ stDOX and Bmal1st/stDOX). Thus, in DOX-treated

Bmal1st/stDTA animals, peripheral blood glycemia was ~10 mmol/L higher than in heterozygotes control mice in the middle of the activity phase (ZT16). This difference was slightly smaller, but still significant, at ZT4 (Fig. 5A). Bmal1^{st/st}DTA and heterozygotes mice exhibited similar levels of hypoinsulinemia after DOX treatment at ZT16 as compared with nontreated Bmal1 st/stDTA and control mice, with no significant changes in blood insulin observed at ZT4 (Fig. 5A). Bmal1st/stDTA mice not treated with DOX exhibited higher levels of blood glucagon as compared with the clock proficient controls. Strikingly, β -cell ablation resulted in a significantly more dramatic hyperglucagonemia in Bmal1+/stDTA mice at ZT16. This phenotype was even more pronounced in Bmal1st/ stDTA mice. A trend for hyperglucagonemia was also observed for $Bmal1^{+/st}$ DTA and $Bmal1^{\bar{s}t/st}$ DTA mice treated with DOX at ZT4; however this tendency did not reach statistical significance (Fig. 5A, Bmal1+/st DOX, Bmal1^{st/st}DOX).

Petrenko et al.

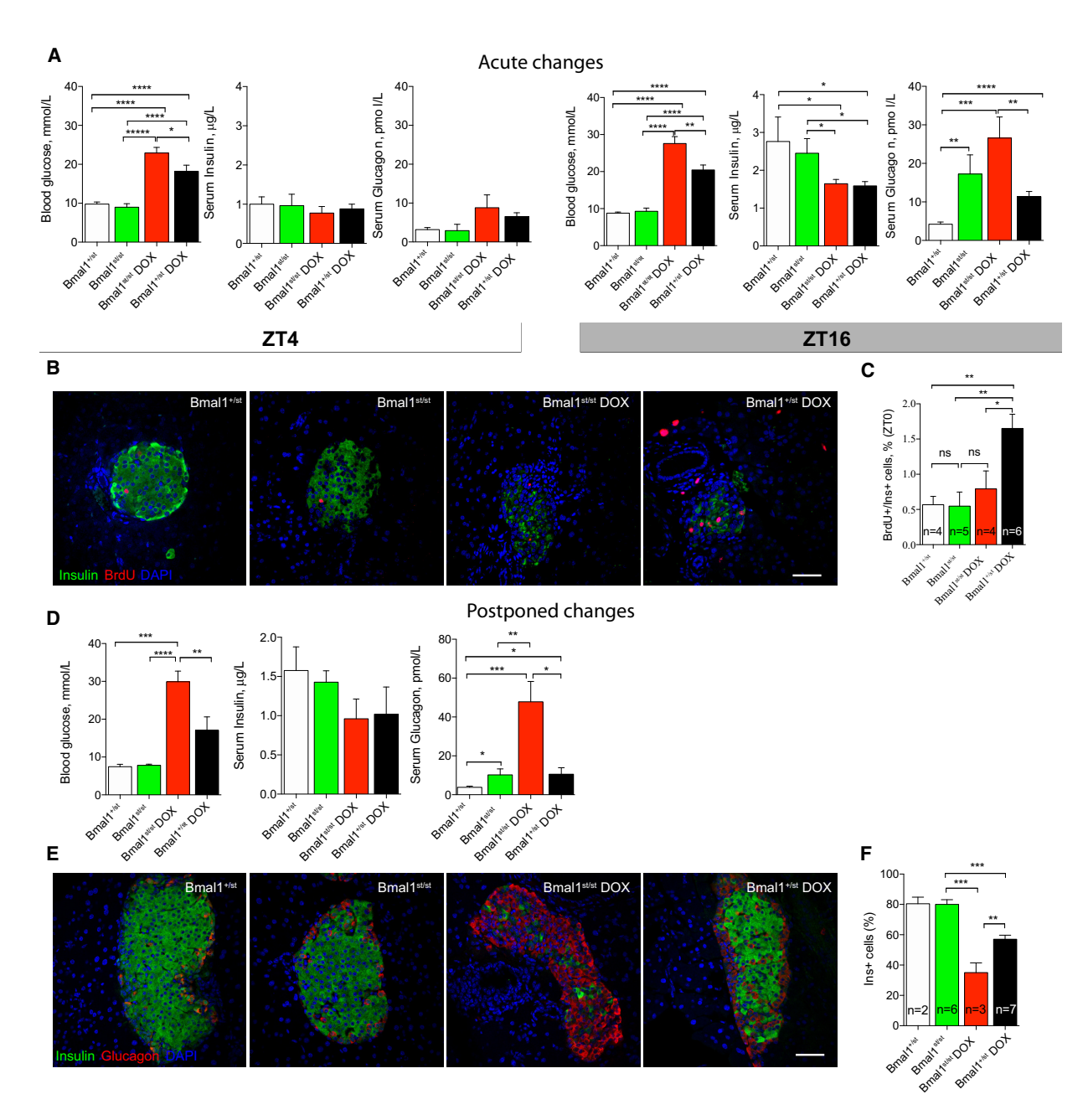


Figure 5. Bmall is required for functional recovery and compensatory β-cell proliferation following massive β-cell loss. (*A*) Assessment of blood glucose, insulin and glucagon levels 12 d after beginning of DOX administration at ZT16 and ZT4. Data are expressed as mean ± SEM for n = 8-16 mice per group. One-way ANOVA was applied to test the difference between groups, followed by *t*-test comparisons. (*) P < 0.05, (**) P < 0.01, (***) P < 0.001, (***) P

Circadian clocks drive **\beta-cell** regeneration

Next, we assessed the proliferation rate of remnant β cells by injecting the thymidine analog BrdU intraperitoneally 2 h before sacrificing the animals at ZTO. In agreement with our previous data (Fig. 1A,B), the number of BrdU/Insulin double-positive β cells was significantly increased in DOX-treated $Bmal1^{+/st}DTA$ mice following β -cell ablation as compared with both $Bmal1^{+/st}DTA$ and $Bmal1^{st/st}DTA$ control mice without DOX treatment (Fig. 5B,C). In striking contrast, β -cell loss failed to enhance the number of BrdU/Insulin double-positive cells in DOX-treated $Bmal1^{st/st}DTA$ ($Bmal1^{st/st}DOX$) (Fig. 5B, C; Supplemental Fig. S7).

Finally, we followed the regeneration and functional recovery of β cells during a longer period after massive ablation. Four weeks after DOX withdrawal the blood glucose levels measured at ZT4 in Bmal1st/stDTA animals stayed consistently high when compared with Bmal1+/stDTA counterparts (Fig. 5D, left panel, cf. Bmal1st/stDOX and Bmal1^{+/st}DOX). The level of serum insulin was comparable between DOX-treated Bmal1+/stDTA and Bmal1st/st DTA animals, with a tendency to be lower in Bmal1st/st group that did not reach statistical significance (Fig. 5D, middle panel). Furthermore, untreated Bmal1st/stDTA mice exhibited a significantly more pronounced hyperglucagonemia as compared with heterozygous controls. Observed hyperglucagonemia was further elevated in DOX treated Bmal1st/stDTA animals compared with their Bmal1st/st counterparts without such a treatment (Fig. 5D, right panel).

Strikingly, 6 wk following DOX withdrawal the survival rate for *Bmal1* st/stDTA animals was ~33% only (three out of nine mice), whereas all of the *Bmal1*+/stDTA animals (*n* = 8) survived at this point. Consistent with the blood glycemia and hormone status, histological examination of the pancreas from the animals following 6 wk of recovery after DOX administration revealed a significantly lower proportion of insulin-positive β cells in Bmal1st/stDTA mice among overall insulin- and glucagon-labeled cells as compared with their Bmal1+/st counterparts (Fig. 5E,F, cf. Bmal1^{st/st}DOX and Bmal1^{+/st}DOX). Hence, in contrast to the β-cell regeneration and recovery from diabetes observed in rhythmic mice, β -cell regeneration did not occur in Bmal1st/st arrhythmic mice. Consequently, this led to a life-threatening diabetes, with pronounced hyperglycemia and hyperglucagonemia.

The expression of cell cycle-regulating genes is strongly inhibited in residual β cells of Bmall st/stDTA mice following β -cell ablation

In an attempt to dissect the molecular mechanism underlying the failure of β -cell regeneration in the absence of the core clock transcription factor BMAL1, we performed RNA-seq on FACS-purified residual β cells from $\mathit{Bmal1}^{st/st}$ DTA mice 10 d following DOX administration (Fig. 6A; Supplemental Data Set S7). First, we compared DOX-treated $\mathit{Bmal1}^{st/st}$ DTA with untreated controls (Supplemental Data Set S8). We identified only three differentially expressed genes between these two conditions: transcripts related to fructose metabolism Aldob and

Pfkfb3 were up-regulated, while H2-Ea-ps was down-regulated. We failed to observe activation of cell cycle related pathways. When compared DOX-treated $Bmal1^{\text{st/st}}$ DTA and $Bmal1^{\text{+/st}}$ DTA mice, an impaired expression of functional Bmal1 pre-mRNA in $Bmal1^{\text{st/st}}$ DTA mice was confirmed by a decreased RNA sequence read coverage of the Bmal1 gene region downstream from the stop cassette (between exon 5 and 6) as compared with heterozygotes mice (Supplemental Fig. S5A,C). An up-regulation of incomplete Bmal1 transcript was observed in $Bmal1^{\text{st/st}}$ mice (Supplemental Fig. S5E,F; Supplemental Data Set S7), supposedly because the expression levels of REV-ERBα/β, that act as repressors of Bmal1 transcription (Preitner et al. 2002), were diminished in these animals (Supplemental Data Set S7).

Within all of the detected 14,649 expressed genes, a subset of 319 differentially expressed genes (DEGs) defined by $FC \ge 2$ with P < 0.05 was identified between homozygous Bmal1^{st/st}DTA and heterozygous Bmal1^{+/st}DTA counterparts (Fig. 6B,C). The IPA of this DEG subset revealed regulators involved in cell cycle regulation and circadian rhythm in the top 5 canonical pathways (Fig. 6D, green island; Supplemenal Fig. S5D). KEGG pathway enrichment analysis revealed a differential expression of modulators of the neuroactive ligand-receptor interaction pathway, comprising key hormonal regulators of β-cell function Gcgr and Ptger3 up-regulation and Glp1r, Oxtr, Ucn3, and Lpar6 down-regulation (Supplemental Fig. S5G; Supplemental Data Set S7). Functional networks directly linked to impaired Bmal1 expression are presented in Supplemental Figure S5, E andF.

Furthermore, based on the observed changes, the pathways involved in cell cycle regulation were predicted as inhibited (Supplemental Fig. S5D), suggesting a decreased β-cell proliferation in the *Bmal1*^{st/st} mice. Supporting this observation, key cell cycle regulators such as senescence markers Cdkn2a (p16) and Cdkn1a (p21, P-value of overlap 6.82E-28, activation z-score 2.701) and tumor suppressor genes p53 and p73, were inferred in the top predicted upstream transcription regulators with expected activation (Fig. 6E). Furthermore, CcnD1 (cyclin D1) (Fig. 6E) and Foxm1 (Fig. 6E,F) were included in the top predicted upstream regulators inferred as inhibited. Accordingly, cell cycle progression was identified as a top molecular and cellular function of the analyzed DEG set, while cancer was suggested to be the leading predicted associated pathology (Fig. 6E). Strikingly, all three top hits revealed by the network analysis were connected to cell cycle regulation (Fig. 6F). Taken together, these findings may explain the low proliferative potential of *Bmal1* deficient β cells after β-cell ablation (Fig. 5B,C, E,F).

Discussion

In this study, we induced massive β -cell ablation to identify mechanisms participating in the regulation of islet cell regeneration and to characterize the transcriptional landscape in separated α cells and residual β cells. Our results provide evidence that proliferation of residual β cells

Petrenko et al.

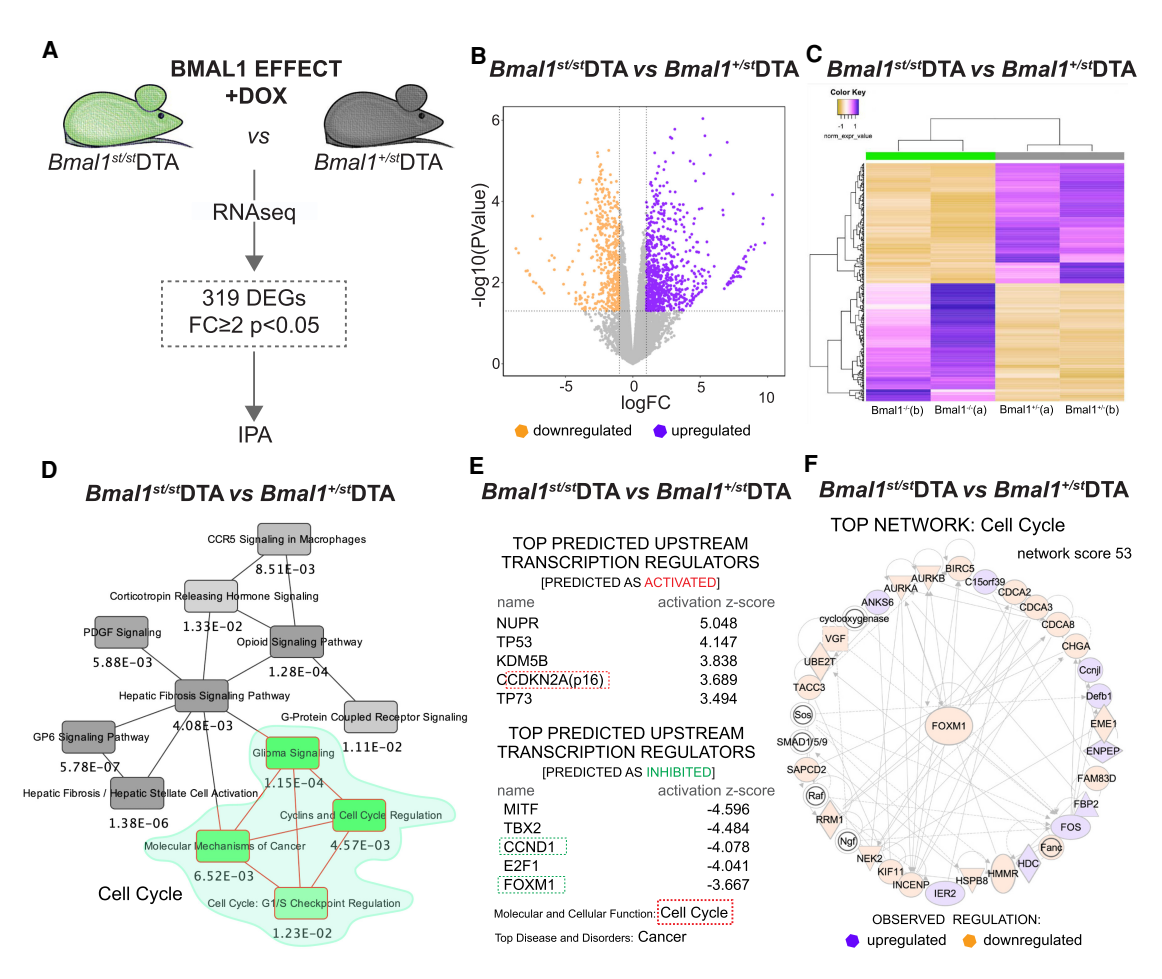


Figure 6. RNA-seq analysis of residual β cells in $Bmal1^{st/st}$ mice following massive β-cell loss. (A) Schematic drawing of RNA-seq differential analysis of FACS-separated β cells from $Bmal1^{st/st}$ and $Bmal1^{+/st}$ mice treated with DOX. Data represent two biological replicates collected at ZT0 (each replicate is a mix of cells from three mice). (B) Volcano plot presenting 319 differentially expressed transcripts (showing significance [$-\log_{10} \{P\text{-value with FDR}\}$] versus fold change [$\log FC$]). Vertical lines highlight \log_2 fold changes of -2 and +2, while a horizontal line represents a P-value with FDR of 0.05. (C) Dendrogram with heat maps highlighting clusters of up-regulated and down-regulated genes between $Bmal1^{st/st}$ and $Bmal1^{+/st}$ mice treated with DOX in two biological replicates (a and b). (D-F) The IPA of differentially expressed genes, revealing the overlapping canonical pathways map (minimum number of common molecules: four; D); top predicted upstream transcription regulators (activated or inhibited), top molecular and cellular function, and top disease and disorders (E); and the top 1 network (F) of the analyzed differential transcriptional landscape, all suggesting the modulation of cell cycle regulation in $Bmal1^{st/st}$ mice.

triggered by massive ablation follows a circadian pattern (Fig. 1). Virtually no compensatory β -cell regeneration occurred in arrhythmic $Bmal1^{\text{st/st}}$ mice that may suggest a role of the functional oscillators in coordinating β -cell division. Importantly, massive β -cell ablation led to a fatal noncompensated diabetes in the absence of the core clock transcription factor BMAL1 (Fig. 5).

Coupling between the circadian clock and β -cell proliferation

Replication of terminally differentiated β cells, rather than differentiation of stem cells, represents a major source of newly generated β cells after birth. This holds true not only under physiological conditions, but also during regeneration following lesions (Dor et al. 2004; Bren-

nand et al. 2007; Nir et al. 2007; Teta et al. 2007; Klochendler et al. 2016). Noteworthy, in the absence of residual $\beta\text{-cell}$ upon near-total ablation the conversion of α or δ cells into insulin-producing cells was also described (Thorel et al. 2010; Chera et al. 2014). Our data indicate that β-cell reparative proliferation follows a daily rhythm and that it requires functional core clock protein Bmall (Figs. 1, 5). We now show that the highest proliferation rate occurs during the activity phase in the middle of night (Fig. 1), and that it coincides with the peaks of rhythmic expression of the genes encoding key regulators of the cell cycle (Fig. 4B). Importantly, whole-body knockout of the core clock component BMAL1 strongly disrupts β cells regeneration following massive ablation in transgenic mice (Fig. 5). A β-cell-specific disruption of the Bmal1 gene was previously reported to prevent a high-fat diet-

Circadian clocks drive **\beta-cell** regeneration

induced expansion of $\beta\text{-cell}$ mass (Rakshit et al. 2016). These previously published data suggest that the lack of $\beta\text{-cell}$ mass expansion following diet-induced obesity takes place in the absence of at least one allele of $\mathit{Bmal1}$ in β cells, and it is likely attributed to the increased cell death, rather than to decreased proliferation per se. Moreover, it is important to highlight that expansion of $\beta\text{-cell}$ mass upon obesity and $\beta\text{-cell}$ regeneration have a different nature. In contrast to the expansion of β cells upon obesity, we show that regeneration requires functional clock and it is still present in rhythmic mice heterozygotes for $\mathit{Bmal1}$.

We found that a number of the up-regulated cell cyclerelated transcripts exhibited a circadian rhythmicity in residual β cells following ablation (Fig. 4C) and were likely under the positive control of the transcription factor FOXM1 (Fig. 2E). The transcription of Foxm1 itself was circadian and peaked in the middle of the active phase, coinciding with the peak of proliferation (Fig. 4C-E). Strikingly, unlike heterozygous animals, no up-regulation of Foxm1 mRNA and transcripts specifying other cell cycle regulators was observed in Bmal1 st/st mice following massive β-cell ablation, as compared with their nontreated counterparts (used as controls) (Fig. 6F; Supplemental Data Set S8). This provides a mechanistic basis for the lack of β-cell regeneration (Fig. 5E,F) and further suggests a key role of circadian clocks in the expression of cell cycle genes. FOXM1 is one of the key transcription factors required for postnatal β-cell proliferation, but not for neogenesis of β cells from progenitors (Zhang et al. 2006; Ackermann Misfeldt et al. 2008). Its expression is enhanced in different models of β-cell expansion associated with obesity (Davis et al. 2010; Yamamoto et al. 2017), pregnancy (Zhang et al. 2010) and regeneration following partial pancreatectomy (Ackermann Misfeldt et al. 2008). Moreover, induction of the activated form of FOXM1 restored the replicative potential of β cells in aged animals (Golson et al. 2015). Finally, stimulation of cell proliferation in juvenile human islets by activation of GLP-1r signaling triggered the expression of Foxm1. This makes FOXM1 a molecular candidate for coupling the cell cycle to molecular clocks. The precise mechanistic details of these interactions need to be elucidated in future work.

Proliferating β cells bear functional clocks

In adulthood, both α and β cells possess cell-autonomous and self-sustained circadian oscillators in mice and humans (Pulimeno et al. 2013; Petrenko et al. 2017b; Petrenko and Dibner 2018). Here we report that in adult mice the residual β cells maintain a circadian rhythmicity both in vivo and in vitro following ablation (Fig. 4B; Supplemental Fig. S4B,C). The characteristics of rhythmic expression patterns of selected core clock genes (*Arntl, RorC*, and *Cry1*) in residual β cells of DOX-treated mice were, however, altered when compared with nontreated mice (Fig. 4B; Supplemental Fig. S4A). These differences may stem from β -cell proliferation, similar to what has previously been reported for dividing and nondividing

NIH3T3 fibroblasts (Nagoshi et al. 2004). Alternatively, altered paracrine or systemic signals along with the observed changes in the molecular landscape of residual β cells may lead to differences in the resetting of the molecular oscillator in residual β cells. For example, the loss of β cells leads to an enhanced proportion of neighboring α cells and an augmented secretion of glucagon (Fig. 5A), a potential synchronizer of molecular clocks in β cells (Petrenko and Dibner 2018).

Interestingly, residual β cells exhibited decreased levels of the mRNA encoding the important differentiation regulator MafA (Fig. 2B,C). This may be the consequence of dedifferentiation and dysfunction of these cells (Wang et al. 2007; Aguayo-Mazzucato et al. 2011; Swisa et al. 2017). Moreover, the circadian amplitude and magnitude of MafA mRNA accumulation were attenuated (Supplemental Fig. S4D) in DOX-treated mice. Besides core clock transcripts and MafA mRNA, numerous groups of transcripts changed their temporal expression profiles in residual β cells and neighboring α cells (Fig. 3), suggesting a modified temporal transcription landscape within regenerating islets upon diabetes.

Activation of β -cell regeneration following ablation

The massive β -cell loss induced the transcription of genes involved in cell cycle progression and replication in the residual β cells (Fig. 2D; Supplemental Data Set S3; Dor et al. 2004), but not in neighboring α cells (Fig. 2A). Likewise, the activation of GLP-1 signaling by exendine-4 exclusively induced proliferation in β-cell, and not in α or δ cells (Dai et al. 2017). This raises the question of which β-cell-specific mitogenic signals become important after β-cell ablation. The function of pancreatic islet is regulated by systemic and paracrine stimuli mediating distinct cell type-specific effects (Koh et al. 2012; Petrenko et al. 2018). Such differences in receptor repertoire and signaling molecules between α and β cells also define the cellspecific entrainment of circadian oscillators by physiologically relevant inputs that may regulate coupling between cell cycle and circadian oscillators (Petrenko et al. 2017b; Petrenko and Dibner 2018). In addition, the difference in glucose sensing and metabolism in α and β cells (Olsen et al. 2005) may account for the cell type-specific activation of β-cell proliferation. Indeed, high glucose plays a role in triggering β-cell proliferation capacity via the glucose sensor glucokinase (Porat et al. 2011). This conjunction may involve the molecular clocks machinery, as the core clock component RORy was reported to regulate glucose-stimulated proliferation in INS-1E cells in vitro (Schmidt et al. 2016). Concordantly, our data indicate that the enhanced proliferation rate following β-cell ablation parallels a hyperglycemia. Nonetheless, no significant proliferation of residual β cells was induced following ablation in absence of BMAL1, although the levels of glycemia were even higher in Bmal1st/st animals. These data suggest that high glucose alone is insufficient to trigger proliferation of β cells, and that functional oscillators are required to induce β -cell proliferation. We wish to emphasize, however, that we do not know whether the

Petrenko et al.

effects on glucose metabolism and β -cell proliferation observed in $\mathit{Bmal1}^{st/st}$ mice (Figs. 5, 6) were attributed to the elimination of the transcriptional factor BMAL1 per se, or to its function as a key core clock regulator. The discrimination between circadian and noncircadian activities of core clock transcription factors has been a notoriously difficult problem in the field. So-called "resonance experiments," in which phenotypes are compared in organisms whose oscillators do or do not resonate with environmental cycles (T cycles), are probably the only approaches revealing the importance of rhythmic functions (Ma et al. 2013). Unfortunately, such endeavors are not feasible in the system described here.

Elegant work by Okamura and colleagues (Matsuo et al. 2003) reported that the initiation of mitotic division in regenerating mouse livers follows a robust circadian rhythm. These investigators provided compelling evidence that rhythmic cell cycle progression in regenerating livers is governed by the circadian expression of Weel, a key regulator of mitosis. Interestingly, the kinetics of Sphase hepatocytes was not controlled by molecular clock. In our study, the kinetics of S-phase regenerating β cells was circadian, and the temporal expression levels of *Wee1* transcript were rhythmic in β cells in both control and DOX conditions, with absolute levels being unchanged (Supplemental Fig. S4E). Wee1 expression exhibited a tendency for down-regulation in Bmal1st/st mice as compared with $Bmal1^{+/st}$ controls (FC = -1.45) (Supplemental Data Set S7) that did not reach statistical significance. Moreover, liver regeneration was delayed, but not arrested, in arrhythmic Cry1/Cry2 knockout mice. In contrast, the regeneration of pancreatic β cells did not proceed in the absence of the essential core clock component BMAL1, leading to fatal diabetes in a high proportion of animals (Fig. 5).

Systemic loss of BMAL1 aggravates diabetes

Disruption of the core clock components impairs insulin secretion by mouse and human β cells (Perelis et al. 2015; Petrenko et al. 2020) and results in a diabetic phenotype in mice (Marcheva et al. 2010). We now demonstrate that in the absence of a functional clock mice develop severe fatal diabetes following massive β-cell loss, contrary to their rhythmic counterparts that partially recover from thus-induced diabetes (Fig. 5D-F; Nir et al. 2007). While we failed to demonstrate a difference in blood insulin levels between Bmal1st/st mice and heterozygotes counterparts at the examined time points, arrhythmic animals developed strong hyperglucagonemia (Fig. 5D). Since glucagon stimulates gluconeogenesis in the liver (Perry et al. 2020), this may contribute to the strongly elevated blood glucose levels following massive β -cell ablation in *Bmal1* st/st mice. In addition, loss of functional clocks evoked insulin resistance in skeletal muscles (Dyar et al. 2014; Harfmann et al. 2016) and impaired cell-autonomous adoptative changes to increased insulin needs upon diet-induced obesity (Rakshit et al. 2016). Taken together, these data suggest that complex interaction between different pathogenetic pathways in pancreatic islets and metabolic

tissues may account for the deterioration of diabetes upon dysfunctional clocks.

In summary, our data strongly suggest that regeneration of β cells is tightly coupled to diurnal rhythm. Moreover, loss of functional clocks aggravates the development of diabetic phenotype in mice. Indeed, human pancreatic islets from T2D individuals bear dysfunctional clocks associated with perturbed temporal regulation of insulin and glucagon secretion (Petrenko et al. 2020). These findings have important translational potential and should be considered in patients with T1D and T2D, as reboosting circadian rhythms by lifestyle adaptations may help preventing the aggravation of the disease.

Materials and methods

Animals

Animal studies were performed according to the regulations of the veterinary office of the State of Geneva (authorization number GE/47/19). Experimental mouse strain proGcg-Venus/RIP-Cherry/PER2::Luc/Insulin-rtTA/TET-DTA was established by crossing triple reporter mouse line proGcg-Venus/RIP-Cherry/ PER2::Luc (Petrenko et al. 2017b) to Insulin-rtTA/TET-DTA mice (Supplemental Fig. S1; Nir et al. 2007). ProGcg-Venus and RIP-Cherry reporters exhibited very high specificity and expression levels in α and β cells, respectively (Dusaulcy et al. 2016; Petrenko et al. 2017a). Bmal1st/st mice were developed by introducing (knock-in) a transcriptional-translational stop cassette between exons 5 and 6 of the Bmal1 locus, containing a splice acceptor and a triple repeat of a polyadenylation signal sequence, flanked by LoxP sites. Bmal1st/st mice were crossed to proGcg-Venus/RIP-Cherry/PER2::Luc/Insulin-rtTA/TET-DTA. The obtained proGcg-Venus/RIP-Cherry/PER2::Luc/InsulinrtTA/TET-DTA/Bmal1st/st mice allowed to genetically induce massive β -cell ablation in the absence of functional clocks by administering 300 mg of doxycycline (DOX) in the drinking water supplemented with 2% sucrose. The control group received only water supplemented with 2% sucrose. All the experiments were done in mice aged 6-8 wk, under standard animal housing conditions with ad libitum access to food and water and under 12-h light/12-h dark cycles (LD; lights on at 7:00 a.m., lights off at 7:00 p.m.). For the islet isolation and BrdU experiments, male mice were fed exclusively during the night 10 d prior to the experiment and during the experiment (Supplemental Fig. S1A), allowing to reduce the effect of individual feeding rhythm (Atger et al. 2015). For the islet isolation across the 24-h period, half of the animals were entrained by inverted LD and feeding cycles for 2 wk preceding the experiments.

Pancreatic islet isolation and separation of α and β cells

Islets of Langerhans were isolated by standard procedure based on collagenase (type XI; Sigma) digestion of pancreas followed by Ficoll purification (Petrenko et al. 2017a). Islet cells were gently dissociated by 0.05% trypsin (GIBCO) treatment, resuspended in KRB solution (pH 7.4, supplemented with 0.3% free fatty acid bovine serum albumin [BSA; Sigma], 1.4 mM glucose, 0.5 mM EDTA). α -Cell and β -cell populations were separated by flow cytometry fluorescence activated cell sorting (FACS; Astrios sorter [Beckman Coulter]) based on fluorescence wavelength and intensity, cell singlet nature, size, and viability as described previously (Petrenko et al. 2017b).

Circadian clocks drive **\beta-cell** regeneration

RNA sequencing (RNA-seq)

For around-the-clock RNA-seq experiments underlying Figures 2 and 3, total RNA was prepared from FACS-sorted α and β cells collected from male $proGcg\text{-}Venus/RIP\text{-}Cherry/PER2::}Luc/InsulinrtTA/TET-DTA control and DOX-treated mice every 4 h around the clock in biological duplicates, using RNeasy Plus microkit (Qiagen). A total of 48 samples, representing RNA pool of three to six mice each, was prepared. RNA-seq was performed by the iGE3 Genomics Platform (University of Geneva, Switzerland). The Illumina TruSeq RNA sample preparation kits were used for the library preparation with 25–50 ng of total RNA as input. Library molarity and quality was assessed with Qubit (Life Technologies) and Tapestation using a DNA high sensitivity chip (Agilent Technologies). Paired-end reads of 50 bases were generated using SMART-Seq v4 chemistry on an Illumina HiSeq 2000 (first replicate) and Illumina HiSeq 4000 (second replicate) sequencers.$

For RNA-seq experiments in Bmal1st/st mice (Fig. 6), total RNA was prepared from FACS-sorted β cells collected from males and females of proGcg-Venus/RIP-Cherry/PER2::Luc/Insulin-rtTA/ TET-DTA/Bmal1st/st mice and their proGcg-Venus/RIP-Cherry/ PER2::Luc/Insulin-rtTA/TET-DTA/Bmal1+/st littermates following 10 d of DOX administration at ZT0 in biological duplicates, using RNeasy Plus microkit (Qiagen) (a total of four samples, representing RNA pool of ~7000 cells from three mice each). RNAseq was performed by the iGE3 Genomics Platform (University of Geneva, Switzerland). The Clontech SMARTer ultralow input RNA was used to generate cDNA followed by Nextera XT kit for library preparation on samples with low RNA input. Library molarity and quality was assessed with Qubit (Life Technologies) and Tapestation using a DNA high sensitivity chip (Agilent Technologies). Single-end reads of 50 bases were generated using on an Illumina HiSeq 4000 sequencer.

RNA-seq data processing and analysis

For around-the-clock gene expression assessments, paired end reads were aligned to the mouse genome (assembly GRCm38/ mm10) using STAR v2.5.3ausing Gencode vM16 annotation. The quantification was performed with QTLtools quan (https ://qtltools.github.io/qtltools/). The mapping quality threshold was set at 255, and the number of mismatches allowed in both reads together was set at five (reads below these thresholds were not considered for the quantification) (Dobin et al. 2013). The genome index was built using Ensembl annotation to improve splice junction's accuracy. For each Ensembl gene, all of the exons of the respective annotated protein-coding transcripts were considered. Using custom Perl script, reads up to one mismatch were counted considering only reads in the right gene orientation. Both uniquely mapping and multimapping reads were reported. Normalization and differential expression analysis were performed with the R/Bioconductor packages edgeR v.3.28 (Robinson et al. 2010) and limma 3.42.2 (Ritchie et al. 2015). Log2 expression levels were calculated.

For the assessment of differential gene expression in β cells between $Bmal1^{st/st}$ and $Bmal1^{st/st}DOX_i$ and between $Bmal1^{st/st}DOX$ and $Bmal1^{st/st}DOX_i$ a quality control was performed with FastQC v.0.11.5. Single-end reads were mapped to mouse genome (assembly GRCm38/mm10) using STAR v.7.0f (Dobin et al. 2013). The biological quality control was done with Picard-Tools v.2.21.6. Raw counts were obtained using HTSeq v.0.9.1. Normalization and differential expression analysis were performed with the R/Bioconductor package edgeR v.3.26.8 (Robinson et al. 2010). The overall workflow of RNA-seq analysis is presented in Supplemental Figure S8.

Differential and temporal analysis

For around-the-clock gene expression assessment, genes with less than one CPM in half of the all measurements were discarded. Differential expression analysis between α and β cells was assessed using the EdgeR and limma packages, following the protocol of (Chen et al. 2016). A gene was defined as differentially expressed when the absolute value of the log₂ fold change (log₂FC) was >0.5 (same cell type) or 1 (otherwise), and the FDR-corrected P-value was < 0.05 from the resulting differential expression analysis. Genes were considered as "nonexpressed" (Ne in Fig. 3) if their respective expression value was below an arbitrary threshold of 1 RPKM averaged over time. Rhythmicity of the transcript profiles was determined in two steps: First, 17 sin/cos models with intercept were regressed on each of two independent experiments corresponding to different periods in 20-28 h. The model with the lowest P-value from the F test was kept. Second, the gene was deemed rhythmically expressed based on a logistic regression model with the previous *P*-value for the two samples used as the input. The logistic regression was trained on a gold standard of 31 manually labeled genes (see Supplemental Data Set S9). All fitted coefficients were significant (P-value < 0.008). Based on a ROC curve, a cutoff of 0.6 was decided leading to a 95% accuracy on the golden standard between 0.849 and 0.988. Rhythmic parameters (i.e., phase, period length, and amplitude) can be shared between the two different cell types and between two conditions (CTR and DOX).

Differential gene expression analysis for β cells between $Bmal1^{st/st}$ and $Bmal1^{st/st}$ DOX, and between $Bmal1^{st/st}$ DOX and $Bmal1^{+/st}$ DOX was assessed using a generalized linear model with quasi-likelihood F-test of the EdgeR package (v 3.26.8). A gene was defined as differentially expressed when the absolute value of the \log_2 fold change (\log_2 FC) was >1 and the FDR-corrected P-value was <0.05 (Benjamini and Hochberg correction).

Ingenuity pathway analysis (IPA) and KEGG pathway enrichment analysis

The pathway analyses were generated by Qiagen's IPA program (IPA; Qiagen, http://www.qiagen.com/ingenuity). Briefly, the analyses were performed with the following settings: expression value type (exp fold change), reference set (ingenuity knowledge base [genes only]), relationships to consider (direct and indirect relationships), interaction networks (35 molecules/network; 25 networks/analysis), node types (all), data sources (all), confidence (experimentally observed), species (human, mouse, rat), tissue and cell lines (all), and mutations (all).

The KEGG pathway enrichment analysis was generated by Database for Annotation, Visualization and Integrated Discovery (DAVID) v6.8 based on the gene lists (Supplemental Data Set S6) comprising rhythmic genes with phase difference >2 h (Supplemental Fig. S4A), and on the gene list (Supplemental Data Set S7) comprising differentially expressed genes between Bmal1st/stDOX and Bmal1+/stDOX phenotypes.

Quantitative polymerase chain reaction (qPCR)

Total RNA was prepared from FACS separated islet cells using RNeasy Plus microkit (Qiagen). The RNA concentration was measured by Qubit RNA SH kit (Invitrogen). Next, 0.1 µg of total RNA was reverse-transcribed using TAKARA (Roche) and random hexamers and was PCR-amplified on a LightCycler 480 (Roche Diagnostics AG). Mean values for each sample were calculated from technical duplicates of each quantitative RT-PCR (qRT-PCR) analysis and normalized to the mean of housekeeping genes hypoxanthine-guanine phosphoribosyltransferase (Hprt)

Petrenko et al.

and S9. Primers used for this study are listed in Supplemental Table S1.

Assessment of blood glucose, insulin, and glucagon levels

Blood glucose (Fig. 5) was measured by the Accu-Chek glucometer (Roche). For insulin and glucagon assessment, blood was collected from the tail vein at ZT4 (11:00), or at ZT16 (23:00) with subsequent serum preparation by immediate centrifugation at 94,000 rcf for 15 min at 4°C and stored at -80°C . Protease inhibitors aprotinin (Sigma) and DPP4 (Millipore) were added to the samples to preserve the hormones from degradation. Insulin and glucagon concentrations were assessed by ultrasensitive mouse insulin and glucagon $100\mu\text{L}$ ELISA kits (Mercodia).

Assessment of cell proliferation

5-bromo-2'-deoxyuridine (BrdU; Sigma-Aldrich) was injected intraperitoneally (100 mg/kg) 2 h prior to sacrifice at the indicated time points.

Immunostaining

Paraffin sections (5 μ m thick) were rehydrated, and antigen retrieval was performed using a Biocare pressure cooker and citrate (pH 6) buffer. The following primary antibodies were used: guinea pig anti-insulin (1:200; Dako), mouse anti-glucagon (1:800; Abcam), rabbit anti-glucagon (1:8000; Abcam), and mouse anti-BrdU (1:300; GE healthcare). For DNA counterstaining we used DAPI (Sigma). Secondary antibodies from Jackson ImmunoResearch were as follows: anti-guinea pig Alexa Fluor 488 (1:200), anti-mouse Cy3 (1:500), and anti-mouse Alexa Fluor 647 (1:500). Immunofluorescence images were captured using a Nikon confocal microscope. To assess β cell replication, at least 2000 β cells were counted per animal, and at least two slides at a distance of >200 μ m were analyzed.

Image analysis

All immunofluorescence images were captured on a Nikon C1 confocal microscope at a magnification of $40\times$ randomly from at least two different slices. The islets were identified by insulin labeling and captured throughout the entire slide. The number of labeled cells was quantified using Fiji software. The numbers of insulin-labeled cells bearing BrdU-labeled nuclei was normalized to the total number of insulin-positive cells in islet, and expressed in percentage. The numbers of insulin- and glucagon-labeled cells were quantified on slices immunostained for these two hormones. The proportion of β cells was expressed as the ratio between number of insulin-positive cells among overall insulinand glucagon-labeled cells.

Quantification and statistical analysis

The results are expressed as means \pm SEM (standard error of mean) for the indicated number of donors (as given in the figure legends) or illustrated as mean value of all experiments (for bioluminescence profiles). The statistical difference was tested by a Student's t-test to compare the two groups. A nonpaired Student's t-test was used to compare group donors. A one-way ANOVA test followed by a nonpaired Student's t-test comparisons was used to compare multiple conditions. All statistical tests were conducted with GraphPad Prism 8 software. Statistical significance was defined at P < 0.05 (*), P < 0.01 (***), P < 0.001 (***), and P < 0.0001 (****). To assess the circadian characteristics of proliferation a

JTK_Cycle fitting method was used (Hughes et al. 2010). The profile was considered as circadian if adjusted *P*-value were <0.05.

Data availability

The accession numbers for the deposited data in GEO are GSE151338 and GSE152751.

Acknowledgments

We thank the colleagues from the University of Geneva-Ueli Schibler, Jacques Philippe, and Claes Wollheim—for constructive discussions; Marie-Claude Brulhart-Meynet for skillful technical assistance; Mylène Docquier, Céline Delucinge-Vivier, Didier Chollet, Emmanouil Dermitzakis, Luciana Romano, Deborah Bielser, Cédric Howald, and Keith Harshman for conducting RNA sequencing; Jean-Pierre Aubry-Lachainaye for help with cell sorting; and Charles Weitz from Harvard Medical School for generously sharing the Bmal1st/st mouse strain. This work was funded by Swiss National Science Foundation grants 31003A_166700/1, and 310030_184708/1; European Foundation for the Study of Diabetes/Novo Nordisk Programme for Diabetes Research: the Vontobel Foundation: the Novartis Consumer Health Foundation; the Bo and Kerstin Hjelt Foundation for diabetes type 2; the Swiss Life Foundation; the Olga Mayenfisch Foundation (to C.D.); University of Geneva-The Hebrew University of Jerusalem Joint Seed Money Funding Scheme (to Y.D. and C.D.); Research Council of Norway (NFR 251041, SC); and the Novo Nordic Foundation (NNF15OC0015054 to S.C.).

Author contributions: C.D., Y.D., and V.P. designed the study, conducted data analysis, and wrote the manuscript. V.P. performed the experiments. M.S.-R. performed histological data collection. K.-F.S. developed the *Bmal1*^{st/st} mouse line. L.G. participated in the islet isolations. B.V. and S.C. conducted RNA-seq data analyses. All authors contributed to the manuscript preparation and approved the final version.

References

Ackermann Misfeldt A, Costa RH, Gannon M. 2008. β-Cell proliferation, but not neogenesis, following 60% partial pancreatectomy is impaired in the absence of FoxM1. *Diabetes* 57: 3069–3077. doi:10.2337/db08-0878

Aguayo-Mazzucato C, Koh A, El Khattabi I, Li WC, Toschi E, Jermendy A, Juhl K, Mao K, Weir GC, Sharma A, et al. 2011. Mafa expression enhances glucose-responsive insulin secretion in neonatal rat β cells. *Diabetologia* **54:** 583–593. doi:10.1007/s00125-010-2026-z

Aryal RP, Kwak PB, Tamayo AG, Gebert M, Chiu PL, Walz T, Weitz CJ. 2017. Macromolecular assemblies of the mammalian circadian clock. *Mol Cell* **67:** 770–782.e6. doi:10.1016/j.molcel.2017.07.017

Atger F, Gobet C, Marquis J, Martin E, Wang J, Weger B, Lefebvre G, Descombes P, Naef F, Gachon F. 2015. Circadian and feeding rhythms differentially affect rhythmic mRNA transcription and translation in mouse liver. *Proc Natl Acad Sci* 112: E6579–E6588. doi:10.1073/pnas.1515308112

Bellet MM, Masri S, Astarita G, Sassone-Corsi P, Della Fazia MA, Servillo G. 2016. Histone deacetylase SIRT1 controls proliferation, circadian rhythm, and lipid metabolism during liver regeneration in mice. *J Biol Chem* **291:** 23318–23329. doi:10.1074/jbc.M116.737114

Bieler J, Cannavo R, Gustafson K, Gobet C, Gatfield D, Naef F. 2014. Robust synchronization of coupled circadian and cell

- cycle oscillators in single mammalian cells. $Mol~Syst~Biol~{\bf 10:}$ 739. doi:10.15252/msb.20145218
- Bjarnason GA, Jordan RC, Wood PA, Li Q, Lincoln DW, Sothern RB, Hrushesky WJ, Ben-David Y. 2001. Circadian expression of clock genes in human oral mucosa and skin: association with specific cell-cycle phases. *Am J Pathol* **158:** 1793–1801. doi:10.1016/S0002-9440(10)64135-1
- Brennand K, Huangfu D, Melton D. 2007. All β cells contribute equally to islet growth and maintenance. *PLoS Biol* **5:** e163. doi:10.1371/journal.pbio.0050163
- Chakravarthy H, Gu X, Enge M, Dai X, Wang Y, Damond N, Downie C, Liu K, Wang J, Xing Y, et al. 2017. Converting adult pancreatic islet α cells into β cells by targeting both Dnmt1 and Arx. *Cell Metab* **25:** 622–634. doi:10.1016/j.cmet.2017 01 009
- Chatterjee S, Yin H, Nam D, Li Y, Ma K. 2015. Brain and muscle Arnt-like 1 promotes skeletal muscle regeneration through satellite cell expansion. *Exp Cell Res* **331**: 200–210. doi:10 .1016/j.yexcr.2014.08.041
- Chen Y, Lun AT, Smyth GK. 2016. From reads to genes to pathways: differential expression analysis of RNA-seq experiments using rsubread and the edgeR quasi-likelihood pipeline. F1000Res 5: 1438.
- Cheng CW, Villani V, Buono R, Wei M, Kumar S, Yilmaz OH, Cohen P, Sneddon JB, Perin L, Longo VD. 2017. Fasting-mimicking diet promotes Ngn3-driven β-cell regeneration to reverse diabetes. *Cell* 168: 775–788.e12. doi:10.1016/j.cell .2017.01.040
- Chera S, Baronnier D, Ghila L, Cigliola V, Jensen JN, Gu G, Furuyama K, Thorel F, Gribble FM, Reimann F, et al. 2014. Diabetes recovery by age-dependent conversion of pancreatic δ-cells into insulin producers. *Nature* **514:** 503–507. doi:10.1038/nature13633
- Cox KH, Takahashi JS. 2019. Circadian clock genes and the transcriptional architecture of the clock mechanism. J Mol Endocrinol 63: R93–R102. doi:10.1530/JME-19-0153
- Dai C, Hang Y, Shostak A, Poffenberger G, Hart N, Prasad N, Phillips N, Levy SE, Greiner DL, Shultz LD, et al. 2017. Age-dependent human β cell proliferation induced by glucagon-like peptide 1 and calcineurin signaling. *J Clin Invest* **127:** 3835–3844.
- Davis DB, Lavine JA, Suhonen JI, Krautkramer KA, Rabaglia ME, Sperger JM, Fernandez LA, Yandell BS, Keller MP, Wang IM, et al. 2010. Foxm1 is up-regulated by obesity and stimulates β-cell proliferation. *Mol Endocrinol* **24:** 1822–1834.
- Dibner C. 2020. The importance of being rhythmic: living in harmony with your body clocks. *Acta Physiol (Oxf)* **228:** e13281. doi:10.1111/apha.13281
- Dibner C, Schibler U, Albrecht U. 2010. The mammalian circadian timing system: organization and coordination of central and peripheral clocks. *Annu Rev Physiol* **72:** 517–549. doi:10.1146/annurev-physiol-021909-135821
- Dobin A, Davis CA, Schlesinger F, Drenkow J, Zaleski C, Jha S, Batut P, Chaisson M, Gingeras TR. 2013. STAR: ultrafast universal RNA-seq aligner. *Bioinformatics* 29: 15–21. doi:10 .1093/bioinformatics/bts635
- Dor Y, Brown J, Martinez OI, Melton DA. 2004. Adult pancreatic β-cells are formed by self-duplication rather than stem-cell differentiation. *Nature* **429**: 41–46. doi:10.1038/nature02520
- Dusaulcy R, Handgraaf S, Heddad-Masson M, Visentin F, Vesin C, Reimann F, Gribble F, Philippe J, Gosmain Y. 2016. α-Cell dysfunctions and molecular alterations in male insulinopenic diabetic mice are not completely corrected by insulin. *Endocrinology* **157:** 536–547. doi:10.1210/en.2015-1725

- Dyar KA, Ciciliot S, Wright LE, Biensø RS, Tagliazucchi GM, Patel VR, Forcato M, Paz MI, Gudiksen A, Solagna F, et al. 2014. Muscle insulin sensitivity and glucose metabolism are controlled by the intrinsic muscle clock. *Mol Metab* 3: 29–41. doi:10.1016/j.molmet.2013.10.005
- Gaucher J, Montellier E, Sassone-Corsi P. 2018. Molecular cogs: interplay between circadian clock and cell cycle. *Trends Cell Biol* 28: 368–379. doi:10.1016/j.tcb.2018.01.006
- Golson ML, Dunn JC, Maulis MF, Dadi PK, Osipovich AB, Magnuson MA, Jacobson DA, Gannon M. 2015. Activation of FoxM1 revitalizes the replicative potential of aged β-cells in male mice and enhances insulin secretion. *Diabetes* 64: 3829–3838. doi:10.2337/db15-0465
- Harfmann BD, Schroder EA, Kachman MT, Hodge BA, Zhang X, Esser KA. 2016. Muscle-specific loss of Bmall leads to disrupted tissue glucose metabolism and systemic glucose homeostasis. *Skelet Muscle* **6:** 12. doi:10.1186/s13395-016-0082-x
- Hughes ME, Hogenesch JB, Kornacker K. 2010. JTK_Cycle: an efficient nonparametric algorithm for detecting rhythmic components in genome-scale data sets. *J Biol Rhythms* 25: 372–380. doi:10.1177/0748730410379711
- Karpowicz P, Zhang Y, Hogenesch JB, Emery P, Perrimon N. 2013. The circadian clock gates the intestinal stem cell regenerative state. Cell Rep 3: 996–1004. doi:10.1016/j.celrep.2013.03.016
- Klochendler A, Caspi I, Corem N, Moran M, Friedlich O, Elgavish S, Nevo Y, Helman A, Glaser B, Eden A, et al. 2016. The genetic program of pancreatic β-cell replication in vivo. *Diabetes* **65:** 2081–22093. doi:10.2337/db16-0003
- Koh DS, Cho JH, Chen L. 2012. Paracrine interactions within islets of Langerhans. J Mol Neurosci 48: 429–440. doi:10.1007/s12031-012-9752-2
- Ma P, Woelfle MA, Johnson CH. 2013. An evolutionary fitness enhancement conferred by the circadian system in cyanobacteria. *Chaos Solitons Fractals* **50:** 65–74. doi:10.1016/j.chaos .2012.11.006
- Mannic T, Meyer P, Triponez F, Pusztaszeri M, Le Martelot G, Mariani O, Schmitter D, Sage D, Philippe J, Dibner C. 2013. Circadian clock characteristics are altered in human thyroid malignant nodules. *J Clin Endocrinol Metab* 98: 4446–4456. doi:10.1210/jc.2013-2568
- Marcheva B, Ramsey KM, Buhr ED, Kobayashi Y, Su H, Ko CH, Ivanova G, Omura C, Mo S, Vitaterna MH, et al. 2010. Disruption of the clock components CLOCK and BMAL1 leads to hypoinsulinaemia and diabetes. *Nature* **466**: 627–631. doi:10.1038/nature09253
- Matsuo T, Yamaguchi S, Mitsui S, Emi A, Shimoda F, Okamura H. 2003. Control mechanism of the circadian clock for timing of cell division in vivo. *Science* 302: 255–259. doi:10.1126/sci ence.1086271
- Nagoshi E, Saini C, Bauer C, Laroche T, Naef F, Schibler U. 2004. Circadian gene expression in individual fibroblasts: cell-autonomous and self-sustained oscillators pass time to daughter cells. Cell 119: 693–705. doi:10.1016/j.cell.2004.11.015
- Nir T, Melton DA, Dor Y. 2007. Recovery from diabetes in mice by β cell regeneration. *J Clin Invest* **117:** 2553–2561. doi:10 .1172/JCI32959
- Olsen HL, Theander S, Bokvist K, Buschard K, Wollheim CB, Gromada J. 2005. Glucose stimulates glucagon release in single rat α-cells by mechanisms that mirror the stimulus-secretion coupling in β-cells. *Endocrinology* **146:** 4861–4870. doi:10.1210/en.2005-0800
- Perelis M, Marcheva B, Ramsey KM, Schipma MJ, Hutchison AL, Taguchi A, Peek CB, Hong H, Huang W, Omura C, et al. 2015. Pancreatic β cell enhancers regulate rhythmic transcription of

Petrenko et al.

- genes controlling insulin secretion. *Science* **350**: aac4250. doi:10.1126/science.aac4250
- Perry RJ, Zhang D, Guerra MT, Brill AL, Goedeke L, Nasiri AR, Rabin-Court A, Wang Y, Peng L, Dufour S, et al. 2020. Glucagon stimulates gluconeogenesis by INSP3R1-mediated hepatic lipolysis. *Nature* **579:** 279–283. doi:10.1038/s41586-020-2074-6
- Petrenko V, Dibner C. 2018. Cell-specific resetting of mouse islet cellular clocks by glucagon, glucagon-like peptide 1 and somatostatin. *Acta Physiol (Oxf)* **222:** e13021. doi:10.1111/apha
- Petrenko V, Gosmain Y, Dibner C. 2017a. High-resolution recording of the circadian oscillator in primary mouse α and β -cell culture. Front Endocrinol (Lausanne) 8: 68. doi:10.3389/fendo.2017.00068
- Petrenko V, Saini C, Giovannoni L, Gobet C, Sage D, Unser M, Heddad Masson M, Gu G, Bosco D, Gachon F, et al. 2017b. Pancreatic α- and β-cellular clocks have distinct molecular properties and impact on islet hormone secretion and gene expression. *Genes Dev* **31:** 383–398. doi:10.1101/gad.290379
- Petrenko V, Philippe J, Dibner C. 2018. Time zones of pancreatic islet metabolism. *Diabetes Obes Metab* **20:** 116–126. doi:10 .1111/dom.13383
- Petrenko V, Gandasi NR, Sage D, Tengholm A, Barg S, Dibner C. 2020. In pancreatic islets from type 2 diabetes patients, the dampened circadian oscillators lead to reduced insulin and glucagon exocytosis. *Proc Natl Acad Sci* **117:** 2484–2495. doi:10.1073/pnas.1916539117
- Porat S, Weinberg-Corem N, Tornovsky-Babaey S, Schyr-Ben-Haroush R, Hija A, Stolovich-Rain M, Dadon D, Granot Z, Ben-Hur V, White P, et al. 2011. Control of pancreatic β cell regeneration by glucose metabolism. *Cell Metab* **13:** 440–449. doi:10.1016/j.cmet.2011.02.012
- Preitner N, Damiola F, Lopez-Molina L, Zakany J, Duboule D, Albrecht U, Schibler U. 2002. The orphan nuclear receptor REV-ERB α controls circadian transcription within the positive limb of the mammalian circadian oscillator. *Cell* **110**: 251–260. doi:10.1016/S0092-8674(02)00825-5
- Pulimeno P, Mannic T, Sage D, Giovannoni L, Salmon P, Lemeille S, Giry-Laterriere M, Unser M, Bosco D, Bauer C, et al. 2013. Autonomous and self-sustained circadian oscillators displayed in human islet cells. *Diabetologia* 56: 497– 507. doi:10.1007/s00125-012-2779-7
- Rakshit K, Hsu TW, Matveyenko AV. 2016. Bmall is required for β cell compensatory expansion, survival and metabolic adaptation to diet-induced obesity in mice. *Diabetologia* **59:** 734–743. doi:10.1007/s00125-015-3859-2
- Ritchie ME, Phipson B, Wu D, Hu Y, Law CW, Shi W, Smyth GK. 2015. limma powers differential expression analyses for RNA-sequencing and microarray studies. *Nucleic Acids Res* **43:** e47. doi:10.1093/nar/gkv007
- Robinson MD, McCarthy DJ, Smyth GK. 2010. Edger: a bioconductor package for differential expression analysis of digital

- gene expression data. *Bioinformatics* **26:** 139–140. doi:10 .1093/bioinformatics/btp616
- Schmidt SF, Madsen JG, Frafjord KO, Poulsen L, Salö S, Boergesen M, Loft A, Larsen BD, Madsen MS, Holst JJ, et al. 2016. Integrative genomics outlines a biphasic glucose response and a ChREBP–ROR γ axis regulating proliferation in β cells. *Cell Rep* **16:** 2359–2372. doi:10.1016/j.celrep.2016.07.063
- Sinturel F, Petrenko V, Dibner C. 2020. Circadian clocks make metabolism run. *J Mol Biol* **432**: 3680–3699. doi:10.1016/j.jmb.2020.01.018
- Stokes K, Cooke A, Chang H, Weaver DR, Breault DT, Karpowicz P. 2017. The circadian clock gene BMAL1 coordinates intestinal regeneration. *Cell Mol Gastroenterol Hepatol* **4:** 95–114. doi:10.1016/j.jcmgh.2017.03.011
- Stolovich-Rain M, Hija A, Grimsby J, Glaser B, Dor Y. 2012. Pancreatic β cells in very old mice retain capacity for compensatory proliferation. *J Biol Chem* **287:** 27407–27414. doi:10.1074/jbc.M112.350736
- Swisa A, Glaser B, Dor Y. 2017. Metabolic stress and compromised identity of pancreatic β cells. Front Genet 8: 21. doi:10.3389/fgene.2017.00021
- Teta M, Rankin MM, Long SY, Stein GM, Kushner JA. 2007. Growth and regeneration of adult β cells does not involve specialized progenitors. *Dev Cell* **12:** 817–826. doi:10.1016/j.devcel.2007.04.011
- Thorel F, Népote V, Avril I, Kohno K, Desgraz R, Chera S, Herrera PL. 2010. Conversion of adult pancreatic α-cells to β-cells after extreme β-cell loss. *Nature* **464:** 1149–1154. doi:10.1038/nature08894
- Wang H, Brun T, Kataoka K, Sharma AJ, Wollheim CB. 2007. MAFA controls genes implicated in insulin biosynthesis and secretion. *Diabetologia* 50: 348–358. doi:10.1007/s00125-006-0490-2
- Xu X, D'Hoker J, Stangé G, Bonné S, De Leu N, Xiao X, Van de Casteele M, Mellitzer G, Ling Z, Pipeleers D, et al. 2008. β Cells can be generated from endogenous progenitors in injured adult mouse pancreas. Cell 132: 197–207. doi:10.1016/j.cell .2007.12.015
- Yamamoto J, Imai J, Izumi T, Takahashi H, Kawana Y, Takahashi K, Kodama S, Kaneko K, Gao J, Uno K, et al. 2017. Neuronal signals regulate obesity induced β -cell proliferation by FoxM1 dependent mechanism. *Nat Commun* **8:** 1930. doi:10 .1038/s41467-017-01869-7
- Zhang H, Ackermann AM, Gusarova GA, Lowe D, Feng X, Kopsombut UG, Costa RH, Gannon M. 2006. The FoxM1 transcription factor is required to maintain pancreatic β-cell mass. *Mol Endocrinol* **20:** 1853–1866. doi:10.1210/me.2006-0056
- Zhang H, Zhang J, Pope CF, Crawford LA, Vasavada RC, Jagasia SM, Gannon M. 2010. Gestational diabetes mellitus resulting from impaired β -cell compensation in the absence of FoxM1, a novel downstream effector of placental lactogen. *Diabetes* **59:** 143–152. doi:10.2337/db09-0050



The core clock transcription factor BMAL1 drives circadian $\beta\text{-cell}$ proliferation during compensatory regeneration of the endocrine pancreas

Volodymyr Petrenko, Miri Stolovich-Rain, Bart Vandereycken, et al.

Genes Dev. published online November 12, 2020 Access the most recent version at doi:10.1101/gad.343137.120

Supplemental Material	http://genesdev.cshlp.org/content/suppl/2020/11/11/gad.343137.120.DC1
	Published online November 12, 2020 in advance of the full issue.
Creative Commons License	This article is distributed exclusively by Cold Spring Harbor Laboratory Press for the first six months after the full-issue publication date (see http://genesdev.cshlp.org/site/misc/terms.xhtml). After six months, it is available under a Creative Commons License (Attribution-NonCommercial 4.0 International), as described at http://creativecommons.org/licenses/by-nc/4.0/ .
Email Alerting Service	Receive free email alerts when new articles cite this article - sign up in the box at the top right corner of the article or click here .

original article

A functional circadian clock is required for proper insulin secretion by human pancreatic islet cells

C. Saini^{1,2,†}, V. Petrenko^{1,2,†}, P. Pulimeno^{1,3,†}, L. Giovannoni¹, T. Berney⁴, M. Hebrok³, C. Howald^{2,5,6}, E. T. Dermitzakis^{2,5,6} & C. Dibner^{1,2}

Aim: To determine the impact of a functional human islet clock on insulin secretion and gene transcription.

Methods: Efficient circadian clock disruption was achieved in human pancreatic islet cells by small interfering RNA-mediated knockdown of *CLOCK*. Human islet secretory function was assessed in the presence or absence of a functional circadian clock by stimulated insulin secretion assays, and by continuous around-the-clock monitoring of basal insulin secretion. Large-scale transcription analysis was accomplished by RNA sequencing, followed by quantitative RT-PCR analysis of selected targets.

Results: Circadian clock disruption resulted in a significant decrease in both acute and chronic glucose-stimulated insulin secretion. Moreover, basal insulin secretion by human islet cells synchronized *in vitro* exhibited a circadian pattern, which was perturbed upon clock disruption. RNA sequencing analysis suggested alterations in 352 transcript levels upon circadian clock disruption. Among them, key regulators of the insulin secretion pathway (GNAQ, ATP1A1, ATP5G2, KCNJ11) and transcripts required for granule maturation and release (VAMP3, STX6, SLC30A8) were affected.

Conclusions: Using our newly developed experimental approach for efficient clock disruption in human pancreatic islet cells, we show for the first time that a functional β -cell clock is required for proper basal and stimulated insulin secretion. Moreover, clock disruption has a profound impact on the human islet transcriptome, in particular, on the genes involved in insulin secretion.

Keywords: circadian bioluminescence, circadian clock, human pancreatic islet, insulin secretion, RNA sequencing

Date submitted 15 September 2015; date of first decision 8 October 2015; date of final acceptance 1 December 2015

Introduction

The circadian system drives intrinsic biological clocks with near 24-h oscillation periods, regulating physiology and behaviour in most living beings, including humans. This network of timekeepers is organized in a hierarchical manner, with a master pacemaker located in the suprachiasmatic nucleus of the hypothalamus [1]. The central clock is synchronized every day to the photoperiod and readjusts the phases of the peripheral oscillators. In mammals, Circadian Locomotor Output Cycles Kaput (CLOCK) and Brain and Muscle ARNT-like Protein 1 (BMAL1) transcription factors activate the expression of *Per* and *Cry* genes. Period (PER) and Cryptochrome (CRY) proteins attenuate the CLOCK/BMAL1-mediated activation of their own synthesis in a negative feedback loop. Nuclear receptors reverse-erb alpha (*Rev-erbα*) and retinoid-related orphan receptor alpha (*RORα*), as well as post-translational

Correspondence to: Charna Dibner, Department of Endocrinology, Diabetes, Nutrition and Hypertension, Faculty of Medicine, University of Geneva, Aile Jura 4-774, Rue

Gabrielle-Perret-Gentil, 4, CH-1211 Geneva 14, Switzerland. E-mail: Charna.Dibner@hcuge.ch

[†]C. S., V. P. and P. P. contributed equally to the manuscript.

protein modifications, play a critical role in this molecular circuitry [2].

Accumulating data from rodent studies suggest an essential role of the circadian system in the coordination of body metabolism [3]. Genome-wide transcriptome profiling studies, as well as a dominant role of feeding–fasting cycles for the synchronization of peripheral oscillators, indicate that the temporal orchestration of metabolism and xenobiotic detoxification is the major purpose of circadian clocks in peripheral tissues [3,4]. This conjecture is further supported by metabolomic and lipidomic approaches, indicating that large numbers of metabolites exhibit circadian profiles in tissues, plasma and saliva [5,6]. Mutations in the essential clock genes *Bmal1* and *Clock* [7] cause various metabolic disorders. Conversely, perturbations of metabolic pathways in mice fed a high-fat diet dampen the amplitude of circadian oscillations and lengthen their period [8].

Several studies have shown the presence of circadian oscillators in rodent pancreatic islets, pointing out their impact on islet gene expression [9] and function [10]. Importantly, Marcheva et al. [7] provided a direct link between a functional circadian islet clock in rodents, insulin secretion and the aetiology of type 2 diabetes (T2D). Their pioneering study highlights

¹ Endocrinology, Diabetes, Hypertension and Nutrition, Diabetes Centre, Faculty of Medicine, University of Geneva, Geneva, Switzerland

² Institute of Genetics and Genomics in Geneva (iGE3), Geneva, Switzerland

³ Diabetes Center, UCSF, San Francisco, CA, USA

⁴ Department of Surgery, Cell Isolation and Transplantation Centre, University Hospital of Geneva, Geneva, Switzerland

⁵ Department of Genetic Medicine and Development, University of Geneva Medical School, Geneva, Switzerland

⁶ Swiss Institute of Bioinformatics, Geneva, Switzerland

original article

the key role of the endocrine pancreas clock for proper islet function, in particular for insulin secretion.

The prevalence of T2D in modern society is taking on enormous proportions. It is therefore of major importance to further identify the molecular basis of circadian rhythmicity in human islets under physiological conditions and its effect on T2D. Despite accumulating evidence on the role of the circadian system in the regulation of glucose homeostasis in humans [2,3], very few studies are available so far that provide a molecular link between the human islet clockwork and insulin secretion. Gene expression analysis in pancreatic islets, isolated from human T2D donors, suggested that mRNA levels of core clock components are deregulated in people with T2D [11]. Our recent work has demonstrated the existence of cell-autonomous, self-sustained circadian oscillators, operative in human pancreatic islets at the population level and at single islet level, that were synchronized between β and non- β cells [12]. In the present study, we aimed to assess the physiological relevance of the circadian oscillator in human pancreatic islets for regulating insulin secretion and for its impact on the islet cell transcriptome.

Materials and Methods

Human Islet Preparation and Cell Culture

Human islets were isolated from pancreases of brain-dead multi-organ donors, obtained either from the Islet Transplantation Centre at the University Hospital of Geneva (Switzerland) as described by us in a previous study [12] or by Prodo Laboratories (Irvine, CA, USA). The use of human islets for research was approved by the local ethics committee. Details of the islet donors are summarized in Table S1 in Appendix S1. After purification, islets were cultured in Connaught Medical Research Laboratories medium (CMRL; 1066 CR1136, SAFC Biosciences) with subsequent gentle dissociation by Accutase (Innovative Cell Technologies, San Diego, CA, USA). Dissociated islet cells were attached to 35-mm dishes or multi-well plates, pre-coated with a laminin-5-rich extracellular matrix derived from 804G cells [13].

Small Interfering RNA Transfection and Lentiviral Transduction

Dissociated adherent human islet cells were transfected twice with 50 nM small interfering RNA (siRNA) targeting *CLOCK* (siClock) or with non-targeting siControl (Dharmacon, GE Healthcare, Little Chalfont, UK), using Lipofectamine® RNAiMAX reagent (Invitrogen, Carlsbad, CA, USA), with subsequent experiments performed 4–7 days post-transfection. To produce lentiviral particles, Bmal1-luciferase reporter (Bmal1-luc) [14] lentivectors were transfected into 293T cells using the polyethylenimine method (for details see Pulimeno et al. [12]). Human islet cells were transduced with a multiplicity of infection = 3.

In vitro Islet Cell Synchronization and Bioluminescence Monitoring

Adherent transfected and transduced islet cells were synchronized by a 1-h forskolin pulse (10 μ M; Sigma, Saint-Louis, MO,

USA), and subjected to continuous bioluminescence recording in CMRL medium containing $100 \,\mu\mathrm{M}$ luciferin (D-luciferin 306-250, NanoLight Technology) as described in detail previously [12], with the following modifications: bioluminescence pattern was monitored by a home-made robotic device equipped with photomultiplier tube detector assemblies, allowing the recording of 24-well plates. Photon counts of each well were integrated during 1 min, over 24-min intervals. In order to analyse the amplitude of time series without the variability of magnitudes, raw data were processed in parallel graphs by moving average with a window of 24 h as described previously [15]. Briefly, the ratio of each data point was calculated on the average of data points in an interval of 24 h (12 h before and 12 h after the analysed data point).

Insulin Secretion Measurements

Insulin secretion assays were performed on ~100 000 attached islet cells in three drops of 50 µl per dish, transfected with either siClock or siControl. For standard glucose-stimulated insulin secretion (GSIS) assays, cells were washed in KRB solution (Krebs-Ringer bicarbonate, pH 7.4, supplemented with 0.3% free fatty acid bovine serum albumin (BSA; Sigma, St Louis, MO, USA) containing 2.8 mM glucose for 2 h. Cells were subsequently incubated in KRB solution containing 2.8 mM glucose for 1 h at 37 °C (basal condition), followed by 1 h stimulation with 16.7 mM glucose, with or without 5 mM theophylline (Sigma; stimulated conditions; modified from Paget et al. [16]). After additional 1 h incubation in KRB solution containing 2.8 mM glucose (re-basal condition), cells were lysed in acid-ethanol solution (1.5% HCl and 75% ethanol) for 1 h at room temperature. For the prolonged insulin release assay, cells were briefly washed in serum-free CMRL medium, supplemented with 0.5% BSA, and statically incubated in the same medium, containing either 5.6 mM glucose (basal condition) or 20 mM glucose (stimulated condition) for 7 h at 37 °C. To assess the total insulin content, cells were lysed in acid-ethanol buffer overnight at −20 °C. All collected samples were supplemented with the protease inhibitors PMSF (Axonlab, Reichenbach an der Fils, Germany), aprotinin (Sigma) and dipeptidyl peptidase-4 (Millipore, Billerica, MA, USA). Insulin was quantified in supernatants and cell lysates using a human insulin ELISA kit (Mercodia, Uppsala, Sweden). Insulin secretion values were obtained by normalization of the supernatant content to the cellular total insulin content. Additional secretion assays are described in Appendix S1.

Circadian Analysis of Basal Insulin Secretion by Continuously Perifused Human Islet Cells

Human islet cells, transduced with the *Bmal1-luc* reporter and synchronized *in vitro* with a 1-h forskolin pulse, were placed into an in-house developed two-well horizontal perifusion chamber connected to the LumiCycle [17]. Cells were continuously perifused for 48 h with CMRL (with supplements, in the absence of sodium pyruvate) containing 5.6 mM glucose and $100 \,\mu\text{M}$ luciferin. Bioluminescence recordings were performed in parallel to the 4 h interval-automated collection of the outflow medium. Basal insulin levels were quantified in the outflow

356 | Saini et al. Volume 18 | No. 4 | April 2016

medium using the human insulin ELISA kit, and were normalized to the total intracellular insulin content measured from cells lysed in acid-ethanol buffer overnight at $-20\,^{\circ}$ C. The circadian character of insulin secretion was evaluated using the JTK_CYCLE algorithm [18].

RNA Analysis by Quantitative RT-PCR

Total RNA was prepared from homogenized (QIAshredder, Qiagen, Hombrechtikon, Switzerland) islet cells using RNeasy® Plus Micro Kit (Qiagen). Then 0.2 μg of total RNA was reverse-transcribed using Superscript III (Invitrogen) and random hexamers and was PCR-amplified on a LightCycler 480 (Roche Diagnostics AG, Basel, Switzerland). Mean values for each sample were calculated from technical duplicates of each quantitative RT-PCR (qRT-PCR) analysis and normalized to the housekeeping gene S9, or to the mean of hypoxanthine-guanine phosphoribosyltransferase (HPRT) and S9. Primers used for this study are listed in Table S2 in Appendix S1.

RNA Sequencing

Human islet cells from eight human islet preparations, transfected with siControl or siClock (total of 16 samples), were sequenced according to a previously described procedure [19,20]. Total RNA libraries were prepared from 150 ng of RNA, following customary Illumina TruSeq protocols for next-generation sequencing. PolyA-selected mRNAs were purified, size-fractioned, and subsequently converted to single-stranded cDNA by random hexamer priming. Following second-strand synthesis, double-stranded cDNAs were blunt-end fragmented and indexed using adapter ligation, after which they were amplified and sequenced according to protocol. RNA libraries were 49 bp paired-end sequenced in one lane on the Illumina HiSeq 2000. Standard quality checks for material degradation (Bioanalyzer, Agilent Technologies, Santa Clara, CA, USA) and concentration (Qubit, Life Technologies, Carlsbad, CA, USA) were carried out before and after library construction, ensuring that samples were suitable for sequencing. Data analysis was performed as described in detail in Appendix S1.

Statistics

Data are presented as mean \pm (standard error of mean) and analysed using a paired Student's t-test. Statistical significance was defined at p < 0.05 (*), p < 0.01 (**) or p < 0.001 (***). The statistical analysis for RNA sequencing (RNAseq) is described in Appendix S1.

Results

CLOCK Knockdown Disrupts the Circadian Oscillator in Human Pancreatic Islet Cells

We have previously characterized self-sustained, cell-autonomous circadian clocks in human pancreatic islets [12]. To unravel the potential impact of this molecular circuitry on the gene expression and physiological function of

islet cells, we set up an efficient siClock transfection protocol, resulting in >80% knockdown of CLOCK transcript levels (Figure 1A). Concomitantly with CLOCK transcript depletion, levels of endogenous REV-ERBα, D-albumin binding protein (DBP) and PER3 transcripts were downregulated by 52, 57 and 51%, respectively, in siClock-transfected cells, as compared with siControl counterparts (Figure 1B). By contrast, BMAL1 and CRY1 levels were upregulated by 50 and 140% (Figure 1B). To further assess the impact of CLOCK knockdown on the functional circadian oscillator in cultured human islet cells, continuous recording of the bioluminescent circadian reporter Bmal1-luc was performed. Consistent with our recent findings [12], human islet cells transfected with siControl exhibited pronounced self-sustained circadian oscillations of the Bmal1-luc reporter following forskolin-induced in vitro synchronization with a period length of 25.81 ± 0.3 h; however, these oscillations were strongly dampened in synchronized islet cells transfected with siClock (Figure 1C, D).

Insulin Secretion is Altered Upon Human Islet Clock Disruption

Functional peripheral clocks are required for sustaining the physiological functions of their corresponding tissues. We therefore aimed to evaluate the impact of a disrupted molecular clock on the endocrine function of human pancreatic islet. Since the majority of cells in islet preparations are β cells (\sim 65%, Figure S1 in Appendix S1), we focused on insulin secretion for our functional studies.

The efficiency of insulin secretion by human islet cells was first assessed by GSIS. In the presence of high glucose (16.7 mM), a significant (30%) decrease in insulin secretion was recorded in siClock-transfected cells (Figure 2A). By adding theophylline, previously reported to allow for enhanced stimulated secretory capacity by human islet cells [16], we achieved an even clearer discrimination in the insulin secretion levels between control situation and disrupted clock condition. Indeed, higher fold induction was observed under these settings, with insulin secretion being significantly reduced in the presence of both low (2.8 mM) and high (16.7 mM) glucose levels upon clock disruption (Figure 2B). We next evaluated the long-term release of insulin by β cells under physiological glucose concentration (5.6 mM), and in the presence of high glucose levels (20 mM) in the medium. In concordance with the acute GSIS test, the long-term (7 h) release of insulin in the presence of physiological glucose concentration was ~50% reduced in islet cells bearing siClock, as compared with matched siControl samples (Figure 2C). A similar trend was observed for the long-term insulin release upon high glucose concentration (Figure 2C).

Furthermore, reduction in stimulated insulin secretion was observed in *siClock* transfected cells in comparison with their *siControl* counterparts on stimulation with the non-glucose secretagogues cholinomimetic carbachol, and the depolarizing agent KCl (Figure S2A and B in Appendix S1). Notably, the insulin content was not affected by clock disruption in all cases, and relative fold increase stayed unchanged between *siControl* and *siClock* conditions (not shown).

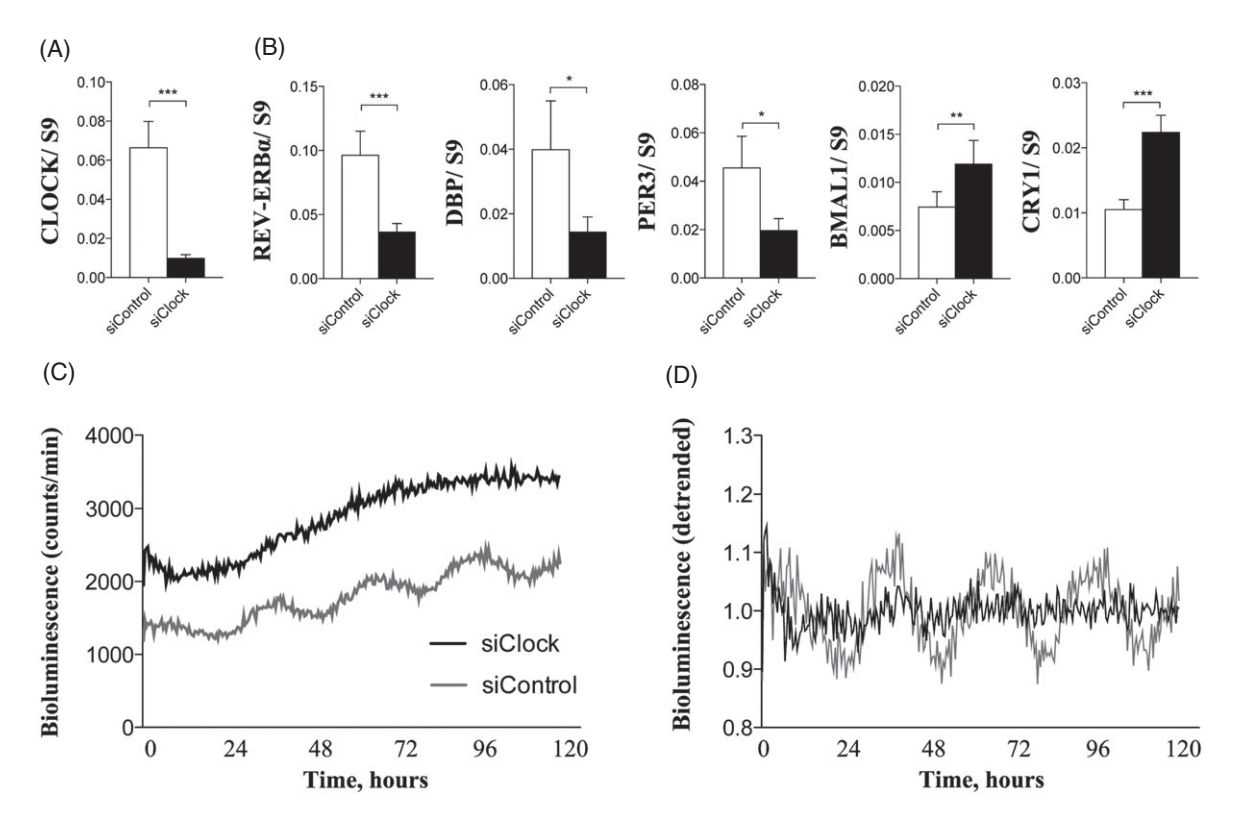


Figure 1. CLOCK knockdown efficiently disrupts the molecular clocks present in human islet cells. Human islet cells were attached to a laminin-coated surface and transfected with scrambled siRNA (siControl) or siRNA targeting CLOCK (siClock). Cells were harvested 7 days later for quantitative RT-PCR analysis of CLOCK (A), $REV-ERB\alpha$, DBP, PER3, BMAL1 and CRY1 transcript levels (B), and normalized to the housekeeping gene S9. Data are presented as mean \pm standard error or the mean of 13 experiments, each using islets from one donor each. (C) Representative oscillatory profiles of forskolin-synchronized human islet cells transduced with Bmal1-luc lentiviruses, and transfected with siControl or siClock. Bmal1-luc oscillation profiles were recorded for two parallel dishes for each of the three donors. (D) To compare bioluminescence values with regard to amplitude, we eliminated variations in the magnitude of the signals by detrending the data presented in (C) as described in Materials and Methods. The y-axis shows detrended bioluminescence.

To further unravel the temporal profile of insulin secretion by isolated human pancreatic islets, we monitored insulin secretion upon constant physiological glucose concentration (5.6 mM glucose) by forskolin-synchronized human islet cells over 48 h. To this end, our recently developed in-house perifusion system, connected to the LumiCycle chamber which allows parallel cell perifusion and bioluminescence profile recordings, was used [17]. The perifusion experiments, paralleled by circadian bioluminescence recording, suggested that forskolin-synchronized human islet cells exhibited a circadian profile of insulin secretion over 48 h (Figure 2D, siControl). Application of JTK CYCLE algorithm [18] confirmed that the average profile of secreted insulin was circadian within 48 h, with a period length of 24.19 ± 0.89 h (**p = 0.009; n = 7 donors). This circadian pattern of insulin secretion was strongly disrupted upon siClock transfection (Figure 2D).

Taken together, these data indicate that operative circadian oscillators in human pancreatic islets are required for proper insulin secretion by β cells.

Impact of CLOCK Knockdown on the Human Pancreatic Islet Cell Transcriptome

To obtain an insight into possible mechanisms of the observed effect of clock disruption on insulin secretion, a transcriptome analysis was performed in human pancreatic islet cells. To this end, *siClock* and *siControl*-transfected islet cells from eight donors were subjected to RNAseq. Out of 21451 expressed coding transcripts, 352 (1.6%) were significantly modified by clock disruption, with 145 being upregulated and 207 being downregulated (Figure 3A; Tables S3 and S4 in Appendix S1). For initial validation, expression levels obtained by RNAseq for *CLOCK*, *REV-ERBa*, *DBP* and *BMAL1* levels were also assessed by qRT-PCR in the same samples, with comparable levels observed by both methods (Figure S3 in Appendix S1).

Significantly up- or downregulated genes were manually curated and analysed as described in the Supplementary Appendix. Differentially expressed genes were clustered into common functional groups (Figure 3B). Consistent with the qRT-PCR results (Figure 1A, B; Figure S3 in Appendix S1), RNAseq confirmed disruption of the molecular circadian clock. Moreover, pathway analysis based on the Kyoto Encyclopedia of Genes and Genomes (KEGG) database suggested that among the five principal pathways that were significantly altered by siClock (Figure 3C), circadian rhythm was ranked number one. CLOCK knockdown resulted in the overexpression of its molecular partner BMAL1 (ARNTL) and also led to an increase in CRY1 (Table 1). The expression levels of all PER genes exhibited a tendency for downregulation, with

358 | Saini et al. Volume 18 | No. 4 | April 2016

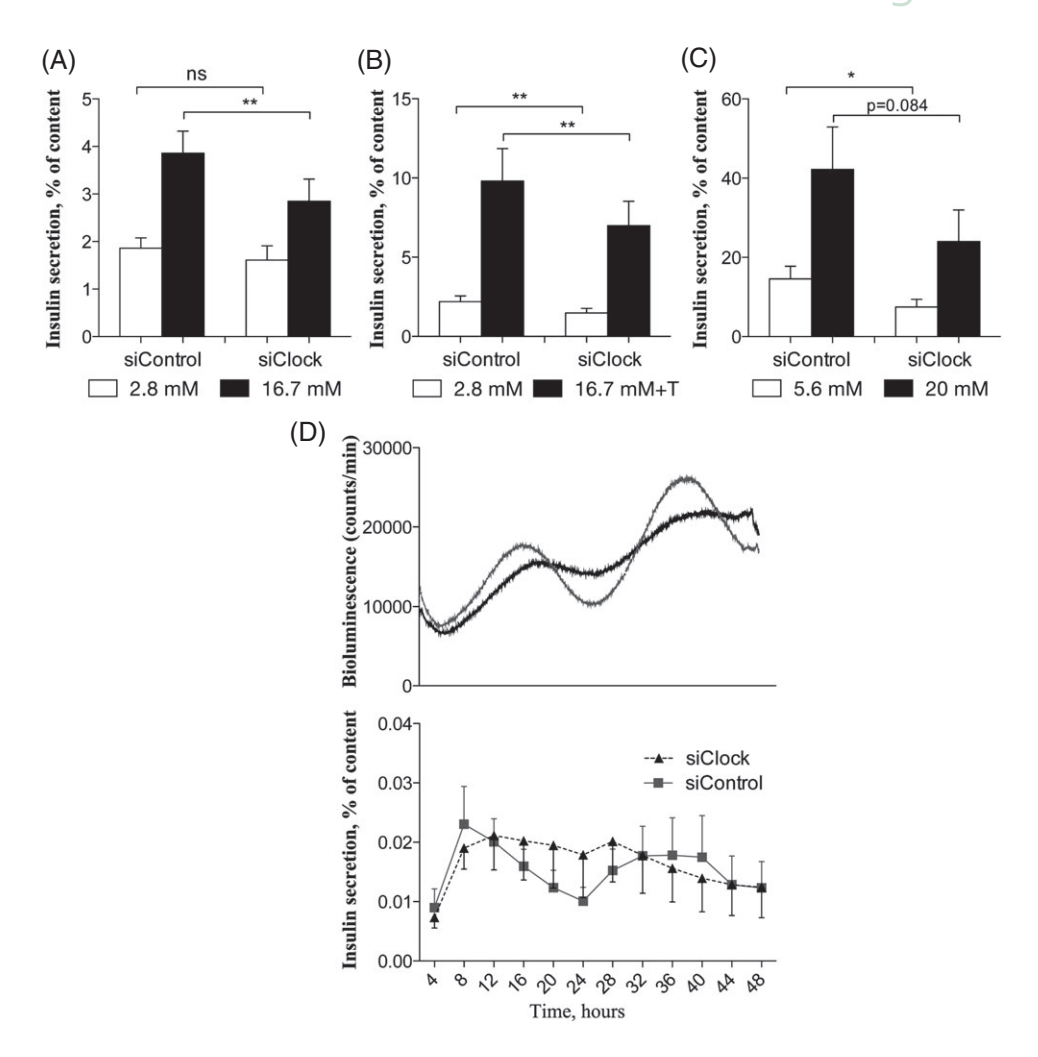


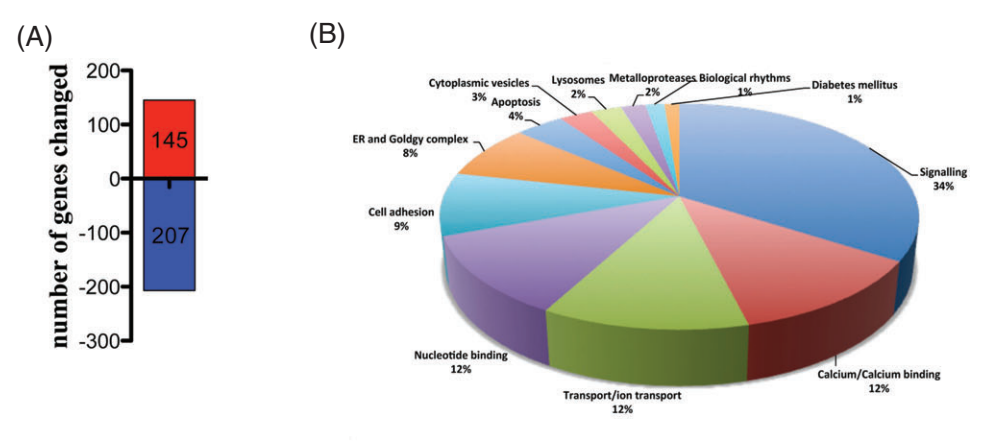
Figure 2. CLOCK knockdown alters basal and glucose-induced insulin secretion in human islet cells. (A) Dissociated human islet cells were transfected with siControl or siClock and were subjected to 1 h incubation with 2.8 mM glucose, followed by 1 h incubation with 16.7 mM glucose (glucose-stimulated insulin secretion) or by 16.7 mM glucose and 5 mM theophylline 'T' (B). (C) Release of insulin by siControl or siClock-transfected cells was assessed after 7 h incubation in the presence of 5.6, or 20 mM glucose. (D) Human islet cells transfected either with siControl or siClock and transduced with Bmal1-luc reporter were constantly perifused with culture medium containing 5.6 mM glucose. Insulin levels were assessed by ELISA (Mercodia) in the outflow samples collected every 4 h during 48 h (bottom panel) upon monitoring of circadian bioluminescence profile (top panel). Data are presented as % of secreted hormone from the total hormone content (mean ± standard error of the mean) for nine donors (at least two technical replicates each) (A), eight donors (at least two technical replicates each) (B), four donors (at least two technical replicates each) (C) and seven donors (one replicate for each donor) (D). Paired Student's t-test analysis was used to compare differences between groups (A–C). **p < 0.01, *p < 0.05.

*PER*3 being significantly repressed down to almost 50% of its initial level. The clock output genes *DBP* and *BHLHE41* were also significantly downregulated. Finally, the expression of components of the clock auxiliary loop was increased for *RORγ* (*RORC*) and decreased for *REV-ERBα* (*NR1D1*). Interestingly, glucocorticoid receptor *NR3C1* was downregulated upon siClock transfection, which was confirmed by qRT-PCR analysis in independent human islet preparations (Figure 4).

In agreement with the observed deficit in insulin secretion, a number of genes related to insulin production/secretion were differentially expressed in human islet cells according to the RNAseq results (Table 1, Figure 3D, schema is adopted from KEGG pathway map, Figure 4, Tables S3 and S4 in Appendix S1). While insulin (*INS*) expression itself was not

affected, genes involved in insulin granule formation and secretion (SLC30A8, VAMP3, STX6) were downregulated. Although downregulation of STX6 levels upon siClock did not reach significance according to RNAseq, further analysis by qRT-PCR performed on cells from 10 independent donors, confirmed significant downregulation (Figure 4A, B). At the same time, levels of the β -cell-specific transcription factors MAFA, NEUROD1 and NKX6-1 were upregulated (Table 1 and Figure 4).

An additional group of transcripts, affected by *siClock*, included genes involved in the execution of stimulatory signals for insulin secretion. We found that transcription of the guanine nucleotide-binding protein G (q-subunit; *GNAQ*), the subunit of mitochondrial ATP synthase (*ATP5G2*) and the principal subunit of the Na⁺/K⁺-ATPase (*ATP1A1*) were



KEGG pathway	Number of genes altered upon siClock out of total	Adjusted p-value	Transcripts altered by siClock
Circadian rhythm mammal	7/22	1.86E-05	RORC,CLOCK,PER3,CRY1,NR1D1, BHLHE41,ARNTL
Lysosome	11/114	0.0011	GNS,LAMP1,SCARB2,HEXB,ABCA, ATP6AP1,PSAP,NPC2,GGA2 NPC1,NEU1.
Phagosome	11/132	0.0029	LAMP1,THBS2,ATP6V1A, HLA-E,VAMP3,ATP6AP1,HLA-C, TUBB6,ATP6V1B2,CANX,THBS1
Focal adhesion and Extracellular matrix-receptor interaction	13/190	0.0046	LAMA4,FLNC,COL5A2,THBS2, MYLK,COL1A2,ITGA1,VCL,PDGFB, PDGFRA,PIK3CB,COL3A1, THBS1
TGF-beta signaling pathway	7/77	0.01689	ACVR1B, SMAD9, PPP2CB, ID4, THBS1, THBS2, TFDP1
Type I diabetes	4/31	0.043	HLA-C,CPE,HLA-E,PTPRN

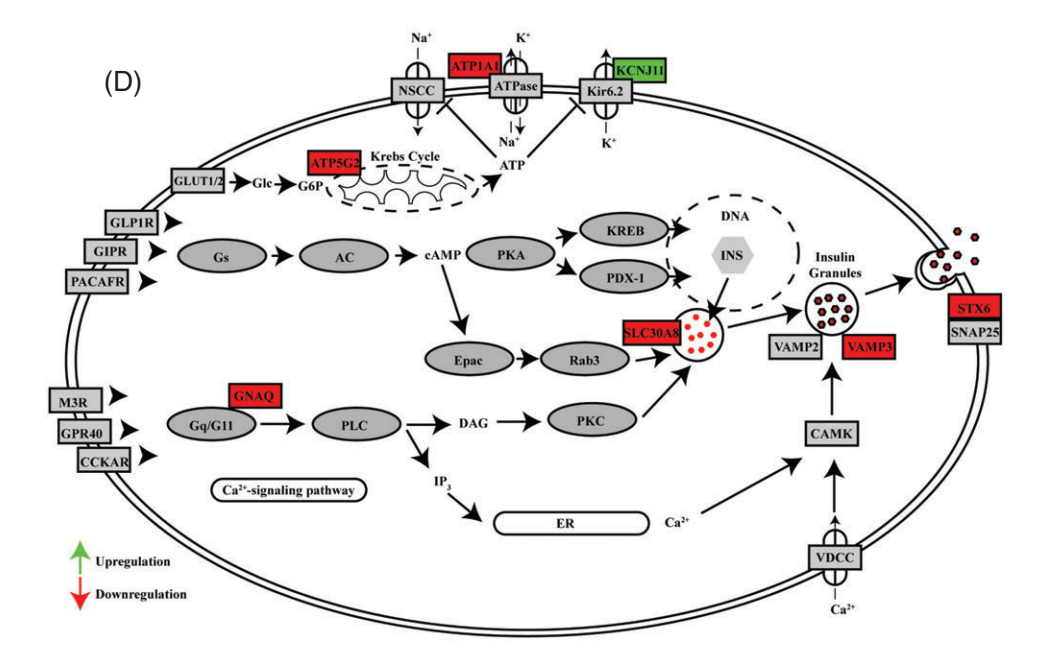


Figure 3. Effect of CLOCK knockdown on human islet cell transcriptome. (A) Number of differentially expressed genes according to the Fisher's exact test with Benjamini Hochberg correction (p < 0.05; gene expression was changed significantly in one direction in at least six out of eight islet preparations and no significant change was observed in the opposite direction). (B) Principal functional categories of the transcripts modified by siClock. Gene ontology analysis was carried out using the WebGestalt and Database for Annotation, Visualization and Integrated Discovery (DAVID) software, with functional groups of genes appearing in both analyses expressed on the diagrams (p < 0.05). (C) Pathways, which include genes that were significantly altered by CLOCK knockdown have been tested in the Kyoto Encyclopedia of Genes and Genomes (KEGG) database with the WebGestalt software and double-checked with the DAVID software (adjusted by Benjamini-Hochberg correction p < 0.05). (D) Schematic presentation of insulin synthesis/secretion KEGG pathways including genes, whose expression was altered by siClock (http://www.genome.jp/kegg-bin/show_pathway?map=hsa04911&show_description=show).

360 | Saini et al. Volume 18 | No. 4 | April 2016

Table 1. Fold changes for selected transcript expression obtained by RNA sequencing analysis upon the CLOCK knockdown.

		Log ₂ fold	Ensemble ID	
	Gene	change	and full name	Source
Circadian clock	CLOCK	-2.7 ↓	ENSG00000134852.10	KEGG database
			Circadian Locomotor Output Cycles Kaput	
	NR1D1	-1.6↓	ENSG00000126368.5	KEGG database
			Nuclear receptor subfamily 1, group D, member 1	
	CRY1	0.87 ↑	ENSG00000008405.7	KEGG database
			Cryptochrome circadian clock 1	
	NR1D2	-0.87 ↓	ENSG00000174738.8	[21]
	4 D. 1771	0.50.4	Nuclear receptor subfamily 1, group D, member 2	WDGG L . I
	ARNTL	0.72 ↑	ENSG00000133794.13	KEGG database
	PER3	0.0.1	Aryl hydrocarbon receptor nuclear translocator-like ENSG00000049246.10	KEGG database
	PEK3	-0.9 ↓	Period circadian clock 3	KEGG database
	RORC	0.63 ↑	ENSG00000143365.12	[22]
	RORC	0.03	RAR-related orphan receptor gamma	[22]
	BHLHE41	-0.25↓	ENSG0000123095.5	[23]
	211211211	0.25 4	Basic helix-loop-helix family, member E41	[20]
	DBP	-0.95↓	ENSG00000105516.6	[24]
		·	D site of albumin promoter binding protein	
Insulin production and secretion	SLC30A8	-0.31 ↓	ENSG00000164756.8	GOTERM database
			Solute carrier family 30 (zinc transporter), member 8	
	VAMP3	-0.67↓	ENSG00000049245.8	[25]
			Vesicle-associated membrane protein 3	
	MAFA	0.45 ↑	ENSG00000182759.3	[26]
			V-Maf avian musculoaponeurotic fibrosarcoma	
			oncogene homologue A	rmag I . I
	ATP1A1	-0.21 ↓	ENSG00000163399.11	KEGG database
	CNIAO	0.46 1	ATPase, Na+/K+ transporting, alpha 1 polypeptide	VECC database
	GNAQ	-0.46 ↓	ENSG00000156052.6 Guanine nucleotide binding protein (G protein), q	KEGG database
			polypeptide	
	KCNJ11	0.2 ↑	ENSG00000187486.5	KEGG database
			Potassium channel, inwardly rectifying subfamily J,	
			member 11	
	NKX6-1	0.34 ↑	ENSG00000163623.5	[26]
			NK6 homeobox 1	
	STX6	-0.33 ↓	ENSG00000135823.9	[27]
			Syntaxin 6	
	NEUROD1	0.2 ↑	ENSG00000162992.3	GOTERM database
	ATTRECE	0.05.1	Neuronal differentiation 1	WEGG 1 . 1
	ATP5G2	-0.25 ↓	ENSG00000135390.13	KEGG database
			ATP synthase, H+ transporting, mitochondrial F0	
Glucocarticoid recentor	NR3C1	-0.38↓	complex, subunit C2 (subunit 9) ENSG00000113580.10	[28]
Glucocorticoid receptor	NKJCI	-0.56 ↓	Nuclear receptor subfamily 3, group C, member 1	[20]
			racical receptor subtaining 3, group 6, member 1	

KEGG, Kyoto Encyclopedia of Genes and Genomes.

repressed, while expression of the ATP-sensitive inward rectifier potassium ion channel (*KCNJ11*) was upregulated. The RNAseq results for these transcripts were also confirmed by qRT-PCR analysis in independent human islets preparations. High similarity in the level of transcript alterations was obtained between the RNAseq findings and qRT-PCR analysis in all cases (Figure 4A, B).

Taken together, these data suggest that *CLOCK* depletion leads to the disruption of insulin synthesis/secretion at the level of granular maturation, membrane fusion and intracellular signal transduction in human islet cells.

Discussion

Studies on peripheral clocks in isolated organ explants/primary cells hold promise for gaining information on the human circadian timing system. Indeed, robust circadian oscillations have been recently characterized by us and others in human primary fibroblasts [29], thyrocytes [30], skeletal myotubes [17] and pancreatic islets [12] kept in organotypic cultures and synchronized *in vitro*. In the present study, we provide new insights into the role of the human circadian clock in the transcriptional and functional regulation of the islet.

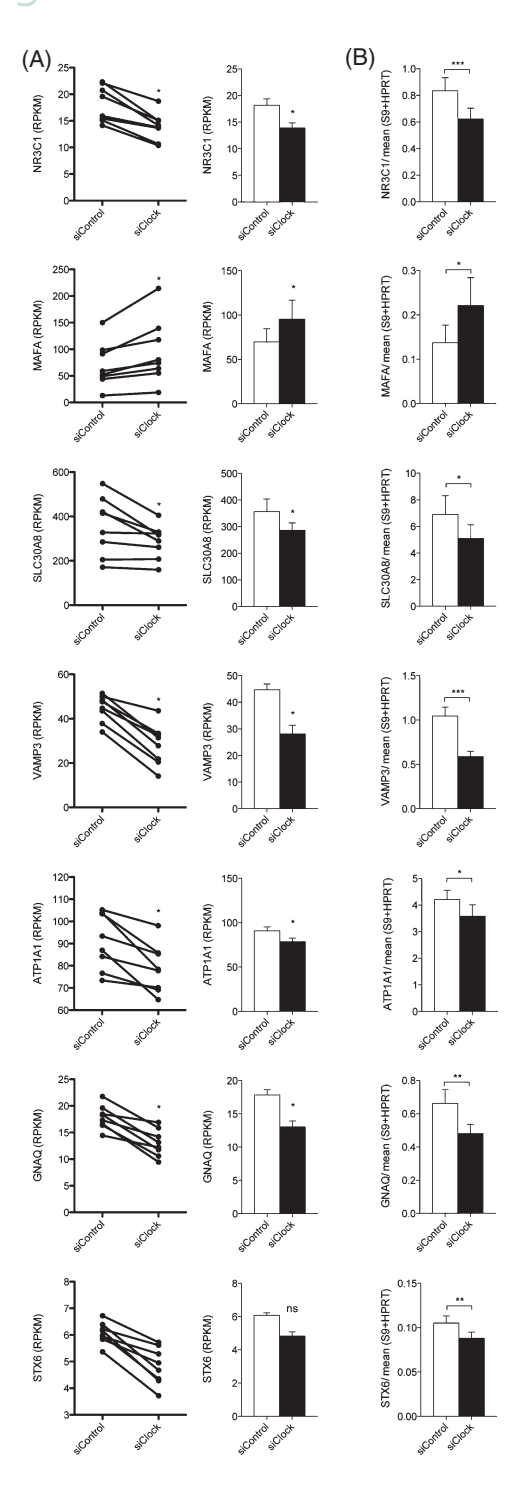


Figure 4. *CLOCK* disruption affects insulin secretion-related transcripts and glucocorticoid receptor levels. (A) reads per kilobase of transcript per million (RPKM) values for each donor (left panels) and average (mean \pm standard error of the mean) obtained by RNA sequencing (eight donors; Fisher's test, p < 0.05 for each donor, gene expression was changed significantly in one direction in at least six of eight islet preparations and no significant change in the opposite direction). (B) Quantitative RT-PCR of the same transcripts performed in 9 (for *NR3C1*, *MAFA*, *VAMP3*, *GNAQ*) or 10 (for *STX6*, *SLC30A8*, *ATP1A1*) independent human islets preparations (data are expressed as relative expression of the target gene to the average of two housekeeping genes *S9* and *HPRT*), paired Student's *t*-test. ***p < 0.001, **p < 0.01, *p < 0.05.

The circadian oscillator was perturbed in human islet cells by a highly reproducible siRNA-mediated CLOCK transcript knockdown of >80% (Figure 1A and Figure S3 in Appendix S1). Upon such CLOCK silencing, significant upregulation of endogenous BMAL1 and CRY1, as well as downregulation of REV-ERB α , PER3 and DBP transcripts was observed by qRT-PCR and RNAseq analyses (Figure 1B and Figure S3 in Appendix S1). Moreover, the circadian amplitude of the Bmal1-luc reporter, assessed in synchronized human islet cells in vitro, was strongly flattened (Figure 1C, D), further validating siClock-mediated core clock disruption in this experimental system. These results are consistent with our recent observations in human skeletal muscle [17], and with data published for the Clock-mutant mouse model [7]. In view of the correlation between in vitro assessed oscillator properties and the in vivo human circadian phenotype, it might be feasible to employ this informative methodology to study peripheral clock alterations, which are considered a hallmark of multiple diseases (reviewed in Saini et al. [31]). Beyond potential diagnostic implications, this approach would allow significant insights to be gained into the impact of the core clock, or its components, on the transcriptional regulation and the physiological function of the respective organ. By disrupting human skeletal muscle clock, we have recently shown that a functional myotube oscillator is required for the basal secretion of IL6, MCP1 and additional myokines [17]. Using a similar experimental system, we now show for the first time that basal insulin secretion exhibits a circadian pattern in in vitro synchronized human pancreatic islet cells monitored during 48 h, which is altered upon clock disruption (Figure 2D). This finding shows that diurnal insulin secretion is modulated by β -cell-autonomous clocks. Such daily regulation gates time windows of insulin secretion, which predisposes the cell to respond to feeding/fasting episodes. With regard to the phase relationship between clock gene expression (reflected by the Bmal1-luc profile) and insulin secretion, we found that the maximum level of secreted insulin precedes the zenith of *BMAL1* expression by \sim 4–6 h (Figure 2D). Importantly, although few studies are available, and taking into account the variability inherent to human studies, such correlation seems to closely recapitulate the phase relationship observed in vivo in patients on a controlled equicaloric diet [32,33], highlighting the potency of our in vitro system for further dissecting the interplay between the human pancreatic islet circadian clock and its physiological function.

Importantly, the present work shows that functional circadian oscillators are necessary for chronic and acute insulin secretion by human pancreatic islet cells in response to glucose and non-glucose (KCl, carbachol and theophylline) stimulators (Figure 2A–C and Figure S2A, B in Appendix S1), indicating that islet cellular clocks are required for the proper ability of the tissue to respond to daily insulin needs. Our experimental results are corroborating well with findings from genetic rodent models [7,34], suggesting that the circadian clock is essential for proper insulin secretion, and that disruption of the islet clock may be a direct cause of T2D development [7,10,35]. In humans, there is accumulating evidence that the circadian oscillator regulates insulin secretion and glucose metabolism [36,37]. Furthermore, misalignment between the endogenous

362 | Saini et al. Volume 18 | No. 4 | April 2016

circadian clock and behavioural rhythms, for example as a result of sleep disturbance or shift work, might be linked to an increased risk of metabolic syndrome and diabetes [3,38]. Consistent with the outcome of these epidemiological and genetic studies, our experiments in cultured human pancreatic islets provide the link between disruption of the islet oscillator and impaired basal and stimulated insulin secretion.

Consistent with the effect of siClock on insulin secretion, the whole transcriptome analysis by RNAseq identified alterations in several functional groups of genes related to impaired insulin secretion (Figure 3B, D, Table 1 and Tables S3 and S4 in Appendix S1). According to the gene ontology analysis, a number of transcripts involved in protein synthesis, granule formation and traffic were affected by siClock. These results were further confirmed by qRT-PCR (Figure 4). For instance, expression of the Zinc-transporter SLC30A8, which is required for normal insulin synthesis, storage and secretion [39], was significantly inhibited by siClock (Figure 4). In rodents, the deletion of Slc30A8 was accompanied by impairment of insulin secretion in vivo [40], consistent with the phenotype observed in the present study (Figure 2; and Figure S2 in Appendix S1). Once insulin is packed into granules, its release requires granule fusion with the plasma membrane. The final step of granule fusion is dependent on the functional SNAP25/VAMP/STX complex, with VAMP3 and STX6 being part of this complex in β cells [41,42]. In the present study, we report downregulation of VAMP3 and STX6 transcripts upon clock disruption (Figures 3 and 4). Importantly, these genes were also differentially expressed in Clock mutant mice [7]; thus, our data are in a good agreement with the assumption that these genes could be responsible for disrupted insulin exocytosis upon clock dysfunction [27].

In addition to mechanisms of granule formation and trafficking, probably responsible for the observed deficit in basal insulin secretion (Figure 2 and Figure S2 in Appendix S1), we found significant changes in genes regulating insulin secretion on-demand. Among them ATP5G2 [ATP synthase, mitochondrial F0 complex, H+ transporting, subunit C2 (subunit 9)], ATP1A1 (Na+/K+-transporting ATPase, subunit α -1) and KCNJ11 (potassium channel, inwardly rectifying subfamily J member 11) are components of the principal ATP-mediated pathway of stimulated insulin secretion in response to high glucose. The expression of ATP5G2 was repressed upon CLOCK knockdown (Table 1). This mitochondrial enzyme is required for ATP synthesis by utilizing an electrochemical gradient of protons across the inner membrane during oxidative phosphorylation; thus, its downregulation might decrease glucose-stimulated ATP production in mitochondria. Notably, studies in Bmal1KO mice suggested that the defect in GSIS occurs as a result of increased mitochondrial uncoupling because of upregulation of Ucp2 (uncoupling protein 2), with consequent impairment of glucose-induced mitochondrial potential generation and decrease in ATP production [25]. In our experiments, CLOCK knockdown resulted in the downregulation of ATP1A1 expression, required for membrane depolarization preceding the insulin granule release (Figure 4 and Table 1 [43]). Moreover the transcription of KCNJ11 encoding an ATP-sensitive inward rectifier potassium ion

channel was upregulated (Table 1). Indeed, an activating mutation of KCNJ11 was shown to inhibit insulin secretion and to cause neonatal diabetes [44]. Furthermore, in a mouse model of neonatal diabetes, a β -cell-specific activating mutation of KCNJ11 induced membrane hyperpolarization altering both basal and glucose-induced insulin secretion [45].

Additionally, insulin secretion is regulated by numerous signalling pathways that use G proteins as second messengers. We found that transcription of GNAQ, a component of the stimulatory G protein α subunit that is required for phospholipase C activation [46] was downregulated by siClock, in a good agreement with a recent work identifying GNAQ as a clock controlled gene in synchronized human islets [37]. Using the cholinomimetic carbachol, a specific activator of the Gq/G11 pathway, we show that this pathway is also altered upon clock disruption in human islet cells (Figure S2C in Appendix S1).

Taken together, our findings suggest that the mechanism underlying reduced insulin release upon islet clock disruption is related to a perturbed insulin secretion pathway at the steps of granular maturation, membrane fusion, and intracellular signal transduction (Figure 3D).

Unexpectedly, we found that *CLOCK* knockdown upregulated the expression of the key β -cell transcription factors *MAFA*, *NEUROD1* and *NKX6-1* (Figure 4 and Table 1 [26]). We speculate that this might reflect a compensatory adaptation to the acute clock disruption induced in human adult islets, in contrast to the mouse *Clock*-mutant model where transcription of *NeuroD1* was repressed [7], possibly as a result of chronic perturbation of the circadian clock.

Interestingly, the expression of glucocorticoid receptor NR3C1 was significantly reduced by clock disruption (Figure 4 and Table 1), which might have an impact on islet cell synchronization, in view of the essential role of glucocorticoid signalling as synchronizer for peripheral oscillators [47]; thus, NR3C1 downregulation might reduce the sensitivity of human islets to glucocorticoids, further exacerbating the dysfunction of the peripheral clock system. From a clinical perspective, this conjunction should be taken into account with respect to the widely used glucocorticoid therapy. In addition, insulin itself represents a powerful systemic regulator of molecular clocks in insulin-sensitive tissues [28,48]. Thereby, a decrease in insulin levels and reduced sensitivity to glucocorticoids due to clock disruption and/or T2D might have a systemic impact in a feed-forward loop mechanism, leading to further disruption of peripheral oscillators in this tissue.

Dysfunction and death of pancreatic β cells represent a key factor in the pathogenesis of diabetes mellitus [49]. For instance, the observed overexpression of pro-apoptotic genes (*PSEN2*, *SQSTM1*, *ACVR1B*, *GCH1*, *HTT*, *ARHGEF3*) and downregulation of anti-apoptotic genes (*FURIN*, *PRDX3*, *PPP2CB*, *BTG*) by *siClock* could trigger β -cell death, which might contribute to the development of T2D. Our analysis of the global transcription response of islet cells to a disrupted circadian clock also revealed significant changes in pathways involved in autoimmunity, such as type 1 diabetes mellitus (Figure 3B, C; Table 1). Although some isoforms of HLA-C and HLA-E were shown to be a prediction factor for type 1 diabetes, it is unclear to what extent the overexpression of both

HLA genes and of the autoantigen *PTPRN* observed in the present study (Figure 3C [50]) could induce an autoimmune response.

Modern lifestyles, including social jet lag and shift work, are associated with the development of metabolic syndrome and T2D [3]. Given that T2D is reaching epidemic proportions in our society, this first demonstration of a link between a functional molecular clock in human pancreatic islets and insulin secretion may represent an important target for future clinical investigations.

Acknowledgements

We are grateful to our colleagues from the University of Geneva Jacques Philippe, Ueli Schibler, Philippe Halban and Ursula Loizides-Mangold for constructive comments on this study and to Andre Liani and George Severi for assistance with the perifusion experiments. This work was funded by the SNSF Grant 31003A_146475/1, Bo Hjelt Foundation, Novartis Consumer Health Foundation, Fondation Romande pour la recherché sur le Diabète, EFSD/Boehringer Ingelheim Basic Research Programme, Société Francophone du diabète and Fondation Ernst et Lucie Schmidheiny (CD). Human islets were obtained through grant #1-RSC-2014-100-I-X from the Juvenile Diabetes Research Foundation (TB). Work in the MH laboratory was supported by the grant NIH (R01 DK105831), and by the SNSF grant P2GEP3-151831 (PP).

Conflict of Interest

None of the authors has a conflict of interest to declare. CS, VP, PP, LG and CH contributed to data acquisition, analysis and interpretation, TB facilitated experiments through the provision of reagents, TB, MH and ED contributed to the conception and design, VP drafted the manuscript, CD designed the study, contributed to the data acquisition and analysis, and drafted the manuscript. All authors took part in the revision of the manuscript and approved the final version.

Supporting Information

Additional Supporting Information may be found in the online version of this article:

Appendix S1. Text file describing supplementary methods, legends to supplementary figures and supplementary tables.

Figure S1. Endocrine cell types representation in dissociated human islet cells.

Figure S2. *CLOCK* knockdown reduces stimulated insulin secretion in human islet cells.

Figure S3. Proof-of-principle validation of RNA sequencing data by qRT-PCR analysis.

References

- Partch CL, Green CB, Takahashi JS. Molecular architecture of the mammalian circadian clock. Trends Cell Biol 2014; 24: 90–99.
- Dibner C, Schibler U. Circadian timing of metabolism in animal models and humans. J Intern Med 2015; 277: 513–527.
- Marcheva B, Ramsey KM, Peek CB, Affinati A, Maury E, Bass J. Circadian clocks and metabolism. Handb Exp Pharmacol 2013; 217: 127–155.

- Dibner C, Schibler U, Albrecht U. The mammalian circadian timing system: organization and coordination of central and peripheral clocks. Annu Rev Physiol 2010; 72: 517–549.
- Dallmann R, Viola AU, Tarokh L, Cajochen C, Brown SA. The human circadian metabolome. Proc Natl Acad Sci U S A 2012: 109: 2625–2629.
- Adamovich Y, Rousso-Noori L, Zwighaft Z et al. Circadian clocks and feeding time regulate the oscillations and levels of hepatic triglycerides. Cell Metab 2014; 19: 319–330.
- Marcheva B, Ramsey KM, Buhr ED et al. Disruption of the clock components CLOCK and BMAL1 leads to hypoinsulinaemia and diabetes. Nature 2010; 466: 627–631
- 8. Turek FW, Joshu C, Kohsaka A et al. Obesity and metabolic syndrome in circadian Clock mutant mice. Science 2005; **308**: 1043–1045.
- 9. Muhlbauer E, Wolgast S, Finckh U, Peschke D, Peschke E. Indication of circadian oscillations in the rat pancreas. FEBS Lett 2004; **564**: 91–96.
- Qian J, Block GD, Colwell CS, Matveyenko AV. Consequences of exposure to light at night on the pancreatic islet circadian clock and function in rats. Diabetes 2013; 62: 3469–3478.
- Stamenkovic JA, Olsson AH, Nagorny CL et al. Regulation of core clock genes in human islets. Metabolism 2012; 61: 978–985.
- Pulimeno P, Mannic T, Sage D et al. Autonomous and self-sustained circadian oscillators displayed in human islet cells. Diabetologia 2013; 56: 497–507.
- Parnaud G, Bosco D, Berney T et al. Proliferation of sorted human and rat beta cells. Diabetologia 2008; 51: 91–100.
- Liu AC, Tran HG, Zhang EE, Priest AA, Welsh DK, Kay SA. Redundant function of REV-ERBalpha and beta and non-essential role for Bmal1 cycling in transcriptional regulation of intracellular circadian rhythms. PLoS Genet 2008; 4: e1000023.
- Saini C, Morf J, Stratmann M, Gos P, Schibler U. Simulated body temperature rhythms reveal the phase-shifting behavior and plasticity of mammalian circadian oscillators. Genes Dev 2012; 26: 567–580.
- Paget MB, Murray HE, Bailey CJ, Flatt PR, Downing R. Rotational co-culture of clonal beta-cells with endothelial cells: effect of PPAR-gamma agonism in vitro on insulin and VEGF secretion. Diabetes Obes Metab 2011; 13: 662–668.
- Perrin L, Loizides-Mangold U, Skarupelova S et al. Human skeletal myotubes display a cell-autonomous circadian clock implicated in basal myokine secretion. Mol Metab 2015; 4: 834–845.
- Hughes ME, Hogenesch JB, Kornacker K. JTK_CYCLE: an efficient nonparametric algorithm for detecting rhythmic components in genome-scale data sets. J Biol Rhythms 2010; 25: 372–380.
- Lappalainen T, Sammeth M, Friedlander MR et al. Transcriptome and genome sequencing uncovers functional variation in humans. Nature 2013; 501: 506–511.
- Mele M, Ferreira PG, Reverter F et al. Human genomics. The human transcriptome across tissues and individuals. Science 2015; 348: 660–665.
- 21. Cho H, Zhao X, Hatori M et al. Regulation of circadian behaviour and metabolism by REV-ERB-alpha and REV-ERB-beta. Nature 2012; **485**: 123–127.
- Takeda Y, Jothi R, Birault V, Jetten AM. RORgamma directly regulates the circadian expression of clock genes and downstream targets in vivo. Nucleic Acids Res 2012; 40: 8519–8535.
- Honma S, Kawamoto T, Takagi Y et al. Dec1 and Dec2 are regulators of the mammalian molecular clock. Nature 2002; 419: 841–844.
- Wuarin J, Schibler U. Expression of the liver-enriched transcriptional activator protein DBP follows a stringent circadian rhythm. Cell 1990; 63: 1257–1266.
- Lee J, Kim MS, Li R et al. Loss of Bmal1 leads to uncoupling and impaired glucose-stimulated insulin secretion in beta-cells. Islets 2011; 3: 381–388.
- Cerf ME. Transcription factors regulating beta-cell function. Eur J Endocrinol 2006; 155: 671–679.

original article

- Marcheva B, Ramsey KM, Bass J. Circadian genes and insulin exocytosis. Cell Logist 2011: 1: 32–36.
- Sato M, Murakami M, Node K, Matsumura R, Akashi M. The role of the endocrine system in feeding-induced tissue-specific circadian entrainment. Cell Rep 2014; 8: 393–401
- 29. Brown SA, Kunz D, Dumas A et al. Molecular insights into human daily behavior. Proc Natl Acad Sci U S A 2008; **105**: 1602–1607.
- Mannic T, Meyer P, Triponez F et al. Circadian clock characteristics are altered in human thyroid malignant nodules. J Clin Endocrinol Metab 2013; 98: 4446–4456
- Saini C, Brown SA, Dibner C. Human peripheral clocks: applications for studying circadian phenotypes in physiology and pathophysiology. Front Neurol 2015; 6: 95
- Akashi M, Soma H, Yamamoto T et al. Noninvasive method for assessing the human circadian clock using hair follicle cells. Proc Natl Acad Sci U S A 2010; 107: 15643–15648.
- Chua EC, Shui G, Lee IT et al. Extensive diversity in circadian regulation of plasma lipids and evidence for different circadian metabolic phenotypes in humans. Proc Natl Acad Sci U S A 2013; 110: 14468–14473.
- Gale JE, Cox HI, Qian J, Block GD, Colwell CS, Matveyenko AV. Disruption of circadian rhythms accelerates development of diabetes through pancreatic beta-cell loss and dysfunction. J Biol Rhythms 2011; 26: 423–433.
- Qian J, Yeh B, Rakshit K, Colwell CS, Matveyenko AV. Circadian disruption and diet-induced obesity synergize to promote development of beta cell failure and diabetes in male rats. Endocrinology 2015; 156: en20151516.
- Kalsbeek A, la Fleur S, Fliers E. Circadian control of glucose metabolism. Mol Metab 2014: 3: 372–383
- Perelis M, Marcheva B, Ramsey KM et al. Pancreatic beta cell enhancers regulate rhythmic transcription of genes controlling insulin secretion. Science 2015; 350: aac4250.
- Morris CJ, Yang JN, Garcia JI et al. Endogenous circadian system and circadian misalignment impact glucose tolerance via separate mechanisms in humans. Proc Natl Acad Sci U S A 2015; 112: E2225–E2234.

- Davidson HW, Wenzlau JM, O'Brien RM. Zinc transporter 8 (ZnT8) and beta cell function. Trends Endocrinol Metab 2014: 25: 415–424.
- Nicolson TJ, Bellomo EA, Wijesekara N et al. Insulin storage and glucose homeostasis in mice null for the granule zinc transporter ZnT8 and studies of the type 2 diabetes-associated variants. Diabetes 2009; 58: 2070–2083.
- 41. Kuliawat R, Kalinina E, Bock J et al. Syntaxin-6 SNARE involvement in secretory and endocytic pathways of cultured pancreatic beta-cells. Mol Biol Cell 2004; **15**: 1690–1701.
- Regazzi R, Wollheim CB, Lang J et al. VAMP-2 and cellubrevin are expressed in pancreatic beta-cells and are essential for Ca(2+)-but not for GTP gamma S-induced insulin secretion. EMBO J 1995; 14: 2723–2730.
- Tarasov A, Dusonchet J, Ashcroft F. Metabolic regulation of the pancreatic beta-cell ATP-sensitive K+ channel: a pas de deux. Diabetes 2004; 53(Suppl. 3): S113–S122.
- Gloyn AL, Siddiqui J, Ellard S. Mutations in the genes encoding the pancreatic beta-cell KATP channel subunits Kir6.2 (KCNJ11) and SUR1 (ABCC8) in diabetes mellitus and hyperinsulinism. Hum Mutat 2006; 27: 220–231.
- Girard CA, Wunderlich FT, Shimomura K et al. Expression of an activating mutation in the gene encoding the KATP channel subunit Kir6.2 in mouse pancreatic beta cells recapitulates neonatal diabetes. J Clin Invest 2009; 119: 80–90.
- Sassmann A, Gier B, Grone HJ, Drews G, Offermanns S, Wettschureck N. The Gq/G11-mediated signaling pathway is critical for autocrine potentiation of insulin secretion in mice. J Clin Invest 2010; 120: 2184–2193.
- Balsalobre A, Brown SA, Marcacci L et al. Resetting of circadian time in peripheral tissues by glucocorticoid signaling. Science 2000; 289: 2344–2347.
- Balsalobre A, Marcacci L, Schibler U. Multiple signaling pathways elicit circadian gene expression in cultured Rat-1 fibroblasts. Curr Biol 2000; 10: 1291–1294.
- Cnop M, Abdulkarim B, Bottu G et al. RNA sequencing identifies dysregulation of the human pancreatic islet transcriptome by the saturated fatty acid palmitate. Diabetes 2014; 63: 1978–1993.
- Arvan P, Pietropaolo M, Ostrov D, Rhodes CJ. Islet autoantigens: structure, function, localization, and regulation. Cold Spring Harb Perspect Med 2012; 2: a007658.



In pancreatic islets from type 2 diabetes patients, the dampened circadian oscillators lead to reduced insulin and glucagon exocytosis

Volodymyr Petrenko^{a,b,c,d}, Nikhil R. Gandasi^{e,f}, Daniel Sage^g, Anders Tengholm^e, Sebastian Barg^e, and Charna Dibner^{a,b,c,d,1}

^aDivision of Endocrinology, Diabetes, and Nutrition, Department of Medicine, University of Geneva, 1211 Geneva, Switzerland; ^bDepartment of Cell Physiology and Metabolism, Faculty of Medicine, University of Geneva, 1211 Geneva, Switzerland; ^cDiabetes Center, Faculty of Medicine, University of Geneva, 1211 Geneva, Switzerland; ^cDepartment of Geneva, 1211 Geneva, Switzerland; ^cDepartment of Medical Cell Biology, Uppsala University, 751 23 Uppsala, Sweden; ^cDepartment of Physiology, Institute of Neuroscience and Physiology, University of Göteborg, Sweden; and ^gBiomedical Imaging Group, Ecole Polytechnique Fédérale de Lausanne, 1015 Lausanne, Switzerland

Edited by Joseph S. Takahashi, The University of Texas Southwestern Medical Center, Dallas, TX, and approved December 21, 2019 (received for review September 25, 2019)

Circadian clocks operative in pancreatic islets participate in the regulation of insulin secretion in humans and, if compromised, in the development of type 2 diabetes (T2D) in rodents. Here we demonstrate that human islet α - and β -cells that bear attenuated clocks exhibit strongly disrupted insulin and glucagon granule docking and exocytosis. To examine whether compromised clocks play a role in the pathogenesis of T2D in humans, we quantified parameters of molecular clocks operative in human T2D islets at population, single islet, and single islet cell levels. Strikingly, our experiments reveal that islets from T2D patients contain clocks with diminished circadian amplitudes and reduced in vitro synchronization capacity compared to their nondiabetic counterparts. Moreover, our data suggest that islet clocks orchestrate temporal profiles of insulin and glucagon secretion in a physiological context. This regulation was disrupted in T2D subjects, implying a role for the islet cell-autonomous clocks in T2D progression. Finally, Nobiletin, an agonist of the core-clock proteins $ROR\alpha/\gamma$, boosted both circadian amplitude of T2D islet clocks and insulin secretion by these islets. Our study emphasizes a link between the circadian clockwork and T2D and proposes that clock modulators hold promise as putative therapeutic agents for this frequent disorder.

circadian clock | exocytosis | human pancreatic islet | type 2 diabetes | real-time bioluminescence

he circadian clocks allow most of the organisms to anticipate periodical changes of geophysical time. In mammals, this time-keeping system governs most aspects of physiology and behavior. It comprises a master pacemaker, located in the paired suprachiasmatic nuclei (SCN) of the hypothalamus, that on a daily basis synchronizes peripheral oscillators situated in the organs (1). The circadian system orchestrates body metabolism via diverse neural and humoral pathways, thus ensuring the finetuning of the metabolic processes to the rest-activity and feeding-fasting cycles. In turn, the metabolites are feeding back on the circadian oscillators at the cellular and whole-body levels (2– 6). Mouse strains lacking a functional clock due to the disruption of essential core-clock genes in the whole body, or in a tissuespecific manner, develop hyperglycemia, hypoinsulinemia, and glucose intolerance (7-10). Emerging works in humans suggest that a considerable portion of the transcripts in metabolic organs exhibit rhythmic expression (7, 11, 12). Human metabolomics and lipidomics studies have demonstrated diurnal profiles for a wide panel of metabolites in different peripheral tissues and in the blood (13–15). Moreover, epidemiological studies in humans strongly suggest that circadian misalignment may lead to the development of metabolic diseases, such as obesity and type 2 diabetes (T2D) (16, 17).

Several articles have provided a detailed characterization of molecular clocks operative in rodent pancreatic islets, highlighting primordial importance of functional islet clocks for insulin secretion and maintenance of glucose homeostasis (7, 8, 18). Such clock-mediated regulation of insulin secretion has been suggested to be exerted on insulin granule exocytosis, rather than on hormone synthesis, although direct evidence is still missing (7, 19, 20). Genetic mouse models with the pancreas-specific clock perturbation exhibit a phenotype of strongly disrupted insulin secretion, severe glucose intolerance, and all of the features of T2D from an early age, strongly suggesting implication of the islet clocks in T2D development (7, 8). Furthermore, the roles of the α-cellular clocks in regulating glucagon secretion in rodents have been highlighted, underscoring the importance of the interactions between the oscillators operative in α - and β -cells for islet function (20, 21). In line with these findings in rodents, studies in human islets unraveled the molecular makeup of the cell-autonomous local oscillators, and their primordial role in

Significance

Here we report that intact islets and islet cells from type 2 diabetes (T2D) donors exhibit attenuated molecular oscillators bearing lower circadian amplitude and compromised synchronization capacity in vitro. Furthermore, we reveal that secretion profiles of insulin, proinsulin, and glucagon were circadian rhythmic under physiological conditions. The temporal coordination of the islet hormone secretion was perturbed in human T2D islets, concomitant with the islet molecular clock alterations. Strikingly, clock-deficient human islet cells exhibited disrupted insulin and glucagon granule docking and exocytosis. Treating the T2D islets with the clock modulator Nobiletin boosted circadian amplitude and insulin secretion. Our study uncovers a link between human molecular clockwork and T2D, thus considering clock modulators as putative pharmacological intervention to combat this disorder.

Author contributions: V.P. and C.D. designed research; V.P. and N.R.G. performed research; A.T. contributed new reagents/analytic tools; V.P., N.R.G., D.S., S.B., and C.D. analyzed data; and V.P., S.B., and C.D. wrote the paper.

The authors declare no competing interest.

This article is a PNAS Direct Submission.

This open access article is distributed under Creative Commons Attribution-NonCommercial-NoDerivatives License 4.0 (CC BY-NC-ND).

Data deposition: Raw data supporting the Fig. 5 and SI Appendix, Fig. S3 are deposited at http://dx.doi.org/10.17632/bwnrghvcpt.1.

¹To whom correspondence may be addressed. Email: charna.dibner@hcuge.ch.

This article contains supporting information online at https://www.pnas.org/lookup/suppl/doi:10.1073/pnas.1916539117/-/DCSupplemental.

First published January 21, 2020.

functional regulation of the endocrine pancreas, notably in regulating insulin secretion (7, 12, 22). Experiments with human islets cultured in vitro revealed that upon clock disruption by RNA interference-mediated *CLOCK* knockdown human islet cells secreted less insulin. Furthermore, clock perturbation disrupted the rhythmicity of basal insulin secretion observed in islets of healthy human subjects (22). These data suggest a functional link between the pancreatic islet clock and insulin secretion and highlight the importance of islet oscillators in the development of T2D in rodents and possibly in humans.

In this study, we uncover the temporal coordination of insulin, proinsulin, and glucagon secretion profiles by the circadian oscillators operative in human islet cells. Such temporal coordination is likely exerted via an exocytosis process, since our experiments reveal that functional islet clocks are indispensable for proper secretory granule docking and exocytosis of insulin and glucagon. Strikingly, our study reveals that the circadian clockwork is compromised in human α - and β -cells in T2D, evidenced by the altered temporal profiles of insulin, proinsulin, and glucagon secreted by T2D human islets. Finally, the clock modulator Nobiletin shows a significant capacity to boost both the amplitude of circadian gene expression in human T2D islets and their insulin secretion, holding promise in terms of therapeutic implications.

Results

Circadian Oscillators Operative in Human Pancreatic Islet Cells Isolated from T2D Donors Exhibit a Dampened Amplitude and **Altered Synchronization Properties.** We have previously identified molecular makeup of cell-autonomous circadian clocks operative in human islets at population, individual islet, and islet cell levels (12). In order to assess whether alterations may occur in the islet circadian clockwork concomitant with the development of T2D in humans, we first measured the expression levels of core-clock genes in nonsynchronized human islet cells derived from T2D donors, and compared those to nondiabetic (ND) counterparts (*SI Appendix*, Table S1). Expression levels of *PERIOD 1* to 3 (*PERI-3*), *CRY2*, *REV-ERBα*, *CLOCK*, and *DBP* were significantly diminished in T2D compared to ND islet cells (*SI Appendix*, Fig. S1A). *NFIL3* levels were slightly up-regulated, and *BMAL1* and *CRY1* did not change (*SI Appendix*, Fig. S1A).

Since expression levels of the key core-clock genes were strongly altered in T2D islets, we next assessed human islet clockwork by introducing two antiphasic circadian reporters, *Bmal1*-Luciferase (*Bmal1-luc*) or *Per2*-Luciferase (*Per2-luc*), allowing for continuous bioluminescence monitoring in human primary cells (23). In an agreement with previous clock characterization in human islets, primary skeletal myotubes, and skin fibroblasts (22, 24, 25), synchronization in vitro by forskolin pulse induced high-amplitude oscillations of both *Bmal1-luc* and *Per2-luc* reporters that were antiphasic in ND islets (compare ND lines in Fig. 1 *A* and *B*, *Left*). While both reporters were rhythmically oscillating in T2D islets following forskolin synchronization, the amplitude of these oscillations was significantly attenuated (Fig. 1 *A* and *B*). Absolute levels of *Bmal1-luc* expression were

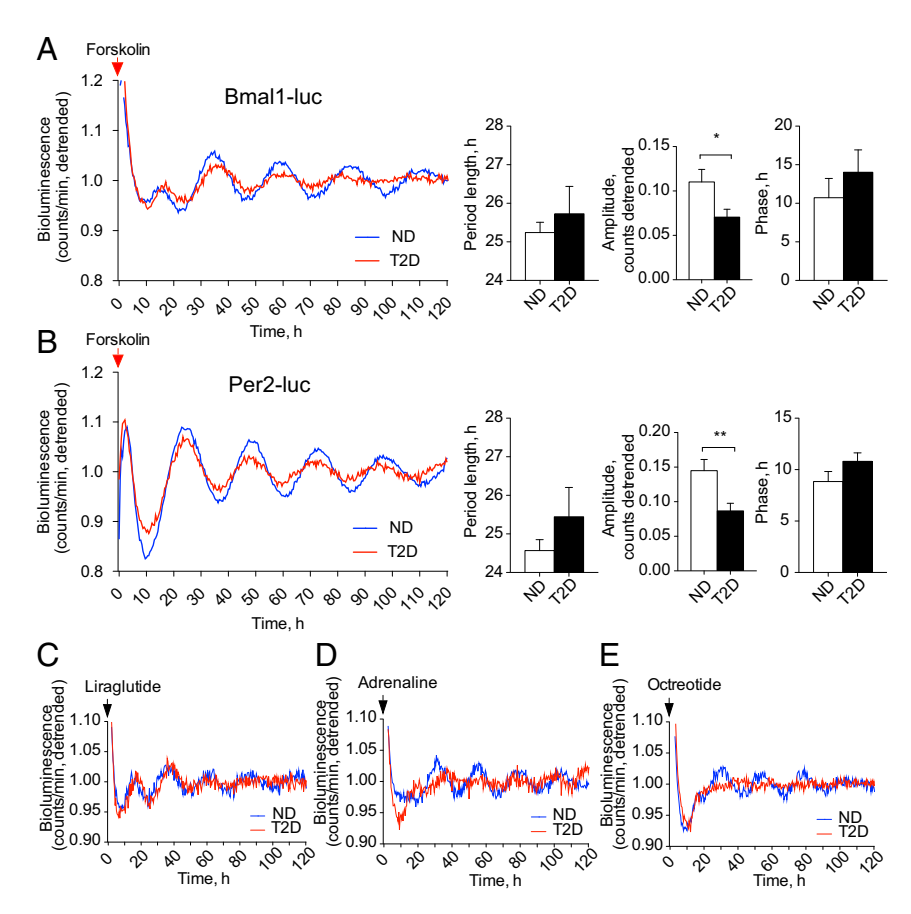


Fig. 1. Pancreatic islets derived from T2D human donors bear disrupted circadian clocks. (A and B) Average detrended oscillatory profiles of forskolin-synchronized human islet cells transduced with Bmal1-luc (A, n = 19 ND; n = 15 T2D donors) or with Per2-luc lentivectors (B, n = 15 ND; n = 12 T2D donors). Comparisons of average period length and amplitude are shown in adjacent histograms. *P < 0.05, **P < 0.01. (C-E) Average detrended Bmal1-luc bio-luminescence profiles for pancreatic islets derived from ND and T2D donors synchronized in vitro with 1-h pulse of GLP-1 receptor agonist Liraglutide (C), adrenaline (D), or synthetic somatostatin analog Octreotide (E). See also SI Appendix, Fig. S1 and Table S2.

comparable and even slightly elevated in T2D islets (SI Appendix, Fig. S1C), whereas those of Per2-luc were strongly decreased in T2D islets compared to ND controls (SI Appendix, Fig. S1D). While no significant alterations in circadian period length and phase of Per2-luc oscillations have been observed overall between ND and T2D groups (Fig. 1 B, Right), nonsignificant tendencies of weak to moderate negative correlations between the circadian oscillation parameters and the blood levels of HbA1c measured in the same subjects have been observed within the T2D group (SI Appendix, Fig. S1 F-H).

Furthermore, we characterized *Bmal1-luc* reporter oscillatory profiles of ND control islets following synchronization by the pulses of Liraglutide, an analog of GLP-1, adrenaline, and Octreotide, an analog of somatostatin. Continuous recording of Bmal1-luc bioluminescence following Liraglutide, adrenaline, or Octreotide synchronization in ND islets (Fig. 1 C-E and SI Appendix, Table S2) revealed significant circadian oscillations as compared to the medium change alone (SI Appendix, Fig. S1E). Circadian amplitude of the oscillations induced by all three synchronizers was inferior to the one resulting from forskolin pulse (Fig. 1A). Period length was shorter for adrenaline-induced oscillations as compared to the other synchronizers, and phase was slightly advanced for adrenaline- and Octreotide-induced oscillations (compare Fig. 1 A and D-E; see also SI Appendix, Table S2). Importantly, when applied to T2D human islets, Octreotide failed to synchronize their clocks (Fig. 1E), whereas adrenaline pulse resulted in Bmal1-luc oscillations with a delayed circadian phase and tendency for dampened amplitude compared to ND controls (Fig. 1D and SI Appendix, Table S2). Reduced expression of SSTR2 and ADRA2A receptor transcripts measured in T2D islets (SI Appendix, Fig. S1B) corroborated compromised synchronizing efficiency of adrenaline and somatostatin in T2D islets. Circadian oscillations resulting from Liraglutide pulse were comparable between ND and T2D islets (Fig. 1C and SI Appendix, Table S2), with significantly faster drop in amplitude by T2D islets as measured by the slope of peaks fading $(-0.015 \pm 0.0023 \text{ versus } -0.007 \pm 0.0018,$ P = 0.024).

Attenuated Individual Cell Oscillations and Perturbed Synchronization Capacity between the Endocrine Cellular Clocks Lead to the Impaired **Islet Clockwork upon T2D.** The perturbation of the islet oscillatory capacity observed in human T2D islets at the islet population level may stem from compromised islet cellular clockwork, or from disrupted synchronization capacity among the individual islets and individual islet cells upon T2D. To distinguish between these scenarios, we visualized *Per2-luc* oscillations of individual islets from T2D and ND donors synchronized by forskolin pulse employing bioluminescence time-lapse microscopy (Fig. 2 A and B and Movies S1 and S2). In line with our recordings at the islet population level (Fig. 1B), average profiles of Per2-luc oscillations in single T2D islets exhibited significantly lower circadian amplitude (Fig. 2 C, Center). Importantly, whereas oscillatory profiles of the individual ND islet clocks were in synchrony among the islets, the phase distribution of T2D islets was wider, indicating disrupted synchronization capacity among the T2D islets (Fig. 2 C, Right, and Movies S1 and S2). Overall, our singleislet recording experiments strongly suggest that T2D islets bear oscillators with lower circadian amplitude, and that synchronization among the individual T2D islet clocks by the most potent synchronizing agent forskolin is less efficient compared to ND counterparts.

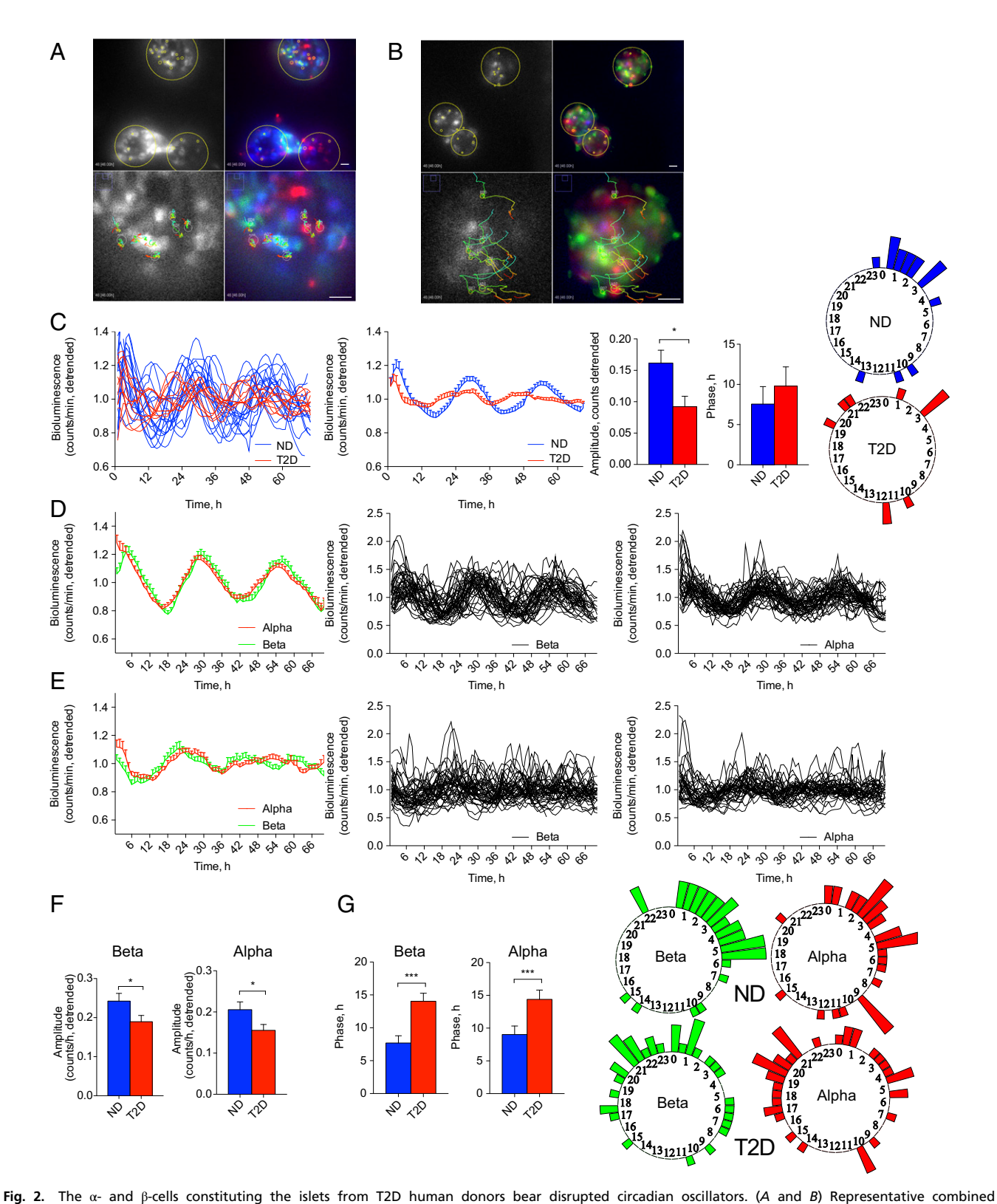
In order to dissect the synchronization and individual oscillator properties in human α - and β -cells, Pppg-mCherry (26) and RIP-GFP (12) viruses were introduced, allowing for efficient and specific cell labeling. Combined bioluminescence-fluorescence time-lapse microscopy of human islet cells transduced with PppgmCherry, RIP-GFP, and Per2-luc viruses has been conducted (Fig. 2 A and B and Movies S1 and S2). Per2-luc profiles in the individual α- and β-cells from ND and T2D donors were traced using modification of a CGE algorithm (12, 27), and analyzed by JTK Cycle (significance threshold of adjusted P value for JTK Cycle analyses was set at 0.1). Most of the traced endocrine cells from ND (86 of 87 islet cells) and T2D donors (76 of 79 islet cells) were rhythmic. Importantly, circadian amplitude was strongly reduced in both α - and β -cellular clocks in the T2D group (Fig. 2 D-F), suggesting clockwork perturbation at the single-cell level. Moreover, both T2D α - and β -cells exhibited significant phase delay and wider phase distribution (Fig. 2G), indicative of less efficient synchronization capacity among the endocrine cells within T2D islets. Thus, both diminished circadian amplitude of individual islet cell clocks and wider phase distribution among the cells contribute to the compromised islet clockwork in T2D donors.

Human α - and β -Cells Synchronized In Vitro Secrete Glucagon, Insulin, and Proinsulin in a Circadian Rhythmic Manner. We recently revealed that human pancreatic islet cells synchronized in vitro exhibited a rhythmic profile of insulin secretion that was compromised in the absence of functional islet clocks (22). We now measured basal insulin secretion by isolated human β-cells. To this end, RIP-GFP-labeled human β-cells were separated by FACS, synchronized in vitro with forskolin pulse, and perifused during 48 h with a culture medium containing 5.5 mM of glucose (Fig. 3 A and B). Basal concentration of insulin secreted by human β -cells exhibited tendency for oscillations that did not reach statistical significance to qualify as circadian according to JTK_Cycle when applied to the time window 0 to 48 h (Fig. 3B). However, the oscillation pattern did qualify as circadian rhythmic in the time window between 4 and 48 h, evaluated to avoid a potential bias from immediate early response. Non- β (GFP⁻)-cells from the same preparations secreted trace amounts of insulin, further validating the quality of β -cell population separation (Fig. 3A).

Next, we measured a temporal profile of glucagon secretion by a mixed human islet cell population (Fig. 3 C and D). Of note, glucagon was secreted in a significantly circadian rhythmic manner by human α -cells (Fig. 3 C and D). The insulin secretion profile by the same mixed islet cell population measured in parallel was rhythmic as well, with the phase of glucagon secretion peak being 2 h behind the peak of insulin secretion (Fig. 3 *C* and *D*).

In addition to mature insulin, β -cells secrete its nonprocessed precursor proinsulin. Our parallel measurements of proinsulin and insulin profiles by the same mixed islet cells revealed that also proinsulin secretion was circadian rhythmic (Fig. 3 E and F). The phase of proinsulin secretion profile was delayed about 2 h as compared to insulin in the same samples. Thus, our data provide evidence for circadian patterns of insulin, proinsulin, and glucagon secretion by human islet cells in physiological situation.

Circadian Profiles of Insulin, Proinsulin, and Glucagon Secretion Are Altered in T2D Islets. Next, temporal secretion profiles of insulin, glucagon, and proinsulin by T2D islet cells were assessed utilizing a perifusion system (Fig. 4 and SI Appendix, Fig. S2). Whereas a temporal pattern of insulin secretion by T2D islet cells still qualified as circadian by JTK Cycle, the magnitude and overall amount of insulin secretion over 48 h were significantly diminished compared to ND controls. This difference was most prominent during the peak of insulin secretion (8 to 12 h and 32 to 36 h) (Fig. 4 A and B and SI Appendix, Fig. S2D). In line with compromised insulin secretion profiles, reduced expression of β-cell-specific genes INS, MAFA, and SLC30A8, and exocytosisrelated genes STX1, SNAP25, and VAMP2 was observed in nonsynchronized T2D islet cells (SI Appendix, Fig. S1B). While we did not detect a significant difference either in absolute values of glucagon secretion by T2D islet cells or in total glucagon



In the second control of the second control



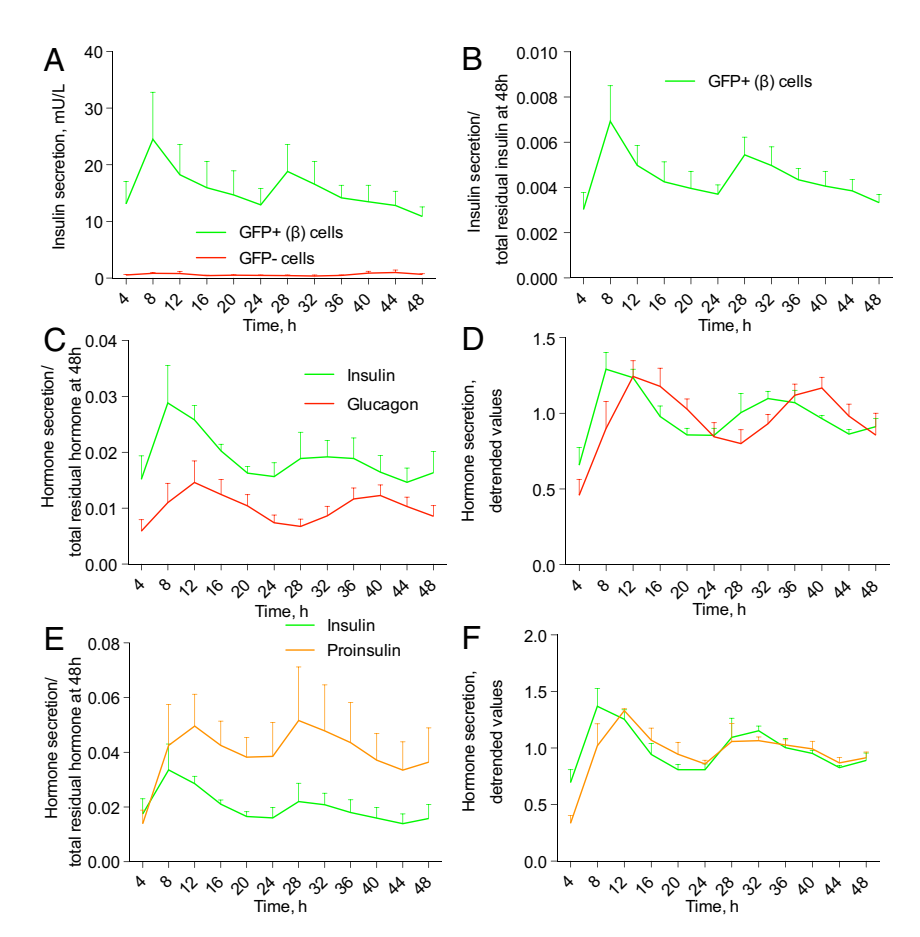


Fig. 3. Glucagon, insulin, and proinsulin are rhythmically secreted by human islet cells synchronized in vitro. (A) Temporal insulin secretion profile by FACSseparated human β-cells (~25,000 cells per dish) assessed by perifusion. (B) Insulin secretion values presented in A were normalized to the total hormone content in the cell lysate at the end of the experiment (at 48 h). When JTK_Cycle was applied to the time window 4 to 44 h, to exclude a possible bias due to immediate-early response to synchronization, the resulting profile of insulin secretion qualified as circadian rhythmic (P = 0.084), with the average period length 24.04 \pm 0.98 h, and phase 10.4 \pm 4.62 h. (C) Insulin and glucagon secretion by \sim 50,000 mixed ND islet cells from n=6 donors subjected to perifusion and normalized to residual respective hormone content at 48 h (C). Note the delayed phase of glucagon secretion as compared to insulin (P = 0.0019, paired Student's t test). (E) Insulin and proinsulin secretion by ND islet cells from n = 4 donors. Note the delayed phase of proinsulin secretion as compared to insulin (P = 0.02, paired Student's t test). (D and F) Detrended values from C and E. JTK_Cycle qualified as circadian rhythmic the average profile of insulin (D, P = 0.057; period length 22.96 \pm 0.75 h); of glucagon (D, P = 0.009, period length 24.3 \pm 0.22 h); and of proinsulin (F, P = 0.097, period length 21.5 \pm 0.96 h).

content in T2D islet cells, the temporal profile of glucagon secretion was altered (Fig. 4 C and \hat{D} and $\hat{S}I$ Appendix, Fig. S2 C and E). Indeed, the circadian rhythmicity of glucagon secretion by T2D islet cells was lost (Fig. 4D). Finally, the proinsulin secretion profile by T2D islet cells was not qualified as circadian rhythmic according to the JTK Cycle (Fig. 4 E and F and SI Appendix, Fig. S2F).

Functional Clock Is Required for Insulin and Glucagon Granule Docking and Exocytosis in Pancreatic α - and β -Cells. Down-regulation of the CLOCK gene has been recently shown to affect expression of genes coding for components of the insulin granule exocytosis machinery (22). We therefore quantified granule docking and exocytosis by total internal reflection fluorescence (TIRF) microscopy in ND human β-cells, in which CLOCK was knocked down using small-interfering RNA (siRNA). The granules were labeled by transducing the cells with the adenoviral granule marker NPY-mCherry (28), and α - or β -cells were identified by using cell specific promoters driving the expression of fluorescent proteins (Materials and Methods). B-Cells showed a pronounced decrease in the density of plasma membrane-docked granules under *CLOCK* knockdown (by 34%, P < 0.0005) (Fig. 5 A and B). The trend was similar in α -cells that also showed a slight decrease in the density of plasma membrane-docked granules in CLOCK knockdown condition (P < 0.05) (Fig. 5 F and G).

We then stimulated exocytosis by elevating extracellular K⁺ to 75 mM for 40 s. Single exocytosis events were observed as a sudden disappearance of granule fluorescence (example in Fig. 5 C and E) (29, 30). As reported previously (28), in control β -cells the rate of exocytosis was initially high but slowed toward the end of the stimulation (Fig. 5D). On average, 0.13 (± 0.016) exocytosis events were recorded during the stimulation in control cells (Fig. 5E). In siCLOCK-transfected cells, both the rapid and the slow phases were still present, but exocytosis was strongly reduced (85% to $0.02 \pm 0.004 \text{ g/µm}^2$, P < 0.0005). In α -cells, we observed a similarly strong reduction in K⁺-stimulated exocytosis after knockdown of *CLOCK* (82% to 0.014 \pm 0.003 g/ μ m², P <0.0005) (Fig. 5 H and I).

Exocytosis and granule docking were also quantified in islets from mice in which Bmal1 was deleted (Bmal1KO). In β-cells, docked granules were reduced by 34% (SI Appendix, Fig. S3 A and B), and K⁺-stimulated exocytosis was reduced by 46% (SI Appendix, Fig. S3C). In α -cells of Bmal1KO mice we observed a similar tendency with reduction of both docked granules (by 20%) (SI Appendix, Fig. S3 D and E) and K⁺-stimulated exocytosis (by 82%) (SI Appendix, Fig. S3F). Collectively, these results further indicate that CLOCK and BMAL1, the two members

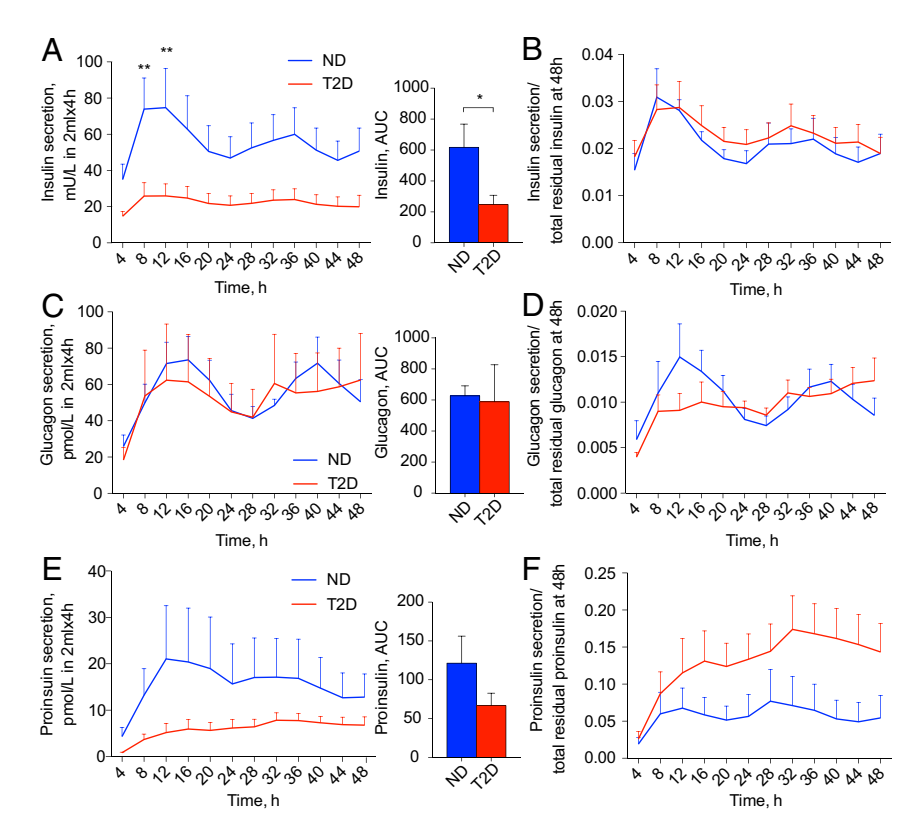


Fig. 4. Circadian rhythmic profiles of insulin, proinsulin, and glucagon secretion are disrupted in T2D. Secretion profiles of insulin (A and B, n = 6 ND; n = 10 T2D donors), glucagon (C and D, n = 6 ND; T2D donors), and proinsulin (E and E, n = 4 ND; n = 5 T2D donors) were measured in the outflow perifusion medium from $\sim 50,000$ synchronized mixed human islet cells. (B, D, and E) Respective raw data from E, E, and E were normalized to the total hormone content in the cell lysate at the end of each experiment. JTK_Cycle analysis qualified insulin secretion profile in ND islets as circadian rhythmic (P = 0.097), with the amplitude of E0.0015 relative units, period length E1.096 h, and phase E2.1096 h. Whereas the insulin secretion profile was still qualified as circadian rhythmic in T2D donors (E2.0012 relative units; period length of E3.67 E3.063 h and phase E3.66 E4.08 h. Glucagon secretion profile qualified as circadian rhythmic in ND donors (E3.0012 relative units; period length of E3.67 E3.0014, period length E4.3 E5.022 h, and phase E6.81 h, whereas it was nonrhythmic in T2D donors (E3.1097) with amplitude of E4.123 h, whereas it was nonrhythmic in T2D donors (E5.15 h, while in T2D donors it was considered noncircadian (E4.1097) with amplitude of E5.1097 with amplitude of E7.1098 period length E7.1098 h, and phase E7.1099 h, while in T2D donors it was considered noncircadian (E5.1099). See also E7.1099 Appendix, Fig. S2. E7.1099 Profiles and E9.1099 Profiles and E9

of the positive limb of the molecular oscillator, are required for proper functioning of the insulin and glucagon granule exocytosis machinery.

High Glucose Levels Alter Molecular Clocks in the Islets from ND, but Not from T2D Donors. To assess the effect of high glucose on the islet clockwork, we recorded *Bmal1-luc* or *Per2-luc* oscillations from ND islets in the presence of 20 mM glucose. Adding high glucose to recording medium resulted in 1 h longer circadian period length for both reporter profiles compared to the physiological concentration of 5.5 mM (Fig. 6A and *SI Appendix*, Fig. S4A). In contrast, the oscillatory profiles of T2D islets in the presence of 5.5 mM (low) and 20 mM (high) glucose in the recording medium were comparable, suggesting that high glucose levels do not induce significant changes in the clockwork (Fig. 6B and *SI Appendix*, Fig. S4B).

When perifused with high glucose, ND islet cells secreted significantly higher insulin levels comparatively to their counterparts perifused with low glucose. This difference was particularly striking during the insulin secretion peaks between 8 to 12 h and 28 to 32 h (Fig. 6C). Interestingly, insulin secretion reached its maximum 2 to 4 h prior to the peak of *Per2-luc* expression recorded in parallel from the same cells (*SI Appendix*, Fig. S4C). In contrast, T2D islet cells perifused with high glucose secreted only slightly more insulin than their counterparts perifused with low glucose (Fig. 6C and *SI Appendix*, Fig. S4D). In an agreement with the outcome of perifusion experiments, static

insulin secretion by nonsynchronized T2D islet cells was slightly elevated in the presence of low glucose, whereas it was decreased at high glucose. This led to a 2.5-fold lower stimulation index for T2D islets (Fig. 6D and SI Appendix, Fig. S4F). Impaired glucose sensitivity of the T2D islet cells might be partly attributed to altered expression levels of insulin-independent glucose transporters GLUT1 and GLUT2 in T2D islet cells (SI Appendix, Fig. S1B) observed in our samples, consistently with the previous reports (31). No significant difference in the islet cell apoptosis has been observed following incubation with high glucose (SI Appendix, Fig. S4E). Collectively, these data indicate that high glucose interferes with the pancreatic islet cell clockwork in ND by lengthening the period, but has little effects on either oscillation of clock gene expression or on temporal insulin secretion in T2D islets.

In Human T2D Islets the Receptor-Related Orphan Receptor Agonist Nobiletin Boosts the Amplitude of Circadian Gene Expression and Increases Basal and Stimulated Insulin Secretion. To examine whether boosting the T2D islet clockwork may have a beneficial effect on insulin secretion, we attempted to restore the dampened circadian amplitude in T2D islets pharmacologically. To this end, we employed Nobiletin, a drug that has been shown to enhance circadian amplitude in clock-deficient mouse fibroblasts via receptor-related orphan receptor (ROR) nuclear receptors (32). Assessment of the expression levels of $ROR\alpha$ transcripts revealed no change between ND and T2D islets (SI Appendix,



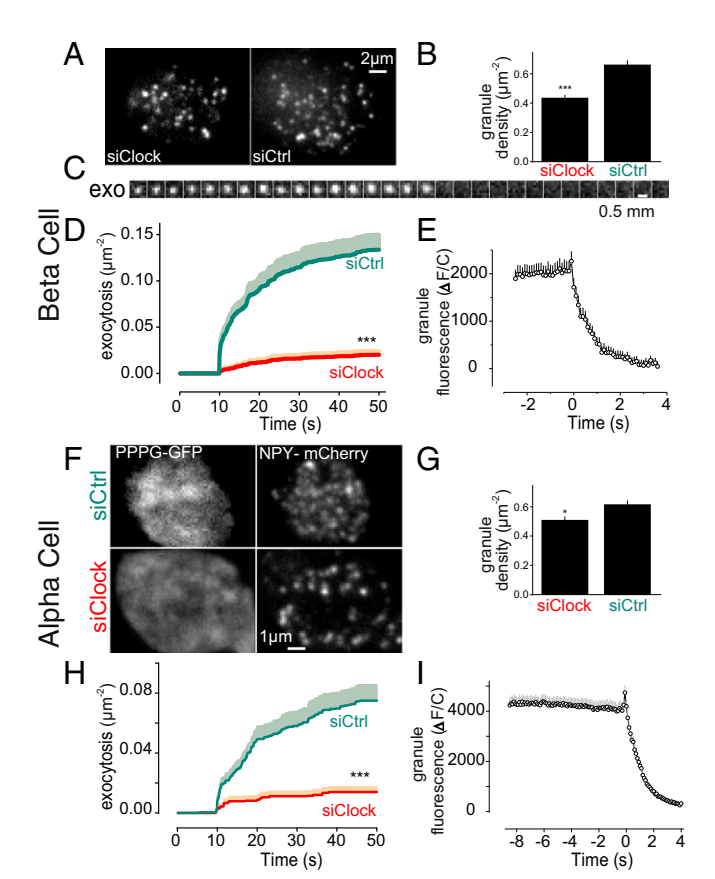


Fig. 5. Molecular clock affects granule docking and exocytosis in human α and β -cells. (A) β -Cells from nondiabetic donors transfected with siRNA targeting CLOCK gene (siClock), or scrambled control siRNA (siCtrl). (B) Density of docked granules in cells as in A. (C) Image sequence (0.1 s per frame) showing an individual insulin granule undergoing K⁺-stimulated exocytosis (exo). (D) Time course of exocytosis constructed from events as in C, in response to elevation of K⁺ to 75 mM for 40 s, 10 s after the experiment was initiated. (E) Average granule fluorescence from all of the exocytosis events seen in siCtrl in D. Note the disappearance of fluorescence signal at time 0. (F) α-Cells of ND donors identified by expression of Pppg-GFP (Left) and coexpressing the granule marker NPY-mCherry (Right) and either transfected with scrambled control (siCtrl, Upper), or siRNA targeting CLOCK (siClock, Lower). (G) Density of docked granules. (H) Time course of exocytosis in α -cells as in F. (I) Average granule fluorescence from all of the exocytosis events seen in siCtrl in (H). Note the disappearance of fluorescence signal at time 0. *P < 0.05, ***P < 0.001. See also SI Appendix, Fig. S3.

Fig. S14). When applied to synchronized T2D human islets, Nobiletin doubled the magnitude and significantly enhanced the amplitude of Bmal1-luc oscillations at least during the first two cycles (Fig. 7 A and B). Similar trend for magnitude was observed for the islets from both ND and T2D donors transduced with Per2-luc reporter; however, the effect on circadian amplitude did not reach statistical significance in this case (SI Appendix, Fig. S5 A and B). Noteworthy, Nobiletin acutely boosted Bmal1-luc expression when applied to forskolin-synchronized T2D islets (SI Appendix, Fig. S5C). Long-term application of Nobiletin to ND and T2D islets did not result in any detectable increase in the islet cell apoptosis (SI Appendix, Fig. S5D).

Next, we investigated the effect of Nobiletin on insulin secretion by human islets. Adding Nobiletin to the medium containing 5.5 mM glucose led to 3.5-fold increase in insulin secretion by ND islets (Fig. 7C). In concordance with static insulin release, a glucose-stimulated insulin secretion (GSIS) test showed significant rise in insulin secretion in basal (fivefold) and glucose-stimulated (twofold) conditions (Fig. 7D). Increased insulin secretion did not stem from the effect on insulin production de novo since the total amount of produced insulin during both tests in the presence of Nobiletin was comparable to the control condition (SI Appendix, Fig. S5 E and F). Subsequently, we tested the capacity of Nobiletin to boost insulin secretion in siCLOCK expressing islet cells that exhibited reduced basal and stimulated insulin secretion (22). GSIS tests conducted in siCLOCK-transfected ND islet cells in the presence of Nobiletin resulted in a marked enhancement of basal and stimulated insulin secretion (Fig. 7E). Remarkably, Nobiletin ameliorated the compromised capacity by T2D islets to release insulin at basal glucose conditions and in the GSIS test (Fig. 7 F and G and SI Appendix, Fig. S5 E and F). Overall, Nobiletin partly restored compromised basal and GSIS by human T2D islets and ND islets bearing disrupted clocks and further enhanced insulin secretion by human ND islets. Noteworthy, Nobiletin also induced glucagon secretion in ND and T2D islets during glucagon release test in the presence of 5.5 mM glucose (SI Appendix, Fig. S5G). Furthermore, we utilized SR9011, a synthetic agonist of REV-ERB receptors (33). Contrary to Nobiletin, SR9011 diminished the magnitude of Per2-luc reporter expression by ND islets, without notable dampening of the circadian amplitude (SI Appendix, Fig. S5H). Of note, application of SR9011 to T2D islet cells throughout all of the stages of GSIS assay significantly reduced the insulin secretion capacity of these cells (Fig. 7H).

Discussion

Rodent studies reported a critical role of the islet circadian clocks in maintaining glucose homeostasis, concomitant with the link between disruption of the islet oscillators and the development of T2D (1, 5, 34). Here we provide a convincing evidence that pancreatic islets isolated from human T2D donors exhibit strongly diminished amplitude of circadian oscillations, as compared to ND counterparts. Furthermore, synchronization capacity of T2D islets by physiologically relevant compounds was reduced. Along with the observed disruption of circadian oscillators, temporal profiles of insulin, proinsulin, and glucagon secretion, that are rhythmic in the case of ND islets, were perturbed in T2D islets. Pancreatic islet oscillators are likely regulating the hormone secretion via the exocytosis process. Indeed, in the model of the islet clock disruption, insulin and glucagon granule docking and exocytosis were strongly decreased, similar to the phenotype observed in T2D islets. Strikingly, the clock modulator Nobiletin enhanced the amplitude of Bmal1-luc circadian oscillations in T2D islets, and partly restored insulin secretory capacity of these islets.

Cell-Autonomous Clocks in Pancreatic Islets Isolated from T2D Donors Exhibit Diminished Circadian Amplitude and Reduced Synchronization Capacity. Pancreatic islets receive numerous systemic and paracrine physiological signals that couple the function of the endocrine pancreas to the metabolic needs on a daily basis, possibly via modulating circadian rhythmicity of α - and β -cells. Indeed, physiologically relevant stimuli such as adrenaline, insulin, glucagon, somatostatin, and GLP-1 analogs (Liraglutide and Exenatide) differentially reset mouse α - and β -cell molecular clocks (20, 21). Forskolin, dexamethasone, and temperature cycles have been shown to efficiently synchronize human pancreatic islet clocks in vitro (7, 12). Here we demonstrate that adrenaline, Octreotide, and Liraglutide are potent synchronizers of circadian clocks in ND human islets. Our data also indicate that chronic application of high glucose levels on ND islets lengthens the circadian period of human islet clocks. The effect of glucose on the islet clocks might be mediated via down-regulation of Per1 and Per2 transcripts, as was reported for cultured fibroblasts (35). In mice, islet cellular clocks in FACS-separated α - and β-cell populations exhibit distinct circadian properties and

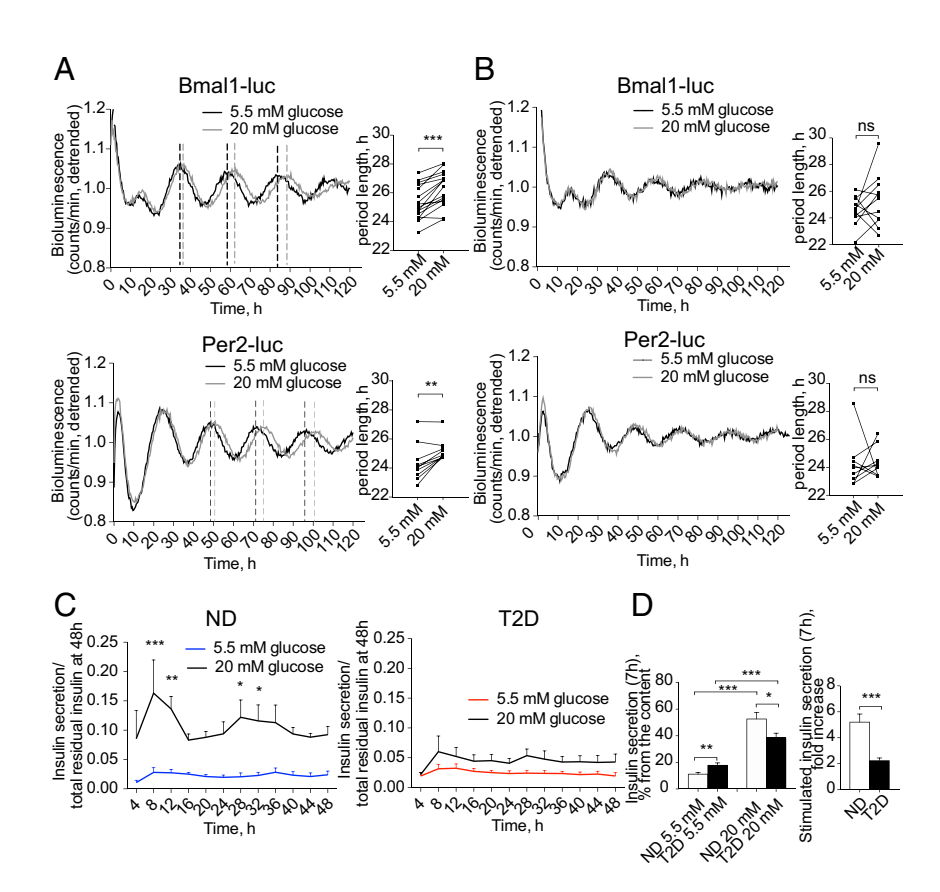


Fig. 6. High glucose levels impact on the molecular clocks in the islets from ND, but not from T2D donors. Average detrended oscillatory profiles of forskolin-synchronized human islet cells from ND (A) and T2D donors (B) transduced with Bmal1-luc (Upper, n=15 for ND and n=10 for T2D) or Per2-luc lentivectors (Lower, n=9 for ND and n=8 for T2D). Adjacent histograms show changes in the period length of islet oscillations recorded in the presence of 20 mM glucose in the medium (difference is tested by paired Student's t test). (C) Insulin secretion by mixed islet cells synchronized with forskolin and perifused in parallel with the medium containing either 5.5 mM or 20 mM glucose across 48 h (n=3 of ND and n=5 T2D donors). Two-way ANOVA test with Bonferroni posttest was used to assess the difference between experimental conditions. (D) Static release (Left) of insulin by dispersed islet cells from ND or T2D donors was measured after 7-h incubation in the presence of 5.5 or 20 mM glucose, and expressed as percent of total residual insulin content in the end of the experiment (mean \pm SEM) for n=10 ND and n=10 T2D preparations. Respective stimulation index is expressed (Right). *P < 0.05, **P < 0.01, and ***P < 0.001. ns, not significant. See also SI Appendix, Fig. S4.

differential responses to physiologically relevant synchronizers (20, 21). Utilizing time-lapse microscopy, we now report that within intact human islets, α - and β -cells possess oscillators with comparable circadian properties, implying the role of the islet cytoarchitecture and paracrine interactions among different endocrine cells for the circadian coupling, similar to those observed in SCN neurons. Although the exact mechanism of coupling among cellular clocks in SCN is not entirely understood, it involves Na+-dependent action potentials relying on the activity of voltage-dependent calcium channels in response to chemical stimuli and transmission of the electrical signaling via gap-junctions (36). Similarly, the coordinated secretory response by the islet to glucose stimulation requires intraislet cell coupling via gap-junctions (37). Furthermore, paracrine glucagon and GLP-1 signaling emanating from α-cells is indispensable for efficient regulation of glucose homeostasis by neighboring β-cells (38). Given that glucose, insulin, adrenaline, glucagon, somatostatin, and GLP-1 mimetics efficiently reset pancreatic islet clocks in mouse and human islets (20, 21), the signaling pathways induced by these molecules might be good candidates for mediators of both circadian and functional coupling among the islet cells.

Pancreatic islets derived from T2D donors exhibited attenuated circadian rhythms as compared to ND counterparts (Figs. 1 and 2 and *SI Appendix*, Fig. S1). In line with previous transcriptomic screening (39), we also show that expression of core-clock components is strongly altered in nonsynchronized cultured

human T2D islets (SI Appendix, Fig. S1A). Observed suppression of one or several components in the principal core-clock loop (CLOCK, PER1-2) may account for dampening the circadian reporter amplitude observed in synchronized T2D islets, as has been previously demonstrated in the skin fibroblasts derived from respective mouse KO models (40, 41). Beyond observed perturbation in the clockwork per se, T2D islet clock oscillators failed responding to physiologically relevant molecules, such as adrenalin, Octreotide, and glucose, further compromising their ability to anticipate and adequately react to feeding-fasting cycles. Loss of the adrenergic resetting effect on the T2D islet clocks might be associated with reduction of ADRA2A expression (SI Appendix, Fig. S1B) (42), or with genetic variant of ADRA2A found in a subset of T2D patients characterized by enhanced adenylate cyclase inhibitory activity in β-cells (43). Similarly, alteration of somatostatin resetting effect on islet clocks might be attributed to reduction of SSTR2 expression levels in T2D islet cells (SI Appendix, Fig. S1B) (42). Furthermore, changes of GLUT2 and GLUT1 transporter expression in T2D islets (SI Appendix, Fig. S1B) (44) may account for the lack of response by the islet cellular oscillators to the high glucose in the medium that was observed in T2D islets, contrary to the ND counterparts (Fig. 6). Of note, while glucose, adrenaline, and somatostatin fail to efficiently synchronize human T2D islet clocks, the GLP-1R mimetic Liraglutide maintained its resetting capacity on T2D oscillators, extending its therapeutic action to the



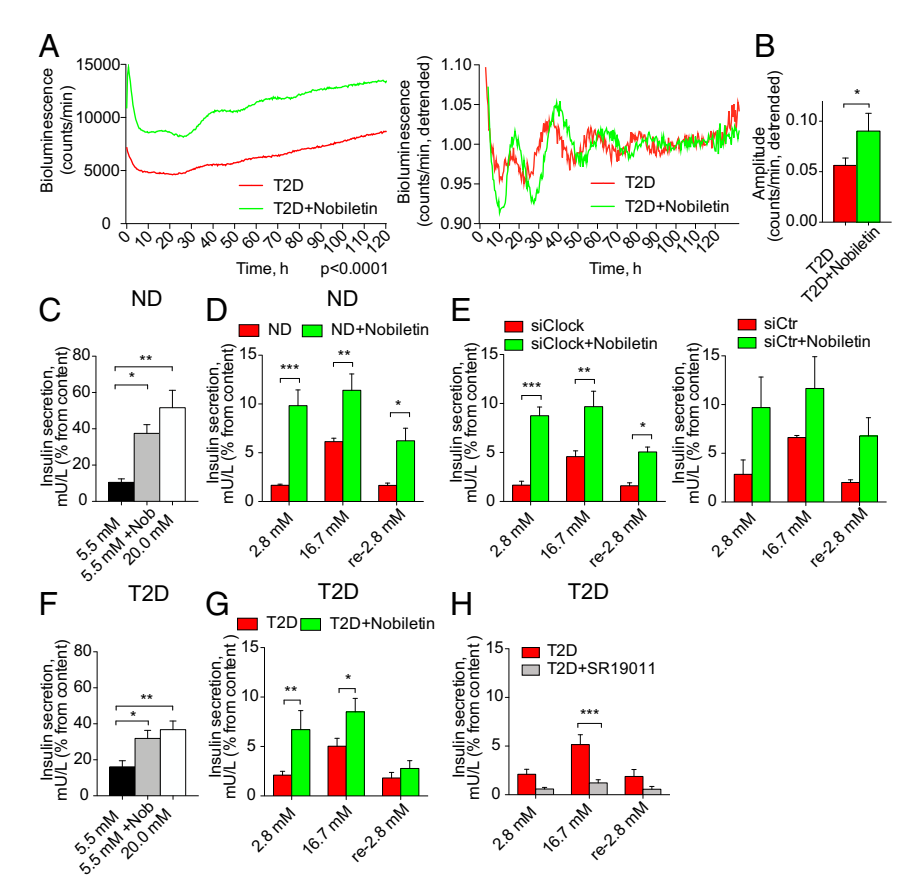


Fig. 7. The ROR agonist Nobiletin boosts disrupted molecular oscillators in human T2D islets, and enhances basal and stimulated insulin secretion by these islets. (A) Nobiletin enhances magnitude (Left) and amplitude (Right) of Bmal1-luc reporter oscillations in T2D islets synchronized with forskolin (n=4 islet batches from individual T2D donors). Difference in circadian magnitude (Left) was tested using two-way ANOVA test, P < 0.0001. Difference in circadian amplitude is shown in the adjacent histogram (B). (C and D) Stimulatory effect of Nobiletin on long-term (C, 7 h) and short-term (D, 1 h) insulin secretion by human islet cells from ND donors (D = 4). (D = Effect of Nobiletin on glucose-induced insulin secretion in human islet cells transfected with siRNA targeting CLOCK leading to the clock perturbation (22, 23). Insulin secretion by SICLOCK-transfected human islet cells (Left, D = 3 independent experiments), or by counterparts treated with scrambled siRNA (siCtr, D = 2 independent experiments). Data are expressed as mean D = 5 SEM (D = 5 donors). See also D = 5 donors), and in short-term glucose-induced insulin secretion tests (D = 5 donors). See also D = 4 donors. The difference is tested by two-way ANOVA test with Bonferroni posttest. D = 0.05, D = 0.01, and D = 0.01.

islet clock modulating function. Interestingly, the oscillation period length within the T2D group showed a tendency for inverse correlation with the T2D severity measured by blood HbA1c levels in the same donors (*SI Appendix*, Fig. S1G) that did not reach statistical significance. A similar negative correlation was observed between period length of cultured skin fibroblasts and blood HbA1c in a different cohort of T2D donors (24).

Perturbed Circadian Oscillators in Human T2D Islets May Affect Temporal Hormone Secretion via Regulating the Islet Hormone Exocytosis. Blood levels of insulin exhibit pronounced daily rhythmic profiles in rodents and in healthy human volunteers (8, 20, 45). These oscillatory profiles are stemming, at least in part, from rhythmic insulin secretion, as was shown by in vitro experiments with isolated mouse and human islets. The latter are compromised in the absence of functional islet clocks (8, 22), suggesting a primordial role of the cell-autonomous circadian oscillators for islet function. Here we show that concordantly with rhythmic secretion of insulin by mixed human islet cells and by pure mouse β -cells, also pure human β -cells synchronized in vitro secrete insulin in a circadian fashion. Additionally, circadian profile of proinsulin secretion was ~2-h phase-delayed compared to insulin secreted by the same islets. Oral glucose tolerance test in humans revealed that release of unprocessed proinsulin follows the one of mature insulin (46), likely reflecting an additional recruitment of proinsulin-containing immature granules upon increased insulin needs. Finally, we show that human islet cells secret glucagon in a circadian fashion. The peak of the rhythmic secretory profile of glucagon was delayed in comparison to that of insulin secreted by the same islets, in agreement with the data in rodents (20, 47). Importantly, rhythmic temporal profiles of proinsulin, insulin, and glucagon secretion by synchronized ND islets were strongly compromised in the T2D islets. In agreement with the data in first-degree relatives of T2D patients, pointing to the absence of the ascending phase of circadian rhythm and the attenuation of the circadian amplitude of insulin secretion rate (48), we found decreased magnitude and amplitude of insulin secretion in T2D islets synchronized in vitro. Strikingly, the circadian rhythmic profile of basal insulin secretion by ND islets was compromised following induced attenuation of molecular clocks (22), providing a parallel between the islet hormone secretion phenotype associated with T2D and with siRNA-mediated islet clock disruption.

Furthermore, our experiments suggest that functional islet clocks are indispensable for a proper docking and exocytosis of insulin and glucagon granules in humans and in mice. Indeed, siCLOCK-mediated clock disruption in human islets and Bmal1 knockout in mice resulted in a similar phenotype comprising

strong decrease in the secretory granule docking and of exocytosis events (Fig. 5 and SI Appendix, Fig. S3). The docking defect in β -cells was more pronounced than in α -cells. In line with these findings, transcriptomic analyses revealed that a large portion of key regulators of the secretory granule trafficking, docking, and exocytosis is under clock regulation in mouse and human islets (6, 7, 20, 22). In concordance with our data (SI *Appendix*, Fig. S1B), the impaired expression of similar groups of genes involved in exocytosis was shown in T2D islets (49) and upon islet clock disruption (22). Thus, the phenotype observed by us in ND human islets bearing disrupted clocks (Fig. 5) recapitulates changes described in human islet cells derived from T2D donors, where reduced granule docking limited sustained insulin secretion (28). The intriguing parallel between the islet transcriptional and functional alterations in human T2D and in human islets bearing compromised clocks supports a potential role of the cell-autonomous islet oscillators in the islet function, glucose homeostasis, and pathogenesis of T2D.

Human studies in controlled laboratory conditions highlighted that even short-term circadian misalignment leads to glucose intolerance and development of metabolic diseases (50). Moreover, disruption of the human islet molecular clocks in vitro attenuates basal and stimulated insulin secretion (22). This work provides evidence linking circadian clock disruption to compromised temporal and absolute levels of islet hormone secretion in the pathogenesis of T2D in humans.

Restoring T2D Islet Oscillators and Insulin Secretion with the Clock Modulator Nobiletin. The ROR nuclear receptor agonist Nobiletin exhibited multiple beneficial effects in rodent models, protecting against development of atherosclerosis, obesity, metabolic syndrome, and insulin resistance in rodents (32, 51, 52). Here we show that the clock modulator Nobiletin efficiently restores flattened amplitude of circadian oscillations in human T2D islets. Strikingly, Nobiletin also enhanced basal and glucose-stimulated insulin secretion in the same T2D islets, and in the islets obtained from ND donors following siCLOCK-mediated clock disruption. In line with original report on metabolic effects of Nobiletin on db/db Clock mutant mice (32), these data suggest that effects of Nobiletin on insulin secretion might be at least partly attributed to the core-clock unrelated action of ROR nuclear receptors. This hypothesis is further supported by the observation that REV-ERB agonist SR9011 exerted inhibitory effect on insulin secretion as opposed to Nobiletin, which was not paralleled by any significant changes in Per2-luc oscillation amplitude. Additionally, recently published RNA-sequencing analyses revealed up-regulation of ROR target genes in skeletal muscle following Nobiletin treatment, comprising the genes encoding for the core-clock components, mitochondrial electron transport chain, and reactive oxygen species scavenging (53). Activation of mitochondrial electron transport chain may potentially represent the clock-unrelated mechanism of Nobiletin action in the islet cells upon clock perturbation. Our in vitro data in human islets, and in vivo treatment of rodents with Nobiletin showed no notable toxicity for this compound (32). Of note, continuous stimulation of insulin secretion exerted by Nobiletin may exhaust the dysfunctional β -cells in T2D and accelerate their failure. Thus, imposing temporal regulation of insulin secretion mirroring the rest-activity cycles by alternated administration of ROR activator to ensure the insulin requirement during the day and ROR inhibitor during the resting state might represent a therapeutic strategy for improving insulin secretion in human T2D.

Materials and Methods

Human Islet Preparations. Human pancreatic islets were obtained from four different sources: 1) Prodo Laboratories LTD company (ND and T2D islets), 2) Alberta Diabetes Institute islet core center (ND and T2D islets), 3) Islet Transplantation Center of Geneva University Hospital (ND islets), and 4)

Pancreatic Tissue Bank of Hospital Universitari de Bellvitge (ND islets). T2D donors had a history of T2D and HbA1c greater than 6.5%. Details of the islet donors are summarized in *SI Appendix*, Table S1. All procedures using human islets were approved by the ethical committee of Geneva University Hospital CCER 2017-00147.

Pancreatic Islet and Islet Cell Culture. Human pancreatic islets were cultured in Connaught Medical Research Laboratories (CMRL) 1066 medium, containing 5.5 mM or 20 mM glucose (where indicated) and supplemented with 10% FBS (Gibco), 110 U/mL penicillin (Gibco), 110 μ g/mL streptomycin (Gibco), 50 μ g/mL gentamicin (Gibco), 2 mM $_{\rm L}$ -glutamine (GlutaMax, Gibco), and 1 mM sodium pyruvate (Gibco). Islet cell gentle dissociation was done using 0.05% Trypsin (Gibco) treatment. For bioluminescence recordings, 100 islets were plated to multiwell plates (LifeSystemDesign). For video time-lapse microscopy experiments, ~20 human islets were plated to a 3.5-cm glass-bottom willco dish (WillCo Wells). For perifusion experiments on purified β -cells (Fig. 3A), ~25,000 FACS-sorted β -cells were attached to 35-mm dishes (Falcon). For the rest of the experiments, ~50,000 dissociated islet cells were attached to 35-mm dishes (Falcon). All dishes were precoated with a homemade laminin-5-rich extracellular matrix derived from 804G cells, as described in ref. 54.

Insulin Secretion Tests. Insulin secretion assays were performed on $\sim\!50,000$ attached islet cells. For GSIS assays, cells were washed in KRB solution (Krebs-Ringer bicarbonate) pH 7.4 supplemented with 0.3% free fatty acid BSA (Sigma) containing 2.8 mM glucose during 2 h, subsequently incubated for 1 h at 37 °C (basal condition), followed by 1-h stimulation with 16.7 mM glucose (stimulated condition), and additional 1-h incubation in KRB solution containing 2.8 mM glucose (rebasal condition). Next, 2.5 μ M SR9011 (Sigma-Aldrich), or 20 μ M Nobiletin (Sigma-Aldrich) were added where indicated. In the end of the experiments, cells were lysed in acid-ethanol solution (1.5% HCl and 75% ethanol) for 1 h at room temperature. For insulin release assay, cells were washed in serum-free CMRL medium supplemented with 0.5% fatty acidfree BSA (Sigma-Aldrich), and incubated in the same medium containing either 5.5 mM glucose or with 20 mM glucose (glucosestimulated condition) for 7 h at 37 °C. Insulin was quantified in supernatants and cell lysates using a human insulin ELISA kit (Mercodia).

Viral Transduction and siRNA Transfection. Human islet cells were transduced with *Bmal1-luc, Per2-luc*, and RIP-GFP lentivectors, as described in ref. 12 and in *SI Appendix, Supplementary Methods*. Pppg-mCherry adenovirus was added at 10⁵ fluorescence forming units (FFU)/islet (26) (see *SI Appendix, Supplementary Methods* for further details). Dissociated adherent human islet cells were transfected twice with 50 nM *siCLOCK* or with the same amount of nontargeting *siControl* (Dharmacon, GE Healthcare) (22, 23).

In Vitro Cell Synchronization and Circadian Bioluminescence Recording. Adherent islets were synchronized by a 1-h pulse of forskolin (10 μ M; Sigma), 5 μM adrenaline (Geneva Hospital Pharmacy), 98 nmol/L Octreotide (Labatec Pharma), or 1.6 μM Liraglutide (Victoza), with a subsequent medium change. The islets were subjected to continuous bioluminescence recording in CMRL medium containing 100 μM luciferin (p-luciferin 306-250, NanoLight Technology) during several days (the experiment duration in hours is indicated in each graph). For the experiments with REV-ERB and ROR agonists, 2.5 μM SR9011 (Sigma-Aldrich) or 20 µM Nobiletin (Sigma-Aldrich), respectively, were applied together with forskolin synchronization pulse, and added to the recording medium for the entire experiment duration. For the experiments with high glucose, the CMRL medium was supplemented with 20 mM D-glucose (Sigma-Aldrich) from the synchronization step and during the entire recording. Bioluminescence pattern was monitored by a home-made robotic device equipped with photomultiplier tube detector assemblies, allowing the recording of 24-well plates (55). In order to analyze the amplitude of time series without the variability of magnitudes, raw data were processed in parallel graphs by moving average with a window of 24 h (22). Cell apoptosis was assessed where indicated with Cell Death Detection ELISA kit (Roche), according to manufacturer instructions.

Continuous Perifusion of Human Islet Cells. Human islet cells were transduced with the *Per2-luc* lentivectors, synchronized in vitro with a 1-h forskolin pulse, and placed into an in-house developed two-well horizontal perifusion chamber connected to the LumiCycle (23, 25). Cells were continuously perifused with sodium pyruvate-free CMRL supplemented with 10% FBS, 2 mM $_{\rm c}$ -glutamine, 50 $_{\rm \mu}$ g/mL gentamycin, 110 U/mL penicillin, 110 $_{\rm \mu}$ g/mL streptomycin, 100 $_{\rm \mu}$ M luciferin, and 5.5 mM glucose or 20 mM glucose. Bioluminescence recordings were performed in parallel to the 4-h interval automated collection of the outflow medium over 48 h. In the end of the

experiments, cells were lysed in acid-ethanol solution (1.5% HCl and 75% ethanol) for 1 h at room temperature. Insulin, glucagon, and proinsulin levels were quantified in the outflow medium using Human Insulin, Glucagon or Human Proinsulin Mercodia ELISA kits (Mercodia). The values were then normalized either to the residual intracellular content at the end of the experiment (48 h) (Figs. 3, 4, and 6C) or to the total RNA extracted from the nonperifused cells plated in parallel dishes (*SI Appendix*, Fig. S2 *D-F*).

Bioluminescence-Fluorescence Video Time-Lapse Microscopy. Human islets attached to glass-bottomed dishes (Willco Wells BV) were transduced with Pppg-mCherry adenovirus to label α -cells, RIP-GFP lentiviruses to label β -cells and with *Per2-luc* bioluminescence reporter. Islets synchronized by forskolin pulse were subjected to combined bioluminescence-fluorescence time-lapse microscopy (12) using Olympus LV200 workstation equipped with a 63× UPLSAPO objective and EM CCD camera (Image EM C9100-13, Hamamatsu). The recorded time-lapse images were analyzed on Fiji application (ImageJ), with individual cells tracked in the bioluminescence and fluorescence channels using a modified version of ImageJ plug-in CGE (27). Bioluminescence signal was measured over α - and β -cells within the encircled cell area (Fig. 2 *A* and *B* and Movies S1 and S2). Measuring of expression levels was performed on the labeled and tracked cells in the bioluminescence images over time. To assess the circadian characteristics of single-cell profiles, a JTK_Cycle fitting method was utilized (56).

TIRF Microscopy. Cells were imaged using a custom-built lens-type TIRF microscope based on an AxioObserver Z1 with a 100×/1.45 objective (Carl Zeiss). Excitation was from two DPSS lasers at 491 and 561 nm (Cobolt) passed through a clean-up filter (zet405/488/561/640x, Chroma) and controlled with an acousto-optical tunable filter (AA-Opto, France). Excitation and emission light were separated using a beamsplitter (ZT405/488/561/640rpc, Chroma). The emission light was chromatically separated onto separate areas of an EMCCD camera (Roper QuantEM 512SC) using an image splitter (Optical Insights) with a cutoff at 565 nm (565dcxr, Chroma) and emission filters (ET525/ 50m and 600/50m, Chroma). Scaling was 160 nm per pixel. Adenovirus-infected cells were imaged for 50 s at 100-ms exposure with 561 (0.2 to 0.5 mW) for exocytosis experiments in β -cells. Similarly, for α -cells the exposure was 561 (0.5 mW) and 491 (0.5 mW). Single images of cells were acquired to measure the number of docked granules at 100-ms exposure and 561 (0.2 mW) for β -cells and 561 (0.5 mW) and 491 (0.5 mW) for α -cells. Further details on the TIRF data analyses are presented in SI Appendix, Supplementary Methods.

- C. Dibner, The importance of being rhythmic: Living in harmony with your body clocks. Acta Physiol. (Oxf.) 228, e13281 (2020).
- G. Asher, P. Sassone-Corsi, Time for food: The intimate interplay between nutrition, metabolism, and the circadian clock. Cell 161, 84–92 (2015).
- A. Kalsbeek, E. Fliers, Daily regulation of hormone profiles. Handb. Exp. Pharmacol. 217, 185–226 (2013).
- S. A. Brown, L. Gaspar, "Circadian metabolomics: Insights for biology and medicine" in A Time for Metabolism and Hormones, P. Sassone-Corsi, Y. Christen, Eds. (Cham, 2016), pp. 79–85.
- F. Gachon, U. Loizides-Mangold, V. Petrenko, C. Dibner, Glucose homeostasis: Regulation by peripheral circadian clocks in rodents and humans. *Endocrinology* 158, 1074–1084 (2017).
- C. Dibner, U. Schibler, METABOLISM. A pancreatic clock times insulin release. Science 350, 628–629 (2015).
- M. Perelis et al., Pancreatic β cell enhancers regulate rhythmic transcription of genes controlling insulin secretion. Science 350, aac4250 (2015).
- 8. B. Marcheva et al., Disruption of the clock components CLOCK and BMAL1 leads to hypoinsulinaemia and diabetes. Nature 466, 627–631 (2010).
- F. W. Turek et al., Obesity and metabolic syndrome in circadian Clock mutant mice. Science 308, 1043–1045 (2005).
- J. E. Gale et al., Disruption of circadian rhythms accelerates development of diabetes through pancreatic beta-cell loss and dysfunction. J. Biol. Rhythms 26, 423–433 (2011).
- L. Perrin et al., Transcriptomic analyses reveal rhythmic and CLOCK-driven pathways in human skeletal muscle. eLife 7, e34114 (2018).
- P. Pulimeno et al., Autonomous and self-sustained circadian oscillators displayed in human islet cells. Diabetologia 56, 497–507 (2013).
- R. Dallmann, A. U. Viola, L. Tarokh, C. Cajochen, S. A. Brown, The human circadian metabolome. *Proc. Natl. Acad. Sci. U.S.A.* 109, 2625–2629 (2012).
- E. C. Chua et al., Extensive diversity in circadian regulation of plasma lipids and evidence for different circadian metabolic phenotypes in humans. Proc. Natl. Acad. Sci. U.S.A. 110. 14468–14473 (2013).
- U. Loizides-Mangold et al., Lipidomics reveals diurnal lipid oscillations in human skeletal muscle persisting in cellular myotubes cultured in vitro. Proc. Natl. Acad. Sci. U.S.A. 114, E8565–E8574 (2017).
- J. T. Bass, The circadian clock system's influence in health and disease. Genome Med. 9, 94 (2017).

Statistics. The results are expressed as means \pm SEM for the indicated number of donors detailed in the figure legends, or illustrated as mean value of all experiments (average bioluminescence profiles). Statistical difference was tested by Student's t test to compare two groups. Paired Student's t test was applied when comparing different treatment for the same donor preparations, and nonpaired Student's t test to compare the values obtained with the islets from ND and T2D donors. Two-way ANOVA test with Bonferroni posttest was used to compare two dependent groups of continuous measurements, where indicated. All statistical tests were realized with GraphPad Prism 5 Software. Statistical significance was defined at *P < 0.05, **P < 0.01, and ***P < 0.001. Correlation was quantified by Pearson coefficient r. To assess the circadian characteristics of hormone secretion or single-cell bioluminescence profiles, a JTK_Cycle fitting method was utilized (56). The profile was considered as circadian if adjusted P value was inferior to 0.1. The parameters of rhythmicity for bioluminescence recording experiments were evaluated based on the detrended values utilizing CosinorJ application.

ACKNOWLEDGMENTS. The authors thank Jacques Philippe, Ueli Schibler, and Claes Wollheim (University of Geneva) for constructive discussions; Marie-Claude Brulhart-Meynet (University Hospital of Geneva) for skillful technical assistance; Domenico Bosco and Thierry Berney (Islet Transplantation Center of Geneva University Hospital), Eduard Montanya Mias and Montserrat Nacher Garcia (Hospital Universitari de Bellvitge, Barcelona) for providing human islets; Etienne Lefai (Institut National de la Recherche Agronomique Auvergne Rhône-Alpes) for adenovirus amplification; Andre Liani and George Severi (University of Geneva) for assistance with perifusion experiments; and Christoph Bauer and Jerome Bosset (University of Geneva) for support with bioimaging experiments. Human islets from the Islet Transplantation Center of Geneva University Hospital were provided through Juvenile Diabetes Research Foundation Award 31-2008-416 (European Consortium for islet transplantation (ECIT) islet for Basic Research program, Thierry Berney). This work was funded by Swiss National Science Foundation Grants 31003A_166700/1, 310030_184708/1, the Vontobel Foundation, the Novartis Consumer Health Foundation, Bo and Kerstin Hjelt Foundation for diabetes type 2, Swiss Life Foundation, and the Olga Mayenfisch Foundation (C.D.); Swedish Research Council 2017-00956, 2018-02871 (to S.B. and A.T.); and Family Ernfors Foundation, European Foundation for the Study of Diabetes, Novo Nordisk Foundation, Diabetes Wellness Network Sweden, Swedish Diabetes Foundation, Exodiab network, Hjärnfonden (S.B.). N.R.G. was supported by the European Foundation for the Study of Diabetes-Rising Star Program and Novo Nordisk Foundation-Young Investigator Program.

- C. Saini, S. A. Brown, C. Dibner, Human peripheral clocks: Applications for studying circadian phenotypes in physiology and pathophysiology. Front. Neurol. 6, 95 (2015).
- L. A. Sadacca, K. A. Lamia, A. S. deLemos, B. Blum, C. J. Weitz, An intrinsic circadian clock of the pancreas is required for normal insulin release and glucose homeostasis in mice. *Diabetologia* 54, 120–124 (2011).
- B. Marcheva, K. M. Ramsey, J. Bass, Circadian genes and insulin exocytosis. *Cell. Logist.* 1, 32–36 (2011).
- V. Petrenko et al., Pancreatic α- and β-cellular clocks have distinct molecular properties and impact on islet hormone secretion and gene expression. Genes Dev. 31, 383–398 (2017).
- V. Petrenko, C. Dibner, Cell-specific resetting of mouse islet cellular clocks by glucagon, glucagon-like peptide 1 and somatostatin. Acta Physiol. (Oxf.) 222, e13021 (2018).
- C. Saini et al., A functional circadian clock is required for proper insulin secretion by human pancreatic islet cells. Diabetes Obes. Metab. 18, 355–365 (2016).
- V. Petrenko, C. Saini, L. Perrin, C. Dibner, Parallel measurement of circadian clock gene expression and hormone secretion in human primary cell cultures. J. Vis. Exp., e54673 (2016).
- 24. F. Sinturel et al., Cellular circadian period length inversely correlates with HbA_{1c} levels in individuals with type 2 diabetes. *Diabetologia* 62, 1453–1462 (2019).
- L. Perrin et al., Human skeletal myotubes display a cell-autonomous circadian clock implicated in basal myokine secretion. Mol. Metab. 4, 834–845 (2015).
- H. Shuai, Y. Xu, Q. Yu, E. Gylfe, A. Tengholm, Fluorescent protein vectors for pancreatic islet cell identification in live-cell imaging. *Pflugers Arch.* 468, 1765–1777 (2016).
- D. Sage, M. Unser, P. Salmon, C. Dibner, A software solution for recording circadian oscillator features in time-lapse live cell microscopy. Cell Div. 5, 17 (2010).
- N. R. Gandasi et al., Glucose-dependent granule docking limits insulin secretion and is decreased in human type 2 diabetes. Cell Metab. 27, 470–478.e4 (2018).
- S. Barg, M. K. Knowles, X. Chen, M. Midorikawa, W. Almers, Syntaxin clusters assemble reversibly at sites of secretory granules in live cells. *Proc. Natl. Acad. Sci. U.S.A.* 107, 20804–20809 (2010).
- N. R. Gandasi et al., Survey of red fluorescence proteins as markers for secretory granule exocytosis. PLoS One 10, e0127801 (2015).
- 31. S. Del Guerra et al., Functional and molecular defects of pancreatic islets in human type 2 diabetes. *Diabetes* **54**, 727–735 (2005).

- B. He et al., The small molecule nobiletin targets the molecular oscillator to enhance circadian rhythms and protect against metabolic syndrome. Cell Metab. 23, 610–621 (2016).
- L. A. Solt et al., Regulation of circadian behaviour and metabolism by synthetic REV-ERB agonists. Nature 485, 62–68 (2012).
- V. Petrenko, J. Philippe, C. Dibner, Time zones of pancreatic islet metabolism. Diabetes Obes. Metab. 20 (suppl. 2), 116–126 (2018).
- T. Hirota et al., Glucose down-regulates Per1 and Per2 mRNA levels and induces circadian gene expression in cultured Rat-1 fibroblasts. J. Biol. Chem. 277, 44244–44251 (2002).
- S. J. Aton, E. D. Herzog, Come together, right...now: Synchronization of rhythms in a mammalian circadian clock. Neuron 48, 531–534 (2005).
- M. A. Ravier et al., Loss of connexin36 channels alters beta-cell coupling, islet synchronization of glucose-induced Ca2+ and insulin oscillations, and basal insulin release. Diabetes 54, 1798–1807 (2005).
- 38. R. Rodriguez-Diaz et al., Paracrine interactions within the pancreatic islet determine the glycemic set point. *Cell Metab.* 27, 549–558.e4 (2018).
- 39. J. A. Stamenkovic *et al.*, Regulation of core clock genes in human islets. *Metabolism* **61**, 978–985 (2012).
- A. C. Liu et al., Intercellular coupling confers robustness against mutations in the SCN circadian clock network. Cell 129, 605–616 (2007).
- Z. Chen et al., Identification of diverse modulators of central and peripheral circadian clocks by high-throughput chemical screening. Proc. Natl. Acad. Sci. U.S.A. 109, 101–106 (2012).
- 42. N. Lawlor et al., Single-cell transcriptomes identify human islet cell signatures and reveal cell-type-specific expression changes in type 2 diabetes. *Genome Res.* 27, 208–222 (2017).
- A. H. Rosengren et al., Overexpression of alpha2A-adrenergic receptors contributes to type 2 diabetes. Science 327, 217–220 (2010).
- B. Thorens, GLUT2, glucose sensing and glucose homeostasis. *Diabetologia* 58, 221–232 (2015).

- G. Boden, J. Ruiz, J. L. Urbain, X. Chen, Evidence for a circadian rhythm of insulin secretion. Am. J. Physiol. 271. E246–E252 (1996).
- A. Fritsche et al., Relationships among age, proinsulin conversion, and beta-cell function in nondiabetic humans. Diabetes 51 (suppl. 1), 5234–5239 (2002).
- M. Ruiter et al., The daily rhythm in plasma glucagon concentrations in the rat is modulated by the biological clock and by feeding behavior. Diabetes 52, 1709–1715 (2003).
- 48. G. Boden, X. Chen, M. Polansky, Disruption of circadian insulin secretion is associated with reduced glucose uptake in first-degree relatives of patients with type 2 diabetes. *Diabetes* 48, 2182–2188 (1999).
- S. A. Andersson et al., Reduced insulin secretion correlates with decreased expression of exocytotic genes in pancreatic islets from patients with type 2 diabetes. Mol. Cell. Endocrinol. 364, 36–45 (2012).
- D. J. Stenvers, F. A. J. L. Scheer, P. Schrauwen, S. E. la Fleur, A. Kalsbeek, Circadian clocks and insulin resistance. *Nat. Rev. Endocrinol.* 15, 75–89 (2019).
- 51. Y. S. Lee et al., Nobiletin improves obesity and insulin resistance in high-fat dietinduced obese mice. J. Nutr. Biochem. 24, 156–162 (2013).
- E. E. Mulvihill et al., Nobiletin attenuates VLDL overproduction, dyslipidemia, and atherosclerosis in mice with diet-induced insulin resistance. *Diabetes* 60, 1446–1457 (2011).
- K. Nohara et al., Nobiletin fortifies mitochondrial respiration in skeletal muscle to promote healthy aging against metabolic challenge. Nat. Commun. 10, 3923 (2019).
- 54. G. Parnaud et al., Proliferation of sorted human and rat beta cells. Diabetologia 51, 91–100 (2008).
- 55. A. Gerber et al., Blood-borne circadian signal stimulates daily oscillations in actin dynamics and SRF activity. Cell 152, 492–503 (2013).
- M. E. Hughes, J. B. Hogenesch, K. Kornacker, JTK_CYCLE: An efficient nonparametric algorithm for detecting rhythmic components in genome-scale data sets. *J. Biol. Rhythms* 25, 372–380 (2010).





Citation: Petrenko V, Sinturel F, Loizides-Mangold U, Montoya JP, Chera S, Riezman H, et al. (2022) Type 2 diabetes disrupts circadian orchestration of lipid metabolism and membrane fluidity in human pancreatic islets. PLoS Biol 20(8): e3001725. https://doi.org/10.1371/journal.pbio.3001725

Academic Editor: Samer Hattar, National Institutes of Health, UNITED STATES

Received: January 25, 2022 Accepted: June 24, 2022 Published: August 3, 2022

Peer Review History: PLOS recognizes the benefits of transparency in the peer review process; therefore, we enable the publication of all of the content of peer review and author responses alongside final, published articles. The editorial history of this article is available here: https://doi.org/10.1371/journal.pbio.3001725

Copyright: © 2022 Petrenko et al. This is an open access article distributed under the terms of the Creative Commons Attribution License, which permits unrestricted use, distribution, and reproduction in any medium, provided the original author and source are credited.

Data Availability Statement: All relevant data are within the paper and its supporting files.

Funding: This work was funded by Swiss National Science Foundation grant 310030_184708/1 (CD);

RESEARCH ARTICLE

Type 2 diabetes disrupts circadian orchestration of lipid metabolism and membrane fluidity in human pancreatic islets

Volodymyr Petrenko 1,2,3,4 , Flore Sinturel 1,2,3,4 , Ursula Loizides-Mangold 1,2,3,4 , Jonathan Paz Montoya 5,6 , Simona Chera 1,2,3,4,7 , Howard Riezman 8 , Charna Dibner 0,1,2,3,4

- 1 Thoracic and Endocrine Surgery Division, Department of Surgery, University Hospital of Geneva, Geneva, Switzerland, 2 Department of Cell Physiology and Metabolism, Faculty of Medicine, University of Geneva, Geneva, Switzerland, 3 Diabetes Center, Faculty of Medicine, University of Geneva, Geneva, Switzerland, 4 Institute of Genetics and Genomics in Geneva (iGE3), Geneva, Switzerland, 5 Proteomics Core Facility, EPFL, Lausanne, Switzerland, 6 Institute of Bioengineering, School of Life Sciences, EPFL, Lausanne, Switzerland, 7 Department of Clinical Science, University of Bergen, Bergen, Norway, 8 Department of Biochemistry, Faculty of Science, NCCR Chemical Biology, University of Geneva, Geneva, Switzerland
- These authors contributed equally to this work.
- * charna.dibner@hcuge.ch

Abstract

Recent evidence suggests that circadian clocks ensure temporal orchestration of lipid homeostasis and play a role in pathophysiology of metabolic diseases in humans, including type 2 diabetes (T2D). Nevertheless, circadian regulation of lipid metabolism in human pancreatic islets has not been explored. Employing lipidomic analyses, we conducted temporal profiling in human pancreatic islets derived from 10 nondiabetic (ND) and 6 T2D donors. Among 329 detected lipid species across 8 major lipid classes, 5% exhibited circadian rhythmicity in ND human islets synchronized in vitro. Two-time point-based lipidomic analyses in T2D human islets revealed global and temporal alterations in phospho- and sphingolipids. Key enzymes regulating turnover of sphingolipids were rhythmically expressed in ND islets and exhibited altered levels in ND islets bearing disrupted clocks and in T2D islets. Strikingly, cellular membrane fluidity, measured by a Nile Red derivative NR12S, was reduced in plasma membrane of T2D diabetic human islets, in ND donors' islets with disrupted circadian clockwork, or treated with sphingolipid pathway modulators. Moreover, inhibiting the glycosphingolipid biosynthesis led to strong reduction of insulin secretion triggered by glucose or KCI, whereas inhibiting earlier steps of de novo ceramide synthesis resulted in milder inhibitory effect on insulin secretion by ND islets. Our data suggest that circadian clocks operative in human pancreatic islets are required for temporal orchestration of lipid homeostasis, and that perturbation of temporal regulation of the islet lipid metabolism upon T2D leads to altered insulin secretion and membrane fluidity. These phenotypes were recapitulated in ND islets bearing disrupted clocks.

the Vontobel Foundation (CD); the Novartis Consumer Health Foundation (CD); European Foundation for the Study of Diabetes EFSD/Novo Nordisk A/S Programme for Diabetes Research in Europe 2020 (CD); the Swiss Life Foundation (CD); the Olga Mayenfisch Foundation (CD); Leenaards Foundation (CD); the Swiss Cancer Research foundation (CD); Fondation pour l'innovation sur le cancer et la biologie (CD); Ligue pulmonaire genevoise (LPGE, CD); Bo and Kerstin Hjelt Foundation for diabetes type 2 (U L-M. and VP); Young Independent Investigator Grant SGED/SSED (VP and FS). SC was supported by funds from the Research Council of Norway (NFR 251041) and Novo Nordic Foundation (NNF150C0015054 and NNF210C0067325). HR was supported by the Swiss National Science Foundation grant 310030 184949 and the NCCR Chemical Biology (51NF40-185898). The funders had no role in study design, data collection and analysis, decision to publish, or preparation of the manuscript.

Competing interests: The authors have declared that no competing interests exist.

Abbreviations: CerS2, ceramide synthase 2; DAL, differentially abundant lipid; GlcCer, glucosylceramide; GP, generalized polarization; GSIS, glucose-stimulated insulin secretion; HexCer, hexosylceramide; HexDHCer, hexosyldihydroceramide; HPRT, hypoxanthine-guanine phosphoribosyltransferase; MUFA, monounsaturated fatty acid; ND, nondiabetic; PC, phosphatidylcholine; PE, phosphatidylethanolamine; PI, phosphatidylinositol; PS, phosphatidylserine; PUFA, polyunsaturated fatty acid; RT, room temperature; SFA, saturated fatty acid; siRNA, small interfering RNA; T2D, type 2 diabetes.

Introduction

Internal circadian clocks have evolved in most living beings to allow anticipation of daily light changes due to the Earth rotation. In mammals, this body timekeeping system relies on a central pacemaker residing in paired suprachiasmatic nuclei in the hypothalamus and multiple peripheral clocks in the organs [1,2]. It comprises myriads of cell-autonomous oscillators operative in most cells that ensure temporal orchestration of all aspects of physiology and metabolism [3,4]. At the same time, a dramatic rise in cardiometabolic diseases including obesity and type 2 diabetes (T2D) worldwide has been associated with the 24/7 lifestyle of our society that leads to chronic desynchrony between internal circadian system and external synchronizing cues (light, eating) dubbed circadian misalignment [3,5,6].

In pancreatic islets, studies in mouse models revealed that functional molecular oscillators are indispensable for absolute and temporal regulation of insulin and glucagon secretion [7– 9], and for compensatory -cell regeneration [10]. Surprisingly, the circadian clocks in neighboring - and -cells are not phase aligned, and they exhibit cell-specific circadian response to physiologically relevant synchronizers such as adrenalin, glucagon, GLP1, or somatostatin [8,11]. Consistently, clock-deficient mice show severe perturbations of glucose and lipid metabolism that are exacerbated upon islet-specific clock disruption and lack of -cell regenerative capacity following massive ablation [7,10,12]. In humans, cell-autonomous clocks operative in - and -cells orchestrate the rhythmic pattern of proinsulin, insulin, and glucagon secretion [13-15]. Disruption of functional oscillators in human islet cells from ND (nondiabetic) donors, mediated by small interfering RNA (siRNA) targeting of CLOCK, resulted in strongly diminished absolute levels and perturbed rhythmicity of basal insulin secretion exerted via reduced secretory granule docking and exocytosis [13,15]. Most strikingly, our recent study reveals that the circadian clockwork is compromised in human - and -cells in T2D. Clock perturbation in T2D islets was paralleled with altered temporal profiles of insulin and glucagon secretion [15].

Lipid metabolites are involved in energy homeostasis, membrane function, and signaling, thus playing essential roles in regulating body metabolism and in pathophysiology of metabolic disorders [16-20]. Mass spectrometry-based shotgun lipidomics allows quantification of over 1,000 phospholipids, sphingolipids, and triacylglycerides with high accuracy [21,22]. Using this powerful approach, it has been demonstrated that in mouse liver, a large portion of lipid species across all major lipid classes display a circadian rhythm, and this rhythmicity is driven by both circadian clocks and feeding [23]. In humans, metabolomics and lipidomics of serial blood samples suggested diurnal profiles for a wide panel of metabolites and lipids [24-26]. Lipidomics of serial human skeletal muscle biopsies obtained across 24 h [27] revealed that about 20% of the lipid species across all major lipid classes display a circadian rhythm in ND patients [28,29]. Strikingly, the rhythmicity of the lipid metabolites has been preserved in human skeletal myotubes differentiated and synchronized in vitro, highlighting that primary cells synchronized in vitro represent invaluable models for studying temporal regulation of lipid metabolism in humans [27]. Oscillating lipids in both skeletal muscle tissue and in cultured myotubes were not only limited to energy-controlling storage lipids such as triglycerides, but also comprised membrane and signaling lipids of different cellular compartments [29]. In line with these findings, parallel RNA-seq analyses based on the same experimental design suggested that key enzymes regulating lipid biosynthesis and glucose metabolism in the skeletal muscle exhibited rhythmic profiles [30]. Furthermore, our earlier works suggest that cellautonomous circadian oscillators are indispensable for the proper coordination of glucose uptake and temporal lipid profiles in human muscle, since glucose uptake was reduced and the

lipid oscillations were blunted upon *siClock*-mediated disruption of the skeletal myotube oscillator [29,30].

Dysregulation of lipid metabolism plays a key role in pathophysiology of metabolic diseases. Lipidomic approaches have pointed to novel mechanistic insights into pathophysiology of obesity and T2D [16,17,20,26,31-34]. The pattern of lipid alterations was tissue and disease specific, allowing to define distinct lipid signatures associated with obesity or T2D [35]. The blood levels of ceramides species and 1-deoxysphingolipids have been proposed as T2D biomarker candidates or therapeutic targets [36-41]. Whereas the roles of lipid metabolites in -cell function and dysfunction upon T2D development have been raised in several studies conducted in immortalized cell lines [42,43] but also in mouse models and in humans [44], no data on human islet lipidomics and its regulation by the circadian system have been provided so far. To fill this gap, we aimed to uncover molecular determinants of circadian regulation of lipid homeostasis in human pancreatic islets under physiological conditions and upon T2D. Employing lipidomic approaches, we demonstrate the circadian rhythmicity of phospho- and sphingolipids in human pancreatic islets from ND donors synchronized in vitro. Most importantly, we provide a novel link between disruption of circadian clock, temporal coordination of lipid metabolism in human pancreatic islet, and islet dysfunction upon T2D in humans, highlighting both molecular oscillator and sphingolipid metabolites as important therapeutic targets for metabolic diseases.

Results

Circadian lipidomics of human pancreatic islets synchronized in vitro

To examine the role of cell-autonomous circadian oscillators operative in human pancreatic islets in temporal orchestration of the islet lipid homeostasis, we conducted lipidomic analysis of intact human pancreatic islets synchronized in vitro. Islets obtained from 6 ND donors (see Table 1 for donor characteristics) were synchronized by a forskolin pulse and collected across 24 h according to the experimental design presented in Fig 1A. Rhythmic expression of key core clock transcripts validated efficient in vitro synchronization of human pancreatic islets (\$1 Fig). Out of 711 measured lipids, a total of 410 lipid species clustered in 8 major lipid classes were detected across all donors (S2A and S2B Fig and S1 Data). The percentage of lipids exhibiting diurnal oscillations according to the METACYCLE algorithm varied from 0.98% to 14.88% among the donors (Fig 1B and S2 Data). A peak of accumulation of rhythmic lipids was observed 12 h to 16 h following in vitro synchronization in most of the donors (Figs 1C and S2C). When the lipid species were clustered by lipid class, the distribution of the rhythmic lipids indicated that certain lipid classes were preferentially subject to circadian oscillations, although this distribution varied across the donors (S2D Fig). Phosphatidylinositol (PI) lipids were particularly enriched among the cyclic species in all donors (Figs 1B and S2D), even when the overall number of rhythmic lipid species was low, like in donor 5. We further investigated the abundance of different PI lipids throughout the circadian cycle. Lyso-, diacyl-, and ether-containing PIs displayed a common pattern of oscillation with a peak at 12 h and a nadir at 32 h after synchronization and up to 2-fold circadian amplitude (Fig 1D). We identified 3 individual lipids significantly rhythmic (p < 0.05) in at least 3 islet batches out of 6, all of them belonging to the PI lipid class: PI(O-)44:4, PI28:3, and PI40:2 (Figs 1E and S2E-S2G), the former being much more abundant than the others in this lipid class (S2H Fig). Noteworthy, the degree of desaturation of these lipids influenced their temporal profiles. Indeed, while PI saturated in their fatty acyl chains (referred to as saturated fatty acids (SFAs)) exhibited circadian rhythmicity with a single peak of abundance at 12 h after in vitro synchronization, the MUFA and PUFA (respectively monounsaturated and polyunsaturated) PIs displayed profiles closer

Table 1. Human donor characteristics.

Donor no.	Sex	Age (years)	BMI (kg/m ²)	HbA _{1c}	Islet purity (%)	Biopsy source
ND 1 ^a	M	51		<6.0	63	BCN
ND 2 ^a	M	54	28.5	<6.0	85	HUG
ND 3 ^a	F	59	23.7	<6.0	70	HUG
ND 4 ^a	F	51	44.1	<6.0	60	HUG
ND 5 ^{a,c}	F	47	33.4	<6.0	60	HUG
ND 6 ^a	M	49	26.2	<6.0	95	HUG
ND 7 ^b	M	20	23.5	<6.0	84	HUG
ND 8 ^b	M	47	23.4	<6.0	80	HUG
ND 9 ^{b,d}	F	59	25.9	<6.0	88	HUG
ND 10 ^b	F	76	19.3	<6.0	80	UAL
ND 11 ^{c,e}	M	23	24	5	90	UAL
ND 12 ^{c,e}	F	46	19	5.8	85-90	Prodo
ND 13 ^{c,e}	M	47	31	5.1	85	UAL
ND 14 ^c	M	45	29.7	5.5	90	UAL
ND 15 ^c	M	46	27.2	<6.0	75	HUG
ND 16 ^{c,e}	F	53	22.7	4.8	90	Prodo
ND 17 ^c	M	59	25.6	<6.0	75	HUG
ND 18 ^c	F	55	21.9	<6.0	60	HUG
ND 19 ^d	M	49	18.6	<6.0	62	HUG
ND 20 ^d	M	60	24.2	<6.0	83	HUG
ND 21 ^d	M	29	23	5.1	85	Prodo
ND 22 ^d	F	24	25.2	<6.0	90-95	Prodo
ND 23 ^e	M	48	19	5.3	85-90	Prodo
ND 24 ^e	F	35	26.7	3.8	95	UAL
ND 25 ^e	M	31	34.9	5.7	80	UAL
M = 15, F	1	46.52 ± 13.21	25.87 ± 5.78	<6.0		
	-		Characteristics of T2D			ı
T2D 1 ^b	M	51	35.6	7.1	90	Prodo
T2D 2 ^b	M	59	27.7	6.5	85	Prodo
T2D 3 ^{b,c}	M	51	35.3	8.6	NA	UAL
T2D 4 ^{b,c}	M	65	21.8	9.9	NA	UAL
T2D 5 ^{b,c}	F	48	30.4	7.5	70	UAL
T2D 6 ^b	M	61	27.4	7.1	90	Prodo
T2D 7 ^c	M	59	27.7	6.5	85	Prodo
T2D 8 ^{c,e}	M	63	22.0	7.3	80-85	Prodo
T2D 9 ^{c,e}	F	43	35.8	1.00	85	UAL
T2D 10 ^{c,e}	M	42	43.7	6.6	95	Prodo
T2D 11 ^c	M	53	30.1	7.8	80	Prodo
T2D 12 ^c	F	37	33	13.1	85	Prodo
M = 9, F = 3		52.67 ± 8.99	30.88 ± 6.25	8.0 ± 1.98		

^aDonors used for whole human islet studies synchronized by forskolin and collected around the clock.

Data in bold represent the mean values per group \pm standard deviation.

BMI, body mass index; ND, nondiabetic; T2D, type 2 diabetes; M, male; F, female.

https://doi.org/10.1371/journal.pbio.3001725.t001

^bDonors used for whole human islet studies collected 12 h and 24 h after forskolin synchronization.

^cDonors used for gene expression analysis by qPCR.

^dDonors used for *siClock/siControl* experiments.

 $^{^{\}mathrm{e}}\mathrm{Donors}$ used for membrane fluidity assessment experiments.

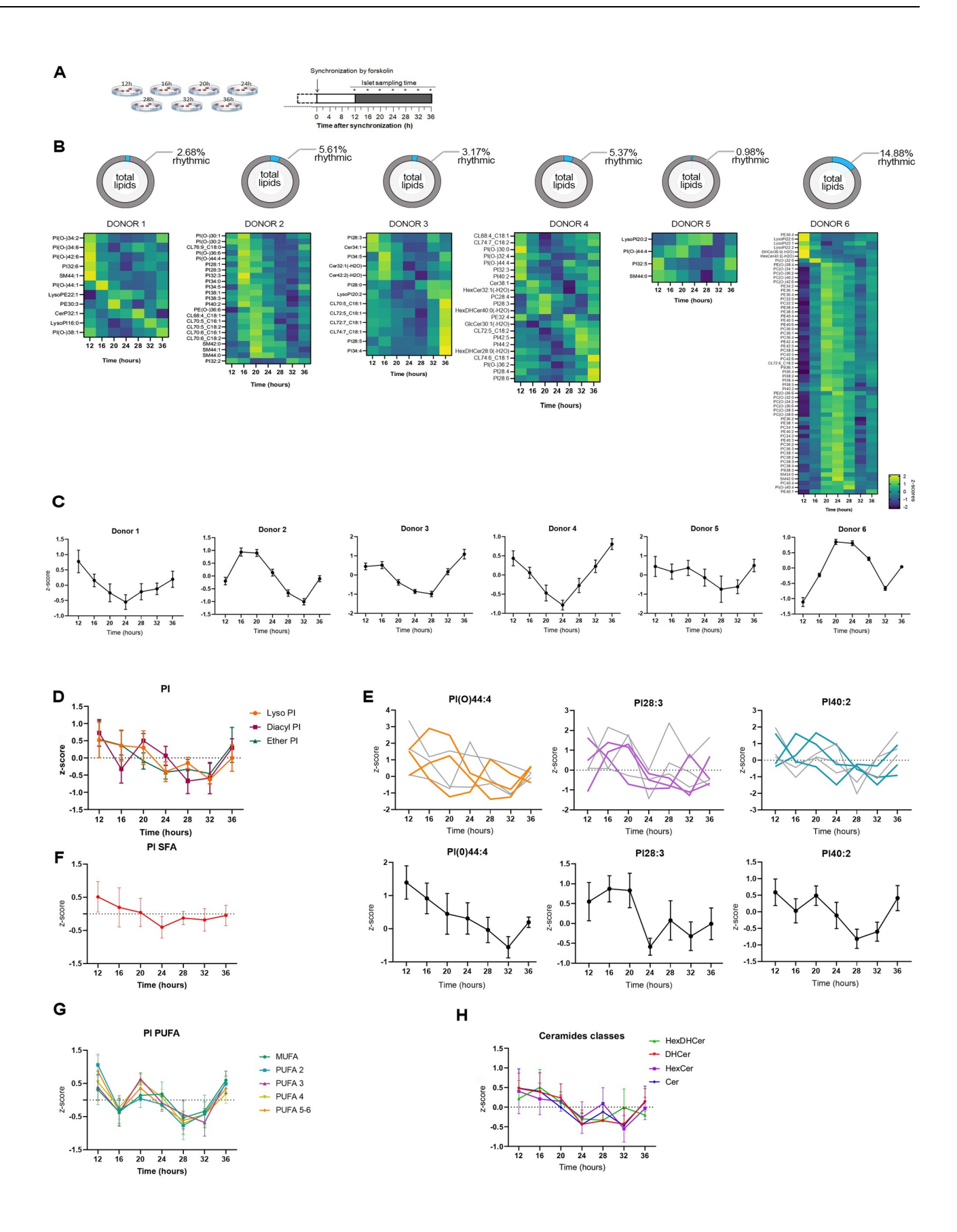


Fig 1. Identification of rhythmic lipid metabolites in human islets. (A) Experimental design for the collection of human pancreatic islets synchronized with forskolin pulse and harvested at the indicated 7 time points (n = 6 donors; asterisks indicate collection time). (B) Percentage of circadian rhythmic lipid species according to METACYCLE in pancreatic islets in each of the analyzed donors and corresponding heatmaps over the 7 time points. Normalized z-scores of lipid metabolites are indicated in yellow (high) and blue (low). See also \$2 Data. (C) Average temporal levels of rhythmic lipids (normalized z-scores) shown in (B) for each islet donors. All profiles were qualified circadian rhythmic (p < 0.05), except for donor 5. Data are represented as mean \pm SEM, n = number of rhythmic lipids for each donor. See also \$2 Data. (D) Average temporal profiles of PI species clustered by subclasses (Lyso-, Diacyl, Ether-PI). LysoPI abundance displays a significant circadian profile (p < 0.05). See also \$1 Data. (E) Representative islet lipids identified as circadian rhythmic in 3 donors: PI(-O) 44:0, PI28:3, and PI40:2. Individual lipid profiles (top panels) with colored traces corresponding to the donors exhibiting a circadian rhythmic profile (p < 0.05); average lipid profiles (bottom panels). See also \$1 Data. (F) Average temporal profiles of SFA PI phospholipid species. See also \$1 Data. (G) Average temporal profiles of PI phospholipid species sorted by degree of saturation, from MUFA lipids to PUFA lipids. See also \$1 Data. (H) Average temporal profiles of ceramide species by subclasses: HexDHCer, DHCer, HexCer, and Cer. DHCer abundance displays a significant circadian profile (p < 0.05). See also \$1 Data. Lipid concentrations of PI shown in (F, G) were corrected for class II isotopic overlaps by performing additional deisotoping analysis on the normalized values. Data for (D-H) are represented as mean \pm SEM, n = 6. See also \$2 Fig. MUFA, monounsaturated fatty acid; PI, phosphatidylinositol; PU

to what we observe for other lipid classes following synchronization (Figs 1F and 1G and S2I–S2K). Indeed, the phosphatidylcholine (PC), phosphatidylethanolamine (PE) and phosphatidylserine (PS), the most abundant classes of membrane lipids along with the PI, exhibited significant temporal changes of their levels across 24 h, but with no clear circadian pattern (S2I Fig). The PC/PE ratio, an indicator of cell membrane integrity, was relatively constant throughout the circadian cycle (S2L Fig).

In addition, we observed heterogenous temporal profiles of various sphingolipids (SL) (S2] Fig). Dihydroceramides exhibit a significantly rhythmic accumulation throughout the 24 h according to METACYCLE, and their temporal accumulation "around the clock" almost overlapped with the one of the ceramides (Cer), hexosylceramides (HexCer), and hexosyldihydroceramides (HexDHCer) (Fig 1H). This similar variation of abundance among the ceramides classes suggests a rhythmic de novo synthesis of the ceramides in pancreatic islets (Fig 1H). In contrast, the profile of the sphingomyelins (SM), the most abundant SL, was closer to that of the glycerophospholipids and cardiolipins (S2I–S2K Fig). Overall, lipid levels strongly changed over the course of 24 h, with variability observed among the islet donors. Importantly, the PI, and to a lesser extent, the Cer and HexCer exhibited oscillatory profiles throughout all the donors, suggesting a widespread impact of the circadian oscillator on these lipid classes metabolism in human pancreatic islets.

Lipidomic profiling reveals major changes in lipid metabolites at 2 time points in human T2D pancreatic islets synchronized in vitro

After identifying circadian rhythmic lipid metabolites in the pancreatic islets from ND donors cultured and synchronized in vitro, we next attempted to measure their temporal alterations in T2D islets. Since we were not able to conduct a complete around the clock study on T2D human islets due to the lack of material, lipid profiles were assessed at 2 opposite time points, 12 h and 24 h following synchronization by forskolin pulse (n = 5 T2D donors) and compared to the ND islet counterpart (n = 4, see Table 1 and S3 Data). The selected time points correspond to peak and trough of the core clock gene BMAL1 expression level (S1 Fig) and of the rhythmic profiles obtained for lipid species in most of the examined ND donors (4 out of 6 donors, Fig 1C). To assess whether T2D is characterized by global changes in lipid homeostasis in human islets, as it was the case in other metabolic tissues [35], we first averaged the levels of lipids detected at the 2 time points and compared those to the lipid class distribution in ND islets (Fig 2A-2D). Hierarchical clustering analysis of the top 30 lipid level changes shows an imperfect separation of the samples collected from T2D and ND donors, since the islet lipids from donor ND 10 clustered closer to the T2D counterpart than the other 3 ND individuals

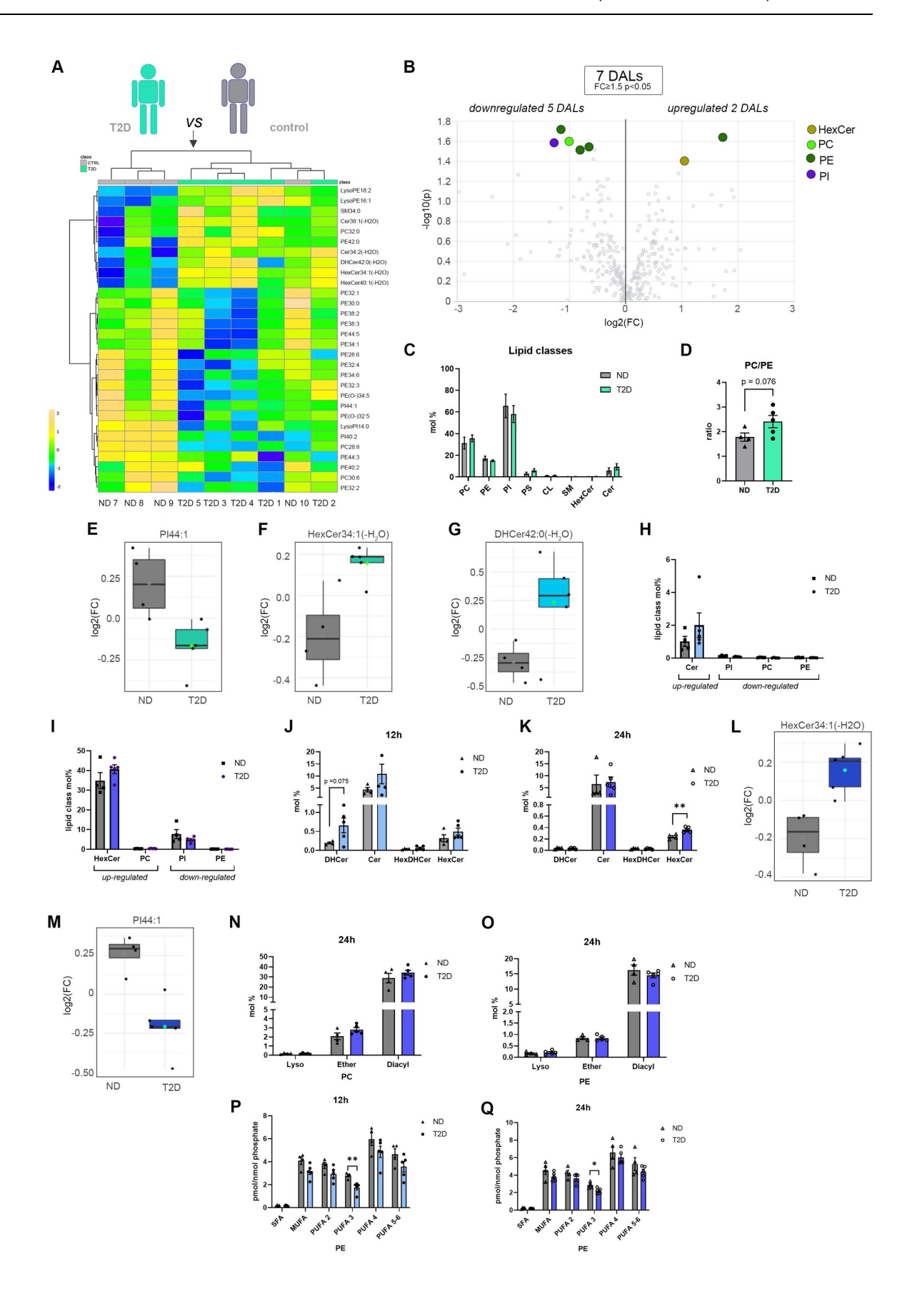


Fig 2. Lipidomic analyses of human islets derived from T2D versus ND donors cultured and synchronized in vitro. (A) Hierarchical clustering analysis (Distance Measure: Euclidian; Clustering algorithm: Ward) of top 30 islet lipids with most contrasting patterns between T2D and control ND counterpart. For each donor, islet lipids levels measured at 12 h and 24 h after forskolin synchronization were averaged (n = 5 for the islets from T2D donors and n = 4 for the islets from ND donors). (B) Volcano plots of differentially abundant islet lipids (fold change ≥ 1.5 and p < 0.05, Welch's corrected) between T2D (n = 5) and ND donors (n = 4). Colored dots highlight significant up- or down-regulated individual lipid species. (C) Lipid class repartition (PC, PE, PI, PS, CL, HexCer, Cer, and SM) in human islets from ND and T2D donors (in mol%), synchronized in vitro and collected at 12 h and 24 h after in vitro synchronization. The data represent the average of the 2 time points (n = 5 for the islets from T2D donors and n = 4 for the islets from ND donors, mean \pm SEM). (D) Comparison of the PC/PE ratio in islets from ND (n = 4) versus islets from T2D donors (n = 5). The data represent the average of the 2 time points (12 h and 24 h) ± SEM. (E, F) Representative examples of individual lipids (PI44:1 and HexCer34:1 (-H2O)) down- (E) and up- (F) regulated in the islets from T2D donors compared to islets from ND donors. The data represent the log2 fold change. (G) DHCer42:0(-H2O) levels in T2D versus ND islets synchronized in vitro and collected after 12 h. (H, I) Abundance of significantly differentially regulated lipids between the control and the T2D groups at 12 h (H) and 24 h (I). Each bar represents the sum of the significantly differentially regulated individual lipids shown in Fig 3E and 3F, as percentage of the total lipids detected from the same class at the same time point. Data are represented as mean ± SEM. (J, K) Relative level changes (mol%) of DHCer, Cer, HexDHCer, and HexCer in islets from T2D (n = 5) and ND (n = 4) donors collected 12 h (J) and 24 h (K) after synchronization, mean ± SEM. (L, M) Representative examples of individual lipids (HexCer34:1(-H2O) and PI44:1) up- (L) and down- (M) regulated in T2D versus ND islets synchronized in vitro and collected after 24 h. The data represent the log2 fold change. (N, O) Relative PC (N) and PE (O) level changes (mol%) in islets from T2D and ND donors collected 24 h after synchronization. Lipids are clustered according to the nature of the fatty acid linkage (diacyl versus alkyl-acyl (ether) or monoacyl (lyso)). T2D donors (n = 5) and ND donors (n = 4), mean \pm SEM. (P, Q) Relative PE level changes (in pmol/nmol of phosphate with lipid concentrations corrected for class II isotopic overlaps) in islets from T2D and ND donors collected 12 h (P) and 24 h (Q) after synchronization represented according to the degree of saturation. T2D donors (n = 5) and ND donors (n = 4), mean \pm SEM. Statistical analyses for (C, D, H–K, and N–Q) are unpaired t test with Welch's correction. *p < 0.05, **p < 0.01. See also \$3 Data. Cer, ceramide; CL, cardiolipin; DHCer, dihydroceramide; HexCer, hexosylceramide; HexDHCer, hexosyldihydroceramide; ND, nondiabetic; PC, phosphatidylcholine; PE, phosphatidylethanolamine; PI, phosphatidylinositol; PS, phosphatidylserine; SM, sphingomyelin; T2D, type 2 diabetes.

https://doi.org/10.1371/journal.pbio.3001725.g002

(Fig 2A). Overall, we observed a concomitant trend of decreased PE lipid levels and increased PC levels in the T2D islet group, resulting in a trend toward an increase PC/PE ratio that did not reach statistical significance (Fig 2C and 2D). Cer and HexCer exhibited a tendency toward increase in the T2D group, whereas several PI lipids were down-regulated (Fig 2A and 2B and 2E–2G). Because various phospholipid species (PE, PI, PC) were either up- or down-regulated in T2D islets (Fig 2A–2G), no significant change in overall amount per lipid class was observed between T2D and ND islets (Fig 2C).

Assuming that differences between the T2D and ND islets could be masked due to the average analysis across 2 time points, we next analyzed the islet lipids level at 12 h and 24 h separately. In this case, the hierarchical clustering showed a clear separation of the samples according to the donor group (T2D and ND) at both time points (Fig 3A and 3B), with a higher number of significant differentially abundant lipids (DALs) observed at 24 h (5 different lipids at 12 h versus 12 at 24 h, with fold change > 1.5 and p < 0.05) (Fig 3C and 3D). None of the lipids differentially abundant between the groups was common across the 2 time points (Fig 3E and 3F), further highlighting the importance of temporal analysis, even if conducted in 2 time points only. Strikingly, several HexCer, representing approximately 40% of all lipids of this class (Fig 2H and 2I), were significantly differentially regulated between the T2D and ND groups (Fig 3F). Consistently, looking at the levels of all major lipid classes (Fig 3G and 3H), we noticed a higher level of total HexCer in the T2D group compared to the ND group at both time points with marked difference at 24 h (Figs 2J-2L and 31). Several C16, C22, and C24 containing HexCer species were particularly increased 24 h after synchronization in the islets from the T2D donors compared to ND counterparts (Fig 3]). Whereas the ceramide levels were only slightly increased in T2D islets, abundant DHCer species were increased in the T2D groups at 12 h after synchronization (Fig 2H and 2J and 2K).

Among the phospholipids, few metabolites were down-regulated in the T2D group that mostly belonged to the PE and PI lipid classes (Figs 2M and 3E), in agreement with the previously observed global differences (Fig 2A and 2B). At 24 h, the concomitant increase of PC

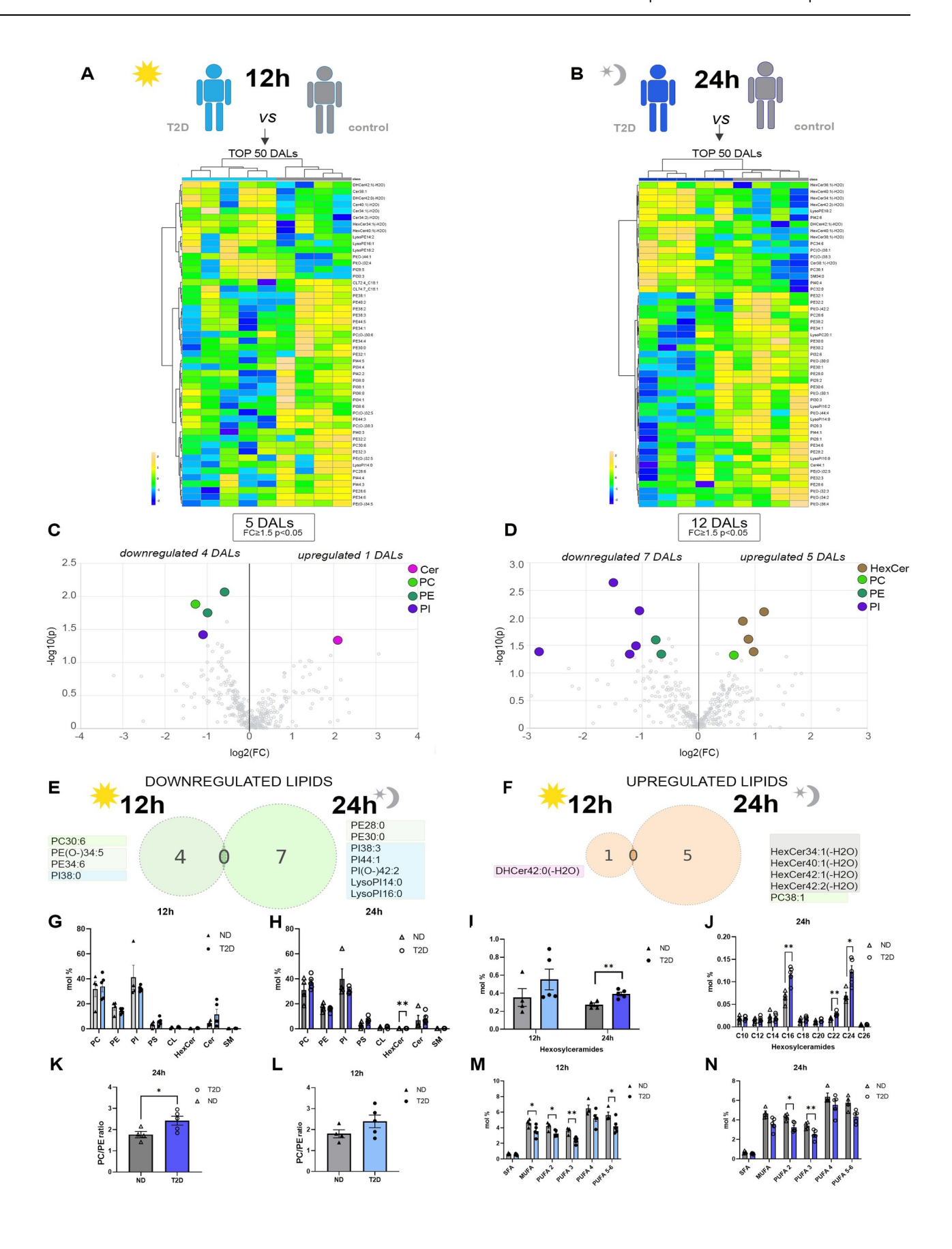


Fig 3. Comparison of human islet lipidome from T2D and ND donors at 12 and 24 h after in vitro synchronization. (A, B) Hierarchical clustering analysis (Distance Measure: Euclidian; Clustering algorithm: Ward) of top 50 islet lipids with most contrasting patterns between T2D and control patients at 12 h (A) and 24 h (B) after forskolin synchronization. (C, D) Volcano plots of differentially abundant islet lipids (fold change ≥ 1.5 and p < 0.05, Welch's corrected) at 12 h (C) and 24 h (D), between T2D and ND donors. Colored dots highlight significant up- or down-regulated individual lipid species. (E, F) Venn diagrams assessing the down-regulated (E) and up-regulated (F) lipid species shared by the 2 indicated time points in islets collected from T2D donors. (G, H) Lipid class repartition (PC, PE, PI, PS, CL, HexCer, Cer, and SM) in human islets from ND and T2D donors (in mol%), synchronized in vitro and collected at 12 h (G) and 24 h (H). (I) Comparison of the relative HexCer level changes (mol%) in ND versus T2D islets collected at 12 h and 24 h after synchronization. (J) Comparison of the relative HexCer level changes, sorted by number of carbons, over the total of islet lipids (mol%) measured in ND and T2D islets collected at 24 h after synchronization. (K, L) Ratio between PC and PE at 12 h (L) and 24 h (K) after synchronization. (M, N) Relative PE level changes (mol%) in islets from T2D and ND donors collected 12 h (M) and 24 h (N) after synchronization represented according to the degree of saturation. Statistics for (G–N) are unpaired 2-tailed t test with Welch's correction. T2D donors (n = 5) and ND donors (n = 4), data are represented as mean ± SEM. * p < 0.05. ** p < 0.01. See also S3 Data. Cer, ceramide; CL, cardiolipin; HexCer, hexosylceramide; ND, nondiabetic; PC, phosphatidylcholine; PE, phosphatidylethanolamine; PI, phosphatidylinositol; PS, phosphatidylserine; SM, sphingomyelin; T2D, type 2 diabetes.

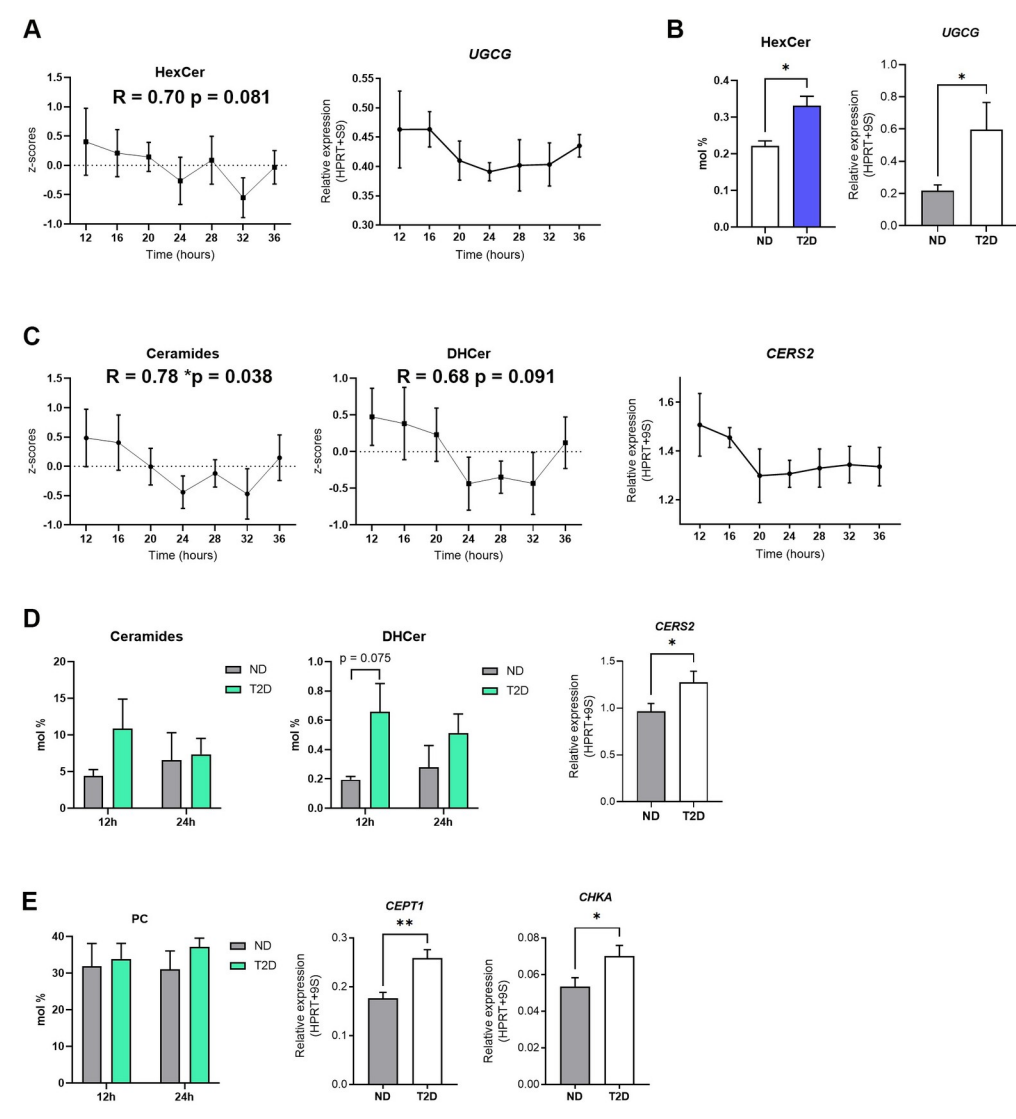
https://doi.org/10.1371/journal.pbio.3001725.g003

and decrease of diacyl PE levels (Fig 2N and 2O) resulted in a significant increase of the PC/PE ratio, known to influence cellular calcium homeostasis and ER function [45] (Fig 3K). A similar change has been observed at 12 h; however, it did not reach statistical significance (Fig 3L). Whereas all unsaturated PE subspecies, regardless of their degree of saturation, exhibited the trend toward the decrease in the T2D group, this difference did not reach significance for PUFA 4 (at both time points) and PUFA 5 to 6 (at 24 h) (Fig 3M and 3N). In contrast, this difference was highly significant for PUFA 3, even after deisotoping correction of the lipid signals (Fig 2P and 2Q). Since increase in PUFAs within the membrane enhances membrane fluidity [46], the decrease in the PUFA-PE content might be indicative of defects in plasma membrane physical properties in the islets derived from T2D patients. Collectively, these experiments reveal major alterations in the pancreatic islet lipid homeostasis in T2D patients, potentially indicative of an increased inflammation and ER stress and reduced membrane plasticity.

Diurnal ceramide levels correlate with transcript profiles encoding key enzymes involved in their turnover

Our data reveal that HexCer display both a rhythmic accumulation pattern around the clock in islets from ND patients synchronized in vitro and higher levels in islets from T2D patients. To explore the molecular determinants, we investigated the temporal gene expression profile of UDP-glucose ceramide glucosyltransferase (UGCG), a key enzyme involved in glucosylceramide biosynthesis that catalyzes the transfer of glucose from UDP-glucose to ceramide. Strikingly, the UGCG mRNA expression measured around the clock in the islets from ND donors exhibited a rhythmic profile (p = 0.05 as assessed by JTK_Cycle) with the trough around 20 to 24 h following in vitro synchronization, corroborating the temporal profile of BMAL1 transcript (S1 Fig), and recapitulating the diurnal accumulation profile of HexCer (Fig 4A). Remarkably, we observe a concordance between the higher level of HexCer in the T2D group at 24 h and the UGCG transcript up-regulation in the same group compared to the ND group (Fig 4B).

We next assessed whether a correlation exists between the levels of Cer and DHCer lipid classes and the temporal mRNA profiles of ceramide synthases, involved in N-acylation of sphinganine and sphingosine bases to form DHCer and Cer. Ceramide synthase 2 (CerS2), the most abundant and ubiquitously expressed ceramide synthase [16,47–49] displays temporal variation in its mRNA expression that correlates with the ceramide and DHCer accumulation profiles (Fig 4C). In addition, the tendency for a higher amount of Cer and DHCer in islets from the T2D donors compared to their counterparts that was especially pronounced for DHCer at 12 h after synchronization, concordantly with the significant increase of *CerS2* transcript in T2D islets (Fig 4D).



Beyond the enzymes involved in lipid metabolism that exhibited oscillatory patterns, we also analyzed the relationship between the enzymes that were significantly differentially expressed in islets from T2D compared to ND donors and the corresponding lipid class abundance in each group. *CEPT1* and *CHKA* genes code for choline/ethanolamine

phosphotransferase and choline kinase alpha enzymes, respectively, that are involved in PC biosynthesis via the CDP-choline pathway. Interestingly, the slight increase in PC levels in the T2D group, more pronounced at 24 h and contributing to a significant increase in the PC/PE ratio at this time point (Fig 3K), was associated with an up-regulation of both *CEPT1* and *CHKA* mRNA expression in the T2D group compared to the ND counterpart (Fig 4E).

Lipid membrane fluidity of the human pancreatic islet cells is diminished in T2D islets and in ND islets upon circadian clock disruption

Collectively, the alterations in lipid metabolites that we observed in human pancreatic islets derived from T2D donors pointed toward a possibility of perturbed membrane organization and fluidity in T2D islet cells, which could impact their secretory function. We therefore measured membrane fluidity in human islet cells from T2D donors compared to ND counterpart (Fig 5A) by bioimaging using a Nile red derivative NR12S that is thought to penetrate only the outer leaflet of the plasma membrane [50]. Fluorescence emission of NR12S is sensitive to the membrane environment in a way that in more ordered membranes fluorescence emission is blue shifted, while in disordered membranes the fluorescence emission spectra is red shifted [50]. This shift in emission profile between liquid-disordered and liquid-ordered phases allows a quantitative assessment of membrane order by calculating the ratio of the fluorescence intensity recorded in 2 spectral channels, known as the generalized polarization (GP) value [51]. GP quantification of NR12S fluorescence emission from ND and T2D islet cell images revealed significant increase in membrane rigidity in T2D islet cells as compared to ND counterparts (Fig 5A).

We have recently demonstrated that functional perturbation of insulin secretion by human pancreatic islets derived from T2D islets was recapitulated in ND human islet cells upon cellautonomous clock disruption, both in terms of diminished absolute secretion and perturbed rhythmic profile, indicating that islet cellular clock disruption may take part in pathophysiology of T2D in humans [13,15]. Whether such a parallel holds true for the changes in lipid homeostasis remains unexplored. Disruption of circadian oscillators in ND islet cells by transfection of siRNA targeting CLOCK following our previously validated protocols [13,52] led to significantly increased expression of UGCG (S3A Fig), similarly to the observed increase in this enzyme in T2D islets (Fig 4B). Moreover, KEGG pathway enrichment analysis of all significantly up-regulated transcripts in clock-compromised islets revealed activation of sphingolipid metabolism pathway (p = 0.0575; S3B Fig). To uncover changes in membrane fluidity in siClock-transfected ND islet cells bearing disrupted oscillators, NR12S fluorescence has been compared between clock-compromised cells and control counterparts transfected with scrambled siControl RNA (Fig 5B, left). Strikingly, membrane fluidity was significantly reduced (Fig 5B, right), pinpointing that disruption of circadian oscillators in islet cells derived from ND donors leads to increased membrane rigidity, thus recapitulating the phenotype observed in T2D islets (compare Fig 5B to 5A).

Perturbation of ceramide metabolism affects insulin secretion by human pancreatic islets and decreases lipid membrane fluidity

Given that major changes that we observed in lipid homeostasis in the islets from T2D donors were related to altered sphingolipid levels, we next assessed the impact of inhibiting ceramide de novo synthesis by myriocin on the islet function. Application of myriocin to ND islet cells resulted in greater GP values of NR12S emission as compared to nontreated control (Fig 5C), suggesting increase in membrane rigidity of these cells. To assess the effect of myriocin on induced insulin secretion by human pancreatic islets, we performed glucose-stimulated insulin

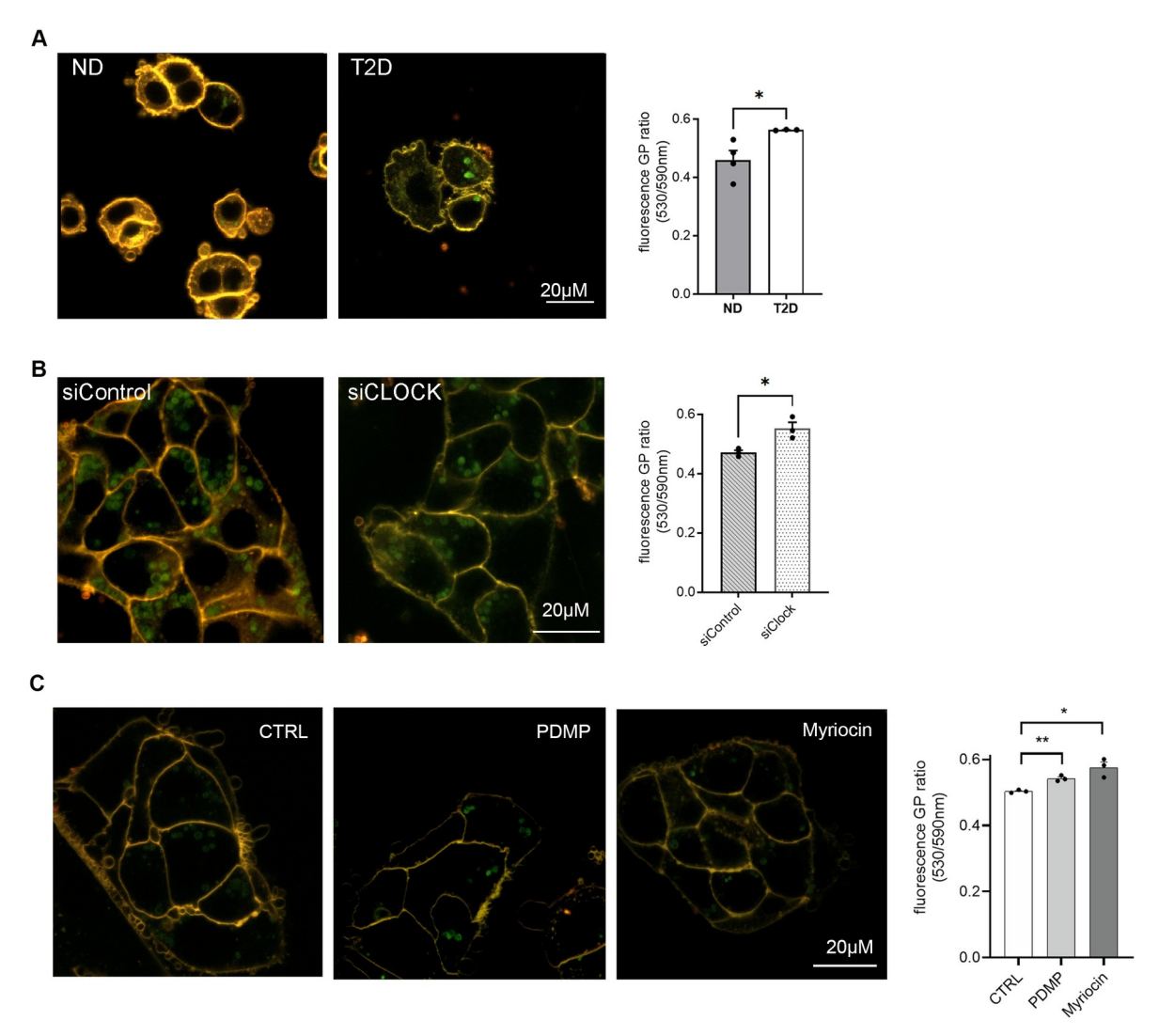


Fig 5. Lipid membrane fluidity of the human pancreatic islet cells is attenuated in T2D islets, in ND islets upon siClock-mediated clock disruption, and in ND islets following perturbation of ceramide metabolism by PDMP or myriocin. Live cell imaging of human islet cells stained with NR12S dye. (A) Representative ND (left) and T2D (right) human islet cells. The graph on the right summarizes the quantification of fluorescence GP ratio for n = 4 ND and n = 3 T2D donors. (B) Representative images of ND islet cells transfected with scrambled siRNA (siControl, left) bearing functional clocks and siClock targeting CLOCK protein that bear perturbed oscillators (right). The graph on the right summarizes the quantification of fluorescence GP ratio for n = 3 donors. (C) Representative images of nontreated control ND islet cells (left), cells following 1-h treatment with PDMP (middle) or myriocin (right). The graph summarizes the quantification of fluorescence GP ratio for n = 3 human donors. Note the significant up-regulation of membrane rigidity for T2D islet cells (A), ND cells with compromised clocks (B, siClock), and ND cells with impaired sphingolipid metabolism (C, PDMP and myriocin). Graph data are represented as mean \pm SEM; unpaired 2-tailed t test as compared to control, t00. See also S3 Fig and S4 Data. GP, generalized polarization; ND, nondiabetic; siRNA, small interfering RNA; T2D, type 2 diabetes.

secretion (GSIS) and KCL-stimulated insulin secretion (KSIS) tests. Application of myriocin to ND as well as to T2D islet cells led to compromised insulin secretion under low glucose conditions and a tendency to inhibiting both GSIS and KSIS that did not reach statistical significance (Fig 6A–6C). We next studied lipid membrane fluidity, GSIS and KSIS in the presence of PDMP that inhibits UCGC, the key enzyme of glycosphingolipid biosynthesis. Similar to myriocin, application of PDMP to ND islet cells significantly increased GP values of NR12S emission (Fig 5C). Strikingly, insulin secretion by ND islets was strongly compromised in the

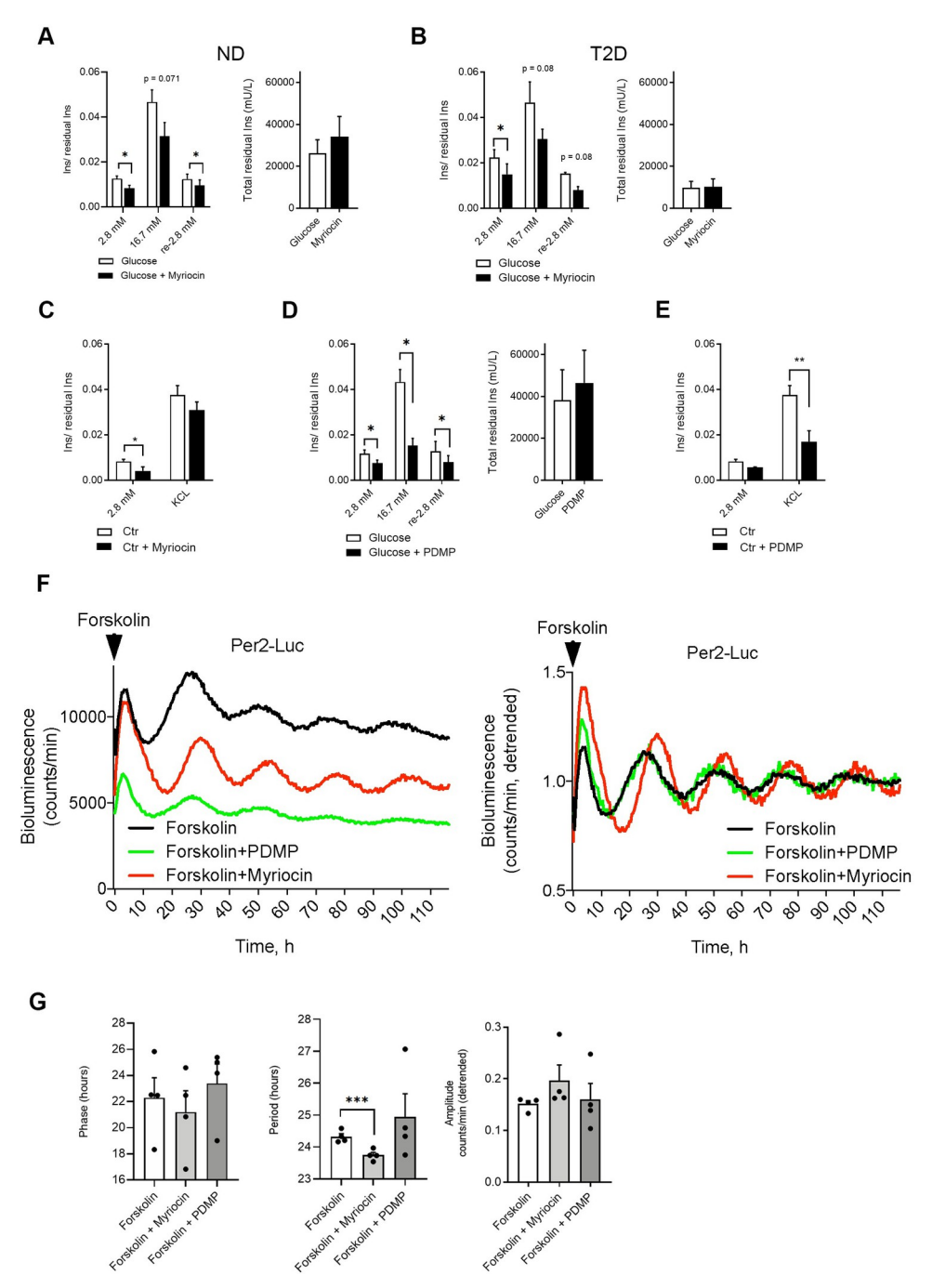


Fig 6. Inhibitors of sphingolipid synthesis, PDMP and myriocin, perturb insulin secretion and circadian oscillations by human pancreatic islets. Inhibitory effects of myriocin (A–C) and ceramide analog PDMP (D, E) on basal (1 h at 2.8 mmol glucose), glucose-induced (1 h at 16.7 mmol), and KCL-induced (1 h at 30 mmol KCL) insulin secretion in human islet cells in vitro. Data represent values normalized (Ins/residual Ins) to the total residual insulin content (total residual Ins (mU/L) presented on adjacent graphs) and are expressed as mean \pm SEM for n=7 ND donors (A), n=3 T2D donors (B), n=3 ND donors (C), n=5 ND donors (D), and n=3 ND donors (E). The difference is tested by paired 2-tailed t test; $p^* < 0.05$, $p^{**} < 0.01$. See also S4 Fig. (F) Representative raw (left) and detrended (right) Per2-luc bioluminescence profiles of human islets in the presence of myriocin or PDMP during the entire bioluminescence recording. (G) Effect of myriocin and PDMP on principal circadian parameters (phase, period length, and amplitude) of Per2-luc oscillations. Data are represented as mean \pm SEM, n=4 ND donors. The difference is tested by 2-way ANOVA test with Bonferroni posttest; $p^* < 0.05$ (as compared to the control counterpart synchronized with forskolin in the absence of these compounds). See also S5 Fig and S4 Data. ND, nondiabetic; T2D, type 2 diabetes.

presence of PDMP at basal glucose levels, and after stimulation by high glucose, or by KCL (Fig 6D and 6E). A similar effect was observed when PDMP was applied to islet cells isolated from T2D patients (S4 Fig). Neither myriocin nor PDMP exerted a significant effect on the islet cell insulin content (Fig 6A and 6B and 6D, right graphs).

Ceramide turnover inhibitors myriocin and PDMP alter circadian oscillations in human pancreatic islets synchronized in vitro

Since the ceramide levels exhibited circadian rhythmicity in ND islets on one hand and were strongly perturbed in T2D islets on the other, we next explored whether disrupted turnover of ceramides may feedback on the islet molecular clockwork. To this end, we recorded circadian bioluminescence of a Period2-luciferase (Per2-luc) lentiviral construct expressed in ND islet cells synchronized in vitro [14,15] in the presence of myriocin or PDMP in the recording medium (Fig 6F). Application of myriocin resulted in period shortening and phase advance of circadian oscillations of Per2-luc, while PDMP had no significant effect on the islet cell rhythmicity (Fig 6G). In contrast to myriocin that did not significantly affect cell mortality, PDMP showed a clear tendency to stimulate islet cell apoptosis following continuous 5-day exposure that did not reach statistical significance as compared to forskolin-treated control (S5 Fig).

Discussion

Our study reveals that in human pancreatic islets derived from ND donors, about 5% of the lipid metabolites across all major lipid classes exhibited pronounced circadian oscillations following in vitro synchronization. In our previous lipidomic analysis, we report that in synchronized human primary myotubes, the circadian oscillating lipid species were more abundant, reaching up to 18.6% [29]. Such discrepancy may reflect tissue-specific lipid composition or stem from the high inter-donor variability, low number of the islet donors (n = 6), limited amount of starting material, and islet cellular heterogeneity.

Among the different lipid species considered circadian in our analysis, we report major oscillations of PIs and SLs. PI metabolites are both components of cellular membranes and signaling molecules that are essential for secretory function of endocrine -cells. Indeed, PI lipids generate soluble inositol second messengers involved in the mobilization of intracellular Ca²⁺ stores and the recruitment of other signaling proteins regulating formation and secretion of granules at the plasma membrane [53]. Moreover, stimulation of insulin secretion influences PI metabolism in plasma membranes of MIN6 -cell line [54,55]. We have previously shown that in vitro synchronized human islets exhibit a circadian profile of insulin secretion, with a respective peak and nadir appearing 12 h and 24 h after synchronization [13,15]. This circadian pattern of insulin secretion positively correlates with the temporal profile of PI abundance, also exhibiting a peak 12 h after forskolin pulse (Fig 1D). We speculate that the circadian oscillations of PI may participate in regulation of temporal secretion of insulin by -cells. Moreover, islets derived from T2D donors exhibited a slight decrease in total PIs and a significant diminution of several individual abundant PI metabolites (Figs 2M and 3A-3E) concomitant with attenuated insulin secretion, further supporting a role of these PIs in the insulin release defects in diabetic -cells.

Cer and HexCer are 2 additional major lipid classes exhibiting temporal variations in synchronized human islets, suggesting rhythmic organization of sphingolipid metabolism. Furthermore, the abundance of the total DHCer species exhibited circadian oscillations (Fig 1H). These temporal variations are correlated with the rhythmic transcription of *CERS2* and *UGCG*, the key enzymes involved in ceramide and glucosylceramide synthesis (Fig 4A and 4C), as well as with the expression of core clock transcripts (S1 Fig). Of note, in some instances,

mRNA measurements were conducted on the islets derived from different donors from those utilized for the lipidomics analyses (see Table 1). In line with these results, a large-scale RNA-seq screening of circadian transcripts in in vitro synchronized human islets reveal circadian rhythmic regulation of transcripts coding for key components of the sphingolipid metabolism (CERKL, SGPL1, NEU2, NEU3, CERS6, CERS4) [7], further highlighting a circadian regulation of this pathway at the transcriptional level. Concordantly, we also observed an up-regulation of CERK, SGPL1 [13], and UGCG transcripts upon siClock condition (S3 Fig), implying interconnection between the islet clockwork and regulation of ceramide synthesis. This finding is in line with our analysis of the human skeletal muscle lipid content upon CLOCK depletion [30] showing that UGCG expression is significantly up-regulated in siClock-transfected primary myotubes compared to siControl-transfected ones. Accordingly, we observed a significant increase of the total HexCer in CLOCK-depleted skeletal muscle myotubes [29].

The interaction between molecular clock and sphingolipids seems to be bidirectional since decrease in sphingolipid levels by myriocin resulted in shortening of a circadian period length and phase advance in human islets (Fig 6F and 6G). Periodicity of clock machinery requires functional interactions of all its molecular components and depends on their expression and/ or posttranscriptional modifications. For example, deletion or mutation of negative limb component PER2 leads to a shortening of period length [56,57]. Nevertheless, our data indicate that myriocin failed to significantly down-regulate Per2-Luc expression, thus not supporting the idea that myriocin may exert its effect via modulation of PER2 absolute levels. On the other hand, phosphorylation of PER2 at different sites modulates the period length [58] and mutations associated with differential phosphorylation of human PER2 underlies familial advanced sleep phase syndrome [59]. Sphingolipids are considered to play an important role in intracellular signaling utilizing lipid-protein interactions [60,61]. Several protein candidates were shown to interact with ceramides, sphingosine 1 phosphate (S1P), and glycosphingolipids. Those comprise insulin receptor, ceramide-activated Ser-Thr phosphatases (PP1, PP2a), protein kinase B, protein kinase C zeta, and others [60–62]. It is not clear whether core clock components may be direct or indirect targets of sphingolipid species [58]. Further studies would be required to shed a light on the mechanisms underlying modulatory effect of sphingolipids on the molecular clock machinery.

Perturbation of islet sphingolipid metabolism takes part in pathogenesis of T2D early in disease development [53,63,64], as well as in T1D [65]. Due to the limited availability of human islets derived from T2D donors, we were unable to perform complete around the clock experiments for this part and compromised on 2-time point design. As a result, the temporal changes in lipid metabolites that are peaking at CT6 and CT18 were likely missed in T2D islets. The comparison of the lipid content between T2D and ND islets in 2 time points revealed an important modification of the sphingolipid fraction in the T2D islets (Fig 3). In line with altered levels of sphingolipids, expression of CERS2 and UGCG was also up-regulated in T2D islets as compared to ND counterparts (Fig 4B and 4D). Ceramide accumulation, in particular in skeletal muscle and white adipose tissue, is associated with impaired insulin signaling and T2D [38,48,66]. However, in our case, the most striking difference between T2D and ND islet lipid content relies on the levels of HexCer, and to some extent on DHCer. UGCG enzyme located in Golgi is essential for the formation of glucosylceramides (GlcCer), precursors for most complex glycosphingolipids [67]. These glycosylated sphingolipids mainly localize in the external leaflet of the plasma membrane. They are involved in various cellular processes, including calcium homeostasis [68], membrane trafficking, and formation of membrane microdomains [69,70] that play important roles in the dynamic aggregation of membrane receptors, as demonstrated for the insulin receptor in mouse adipocytes [71,72]. Noteworthy, -cell metabolic stress induced by acute palmitate treatment stimulates Cer production, while

longer (48 h) palmitate exposure increases, via the up-regulation of *UGCG*, the levels of GlcCer with no significant effect on SM and Cer accumulation, [42,73] thus recapitulating the changes we have detected in T2D human islets. Similarly, stress-induced Cer increase in keratinocytes following exposure to exogenous sphingomyelinase resulted in increased GlcCer synthase expression and GlcCer levels [74]. We hypothesize that enhancing the conversion of Cer into GlcCer, via the up-regulation of *UGCG*, prevents the deleterious effect of excessive Cer amounts and could thus reduce ER stress markers and apoptosis [74,75].

Here, we show that de novo production of sphingolipids is required for normal secretion of insulin by human islet cells in vitro, since application of sphingolipid synthesis inhibitor myriocin dampened the basal levels of secreted insulin in both ND and T2D human islet cells (Fig 6A–6C). Data in mouse islets and in rodent—cell line further support an important role of sphingolipid metabolism for insulin secretion, since inhibition of this pathway in rodent—cells by myriocin or fumonisin B1 attenuates insulin secretion [63,64]. At the same time, we showed that reduction of Cer by shunting them toward HexCer is necessary for proper basal and GSIS by human islet cells. Indeed, inhibition of GlcCer biosynthesis by PDMP significantly reduced basal insulin secretion and completely abolished their response to high glucose challenge or following KCL-triggered depolarization in vitro (Fig 6D and 6E). In addition to glucosylceramide synthase inhibition, the attenuation of mTOR signaling pathway and lysosomal lipid accumulation reported following PDMP treatment [76] may partly account for its inhibitory effect on insulin secretion. Importantly, knockdown of *UGCG* by siRNA in mouse islets also resulted in major insulin secretion defects [77], further suggesting that UGCG plays a key role in the observed phenotype.

Recent studies showed that pharmacological inhibition of 2 other ceramide-shunting pathways (sphingomyelin biosynthesis by D609 and S1P biosynthesis by sphingosine-kinase inhibitor SKI), similarly to described here HexCer biosynthesis inhibition by PDMP, significantly reduces basal and glucose-induced insulin secretion in vitro as well as in vivo in rodents [63,64]. In MIN6 cells, glucose stimulation enhanced conversion of Cer to GlcCer and to SM [78], as well as accumulation of S1P but not Cer [79]. Together, these data suggest that proper Cer homeostasis is required for stimulus-secretion coupling in -cells.

Noteworthy, several DHCer species were increased in T2D islets compared to ND islets, with a marked difference 12 h after synchronization (Figs 2A, 2G, 2J, 3A, 3C, and 3F). The significant increase of DHCer42:0(- H_2O) (C24DHCer) observed in the T2D islets may mask an up-regulation of C24DoxCer. We and others recently reported that noncanonical 1-deoxyceramide (DoxCer) levels were elevated in serum and adipose tissue of T2D patients [35,80]. Given that DoxCer has the exact same m/z ratio as DHCer- H_2O , these 2 lipid species may be misidentified, thus requiring a separate assessment using liquid chromatography mass spectrometry to be properly measured [35]. Deoxysphingolipids were shown to compromise GSIS in rodent islets and Ins-1 cells [34] allowing to envisage a specific role of these toxic sphingolipids in the failure of pancreatic -cells. Further lipidomic analyses in human islets should be conducted to conclude this link in humans.

Importantly, we demonstrate that the plasma membrane of T2D pancreatic islet cells is more rigid compared to ND counterparts (Fig 5A). Lowered membrane fluidity was reported in erythrocytes [81], leukocytes [82], and platelets [83,84] from T2D patients, suggesting a potential generality of membrane stiffness upon T2D. Strikingly, a similar phenotype was observed in clock-compromised islet cells from ND donors that exhibited stiffer plasma membrane than their counterparts bearing functional clocks (Fig 5B) and following direct sphingolipid perturbation by PDMP or myriocin (Fig 5C). Rheological properties of the membrane bilayer rely on lipid composition and cholesterol content [85,86]. Thus, saturated lipids increase membrane rigidity, whereas polyunsaturated phospholipids that bear more flexible

chains facilitate membrane conformational state changes by increasing membrane flexibility and fission [85,87–90]. Consequently, membrane PUFAs might be particularly critical for cells that go through multiple endocytic events such as epithelial cells [89]. Our lipidomic analysis revealed an overall trend for lowering PE species, with the levels of PE-PUFAs being significantly decreased in islets from T2D patients as compared to their ND counterparts (Figs 2P and 2Q and 3M and 3N). At the same time, the levels of PC lipids stayed relatively stable, thus resulting in increased PC/PE ratio that reaches significance at 24 h after synchronization (Fig 3K). Membrane fluidity impacts on cell communication with the environment by affecting the receptor function, signal transduction, endo-, and exocytosis. Indeed, decreased membrane fluidity reduces the insulin signaling in kidney mononuclear leukocytes and in diabetic kidney [82,91]. The exact mechanism of membrane fluidity changes in the clock-compromised and T2D human islet cells and its role on insulin secretion and signal transduction in -cells needs to be assessed in future studies.

In summary, our large-scale lipidomic analyses provide the first systematic characterization of the temporal organization of lipid metabolite landscape in human pancreatic islets from ND donors. Our recent study demonstrated that molecular clocks are compromised in pancreatic islets from T2D human donors, leading to disrupted absolute and temporal profiles of insulin and glucagon secretion [15]. Here, we report time-of-the-day-specific alterations of lipid metabolism in T2D human islets. The changes in lipid composition and saturation degree were concomitant with observed decrease of membrane fluidity in T2D human islets. Strikingly, a drop-in membrane fluidity was recapitulated in ND islets bearing compromised clocks, in line with a similar parallel between disrupted islet hormone secretion between T2D and ND islets transfected with siClock in our previous study [15]. Finally, our data suggest a reciprocal connection between the islet circadian clocks and Cer metabolism. Perturbation of Cer turnover observed in human pancreatic islets upon T2D may lead to exacerbation of the islet clock disruption and thus to further disturbance of lipid homeostasis in a feed-forward loop. Altogether, we provide a novel link between disruption of circadian clock, temporal coordination of lipid metabolism in human pancreatic islet, and islet dysfunction upon T2D in humans, highlighting both molecular oscillator and sphingolipid metabolites as important regulators of insulin secretion and membrane fluidity.

Material and methods

Pancreatic islet and islet cell culture

Human pancreatic islets were obtained from 4 different sources, summarized in Table 1: (i) Prodo Laboratories company (ND and T2D islets); (ii) Alberta Diabetes Institute islet core center (UAL) (ND and T2D islets); and (iii) Islet Transplantation Center of Geneva University Hospital (ND islets). T2D donors had a history of T2D and/or HbA_{1c} greater than 6.5%. Details of the islet donors are summarized in Table 1. All procedures using human islets were approved by the ethical committee of Geneva University Hospital CCER 2017–00147. Human pancreatic islets were cultured in CMRL 1066 medium, containing 5.5 mM glucose and supplemented with 10% fetal bovine serum (Gibco), 110 U/ml penicillin (Gibco), 110 μ g/ml streptomycin (Gibco), 50 μ g/ml gentamicin (Gibco), 2 mM L-glutamine (GlutaMax, Gibco), and 1 mM sodium pyruvate (Gibco). Islet cell gentle dissociation was done using 0.05% Trypsin (Gibco) treatment. For lipidomic analysis, approximately 600 islets were plated to 35-mm dishes (Falcon). For bioluminescence recordings, 100 islets were plated to multi-well plates (LifeSystemDesign). For the rest of the experiments, approximately 50,000 dissociated islet cells were attached to 35-mm dishes (Falcon). All dishes were precoated with a homemade laminin-5-rich extracellular matrix derived from 804G cells as described in [92].

Viral transduction and small interfering RNA transfection

Human islet cells were transduced with Per2-luc lentivectors as described in [14]. Dissociated adherent human islet cells were transfected twice with 50 nM siClock or with the same amount of nontargeting siControl (Dharmacon, GE Healthcare, Little Chalfont, United Kingdom) [13,52].

In vitro cell synchronization and circadian bioluminescence recording

Adherent islets were synchronized by a 1-h pulse of forskolin (10 μ M; Sigma, Saint-Louis, Missouri, United States of America) with a subsequent medium change. The islets were subjected to continuous bioluminescence recording in CMRL medium containing 100 μ M luciferin (D-luciferin 306–250, NanoLight Technology) during at least 5 consecutive days. For the experiments with ceramide and hexosylceramide biosynthesis inhibitors, 100 nM N-[2-hydroxy-1-(4-morpholinylmethyl)-2-phenylethyl]-decanamide, monohydrochloride (PDMP, Cayman Chemical) or 100 nM myriocin (Sigma-Aldrich), respectively, were applied together with forskolin synchronization pulse and added to the recording medium for the entire experiment duration. Bioluminescence pattern was monitored by a homemade robotic device equipped with photomultiplier tube detector assemblies, allowing the recording of 24-well plates [93] or by LumiCycle 96 (Actimetrics). In order to analyze the amplitude, period length, and phase of time series without the variability of magnitudes, raw data were processed in parallel graphs by moving average with a window of 24 h [13]. Cell apoptosis was assessed where indicated with Cell Death Detection ELISA kit (Roche) in the end of bioluminescence recording experiments, according to manufacturer instructions.

Lipid extraction procedures

The lipidomic extractions were performed as described in [35]. A total of 600 human islets were harvested (approximately 6×10^5 cells) at the indicated time points after 1-h pulse of forskolin synchronization (Fig 1A) or as indicated otherwise (Figs 2 and 3) and resuspended in 100 μL H₂O. Lipid extracts were prepared using a modified MTBE (methyl-tert-butyl ether) extraction protocol with addition of internal lipid standards [94]. Briefly, 360 µL methanol and a mix of internal standards were added (400 pmol PC 12:0/12:0, 1,000 pmol PE 17:0/14:1, 1,000 pmol PI 17:0/14:1, 3,300 pmol PS 17:0/14:1, 2,500 pmol SM d18:1/12:0, 500 pmol Cer d18:1/17:0, and 100 pmol GlcCer d18:1/8:0). After addition of 1.2 mL of MTBE, samples were placed for 10 min on a multitube vortexer at 4°C followed by incubation for 1 h at room temperature (RT) on a shaker. Phase separation was induced by addition of 200 μL MS-grade water. After 10 min at RT, samples were centrifuged at 1,000g for 10 min. The upper (organic) phase was transferred into a 13-mm glass tube, and the lower phase was re-extracted with 400 μL artificial upper phase [MTBE/methanol/H₂O (10:3:1.5, v/v/v)]. The combined organic phases were separated into 2 aliquots and dried in a vacuum concentrator (CentriVap, Labconco). Phospholipids were eluted with methanol ($3 \times 500 \,\mu\text{L}$) and divided into 2 aliquots. One aliquot was used for glycerophospholipid and phosphorus assay, respectively, while the other aliquot was treated by mild alkaline hydrolysis to enrich for sphingolipids, according to the method by Clarke [95]. Briefly, 1 mL freshly prepared monomethylamine reagent [methylamine/H₂O/n-butanol/methanol (5:3:1:4, (v/v/v/v)] was added to the dried lipid extract and then incubated at 53°C for 1 h in a water bath. Lipids were cooled to RT and then dried. For desalting, the dried lipid extract was resuspended in 300 µL water-saturated n-butanol and then extracted with 150 µL H₂O. The organic phase was collected, and the aqueous phase was re-extracted twice with 300 µL water-saturated n-butanol. The organic phases were pooled and dried in a vacuum concentrator.

Determination of total phosphorus

Total phosphorus was determined as described in [35]. Briefly, 100 μ L of the total lipid extract, resuspended in chloroform/methanol (1:1), were placed into 13-mm disposable pyrex tubes and dried in a vacuum concentrator, and 0, 2, 5, 10, 20 μ L of a 3 mmol/L KH₂PO₄ standard solution were placed into separate tubes. To each tube, distilled water was added to reach 20 μ L of aqueous solution. After addition of 140 μ L 70% perchloric acid, samples were heated at 180°C for 1 h in a chemical hood. Then, 800 μ L of a freshly prepared solution of water, ammonium molybdate (100 mg/8 mL H₂O), and ascorbic acid (100 mg/6 mL H₂O) in a ratio of 5:2:1 (v/v/v) were added. Tubes were heated at 100°C for 5 min and cooled at RT for 5 min. Approximately 100 μ L of each sample was then transferred into a 96-well microplate, and the absorbance at 820 nm was measured.

Phospho- and sphingolipid analysis by mass spectrometry

Mass spectrometry analysis was performed using multiple reaction monitoring on a TSQ Vantage Extended Mass Range Mass Spectrometer (Thermo Fisher Scientific), equipped with a robotic nanoflow ion source (Triversa Nanomate, Advion Biosciences) as previously described [35]. Optimized fragmentation was generated using appropriate collision energies and s-lens values for each lipid class. Mass spectrometry data were acquired with TSQ Tune 2.6 SP1 and treated with Xcalibur 4.0 QF2 software (Thermo Fisher Scientific). Lipid quantification was carried out using an analysis platform for lipidomics data hosted at EPFL Lausanne Switzerland (http://lipidomes.epfl.ch/). Quantification procedure was described in [96]. Dried lipid extracts were resuspended in 250 μ L MS-grade chloroform/methanol (1:1) and further diluted in either chloroform/methanol (1:2) plus 5 mmol/L ammonium acetate (negative ion mode) or in chloroform/methanol/H2O (2:7:1) plus 5 mmol/L ammonium acetate (positive ion mode).

RNA extraction and qPCR

Total RNA was prepared from cultured islet cells using RNeasy Plus Micro Kit (Qiagen). The RNA concentration was measured by Qubit RNA SH kit (Invitrogen). Then, 0.2 μ g of total RNA was reverse-transcribed using Superscript II (Invitrogen) and random hexamers and was PCR-amplified on a LightCycler 480 (Roche Diagnostics AG, Basel, Switzerland). Mean values for each sample were calculated from technical duplicates of each quantitative RT-PCR (qRT-PCR) analysis and normalized to the mean of housekeeping genes hypoxanthine-guanine phosphoribosyltransferase (*HPRT*) and *S9*. Primers used for this study are listed in S1 Table.

Membrane fluidity experiments

For assessment of membrane fluidity, the islets cells were seeded onto a glass-bottom dishes (Willco) at a density of 30,000 cells/dish. For microscopy imaging, the attached cells were washed once with warm CMRL 1066 medium with no phenol red (Gibco-Invitrogen), supplemented with 2 mM L-glutamine (GlutaMax, Gibco), 1 mM sodium pyruvate (Gibco), and 15 mM HEPES to maintain pH. After that, 200 μ L of a 2 μ M NS12R dye solution (Klymchenko Laboratory [50]) diluted in the same medium was added, and the cells were incubated for 5 min at RT. Cells were washed 3 times with the warm medium and immediately subjected to fluorescence microscopy using a Nikon A1r microscope, equipped with CFI Plan Apo ×60 oil (NA = 1.4) objective. The excitation in confocal mode was provided by a 488-nm laser, while the fluorescence was detected at 2 spectral ranges: 550 to 600 ($I_{550-600}$) and 600 to 650 ($I_{600-650}$)

nm in sequential mode by rapid switching to minimize drift. All the parameters at each channel were left constant. The laser power was set at 1% of maximum intensity to achieve a good signal. At least 10 confocal images were recorded using NIS Elements per 1 dish. The fluorescence shift radiometry was assessed using Fiji after outlaying membrane area. GP was calculated as follows: $GP = (I_{550-600} - gI_{600-650})/(I_{550-600} + gI_{600-650})$. Where coefficient g was previously calculated for the NR12S solution in CMRL.

Data quantification and analyses

Lipid concentrations were calculated relative to the relevant internal standards and normalized to the total phosphate content of each total lipid extract (S1–S3 Data). Then, for comparison between different lipids samples, relative lipid concentrations were normalized to the total lipid content of each lipid extract (mol%). For temporal analysis, normalized lipid values were z-scored within patients. To identify circadian variations within the lipidomic data set, normalized lipid values were further analyzed using the METACYCLE v1.2.0 algorithm in R Bioconductor v3.11 [97]. The period width was set to fit a time frame of 20 to 28 h and a p value of ≤ 0.05 was considered statistically significant.

Lipid concentrations were corrected for class II isotopic overlaps for the analysis of lipid degree of saturation as described in [98]. Briefly, correction factors for deisotoping were derived using theoretical M+2 abundances calculated using the Envipat Web 2.4 tool (https://www.envipat.eawag.ch/) applying a mass resolution of 5,000. These theoretical M+2 abundances were multiplied by a correction factor accounting for the probability at random distribution of two 13 C isotopes within the remaining heavy fragment generated during the fragmentation in the collision chamber (Q2) but not detected in the Q3. The resulting formula for correction is: M + 2_{correction} = (M + 2_{theoretical})×((n_{heavy})/(m_{total}))² with n_{heavy} being the number of carbons in the heavy fragment, and m_{total}, the number of carbons in the entire lipid molecule. For each lipid species, the corrected M + 2 signal was calculated and subtracted from the acquired signal for the lipid species with m/z + 2 within a series of lipid species from the same lipid class, beginning with the most desaturated species, stepwise until reaching the fully saturated form.

Additional data processing (filtering, normalization, transformation, scaling), statistical analyses, and data plotting were performed using MetaboAnalyst 5.0 [97] and Prism Graph Pad 8.0. Statistical tests used for comparison between groups are indicated in the figure legends. Differences were considered significant for $p \le 0.05$ (*), $p \le 0.01$ (***), and $p \le 0.001$ (***).

To determine the clustering, k-NN (nearest neighbors with k clusters) was applied to the phases and amplitudes in polar coordinates of all circadian signals for k = 1, 2, and 3 clusters.

Supporting information

S1 Fig. Oscillations of core clock and clock-related genes in forskolin-synchronized human islets.

(DOCX)

S2 Fig. Lipidomic analyses of human islets derived from T2D versus ND donors cultured and synchronized in vitro.

(DOCX)

S3 Fig. Up-regulation of sphingolipid metabolism in clock-deficient human islet cells. (DOCX)

S4 Fig. PDMP inhibits basal (1 h at 2.8 mmol glucose) and glucose-induced (1 h at 16.7 mmol) insulin secretion in human islet cells from T2D donor in vitro (n = 1). (DOCX)

S5 Fig. Assessment of apoptosis in pancreatic islets treated with myriocin or PDMP during continuous bioluminescence recordings for 5 days.

(DOCX)

S1 Table. Sequences of quantitative RT-PCR primers. (DOCX)

S1 Data. Lipidomic data regarding the human pancreatic islets from ND donors synchronized in vitro.

(XLSX)

S2 Data. Rhythmic islet lipids according to METACYCLE algorithm (p < 0.05). (XLSX)

S3 Data. Lipidomic data regarding the human pancreatic islets from ND and T2D donors collected 12 h and 24 h after synchronization.

(XLSX)

S4 Data. Raw data for Figs 4–6. Naming of sheets corresponds to the relevant figures. Data for assigned figure panels on sheet is introduced with corresponding legend. (XLSX)

S5 Data. Raw data for S1 and S3-S5 Figs. Naming of sheets corresponds to the relevant supplemental figures. Data for assigned figure panels on sheet is introduced with corresponding legend. (XLSX)

Acknowledgments

The authors thank Domenico Bosco and Thierry Berney (Islet Transplantation Center of Geneva University Hospital), Eduard Montanya Mias and Montserrat Nacher Garcia (Hospital Universitari de Bellvitge, Barcelona) and Alberta Diabetes Institute IsletCore for providing human islets; Giovanni d'Angelo (EPFL) for support with the lipidomic analyses and for constructive discussions; François Prodon and Bioimaging platform team, Faculty of Medicine, University of Geneva; Andrey Klymchenko (CNRS, Strasbourg) for generously sharing Nile Red dye NR12S.

Author Contributions

Conceptualization: Volodymyr Petrenko, Flore Sinturel, Howard Riezman, Charna Dibner.

Data curation: Volodymyr Petrenko, Flore Sinturel, Ursula Loizides-Mangold, Jonathan Paz Montoya, Simona Chera, Charna Dibner.

Formal analysis: Volodymyr Petrenko, Flore Sinturel, Ursula Loizides-Mangold, Jonathan Paz Montoya, Simona Chera.

Funding acquisition: Volodymyr Petrenko, Howard Riezman, Charna Dibner.

Investigation: Volodymyr Petrenko, Flore Sinturel, Ursula Loizides-Mangold, Jonathan Paz Montoya, Simona Chera, Charna Dibner.

Methodology: Volodymyr Petrenko, Flore Sinturel, Ursula Loizides-Mangold, Jonathan Paz Montoya, Howard Riezman.

Project administration: Howard Riezman, Charna Dibner.

Resources: Charna Dibner. **Software:** Simona Chera.

Supervision: Howard Riezman, Charna Dibner.

Validation: Volodymyr Petrenko, Flore Sinturel, Ursula Loizides-Mangold, Jonathan Paz Montoya, Simona Chera, Howard Riezman, Charna Dibner.

Visualization: Volodymyr Petrenko, Flore Sinturel, Simona Chera.

Writing – original draft: Volodymyr Petrenko, Flore Sinturel, Charna Dibner.

Writing – review & editing: Volodymyr Petrenko, Flore Sinturel, Ursula Loizides-Mangold, Jonathan Paz Montoya, Simona Chera, Howard Riezman, Charna Dibner.

References

- Dibner C. The importance of being rhythmic: Living in harmony with your body clocks. Acta Physiol (Oxf). 2020; 228(1):e13281. Epub 2019/04/14. https://doi.org/10.1111/apha.13281 PMID: 30980501.
- Dibner C, Schibler U. Circadian timing of metabolism in animal models and humans. J Intern Med. 2015. Epub 2015/01/21. https://doi.org/10.1111/joim.12347 PMID: 25599827.
- Sinturel F, Petrenko V, Dibner C. Circadian Clocks Make Metabolism Run. J Mol Biol. 2020; 432 (12):3680–99. Epub 2020/01/31. https://doi.org/10.1016/j.jmb.2020.01.018 PMID: 31996313.
- Finger AM, Dibner C, Kramer A. Coupled network of the circadian clocks: a driving force of rhythmic physiology. FEBS Lett. 2020; 594(17):2734–69. Epub 2020/08/05. https://doi.org/10.1002/1873-3468. 13898 PMID: 32750151.
- Allada R, Bass J. Circadian Mechanisms in Medicine. N Engl J Med. 2021; 384(6):550–61. Epub 2021/ 02/11. https://doi.org/10.1056/NEJMra1802337 PMID: 33567194; PubMed Central PMCID: PMC8108270.
- Rijo-Ferreira F, Takahashi JS. Genomics of circadian rhythms in health and disease. Genome Med. 2019; 11(1):82. Epub 2019/12/19. https://doi.org/10.1186/s13073-019-0704-0 PMID: 31847894; PubMed Central PMCID: PMC6916512.
- Perelis M, Marcheva B, Ramsey KM, Schipma MJ, Hutchison AL, Taguchi A, et al. Pancreatic beta cell enhancers regulate rhythmic transcription of genes controlling insulin secretion. Science. 2015; 350 (6261):aac4250. https://doi.org/10.1126/science.aac4250 PMID: 26542580; PubMed Central PMCID: PMC4669216.
- Petrenko V, Saini C, Giovannoni L, Gobet C, Sage D, Unser M, et al. Pancreatic alpha- and beta-cellular clocks have distinct molecular properties and impact on islet hormone secretion and gene expression. Genes Dev. 2017; 31(4):383–398. https://doi.org/10.1101/gad.290379.116 PMID: 28275001; PubMed Central PMCID: PMC5358758.
- Petrenko V, Dibner C. Circadian orchestration of insulin and glucagon release. Cell Cycle. 2017;1–2. https://doi.org/10.1080/15384101.2017.1326768 PMID: 28537528.
- Petrenko V, Stolovich-Rain M, Vandereycken B, Giovannoni L, Storch KF, Dor Y, et al. The core clock transcription factor BMAL1 drives circadian beta-cell proliferation during compensatory regeneration of the endocrine pancreas. Genes Dev. 2020; 34(23–24):1650–65. Epub 2020/11/14. https://doi.org/10. 1101/gad.343137.120 PMID: 33184223; PubMed Central PMCID: PMC7706703.
- Petrenko V, Dibner C. Cell-specific resetting of mouse islet cellular clocks by glucagon, glucagon-like peptide 1 and somatostatin. Acta Physiol (Oxf). 2017. https://doi.org/10.1111/apha.13021 PMID: 29271578.
- Marcheva B, Ramsey KM, Buhr ED, Kobayashi Y, Su H, Ko CH, et al. Disruption of the clock components CLOCK and BMAL1 leads to hypoinsulinaemia and diabetes. Nature. 2010; 466(7306):627–31. Epub 2010/06/22. https://doi.org/10.1038/nature09253 [pii] PMID: 20562852; PubMed Central PMCID: PMC2920067.

- Saini C, Petrenko V, Pulimeno P, Giovannoni L, Berney T, Hebrok M, et al. A functional circadian clock is required for proper insulin secretion by human pancreatic islet cells. Diabetes Obes Metab. 2016; 18 (4):355–365. https://doi.org/10.1111/dom.12616 PMID: 26662378.
- Pulimeno P, Mannic T, Sage D, Giovannoni L, Salmon P, Lemeille S, et al. Autonomous and self-sustained circadian oscillators displayed in human islet cells. Diabetologia. 2013; 56(3):497–507. Epub 2012/12/18. https://doi.org/10.1007/s00125-012-2779-7 PMID: 23242133; PubMed Central PMCID: PMC3563957.
- 15. Petrenko V, Gandasi NR, Sage D, Tengholm A, Barg S, Dibner C. In pancreatic islets from type 2 diabetes patients, the dampened circadian oscillators lead to reduced insulin and glucagon exocytosis. Proc Natl Acad Sci U S A. 2020; 117(5):2484–95. Epub 2020/01/23. https://doi.org/10.1073/pnas. 1916539117 PMID: 31964806; PubMed Central PMCID: PMC7007532.
- Chaurasia B, Summers SA. Ceramides in Metabolism: Key Lipotoxic Players. Annu Rev Physiol. 2021; 83:303–30. Epub 2020/11/08. https://doi.org/10.1146/annurev-physiol-031620-093815 PMID: 33158378; PubMed Central PMCID: PMC7905841.
- Meikle PJ, Summers SA. Sphingolipids and phospholipids in insulin resistance and related metabolic disorders. Nat Rev Endocrinol. 2017; 13(2):79–91. https://doi.org/10.1038/nrendo.2016.169 PMID: 27767036.
- Harayama T, Riezman H. Understanding the diversity of membrane lipid composition. Nat Rev Mol Cell Biol. 2018. https://doi.org/10.1038/nrm.2017.138 PMID: 29410529
- Jimenez-Rojo N, Leonetti MD, Zoni V, Colom A, Feng S, Iyengar NR, et al. Conserved Functions of Ether Lipids and Sphingolipids in the Early Secretory Pathway. Curr Biol. 2020; 30(19):3775–87 e7. Epub 2020/08/29. https://doi.org/10.1016/j.cub.2020.07.059 PMID: 32857977.
- Loewith R, Riezman H, Winssinger N. Sphingolipids and membrane targets for therapeutics. Curr Opin Chem Biol. 2019; 50:19–28. Epub 2019/03/22. https://doi.org/10.1016/j.cbpa.2019.02.015 PMID: 30897494.
- Shevchenko A, Simons K. Lipidomics: coming to grips with lipid diversity. Nat Rev Mol Cell Biol. 2010; 11(8):593–8. Epub 2010/07/08. https://doi.org/10.1038/nrm2934 PMID: 20606693.
- Eggers LF, Schwudke D. Shotgun Lipidomics Approach for Clinical Samples. Methods Mol Biol. 2018; 1730:163–74. Epub 2018/01/25. https://doi.org/10.1007/978-1-4939-7592-1 12 PMID: 29363073.
- 23. Adamovich Y, Rousso-Noori L, Zwighaft Z, Neufeld-Cohen A, Golik M, Kraut-Cohen J, et al. Circadian clocks and feeding time regulate the oscillations and levels of hepatic triglycerides. Cell Metab. 2014; 19(2):319–330. https://doi.org/10.1016/j.cmet.2013.12.016 PMID: 24506873; PubMed Central PMCID: PMC4261230.
- Dallmann R, Viola AU, Tarokh L, Cajochen C, Brown SA. The human circadian metabolome. Proc Natl Acad Sci U S A. 2012; 109(7):2625–9. Epub 2012/02/07. https://doi.org/10.1073/pnas.1114410109
 PMID: 22308371; PubMed Central PMCID: PMC3289302.
- 25. Chua EC, Shui G, Lee IT, Lau P, Tan LC, Yeo SC, et al. Extensive diversity in circadian regulation of plasma lipids and evidence for different circadian metabolic phenotypes in humans. Proc Natl Acad Sci U S A. 2013; 110(35):14468–73. Epub 2013/08/16. https://doi.org/10.1073/pnas.1222647110 PMID: 23946426; PubMed Central PMCID: PMC3761633.
- Sinturel F, Spaleniak W, Dibner C. Circadian rhythm of lipid metabolism. Biochem Soc Trans. 2022. Epub 2022/05/24. https://doi.org/10.1042/BST20210508 PMID: 35604112.
- Loizides-Mangold U, Petrenko V, Dibner C. Circadian Lipidomics: Analysis of Lipid Metabolites Around the Clock. Methods Mol Biol. 2021; 2130:169–83. Epub 2020/12/08. https://doi.org/10.1007/978-1-0716-0381-9_13 PMID: 33284444.
- 28. Held NM, Wefers J, van Weeghel M, Daemen S, Hansen J, Vaz FM, et al. Skeletal muscle in healthy humans exhibits a day-night rhythm in lipid metabolism. Mol Metab. 2020; 37:100989. Epub 2020/04/10. https://doi.org/10.1016/j.molmet.2020.100989 PMID: 32272236; PubMed Central PMCID: PMC7217992.
- Loizides-Mangold U, Perrin L, Vandereycken B, Betts JA, Walhin JP, Templeman I, et al. Lipidomics reveals diurnal lipid oscillations in human skeletal muscle persisting in cellular myotubes cultured in vitro. Proc Natl Acad Sci U S A. 2017. https://doi.org/10.1073/pnas.1705821114 PMID: 28973848.
- Perrin L, Loizides-Mangold U, Chanon S, Gobet C, Hulo N, Isenegger L, et al. Transcriptomic analyses reveal rhythmic and CLOCK-driven pathways in human skeletal muscle. Elife. 2018; 7. https://doi.org/10.7554/eLife.34114 PMID: 29658882
- Chaurasia B, Tippetts TS, Mayoral Monibas R, Liu J, Li Y, Wang L, et al. Targeting a ceramide double bond improves insulin resistance and hepatic steatosis. Science. 2019; 365(6451):386–92. Epub 2019/07/06. https://doi.org/10.1126/science.aav3722 PMID: 31273070; PubMed Central PMCID: PMC6787918.

- Chaurasia B, Summers SA. Ceramides—Lipotoxic Inducers of Metabolic Disorders. Trends Endocrinol Metab. 2015; 26(10):538–550. https://doi.org/10.1016/j.tem.2015.07.006 PMID: 26412155.
- Othman A, Saely CH, Muendlein A, Vonbank A, Drexel H, von Eckardstein A, et al. Plasma 1-deoxy-sphingolipids are predictive biomarkers for type 2 diabetes mellitus. BMJ Open Diabetes Res Care. 2015; 3(1):e000073. https://doi.org/10.1136/bmjdrc-2014-000073 PMID: 25815206; PubMed Central PMCID: PMC4368929.
- Zuellig RA, Hornemann T, Othman A, Hehl AB, Bode H, Guntert T, et al. Deoxysphingolipids, novel biomarkers for type 2 diabetes, are cytotoxic for insulin-producing cells. Diabetes. 2014; 63(4):1326–1339. https://doi.org/10.2337/db13-1042 PMID: 24379346.
- Hannich JT, Loizides-Mangold U, Sinturel F, Harayama T, Vandereycken B, Saini C, et al. Ether lipids, sphingolipids and toxic 1-deoxyceramides as hallmarks for lean and obese type 2 diabetic patients. Acta Physiol (Oxf). 2020:e13610. Epub 2020/12/23. https://doi.org/10.1111/apha.13610 PMID: 33351229.
- Hilvo M, Salonurmi T, Havulinna AS, Kauhanen D, Pedersen ER, Tell GS, et al. Ceramide stearic to palmitic acid ratio predicts incident diabetes. Diabetologia. 2018; 61(6):1424–1434. https://doi.org/10.1007/s00125-018-4590-6 PMID: 29546476.
- Hla T, Kolesnick R. C16:0-ceramide signals insulin resistance. Cell Metab. 2014; 20(5):703–705. https://doi.org/10.1016/j.cmet.2014.10.017 PMID: 25440051; PubMed Central PMCID: PMC4393079.
- Holland WL, Brozinick JT, Wang LP, Hawkins ED, Sargent KM, Liu Y, et al. Inhibition of ceramide synthesis ameliorates glucocorticoid-, saturated-fat-, and obesity-induced insulin resistance. Cell Metab. 2007; 5(3):167–179. https://doi.org/10.1016/j.cmet.2007.01.002 PMID: 17339025.
- Chew WS, Torta F, Ji S, Choi H, Begum H, Sim X, et al. Large-scale lipidomics identifies associations between plasma sphingolipids and T2DM incidence. JCI Insight. 2019; 5. Epub 2019/06/05. https://doi. org/10.1172/jci.insight.126925 PMID: 31162145; PubMed Central PMCID: PMC6629294.
- 40. Wigger L, Cruciani-Guglielmacci C, Nicolas A, Denom J, Fernandez N, Fumeron F, et al. Plasma Dihydroceramides Are Diabetes Susceptibility Biomarker Candidates in Mice and Humans. Cell Rep. 2017; 18(9):2269–2279. https://doi.org/10.1016/j.celrep.2017.02.019 PMID: 28249170.
- Othman A, Rutti MF, Ernst D, Saely CH, Rein P, Drexel H, et al. Plasma deoxysphingolipids: a novel class of biomarkers for the metabolic syndrome? Diabetologia. 2012; 55(2):421–431. https://doi.org/10.1007/s00125-011-2384-1 PMID: 22124606.
- 42. Boslem E, MacIntosh G, Preston AM, Bartley C, Busch AK, Fuller M, et al. A lipidomic screen of palmitate-treated MIN6 beta-cells links sphingolipid metabolites with endoplasmic reticulum (ER) stress and impaired protein trafficking. Biochem J. 2011; 435(1):267–76. Epub 2011/01/27. https://doi.org/10.1042/BJ20101867 PMID: 21265737.
- MacDonald MJ, Ade L, Ntambi JM, Ansari IU, Stoker SW. Characterization of phospholipids in insulin secretory granules and mitochondria in pancreatic beta cells and their changes with glucose stimulation. J Biol Chem. 2015; 290(17):11075–92. Epub 2015/03/13. https://doi.org/10.1074/jbc.M114.628420
 PMID: 25762724: PubMed Central PMCID: PMC4409267.
- 44. Sanchez-Archidona AR, Cruciani-Guglielmacci C, Roujeau C, Wigger L, Lallement J, Denom J, et al. Plasma triacylglycerols are biomarkers of beta-cell function in mice and humans. Mol Metab. 2021; 54:101355. Epub 2021/10/12. https://doi.org/10.1016/j.molmet.2021.101355 PMID: 34634522; PubMed Central PMCID: PMC8602044.
- 45. van der Veen JN, Kennelly JP, Wan S, Vance JE, Vance DE, Jacobs RL. The critical role of phosphatidylcholine and phosphatidylethanolamine metabolism in health and disease. Biochim Biophys Acta Biomembr. 2017; 1859(9 Pt B):1558–72. https://doi.org/10.1016/j.bbamem.2017.04.006 PMID: 28411170.
- 46. Harayama T, Shimizu T. Roles of polyunsaturated fatty acids, from mediators to membranes. J Lipid Res. 2020; 61(8):1150–60. Epub 2020/06/04. https://doi.org/10.1194/jlr.R120000800 PMID: 32487545; PubMed Central PMCID: PMC7397749.
- 47. Zitomer NC, Mitchell T, Voss KA, Bondy GS, Pruett ST, Garnier-Amblard EC, et al. Ceramide synthase inhibition by fumonisin B1 causes accumulation of 1-deoxysphinganine: a novel category of bioactive 1-deoxysphingoid bases and 1-deoxydihydroceramides biosynthesized by mammalian cell lines and animals. J Biol Chem. 2009; 284(8):4786–4795. https://doi.org/10.1074/jbc.M808798200 PMID: 19095642; PubMed Central PMCID: PMC2643501.
- 48. Turpin SM, Nicholls HT, Willmes DM, Mourier A, Brodesser S, Wunderlich CM, et al. Obesity-induced CerS6-dependent C16:0 ceramide production promotes weight gain and glucose intolerance. Cell Metab. 2014; 20(4):678–86. Epub 2014/10/09. https://doi.org/10.1016/j.cmet.2014.08.002 PMID: 25295788.
- Mullen TD, Hannun YA, Obeid LM. Ceramide synthases at the centre of sphingolipid metabolism and biology. Biochem J. 2012; 441(3):789–802. Epub 2012/01/18. https://doi.org/10.1042/BJ20111626 PMID: 22248339; PubMed Central PMCID: PMC3689921.

- Kucherak OA, Oncul S, Darwich Z, Yushchenko DA, Arntz Y, Didier P, et al. Switchable nile red-based probe for cholesterol and lipid order at the outer leaflet of biomembranes. J Am Chem Soc. 2010; 132 (13):4907–4916. https://doi.org/10.1021/ja100351w PMID: 20225874.
- Owen DM, Rentero C, Magenau A, Abu-Siniyeh A, Gaus K. Quantitative imaging of membrane lipid order in cells and organisms. Nat Protoc. 2012; 7(1):24–35. https://doi.org/10.1038/nprot.2011.419 PMID: 22157973.
- Petrenko V, Saini C, Perrin L, Dibner C. Parallel Measurement of Circadian Clock Gene Expression and Hormone Secretion in Human Primary Cell Cultures. J Vis Exp. 2016;(117). https://doi.org/10.3791/54673 PMID: 27911383.
- Wuttke A. Lipid signalling dynamics at the beta-cell plasma membrane. Basic Clin Pharmacol Toxicol. 2015; 116(4):281–90. Epub 2014/12/23. https://doi.org/10.1111/bcpt.12369 PMID: 25529872.
- 54. Hagren OI, Tengholm A. Glucose and insulin synergistically activate phosphatidylinositol 3-kinase to trigger oscillations of phosphatidylinositol 3,4,5-trisphosphate in beta-cells. J Biol Chem. 2006; 281 (51):39121–7. Epub 2006/11/01. https://doi.org/10.1074/jbc.M607445200 PMID: 17074763.
- Wuttke A, Idevall-Hagren O, Tengholm A. Imaging phosphoinositide dynamics in living cells. Methods Mol Biol. 2010; 645:219–35. Epub 2010/07/21. https://doi.org/10.1007/978-1-60327-175-2_14 PMID: 20645191.
- Zheng B, Larkin DW, Albrecht U, Sun ZS, Sage M, Eichele G, et al. The mPer2 gene encodes a functional component of the mammalian circadian clock. Nature. 1999; 400(6740):169–73. Epub 1999/07/17. https://doi.org/10.1038/22118 PMID: 10408444.
- 57. Bae K, Jin X, Maywood ES, Hastings MH, Reppert SM, Weaver DR. Differential functions of mPer1, mPer2, and mPer3 in the SCN circadian clock. Neuron. 2001; 30(2):525–36. Epub 2001/06/08. https://doi.org/10.1016/s0896-6273(01)00302-6 PMID: 11395012.
- Brenna A, Albrecht U. Phosphorylation and Circadian Molecular Timing. Front Physiol. 2020;
 11:612510. Epub 2020/12/17. https://doi.org/10.3389/fphys.2020.612510 PMID: 33324245; PubMed Central PMCID: PMC7726318.
- 59. Vanselow K, Vanselow JT, Westermark PO, Reischl S, Maier B, Korte T, et al. Differential effects of PER2 phosphorylation: molecular basis for the human familial advanced sleep phase syndrome (FASPS). Genes Dev. 2006; 20(19):2660–72. Epub 2006/09/20. https://doi.org/10.1101/gad.397006 PMID: 16983144; PubMed Central PMCID: PMC1578693.
- Bartke N, Hannun YA. Bioactive sphingolipids: metabolism and function. J Lipid Res. 2009; 50(Suppl: S91-6). Epub 2008/11/20. https://doi.org/10.1194/jlr.R800080-JLR200 PMID: 19017611; PubMed Central PMCID: PMC2674734.
- Hannun YA, Obeid LM. Principles of bioactive lipid signalling: lessons from sphingolipids. Nat Rev Mol Cell Biol. 2008; 9(2):139–50. Epub 2008/01/25. https://doi.org/10.1038/nrm2329 PMID: 18216770.
- Russo D, Parashuraman S, D'Angelo G. Glycosphingolipid-Protein Interaction in Signal Transduction. Int J Mol Sci. 2016; 17(10). Epub 2016/10/19. https://doi.org/10.3390/ijms17101732 PMID: 27754465; PubMed Central PMCID: PMC5085762.
- 63. Khan SR, Manialawy Y, Obersterescu A, Cox BJ, Gunderson EP, Wheeler MB. Diminished Sphingolipid Metabolism, a Hallmark of Future Type 2 Diabetes Pathogenesis, Is Linked to Pancreatic beta Cell Dysfunction. iScience. 2020; 23(10):101566. Epub 2020/10/27. https://doi.org/10.1016/j.isci.2020. 101566 PMID: 33103069; PubMed Central PMCID: PMC7578680.
- 64. Khan SR, Mohan H, Liu Y, Batchuluun B, Gohil H, Al Rijjal D, et al. The discovery of novel predictive biomarkers and early-stage pathophysiology for the transition from gestational diabetes to type 2 diabetes. Diabetologia. 2019; 62(4):687–703. Epub 2019/01/16. https://doi.org/10.1007/s00125-018-4800-2 PMID: 30645667; PubMed Central PMCID: PMC7237273.
- 65. Holm LJ, Krogvold L, Hasselby JP, Kaur S, Claessens LA, Russell MA, et al. Abnormal islet sphingolipid metabolism in type 1 diabetes. Diabetologia. 2018; 61(7):1650–61. Epub 2018/04/20. https://doi.org/10.1007/s00125-018-4614-2 PMID: 29671030; PubMed Central PMCID: PMC6445476.
- 66. Turpin SM, Lancaster GI, Darby I, Febbraio MA, Watt MJ. Apoptosis in skeletal muscle myotubes is induced by ceramides and is positively related to insulin resistance. Am J Physiol Endocrinol Metab. 2006; 291(6):E1341–50. Epub 2006/07/20. https://doi.org/10.1152/ajpendo.00095.2006 PMID: 16849630.
- 67. Ichikawa S, Sakiyama H, Suzuki G, Hidari KI, Hirabayashi Y. Expression cloning of a cDNA for human ceramide glucosyltransferase that catalyzes the first glycosylation step of glycosphingolipid synthesis. Proc Natl Acad Sci U S A. 1996; 93(10):4638–43. Epub 1996/05/14. https://doi.org/10.1073/pnas.93. 10.4638 PMID: 8643456; PubMed Central PMCID: PMC39331.
- **68.** Lloyd-Evans E, Pelled D, Riebeling C, Bodennec J, de-Morgan A, Waller H, et al. Glucosylceramide and glucosylsphingosine modulate calcium mobilization from brain microsomes via different

- mechanisms. J Biol Chem. 2003; 278(26):23594–9. Epub 2003/04/24. https://doi.org/10.1074/jbc. M300212200 PMID: 12709427.
- 69. Westerlund B, Slotte JP. How the molecular features of glycosphingolipids affect domain formation in fluid membranes. Biochim Biophys Acta. 2009; 1788(1):194–201. Epub 2008/12/17. https://doi.org/10.1016/j.bbamem.2008.11.010 PMID: 19073136.
- Sillence DJ, Puri V, Marks DL, Butters TD, Dwek RA, Pagano RE, et al. Glucosylceramide modulates membrane traffic along the endocytic pathway. J Lipid Res. 2002; 43(11):1837–45. Epub 2002/10/29. https://doi.org/10.1194/jlr.m200232-jlr200 PMID: 12401882.
- Inokuchi J. Membrane microdomains and insulin resistance. FEBS Lett. 2010; 584(9):1864–71. Epub 2009/10/14. https://doi.org/10.1016/j.febslet.2009.10.012 PMID: 19822143.
- 72. Kabayama K, Sato T, Saito K, Loberto N, Prinetti A, Sonnino S, et al. Dissociation of the insulin receptor and caveolin-1 complex by ganglioside GM3 in the state of insulin resistance. Proc Natl Acad Sci U S A. 2007; 104(34):13678–83. Epub 2007/08/19. https://doi.org/10.1073/pnas.0703650104 PMID: 17699617; PubMed Central PMCID: PMC1949342.
- Veret J, Coant N, Berdyshev EV, Skobeleva A, Therville N, Bailbe D, et al. Ceramide synthase 4 and de novo production of ceramides with specific N-acyl chain lengths are involved in glucolipotoxicity-induced apoptosis of INS-1 beta-cells. Biochem J. 2011; 438(1):177–89. Epub 2011/05/20. https://doi.org/10.1042/BJ20101386 PMID: 21592087.
- Uchida Y, Murata S, Schmuth M, Behne MJ, Lee JD, Ichikawa S, et al. Glucosylceramide synthesis and synthase expression protect against ceramide-induced stress. J Lipid Res. 2002; 43(8):1293–302. Epub 2002/08/15. PMID: 12177173.
- 75. Turpin-Nolan SM, Bruning JC. The role of ceramides in metabolic disorders: when size and localization matters. Nat Rev Endocrinol. 2020; 16(4):224–33. Epub 2020/02/16. https://doi.org/10.1038/s41574-020-0320-5 PMID: 32060415.
- 76. Hartwig P, Hoglinger D. The Glucosylceramide Synthase Inhibitor PDMP Causes Lysosomal Lipid Accumulation and mTOR Inactivation. Int J Mol Sci. 2021; 22(13). Epub 2021/07/03. https://doi.org/10.3390/ijms22137065 PMID: 34209164; PubMed Central PMCID: PMC8268262.
- Jennemann R, Kaden S, Volz M, Nordstrom V, Herzer S, Sandhoff R, et al. Gangliosides modulate insulin secretion by pancreatic beta cells under glucose stress. Glycobiology. 2020; 30(9):722–34. Epub 2020/03/10. https://doi.org/10.1093/glycob/cwaa022 PMID: 32149357.
- 78. Pearson GL, Mellett N, Chu KY, Boslem E, Meikle PJ, Biden TJ. A comprehensive lipidomic screen of pancreatic beta-cells using mass spectroscopy defines novel features of glucose-stimulated turnover of neutral lipids, sphingolipids and plasmalogens. Mol Metab. 2016; 5(6):404–14. Epub 2016/06/04. https://doi.org/10.1016/j.molmet.2016.04.003 PMID: 27257600; PubMed Central PMCID: PMC4877660.
- Cantrell Stanford J, Morris AJ, Sunkara M, Popa GJ, Larson KL, Ozcan S. Sphingosine 1-phosphate (S1P) regulates glucose-stimulated insulin secretion in pancreatic beta cells. J Biol Chem. 2012; 287 (16):13457–64. Epub 2012/03/06. https://doi.org/10.1074/jbc.M111.268185 PMID: 22389505; PubMed Central PMCID: PMC3339968.
- 80. Bertea M, Rutti MF, Othman A, Marti-Jaun J, Hersberger M, von Eckardstein A, et al. Deoxysphingoid bases as plasma markers in diabetes mellitus. Lipids Health Dis. 2010; 9:84. Epub 2010/08/18. https://doi.org/10.1186/1476-511X-9-84 PMID: 20712864; PubMed Central PMCID: PMC2931514.
- Kamada T, McMillan DE, Yamashita T, Otsuji S. Lowered membrane fluidity of younger erythrocytes in diabetes. Diabetes Res Clin Pract. 1992; 16(1):1–6. Epub 1992/04/01. https://doi.org/10.1016/0168-8227(92)90128-e PMID: 1576926.
- 82. Tong P, Thomas T, Berrish T, Humphriss D, Barriocanal L, Stewart M, et al. Cell membrane dynamics and insulin resistance in non-insulin-dependent diabetes mellitus. Lancet. 1995; 345(8946):357–8. Epub 1995/02/11. https://doi.org/10.1016/s0140-6736(95)90343-7 PMID: 7845118.
- Watala C, Boncler M, Golanski J, Koziolkiewcz W, Trojanowski Z, Walkowiak B. Platelet membrane lipid fluidity and intraplatelet calcium mobilization in type 2 diabetes mellitus. Eur J Haematol. 1998; 61 (5):319–26. Epub 1998/12/17. https://doi.org/10.1111/j.1600-0609.1998.tb01095.x PMID: 9855247.
- 84. Winocour PD, Bryszewska M, Watala C, Rand ML, Epand RM, Kinlough-Rathbone RL, et al. Reduced membrane fluidity in platelets from diabetic patients. Diabetes. 1990; 39(2):241–4. Epub 1990/02/01. https://doi.org/10.2337/diab.39.2.241 PMID: 2227132.
- 85. Rawicz W, Olbrich KC, McIntosh T, Needham D, Evans E. Effect of chain length and unsaturation on elasticity of lipid bilayers. Biophys J. 2000; 79(1):328–39. Epub 2000/06/27. https://doi.org/10.1016/S0006-3495(00)76295-3 PMID: 10866959; PubMed Central PMCID: PMC1300937.
- 86. Chakraborty S, Doktorova M, Molugu TR, Heberle FA, Scott HL, Dzikovski B, et al. How cholesterol stiffens unsaturated lipid membranes. Proc Natl Acad Sci U S A. 2020; 117(36):21896–905. Epub

- 2020/08/28. https://doi.org/10.1073/pnas.2004807117 PMID: 32843347; PubMed Central PMCID: PMC7486787.
- 87. Pinot M, Vanni S, Pagnotta S, Lacas-Gervais S, Payet LA, Ferreira T, et al. Lipid cell biology. Polyunsaturated phospholipids facilitate membrane deformation and fission by endocytic proteins. Science. 2014; 345(6197):693–7. Epub 2014/08/12. https://doi.org/10.1126/science.1255288 PMID: 25104391.
- 88. Manni MM, Tiberti ML, Pagnotta S, Barelli H, Gautier R, Antonny B. Acyl chain asymmetry and polyunsaturation of brain phospholipids facilitate membrane vesiculation without leakage. Elife. 2018; 7. Epub 2018/03/16. https://doi.org/10.7554/eLife.34394 PMID: 29543154; PubMed Central PMCID: PMC5903860.
- Tiberti ML, Antonny B, Gautier R. The transbilayer distribution of polyunsaturated phospholipids determines their facilitating effect on membrane deformation. Soft Matter. 2020; 16(7):1722–30. Epub 2020/01/10. https://doi.org/10.1039/c9sm02107h PMID: 31916552.
- Maulucci G, Cohen O, Daniel B, Sansone A, Petropoulou PI, Filou S, et al. Fatty acid-related modulations of membrane fluidity in cells: detection and implications. Free Radic Res. 2016; 50(sup1):S40–S50. Epub 2016/09/07. https://doi.org/10.1080/10715762.2016.1231403 PMID: 27593084.
- 91. Mitrofanova A, Mallela SK, Ducasa GM, Yoo TH, Rosenfeld-Gur E, Zelnik ID, et al. SMPDL3b modulates insulin receptor signaling in diabetic kidney disease. Nat Commun. 2019; 10(1):2692. Epub 2019/06/21. https://doi.org/10.1038/s41467-019-10584-4 PMID: 31217420; PubMed Central PMCID: PMC6584700.
- Parnaud G, Bosco D, Berney T, Pattou F, Kerr-Conte J, Donath MY, et al. Proliferation of sorted human and rat beta cells. Diabetologia. 2008; 51(1):91–100. https://doi.org/10.1007/s00125-007-0855-1 PMID: 17994216.
- 93. Gerber A, Esnault C, Aubert G, Treisman R, Pralong F, Schibler U. Blood-borne circadian signal stimulates daily oscillations in actin dynamics and SRF activity. Cell. 2013; 152(3):492–503. Epub 2013/02/05. S0092-8674(12)01549-8 [pii] https://doi.org/10.1016/j.cell.2012.12.027 PMID: 23374345.
- 94. Matyash V, Liebisch G, Kurzchalia TV, Shevchenko A, Schwudke D. Lipid extraction by methyl-tert-butyl ether for high-throughput lipidomics. J Lipid Res. 2008; 49(5):1137–46. Epub 2008/02/19. https://doi.org/10.1194/jlr.D700041-JLR200 PMID: 18281723; PubMed Central PMCID: PMC2311442.
- Clarke NG, Dawson RM. Alkaline O leads to N-transacylation. A new method for the quantitative deacylation of phospholipids. Biochem J. 1981; 195(1):301–6. Epub 1981/04/01. https://doi.org/10.1042/ bj1950301 PMID: 7306057; PubMed Central PMCID: PMC1162886.
- 96. Pietilainen KH, Sysi-Aho M, Rissanen A, Seppanen-Laakso T, Yki-Jarvinen H, Kaprio J, et al. Acquired obesity is associated with changes in the serum lipidomic profile independent of genetic effects—a monozygotic twin study. PLoS ONE. 2007; 2(2):e218. Epub 2007/02/15. https://doi.org/10.1371/journal.pone.0000218 PMID: 17299598; PubMed Central PMCID: PMC1789242.
- 97. Pang Z, Chong J, Zhou G, de Lima Morais DA, Chang L, Barrette M, et al. MetaboAnalyst 5.0: narrowing the gap between raw spectra and functional insights. Nucleic Acids Res. 2021; 49(W1):W388–W96. Epub 2021/05/22. https://doi.org/10.1093/nar/gkab382 PMID: 34019663; PubMed Central PMCID: PMC8265181.
- 98. Cadena Del Castillo CE, Hannich JT, Kaech A, Chiyoda H, Brewer J, Fukuyama M, et al. Patched regulates lipid homeostasis by controlling cellular cholesterol levels. Nat Commun. 2021; 12(1):4898. Epub 2021/08/14. https://doi.org/10.1038/s41467-021-24995-9 PMID: 34385431; PubMed Central PMCID: PMC8361143.